Drug Discoveries & Therapeutics

ISSN 1881-7831 Online ISSN 1881-784X
Volume 4, Number 5, October 2010
www.ddtjournal.com

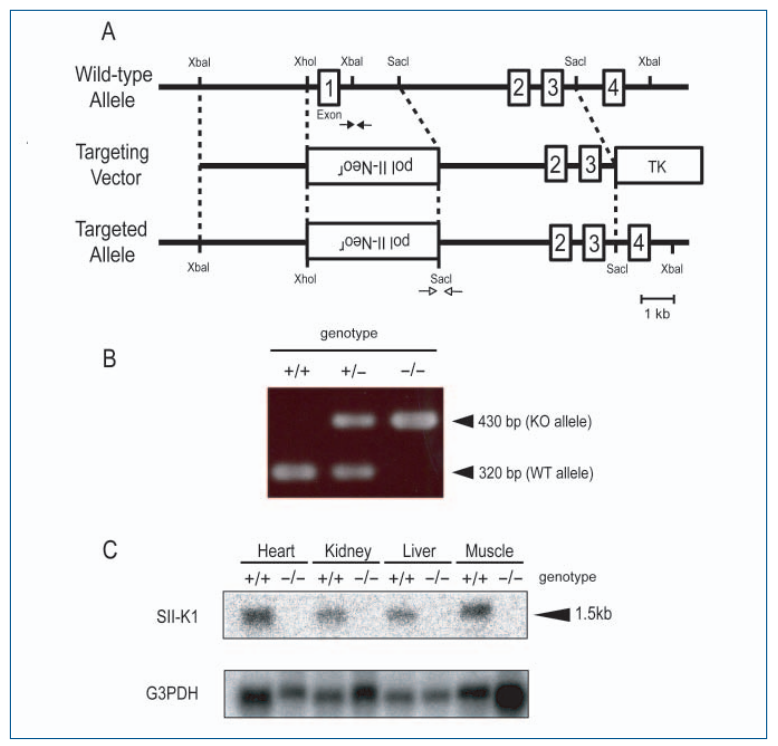

Shandong University China-Japan Cooperation Center for Drug Discovery & Screen
International Advancement Center for Medicine & Health Research

Drug Discoveries & Therapeutics

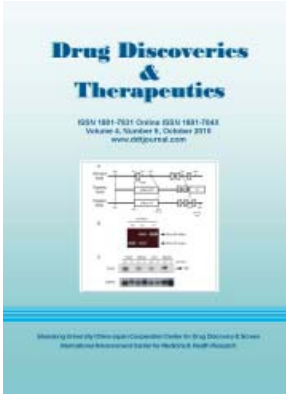

Drug Discoveries & Therapeutics is a peer-reviewed international journal published bimonthly by *Shandong University China-Japan Cooperation Center for Drug Discovery & Screen* (SDU-DDSC) and *International Advancement Center for Medicine & Health Research Co., Ltd.* (IACMHR Co., Ltd.).

Drug Discoveries & Therapeutics mainly publishes articles related to basic and clinical pharmaceutical research such as pharmaceutical and therapeutical chemistry, pharmacology, pharmacy, pharmacokinetics, industrial pharmacy, pharmaceutical manufacturing, pharmaceutical technology, drug delivery, toxicology, and traditional herb medicine. Studies on drug-related fields such as biology, biochemistry, physiology, microbiology, and immunology are also within the scope of this journal.

Subject Coverage: Basic and clinical pharmaceutical research including Pharmaceutical and therapeutical chemistry, Pharmacology, Pharmacy, Pharmacokinetics, Industrial pharmacy, Pharmaceutical manufacturing, Pharmaceutical technology, Drug delivery, Toxicology, and Traditional herb medicine.

Language: English
Issues/Year: 6
Published by: IACMHR and SDU-DDSC
ISSN: 1881-7831 (**Online ISSN** 1881-784X)
CODEN: DDTRBX

Editorial and Head Office

Wei TANG, MD PhD
Executive Editor
Drug Discoveries & Therapeutics
Pearl City Koishikawa 603,
2-4-5 Kasuga, Bunkyo-ku,
Tokyo 112-0003, Japan
Tel: 03-5840-9697
Fax: 03-5840-9698
E-mail: office@ddtjournal.com
URL: www.ddtjournal.com

IACMHR CO., LTD.

Drug Discoveries & Therapeutics

Editorial Board

CONTENTS

Volume 4, Number 5, 2010

Reviews

Original Articles

CONTENTS (*Continued*)

Review

Development in malarial vaccine: A review

Meenakshi Dhanawat*, Nirupam Das, Ramesh C. Nagarwal, J. K. Pandit*

Department of Pharmaceutics, Institute of Technology, Banaras Hindu University, Varanasi, India.

ABSTRACT: Malaria, a vector-borne infectious disease, is currently a grave and universal concern with a significant social, economic, and human cost, mainly in developing countries. In addition, the emergence and spread of resistance to antimalarial therapies have further aggravated the global situation. Currently most of the research is focused on development of antimalarial drugs, drug resistance, and novel formulations to maximize the therapeutic effect. A number of novel molecules potentially active against malarial parasites are being developed. A vaccine is still viewed as a critical part of a long-term malaria control strategy. In the last several years various studies have shown significant progress in the development of vaccines against malaria. Advancement in vaccine technology and immunology is being used to develop malaria subunit vaccines that would open up new vistas for effective treatment and control of malaria. The development of an effective malaria vaccine represents one of the most important approaches that would provide a cost-effective intervention in addition to currently available malaria control strategies. An overview on progress in antimalarial vaccines is presented.

Keywords: Malaria, plasmodium, vaccines, adjuvant

1. Introduction

Malaria is a debilitating parasitic disease. According to the Roll Back Malaria (RBM) Partnership, each year approximately 860,000 (89% were in the African Region, followed by 6% in the Eastern Mediterranean and 5% in the South-East Asia Regions) lives, mainly children and women, succumb to it (*1,2*).

Most of the drugs used in antimalarial chemotherapy are particularly active against the asexual blood forms of the parasite, which are responsible for the clinical symptoms of the disease (*3*). The increasing resistance of the malaria parasite *Plasmodium falciparum* to currently available drugs and especially to chloroquine necessitates a continuous effort to develop more effective therapeutic options (*4,5*).

Malaria continues to exact a devastating social and economic cost across the globe. It strikes hardest at some of the poorest nations and is a significant root and outcome of poverty. This is endemic in many developing nations; additionally malaria is also of serious concern to travelers, especially in the absence of a vaccine and in the face of widespread resistance to several antimalarial drugs (*6*). The most common etiological agent of malaria is *P. falciparum*, a highly evolved unicellular parasite whose life cycle, shared between an Anopheles mosquito vector and the human host, exhibits striking biological features that have been exploited to seek intervention strategies for malaria therapy (*7*). A logical and rational approach for vaccine development is imperatively needed. Devising an effective malaria vaccine would certainly help in limiting unacceptably high morbidity (*8*). Due to the complexity of the malarial parasite's life cycle, a better understanding of its molecular interactions in invasion is required (*9,10*).

Because of the rapid emergence of drug resistance and unclear mechanisms, much money has been wasted in many malaria endemic sites. Therefore a vaccine seems to be an alternative and pragmatic approach to eradicate the disease. Even a modestly efficacious malaria vaccine may protect hundreds of thousands of people from disease and death each year. The development of an effective malaria vaccine represents one of the most important approaches that would provide a cost-effective intervention in addition to currently available malaria control strategies. A number of antigens (a dozen or so) derived from different stages of the parasite's life cycle have been described and are in preclinical or clinical vaccine trials (*11*).

The recent sequencing of genomes of the *Plasmodium* species causing malaria offers immense opportunities to aid in the development of new

**Address correspondence to:*
Dr. J. K. Pandit, Department of Pharmaceutics, Institute of Technology, Banaras Hindu University, Varanasi-221 005, India.
e-mail: dr.jkpandit@gmail.com
Ms. Meenakshi Dhanawat, Senior Research Fellow, Department of Pharmaceutics, Institute of Technology, Banaras Hindu University, Varanasi-221 005, India.
e-mail: mdanawat.rs.phe@itbhu.ac.in

therapeutics and vaccine candidates through Bio-informatics tools and resources. One such database that can significantly promote the vaccine research is the MalVac Database (*12*). Recent launching of a massive vaccine trial spearheaded by British drugmaker GlaxoSmithKline PLC in collaboration with the PATH (Programs for Appropriate Technologies in Health) Malaria Vaccine Initiative has been reported. This initiative might accelerate development of a new generation of malaria vaccines (*http://www.malariavaccine.org/news-press-kits-09252008.php*).

An ideal vaccine should be safe with no or minimal side-effects, easy and cheap to manufacture, stable for storage/transport, easy to administer, could be given to infants (ideally alongside other childhood vaccinations), and should stimulate life-long protection against all forms of the disease. Although much effort is currently directed at disease treatment through the development of new antimalarial drugs, vaccines enjoy many intrinsic advantages. The desirable frequency of vaccine treatment is perhaps in the range of once or twice per lifetime, or at least, once or twice per year. Vaccines are relatively cheap to produce, if albeit not necessarily easy to discover, making them of special interest to developing countries. The ongoing spread of drug-resistant forms of malaria in combination with the side-effects associated with prevention and treatment of this disease have provided impetus for the development of a safe and effective vaccine.

2. Progress in the development of antimalarial vaccines

It is important to understand the pathogenesis of the disease, including the life cycle (Figure 1) of the parasite and the interaction between the host immune response and the parasite, for better preventive and therapeutic modalities against malaria.

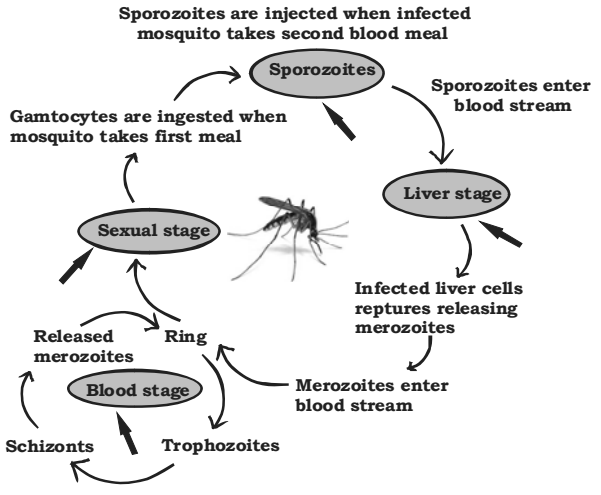

Figure 1. Malaria vaccines targeting life cycles: Targets-sporozoite, liver stage, blood stage, sexual stage. (*www.iavireport.org/Issues/1102/malariavax.asp; http://encarta.msn.com/media_461541582/life_cycle_of_the_malaria_parasite.html*)

The initial stage of infection involves the inoculation of sporozoites into the blood stream known as the pre-erythrocytic stage. This is an asymptomatic phase associated with an initial humoral response. The phase is followed by multiplication and infection of hepatocytes (*13*).

During this phase, a cell-mediated CTL (cytotoxic T lymphocyte) response is elicited. Last comes the erythrocytic phase, where infected hepatocytes rupture, releasing thousands of daughter merozoites back into the blood, where they invade circulating erythrocytes and which is associated with the clinical symptoms of the disease and correlated with both humoral and cellular responses (Figure 1) (*14*).

Vaccines against malaria have been designed to work at these different stages of the life cycle of the parasite (Table 1). Apart from the life cycle one can consider DNA and T-Cell targeting vaccines. Recently developed transmission-blocking vaccines are of considerable importance (*15*). In addition, potentially important targets for naturally acquired immunity have been exploited. The variant surface antigens (VSA) families present on the surface of infected erythrocytes particularly the PfEMP1 is well characterized. A VSA-based vaccine may prolong the protection level by preventing the parasites from expressing the VSA and will render the disease less severe (*16*).

Although promising an individual antibody response may vary between each domain as PfEMP1 exhibits a domain structure. Recent studies simultaneously observed that potential cross-reactivity in response to one of the domains- (Duffy-binding like domain) DBL4γ suggest reconsidering the vaccine for further improvement in triggering an invariable antibody response (*17*).

On the other hand a carbohydrate-based synthetic vaccine is also being developed, which will be discussed in a later part of this review. Based upon the above mentioned targets there are two standard models: (*i*) Vaccines to prevent clinical disease using irradiated sporozoites (*18*) and (*ii*) Vaccines to prevent mortality based on innate immunity (*19*).

Development of an effective malaria vaccine is a daunting task as the parasite undergoes changes in its morphological forms and surface antigens. These features enable the parasite to evade protective immune responses and vaccines based on protective immunity and are unlikely to effectively curtail transmission. As a result, the acquisition of long-term sterilizing immunity characterized by recovery from many infectious diseases does not occur with malaria. Hence vaccines inducing artificially acquired active immunity are the need of the hour and the recombinant pre-erythrocytic vaccine RTS, S might hold promise for the near future.

Table 1. Possible targets and immune mechanism of antimalarial vaccines

S. No.	Targets	Immune mechanism
1	Pre-erythrocytic Stage	
	Sporozoites	Antibodies
	Liver forms	CD4+ and CD8+ T-Cells/antibodies
2	Asexual blood Stage	
	Erythrocytes (infected)	Antibody-includes inhibition of RBC invasion
3	Sexual Stage	
	Gametocytes	Antibody-blocking of activity (pre- and post-fertilization in the mosquito)

Table 2. Summary of antimalarial vaccines

S. No.	Vaccines	Type	Antigen	Mechanism	Site of Action
1.	RTS, S	Pre-erythrocytic	Fusion of C-terminal regions of CSP with the hepatitis B surface antigen	Prevents sporozoites from invading hepatocytes; Eliminating infected hepatocytes	Sporozoite
2.	FFM ME-TRAP	Pre-erythrocytic	Two attenuated POX virus vectors	Both deliver the pre-erythrocytic malaria antigen	Sporozoite
3.	ICC-1132	Pre-erythrocytic	Modified hepatitis B virus core particle (HBc) bearing putative protective T- and B-cell epitopes	Generate a potent anti-CSP antibody response	Sporozoite
4.	Liver Stage Antigen	Pre-erythrocytic	Liver stage antigens-1 and 3 (LSA-1 and LSA-3)	Shows antigenic effect on liver-stage parasites; Expressed solely in infected hepatocytes	Acts in liver schizogony and merozoite release
5.	MSP (Merozoites Surface Protein)	Blood Stage	Merozoite surface protein	Hinders Interactions between merozoites and erythrocytes during initial contact	Merozoite/ Erythrocytes
6.	AMA1 (Apical Membrane Protein)	Blood Stage	Apical membrane antigen-1	Ceases the invasion of host cell immune responses by *Plasmodium* profound parasite-inhibitory effects	Erythrocytes
7.	EBA-175 RII-NG	Blood Stage	Erythrocyte binding antigen (EBA-175)	Blocks incursion of host cells and an intracellular translocation of machinery by parasite	Erythrocytes
8.	PfEMP1	Blood Stage	Erythrocyte Membrane Binding antigen	Immunity to the surface of the trophozoite-infected RBC	Erythrocytes
9.	PfCP2.9	Combination blood stage	AMA1/MSP1 chimeric recombinant antigen	Hinders Interactions between merozoites and erythrocytes during initial contact	Erythrocytes
10.	AMA1-C1/Alhydrogel® plus CPG7909	Asexual Blood-Stage Vaccine	Apical membrane antigen-1	Profound parasite-inhibitory effects.This is the first reported use in humans of an investigational vaccine	Erythrocytes
11.	MSP3/GLURP (GMZ2) AlOH	Combination blood stage	Recombinant GLURP-MSP3 fusion antigen	GLURP and MSP3 antigenicity	Erythrocytes
12.	Pfs230	Sexual stage	Gamete-specific surface antigen	Block the infectivity of gametes	Gametocytes
13.	Pfs25 and Pvs25	Transmission blocking vaccine	Surface antigen of mosquito stage of the malaria parasites	Kills the mosquito stage of parasite	Mosquito stage of parasite
14.	FFM ME-TRAP + PEV3A	Combination Multi-stage Vaccines	Targeting different stages of the malaria life cycle		
15.	NYVAC-Pf7	Single NYVAC genome containing genes encoding seven *Plasmodium falciparum* antigens			
16.	Synthetic GPI vaccine	Endotoxin of parasitic origin	Prevent the pathology and fatalities of severe malaria		

2.1. *Pre-erythrocytic vaccines*

A pre-erythrocytic vaccine is designed to target sporozoites or schizont-infected liver cells and thus prevent the release of primary merozoites from infected hepatocytes. Sporozoites constitute the infective stage of the malarial parasite and they are ideally the target for a malaria vaccine. Vaccines against the pre-erythrocytic stages of malaria hold the greatest promise as an effective intervention tool against malaria. The

pre-erythrocytic stage vaccine (PEV) includes antigens from the sporozoites and liver stages. The PEV is unique in that it can induce a state of strong, sterile immunity both in humans and in animal models (*20*).

The ideal vaccine for this stage would induce high titers of functional antibodies against sporozoites to prevent all parasites from entering the liver stage, and induce potent cytotoxic T-lymphocyte immunogenicity against the liver stage to kill infected hepatocytes, while not harming the human host. The lead candidate vaccine of this type is RTS, S, a recombinant protein vaccine. It targets the sporozoite stage preventing the invasion of hepatocytes by sporozoites or destroys parasites in infected hepatocytes and thus prevents both clinical disease and the transmission of malaria (Figure 2) (*21-23*).

2.1.1. *Circumsporozoite protein (CSP) based vaccines*

CSP expressed on the surface of developing and mature sporozoites are considered to be an important target of antibody and T cell-mediated responses to sporozoites (*24*). Due to high immunogenicity and a crucial role in hepatic cell invasion by CSP this molecule has been considered as an excellent target for antimalarial vaccine development. CSP based vaccine is classified into recombinant and synthetic (*25*). The CSP displays a characteristic common molecular structure in all *Plasmodia*, consisting of a central tandem amino acid repeat region and two relatively conserved domains named regions I and II (containing great genetic variability in some residues), localized at the protein's amino- and carboxy-terminal ends, respectively (Figure 3) (*26,27*). PEV has been primarily based on the CSP. In particular, the central repeat region that contains an immunodominant B cell epitope represented the target of the initial vaccine trials (*28-30*).

(*a*) *RTS, S* – RTS, S is a recombinant pre-erythrocytic vaccine consisting of the circumsporozoite protein found on the surface of the sporozoite stage of *P. falciparum*. It's a fusion of the central repeat and C-terminal flanking regions of CSP with the hepatitis B surface antigen (HBsAg), combined and named RTS, and formulated with the AS02A Adjuvant System (*21*). This antigen elicits antibodies that are capable of preventing sporozoites from invading hepatocytes, and a cellular response that is capable of eliminating infected hepatocytes (*31,32*). Different types of RTS, S vaccines depending upon adjuvant are: RTS, S/AS02A, RTS, S/AS02B, RTS, S/AS02D, RTS, S/AS02E. The most successful malaria vaccine to date, the recombinant protein RTS, S administered with the adjuvant AS02A, has shown protection against experimental and natural *P. falciparum* sporozoite challenge in humans (*33,34*).

A trial in southern Mozambique aimed to assess the safety, immunogenicity, and initial efficacy of the malaria vaccine RTS, S formulated in the AS02 adjuvant

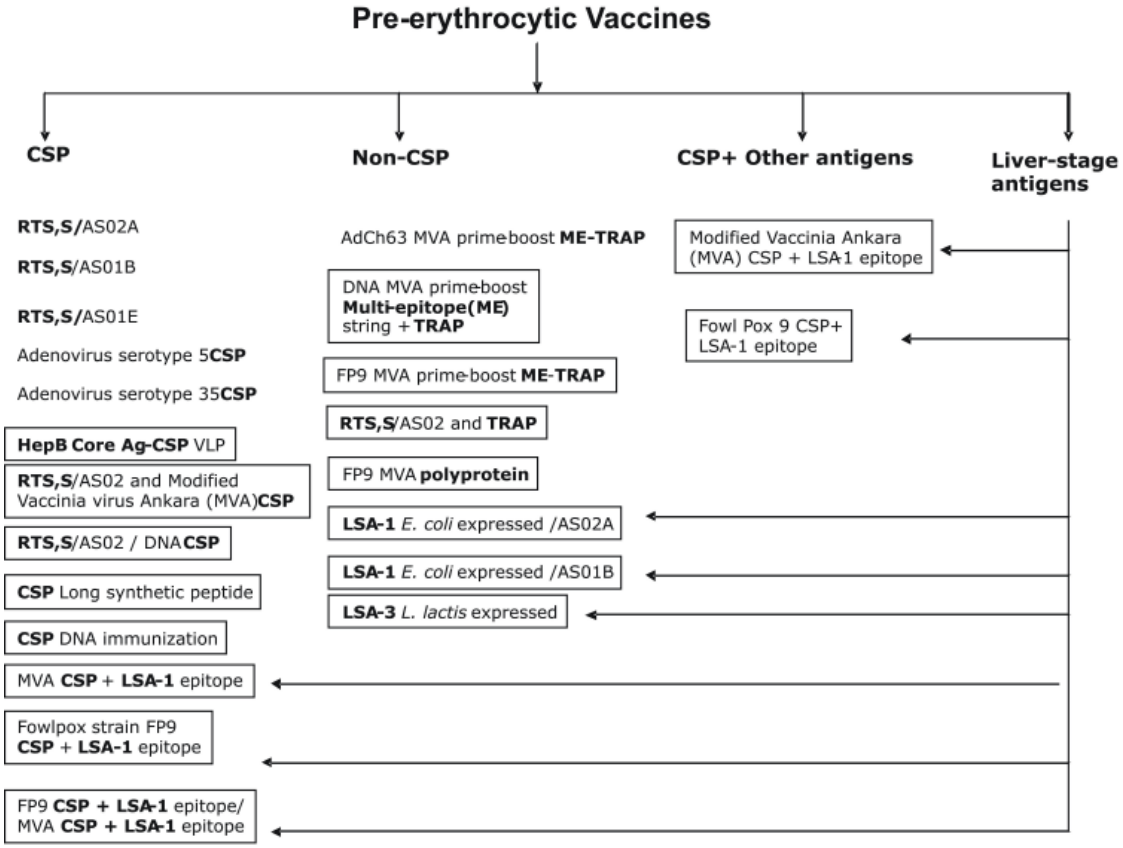

Figure 2. Pre-erythrocytic vaccines in various phases of clinical trials. Vaccines in BOX are withdrawn from clinical trials. (*http://www.who.int/vaccine_research/documents/Malaria%20Vaccine%20Rainbow%20Table_Clinical_Oct_2008.pdf*)

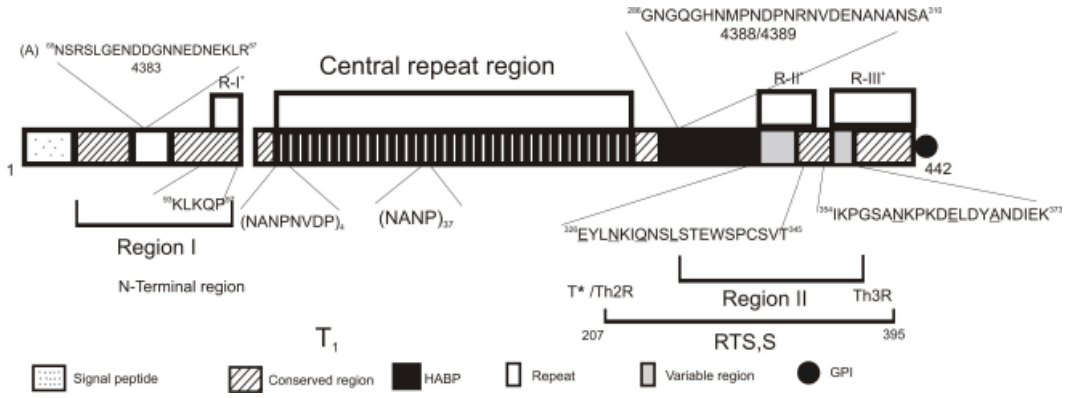

Figure 3. Various regions of CSP vaccine.

system, AS02D (with the letter D indicating the pediatric formulation) has proved that the vaccine is having a good safety profile and is protective in those most vulnerable to the disease-infants less than 1 year old (*35*). This trial was followed by recent Phase IIb studies of the vaccine in Bagamoyo, Tanzania. Although the vaccine was co-administered to infants with other routinely delivered EPI immunizations (the World Health Organization's Expanded Program on Immunization), it did not interfere with the immunogenicity of the multiple co-administered antigens. A 65% rate of protection against new infections was observed (*36*). To confirm the efficacy of RTS, S, a study sponsored by the PATH Malaria Vaccine Initiative (MVI) and GlaxoSmithKline Biologicals found that this particular malaria vaccine has significant efficacy with fewer serious adverse effects in clinical malaria in children 5 to 17 months of age (*37*).

A large scale study (Phase III) of RTS, S/AS01E (Mosquirix®) vaccine developed by GSK (Glaxo Smithkline Biologicals) has been launched and is expected to be undertaken at 11 different sites in seven countries in Sub-Saharan Africa involving 16,000 children and infants (*38*).

(*b*) *FFM ME-TRAP* – FFM ME-TRAP denotes two recombinant viral vectors, attenuated fowl pox strain FP9 (FP9 ME-TRAP) and modified Vaccinia Virus Ankara (MVA ME-TRAP). Both encode the pre-erythrocytic malaria antigen construct thrombospondin-related adhesion protein (TRAP) coupled to the multiple epitope (ME) string (*39*). Outcome from a Phase IIb trial with vaccination regimen FFM ME-TRAP indicated that the vaccine showed weak immune response and was not protective against episodes of clinical malaria among children in a malaria endemic area (*40*).

(*c*) *ICC-1132* – ICC-1132 is a malaria vaccine candidate based on a modified hepatitis B virus core particle (HBc) bearing putative protective T- and B-cell epitopes from the repeat region and a universal T-cell epitope from the C terminus of CSP of *P. falciparum* (Figure 4). It was used to generate a potent anti-CSP antibody response. This vaccine has been found to be highly immunogenic in mice and in *cynomolgus*

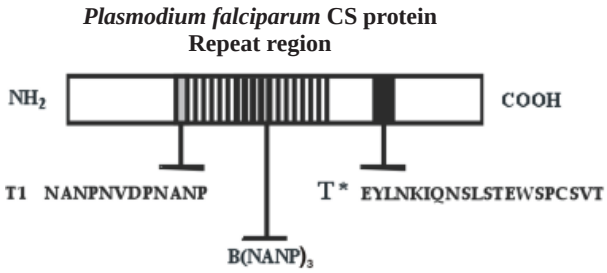

Figure 4. *Plasmodium falciparum* CS proteins [B-cell epitope; $(NANP)_3$; T1-epitope; T*-epitope] (*41,42*).

monkeys. ICC-1132 elicits potent antibody responses in mice primed with *P. falciparum* sporozoites. This suggests a potential advantage of enhancing the sporozoite-primed responses of semi-immune individuals in endemic areas (*41,42*).

In a recent trial of ICC-1132 (Malariavax), a novel CS based malaria vaccine was found to be safe and well tolerated but malaria specific antibody responses were relatively weak as compared to the responses to the immunogen (ICC-1132) and to HBc. When adjuvanted with alum (Alhydrogel® formulation), the vaccine was poorly immunogenic suggesting the use of a more powerful adjuvant system (*43*).

(*d*) *CSP (Long synthetic peptide)* – One of the major targets of antibody and T cell-mediated responses to sporozoites is the CSP expressed on the surface (*54*). CSP derived peptides are presented in association with MHC molecules on the surface of infected liver cells as evidenced by CSP-specific T cell recognition (*44*).

(*e*) *CSP + other antigens* – Modified Vaccinia Ankara (MVA) CSP + LSA-1 epitope, and Fowl Pox 9 CSP + LSA-1 epitope are two types of vaccine which have CSP along with some other antigens like LSA-1. Unfortunately both of them have failed in their Phase Ia clinical trials. Apart from these CSP vaccines, numerous CSPs became obsolete in various stages of their clinical trials. Some of them are: HepB Core Ag-CSP VLP, RTS, S/AS02 and modified vaccinia virus Ankara (MVA), RTS, S/AS02/ DNA CSP (NMRC-GSK), CSP Long synthetic peptide, CSP DNA immunization, MVA CSP + LSA-1 epitope,

Fowl pox strain FP9 CSP + LSA-1 epitope, and FP9 CSP + LSA-1 epitope/MVA CSP + LSA-1 epitope.

2.1.2. *Liver-stage antigens (LSAs)*

The liver plays a crucial role in the *Plasmodium* life cycle, because hepatocytes are an obligatory site for schizogony, a process of amplification and molecular changes for the parasite. In *P. falciparum*, at least two of the relevant antigens (LSA-1 and LSA-3), have been identified and characterized (*45-47*). LSAs 1 and 3 expressed by liver-stage parasites and both pre-erythrocytic and a blood-stage parasites respectively showed promising antigenic and immunogenic properties. LSA-1, from current evidence, is one of the few antigens exclusively expressed in hepatocytes (*48,49*). Immunization studies with various LSA-3 antigens on chimpanzees (*Pan troglodytes*), the primates most closely related to humans, induced protection against successive challenges with large numbers of *P. falciparum* sporozoites. These surface proteins are expressed solely in infected hepatocytes and thought to have a role in liver schizogony and merozoite release (*50*). The different stages of the parasite express different antigens. A vaccine effective in killing liver-stage parasites may not inhibit the growth of blood-stage parasites and the above study did not confirm whether it was liver-stage or blood-stage protection (*51,52*). Although the exact function of LSA-1 for the parasite remains unknown, there is still evidence that this antigen is an attractive target for vaccine design at both the T-cell and B-cell level.

2.2. *Blood-stage/erythrocytic vaccines*

For an asexual stage malaria vaccine, the impetus came from the establishment of parasite culture by Trager and Jensen (*53*) and peptide biology. Blood stage vaccines (Figure 5) aim to impact the disease causing stage of the parasite's life cycle, and research in this area has focused mainly on AMA1 and MSP1 (*54*) antigens that are used by the parasite to invade the human red blood cell and cause disease. There are two possible classes of blood-stage vaccine: anti-invasion and anti-complication. A vaccine that could prevent invasion of red blood cells by merozoites would prevent malaria disease. Blood-stage vaccines reduce morbidity and mortality due to severe malaria, and are not intended to prevent infection (*55*). Development of such vaccines has been hampered by the lack of an established human challenge model, by the limitations of available animal models, and by unclear immunological correlates of protection (*56*). Despite these challenges, several antigens expressed by merozoites, the extra cellular form of the parasite that infects erythrocytes, have emerged as promising vaccine candidates. Druilhe and colleagues put forward encouraging findings from a Phase I trial of merozoite surface protein (MSP) (*57*).

2.2.1. *MSP (merozoite surface protein)*

During initial contact MSPs, often referred as "surface proteins", mediate the interactions between merozoites and erythrocytes (*58,59*). MSPs are situated on the merozoite surface, and are associated with merozoite surface molecules. In *P. falciparum*, this protein ranges in size from 185 to 200 kDa and is attached at its C terminus to the parasite plasma membrane *via* a glycosylphosphatidylinositol anchor (*60*). These proteins are of great importance in developing potential targets as candidates for an anti-malarial vaccine (*61,62*).

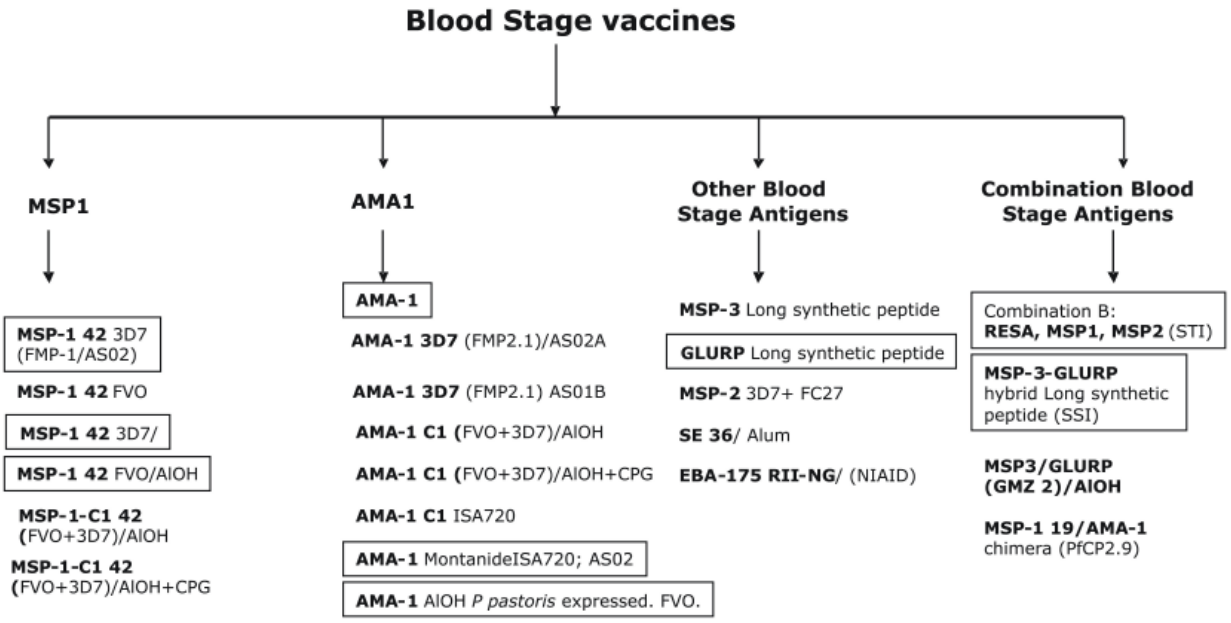

Figure 5. Blood stage vaccines in various phases of clinical trials. Vaccines in BOX are withdrawn from clinical trials. (*http://www.who.int*)

The major MSP-1 is one of the most widely studied parasite antigens from the erythrocyte stage of infection by *P. falciparum* (*63,64*). It is secreted as a 195 kDa protein that is proteolytically cleaved (Figure 6) to form four fragments, of 83 kDa, 30 kDa, 38 kDa, and 42 kDa, during merozoite maturation (*65-67*). The 42 kDa C-terminal fragment (MSP-142) is further processed to 33 kDa and 19 kDa. Only the MSP1-19 fragment remains on the merozoite surface at the time of erythrocyte invasion. It contains two epidermal growth factor-like modules that are anchored to the surface *via* a glycosylphosphatidylinositol moiety. Both MSP-119 and MSP-142 are leading vaccine candidates for the blood stage of *P. falciparum* (*68*).

2.2.2. *Apical membrane antigen (AMA1)*

AMA1 is a micronemal protein of apicomplexan parasites that appears to be essential during the invasion of host cell immune responses by *Plasmodium*. AMA1 can have profound parasite-inhibitory effects; both have been measured *in vitro* and in animal challenge models, suggesting AMA1 as a potential vaccine component (*69,70*). AMA1 is a structurally conserved type I integral membrane protein varying between 556 to 563 amino acids and is an apical membrane antigen 1 of the malarial parasite *P. falciparum* (PfAMA1). It is a merozoite antigen that is considered a strong candidate for inclusion in a malaria vaccine (Figure 7) (*71*).

2.2.3. *AMA1-C1/Alhydrogel® plus CpG 7909*

The AMA1-Combination 1 vaccine was developed by the Malaria Vaccine Development Branch of the National Institute of Allergy and Infectious Diseases (NIAID), National Institutes of Health, USA. It contains an equal mixture of yeast expressed recombinant allelic proteins based on sequences from the FVO (fragment from the Vietnam-Oak Knoll) and 3D7 strains of *P. falciparum*, adsorbed on Alhydrogel (*73*). AMA1, a polymorphic MSP, is a leading asexual blood-stage malaria vaccine candidate. The overall structure of AMA1 appears to be conserved as compared to other surface proteins, but there are numerous amino acid substitutions identified among different *P. falciparum* isolates (*74-76*). This is the first reported use in humans of an investigational vaccine with the novel adjuvant CpG (cytosine and guanine separated by a phosphate) 7909. It is an immunomodulating synthetic oligodeoxynucleotide (ODN). CpG ODN as a vaccine adjuvant has a sequence of 5'-TCG TCG TTT TGT CGT TTT GTC GTT-3' with all nucleotides linked with phosphorothioate bonds and has been found to be considerably more potent than alum in mice. CpG 7909 is needed to induce high antibody levels for malaria proteins, which are generally poor immunogens in humans (*77*). As an adjuvant alhydrogel is known to strongly promote Th2 (T helper)-type responses. Mullen and coworkers showed that the addition of CpG 7909 to AMA1-C1/Alhydrogel vaccine resulted in an increase in antibody titers and functional responses in mice, rats, and guinea pigs. The safety profile of the AMA1-C1/Alhydrogel® (aluminium hydroxide) plus CpG 7909 malaria vaccine is acceptable and a significant increase in immunogenicity was observed (*78,79*).

A Phase I trial of this vaccine in two different formulations (phosphate buffer and saline) and dosing intervals (1 month or 2 months) was conducted in healthy adults of age 18-50 years. AMA1-C1/Alhydrogel® + CPG 7909 in saline was shown to have similar immunogenicity as the AMA1-C1/Alhydrogel® + CPG 7909 buffered with phosphate and both the formulations were well tolerated. Excellent *in vitro* growth-inhibitory activity was reported in this human vaccine trial with AMA1. Based on the tolerability and immunogenicity of the vaccine a Phase II study suggested the development of a more immunogenic formulation of AMA1-C1

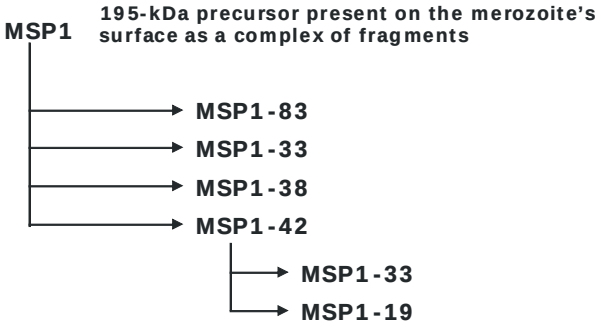

Figure 6. Proteolytic cleavage of MSPs.

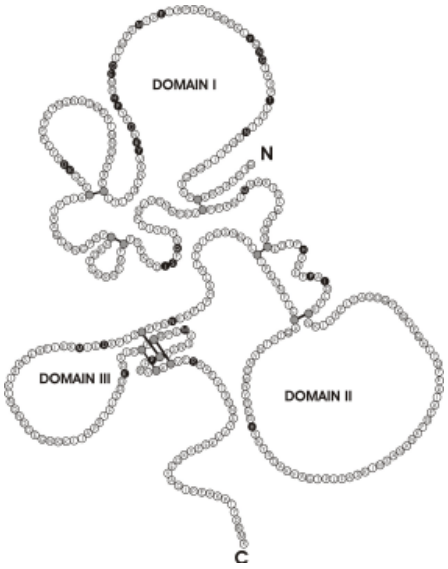

Figure 7. Schematic of Pf AMA1 ectodomain (domains, I, II and III). Locations of eight disulphide bridges are shown in dark grey. D493, F505 and K544, are shaded in grey. Residues shaded in black represent mutations across 11 different naturally occurring *P. falciparum* sequences (*71,72*).

as an effective blood stage vaccine for *P. falciparum* malaria. Further, in the absence of a human blood stage challenge model or a predictive animal model, blood stage malaria vaccine development is empiric and demonstration of protection requires Phase IIb studies in the target population (*55*).

2.2.4. *Other blood stage antigens*

(*a*) *EBA-175 RII-NG* – One approach is to develop vaccines that target the molecular receptors used by the malaria parasite for the incursion of host cells and an intracellular translocation machinery to accentuate the process. The transmembrane erythrocyte binding protein-175 (EBA-175) and TRAP play a vital role in this course of action (*80,81*). The 175 kDa *P. falciparum* erythrocyte binding antigen (EBA-175) (Figure 8) binds sialic acid residues on glycophorin-A to mediate erythrocyte invasion. Two adhesive modules (called F1/F2) located in the extra cellular domain mediate the receptor interaction of EBA-175 (*82-85*). The binding region within EBA-175 is a cysteine-rich region identified as region II. Antibodies against region II block the binding of native EBA-175 to erythrocytes (*84,86*).

(*b*) *PfEMP1* – PfEMP1 (Figure 9) (*P. falciparum* erythrocyte membrane protein 1) is a high-molecular weight (200 to 350 kDa) transmembrane polypeptide consisting of 4 to 7 extracellular domains encoded by the *var* gene family. It has been identified as the rosetting ligand of the malaria parasite *P. falciparum* (*87,88*). PfEMP1 interacts with complement receptor, one on uninfected erythrocytes to form rosettes in the vasculature of the infected organ, and is associated with severe malaria. PfEMP1 could regulate both trophozoite and sexual stage densities (*89,90*). Immunity to the surface of the trophozoite-infected RBC could render protection from further infection. PfEMP1 appears to be the target of naturally acquired protective immunity in humans and immunization of *Aotus* monkeys with a domain of PfEMP1 inducing protection against a lethal *Plasmodium* parasite line (*91*).

(*c*) *PfEMP1 DBL1α-TM-AS* – The primary structure of PfEMP1 consists of a large N-terminal ecto-domain containing a variable number of DBL domains that mediate cytoadherence to various host cell receptors (*94,95*). The cytoadhesion of parasite-infected erythrocytes to a number of host cells is a causative factor in severe pathology of malaria, and PfEMP1 is considered the major virulence determinant of *P. falciparum* (*96*). Vogt *et al.* using recombinant proteins corresponding to the different domains of *P. falciparum* erythrocyte membrane protein 1 (PfEMP1) identified DBL-1α as the ligand for HS (heparan sulfate) (*97*).

2.2.5. *Combination blood stage vaccines*

(*a*) *PfCP2.9* – PfCP2.9 (Figure 10) is the first malaria vaccine candidate based on a chimeric recombinant protein vaccine for *P. falciparum* malaria consisting of AMA1 (domain III) and MSP1(19 kDa portion) expressed from the yeast *Pichia pastoris* with improved immunogenicity.

The enhancement of immunogenicity may be attributed to the presence of more T cell epitopes included in the construct and activity mediated by a combination of growth-inhibitory antibodies generated by the individual MSP1-19 and AMA-1(III) of PfCP-2.9 Vaccine (*98*). It was formulated with the adjuvant Montanide ISA 720 and at a dose of 50 µg, the vaccine appeared safe and highly immunogenic when observed during a preclinical evaluation (*99*).

A Phase I clinical trial was conducted at Shanghai, China to assess the safety, reactivity, and immunogenicity (antigen-specific antibody response) of PfCP2.9/ISA 720 vaccine. In this trial, volunteers developed high ELISA antibody responses to PfCP2.9

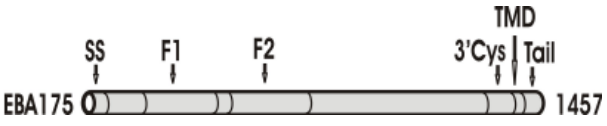

Figure 8. EBA-175 RII-NG-blood stage antigens.

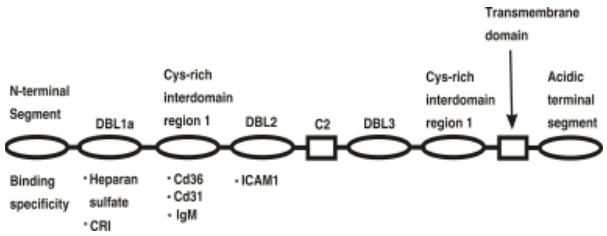

Figure 9. The multi-domain structure of *PfEMP1* (*91-93*). The extracellular domain building blocks: NTS, DBL, CIDR and C2 domains. Based on sequence similarity, DBL domains group as five types (α-ε) and CIDR domains as three types (α-γ)12. DBLα, β and δ types pair with other domains. Abbreviation: CR1, complement receptor 1; ATS, acidic terminal segment; CIDR, cysteine-rich interdomain region; DBL, Duffy-binding-like domain; ICAM-1, intracellular adhesion molecule-1; NTS, N-terminal segment; TM, transmembrane domain.

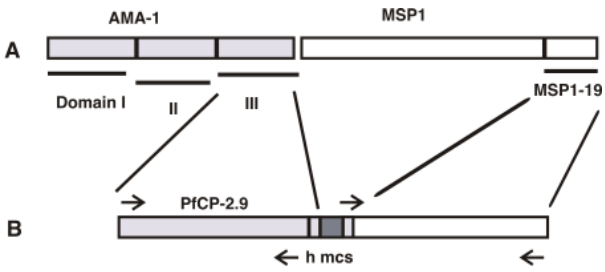

Figure 10. Schematic representation of the PfCP-2.9 gene construct and recombinant protein. (A) Localization of domain III of AMA-1 and MSP1-19 on the two molecules. **(B)** Structure of PfCP-2.9. The AMA-1(III) and MSP1-19 fragments were fused *via* a hinge-MCS (Multiple Cloning Site or polylinker)-hinge fragment (*98*).

but biological function of these antibodies was not reflected by *in vitro* inhibition of parasite growth. Additionally lower IFA (Indirect Immunofluorescent Assay) antibody responses were observed to native AMA1 and MSP1 in parasites (*100*). The most common adverse event was dose dependent reactivity at the injection site as reported earlier (*101*). Sinobiomed Inc., a Shanghai based leading developer of genetically engineered recombinant protein drugs and vaccines is planning to launch the Phase II clinical trial of its patented malaria vaccine candidate, PfCP2.9 (*http://www.redorbit.com/news/health/1385194/phase_ii_clinical_trial_of_sinobiomeds_malaria_candidate_vaccine_to/*).

(*b*) *MSP3/GLURP (GMZ 2)/AlOH – Lactococcus lactis* expressed recombinant is a fusion protein, derived from *P. falciparum* Glutamate-rich protein (GLURP) genetically coupled to *P. falciparum* MSP3 and produced in *L. lactis* as a secreted recombinant GLURP-MSP3 fusion protein. It was designed with an aim to produce high levels of cytophilic antibodies. Antigenic studies suggested that the hybrid molecule provides an adequate presentation of GLURP and MSP3 antigenicity (*11,102*).

2.3. *Sexual-stage vaccines*

Induction of antibodies to gametocyte antigens can prevent fertilization in the mosquito; as well as its blood meal. The mosquito ingests antibodies that block fertilization. As a result, assessment of the efficacy of gametocyte vaccines is possible with a simple *ex vivo* assay. A sexual-stage vaccine consisting of an antigen not expressed in human beings during natural infection would not select for escape mutants. Therefore, combination of such a vaccine with a blood-stage or pre-erythrocytic vaccine could prevent potential immune selection. Sexual-stage vaccination would not protect vaccinated individuals from disease but would protect communities from infection.

2.3.1. *Pfs230*

The 230 kDa gametocyte gamete-specific surface protein of *P. falciparum*, Pfs230, is a target of antibodies which inhibit the development of the parasite inside the mosquito vector (Figure 11). A transmission blocking vaccine based on Pfs230 may be a powerful tool for malaria control. This sexual-stage falciparum surface antigen can elicit antibodies which block the infectivity of gametes in mosquitoes (*103-105*).

2.3.2. *Transmission-blocking vaccine*

Mosquito stage transmission blocking (MSTB) or transmission-blocking vaccine (TBV) (Figure 12) is an anti-mosquito stage vaccine that targets antigens on gametes, zygotes or ookinetes. The idea for TBVs emerged from the 1976 observations of Gwadz (*106*) and Carter & Chen (*107*) which showed that antibodies elicited by gametocytes from the avian malarial parasite, *P. gallinaceum* were capable of killing the emerging gametocytes – not in the avian host but in the mosquito vector. The ultimate goal of TBVs is the interruption of malaria transmission from human to mosquito populations through prevention of parasite development in the mosquito midgut. TBVs do not confer protection to individuals and thus vaccination coverage will likely need to be widespread and sustained.

An underlying assumption of course is that proteins expressed in mammalian cells after immunization with DNA vaccine plasmids, are likely to be folded more like that in the eukaryotic parasite and thus elicit a functionally effective transmission-blocking immune response in experimental animals and ultimately in humans (*108,109*). The intention is to protect communities from infection, rather than the individual, but active clinical development of this approach is still awaited.

The Phase I Trial of Malaria Transmission Blocking

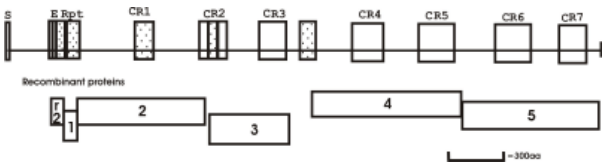

Figure 11. Sequence domains of Pfs230 and the sequences from which recombinant antigens were derived. S, signal sequence; E, poly-glutamate region; Rpt, tetra peptide region; CR, cystein rich motifs; r2-5, recombinant proteins; Shaded area, net negative charge.

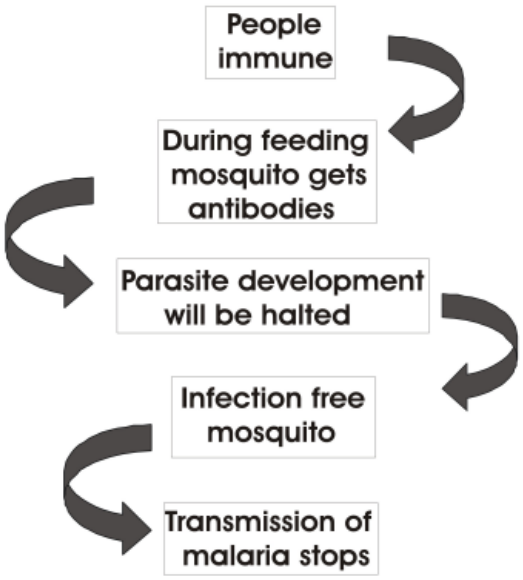

Figure 12. Concept of malaria transmission blocking vaccine Pfs25 and Pvs25.

Vaccine (TBV) Candidates Pfs25 and Pvs25 Formulated with Montanide ISA 51: Pfs25 and Pvs25, surface proteins of mosquito stage of the malaria parasites *P. falciparum* and *P. vivax*, respectively, are leading candidates for vaccines preventing malaria transmission by mosquitoes. It is feasible to induce transmission-blocking immunity in humans using the Pfs25/ISA 51 vaccine (*110*). Two TBVs, which were under clinical trial, withdrawn at Phase Ia were: Pfs25 ISA51 *Pichia pastoris* expressed, Pvs25 AlOH/ISA51 *Saccharomyces* expressed.

2.4. *Combination multi-stage vaccines*

Due to the complex life cycle and high antigenic diversity of the malaria parasite, a multistage vaccine may be necessary for optimal protection against the disease. A combination of pre-erythrocytic and blood-stage antigens is the most feasible approach to obtain a multistage vaccine to prevent malarial parasites from invasion of the host.

2.4.1. *FFM ME-TRAP + PEV3A*

A combination vaccine targeting different stages of the malaria life cycle may provide the most effective malaria vaccine. A new combination malaria vaccine is FFM ME-TRAP + PEV3A. PEV3A consists of peptide derived from both the pre-erythrocytic circumsporozoite protein and the blood stage antigen AMA-1 (*111*). Virosomal PEV3A vaccine given either alone or in combination with ME-TRAP vaccine had no protective effect in the malaria challenge model.

2.4.2. *NYVAC-Pf7*

A recently developed multistage vaccine, NYVAC-Pf7 is a single NYVAC genome containing genes encoding seven *P. falciparum* antigens. NYVAC-Pf7 is a genetically engineered, attenuated vaccinia virus, multistage, multicomponent *P. falciparum* vaccine that includes a TBV candidate Pfs-25, together with six additional leading candidate antigens (three pre-erythrocytic proteins: CS, SSP2/TRAP and LSA-1; and three asexual blood-stage antigens: MSP-1, AMA-1, and SERA) (*112*).

2.5. *T-cell targeting vaccines*

Most currently used vaccines work by getting the body to produce antibodies against the disease. Antibodies are unable to attack the malaria parasite once it has invaded liver cells and thus the approach was to design malaria vaccines that will produce potent T-cell responses against the liver stage of malaria infection (Figure 13). T-cells are a type of white blood cells called lymphocytes that circulate in the blood. There

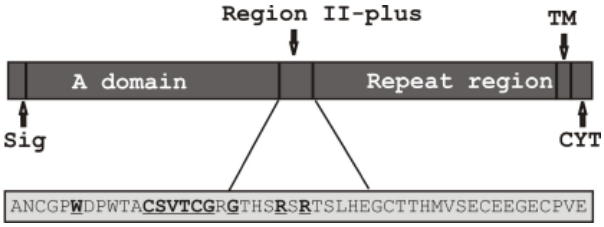

Figure 13. T-cell targeting vaccines.

are two types of T-cells: CD8+ T-cells and CD4+ T-cells and among them CD8+ T-cells play an important role in protective immunity. The vaccines stimulate populations of T-cells that will destroy liver cells that are harboring the malaria parasite and thus prevent parasite development. This approach could prevent both blood-stage infection and also prevent malaria transmission in endemic areas. The T-cells recognize the infected liver cells as they express small peptides from malaria on their surface (*113,114*). They also produce chemokines and cytokines particularly IFN-γ (Interferon-gamma) that can act in highly infection specific mechanisms to interfere with the spread and replication of a microbe. Mutation at a target epitope of the pathogen limits the ability of the T-cell (CD8+ T-cell) to recognize it and also in the presence of a high level of antigens, T-cells get exhausted after a certain time interval (*115*).

For many years the IFN-γ *ex vivo* ELISpot has been a major assay for assessing human T-cell responses generated by malaria vaccines. The ELISpot assay though a sensitive assay is an imperfect correlate of protection against malaria. Developing an ideal assay procedure was considered to be the major limitation for evaluating the efficiency of T-cell vaccines. Flow cytometric analysis of T-cell function that has been developed over time provides valuable insight into vaccine efficacy and protection (*116*). It also allows characterization of multifunctional antigen-specific T-cells following vaccination (*117*).

Flow cytometric analysis facilitates a more precise measurement of MIG (monokine induced by gamma) also known as CXCL9. Measurement of CXCL9, a chemokine induced by INF-γ, has now been considered as a more sensitive assay for the quantitative detection of INF-γ post vaccination (*118*).

2.5.1. *DNA vaccines*

The interest in this novel technology has been enormous and DNA vaccines are quite effective in priming immune responses and inducing immunological memory. Vaccine delivery systems that have been designed to induce protective CD8+ T-cell responses against *Plasmodium*-infected hepatocytes have been studied extensively but have been judged as being suboptimal for inducing protective immunity against

malaria. The key to success for any DNA-based therapy is to design a vector able to serve as a safe and efficient delivery system. Efficient and relatively safe DNA transfection using lipoplexes makes them an appealing alternative to be explored for gene delivery (*119*). The emerging technology of DNA vaccines offers many of the features desired in a malaria vaccine. Plasmid DNA introduced directly into the cells of the vaccine encodes antigen expression which stimulates a specific immunological response. This technique provides a practical and relatively simple approach toward designing a multivalent vaccine capable of delivering those antigens necessary to induce a protective immune response. This capability is especially relevant for a malaria vaccine. There are only a few target epitopes for T-cells and sequences vary from one strain of parasite to another and the specific variants do not often induce immunologically cross-reactive responses. Indeed, an effective DNA vaccine against malaria is expected to be a multi-gene vaccine (*56*). To date no DNA vaccine used alone has been reported to be efficacious in humans.

Although significant successes have been achieved in laboratory animal species, the level of immunity and protection afforded by DNA vaccines in larger animals and humans is often more limited than by conventional vaccines.

2.5.2. *DNA, MVA, and FP9 vaccines*

DNA, MVA and FP9 vaccines used initially encoded an identical DNA sequence consisting of a string of T- and B-cell epitopes from pre-erythrocytic antigens (the multi-epitope or ME string) fused to the entire sequence of TRAP (Figure 14) (*120-122*). TRAP is a pre-erythrocytic antigen that has been shown to be important for gliding motility and infectivity of liver cells and is currently being pursued as a malaria vaccine candidate for *P. falciparum* (*120,123,124*). It is a transmembrane protein that belongs to the TRAP/Micronemal protein 2 (TRAP/MIC2) family required for sporozoite gliding motility and together with the circumsporozoite protein (CS) it has been found to be essential for the process of malaria sporozoite infection to the hepatocyte (*125-127*).

Several sequential clinical trials of DNA ME-TRAP, MVA ME-TRAP and FP9 ME-TRAP vaccines have been conducted to evaluate their safety, immunogenicity and protective efficacy in human volunteers. These vaccines are safe, highly immunogenic for CD4+ and CD8+ T lymphocytes and have shown encouraging and statistically significant results in studies of efficacy against a stringent, heterologous strain sporozoite challenge.

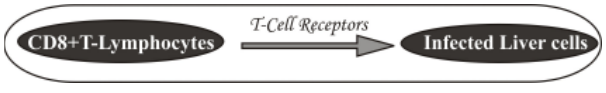

Figure 14. Schematic representation of *Plasmodium vivax* TRAP protein. Bold and underlined characters represent the cell adhesive motifs. Sig, signal sequence; M, transmembrane sequence; CYT, cytoplasmic tail (*128*).

2.6. *Synthetic glycosylphosphatidylinositol (GPI) vaccine*

GPI (Figures 15 and 16), which is a pro-inflammatory endotoxin of parasitic origin and thought to be responsible for malarial acidosis, pulmonary edema and cerebral syndrome, has been synthesized. Hexasaccharide malarial toxin I synthesized by an automated procedure is currently under development as a malaria vaccine candidate (*129*). Using a combination of automated solid phase methods and solution-phase fragment coupling, the target GPI was assembled in a matter of days. Seeberger *et al.* recently reported the total synthesis of *P. falciparum* lipidated GPI by a highly convergent synthetic strategy. They placed three orthogonal protecting groups for the late stage installation of three lipid side chains on the GPI hexasaccharide backbone (*130*).

Synthetic GPI (*P. falciparum* GPI glycan) is a prototype carbohydrate anti-toxic vaccine, which could contribute greatly to prevent the pathology and fatalities of severe malaria (*131,132*).

Regardless of these advances, major improvements

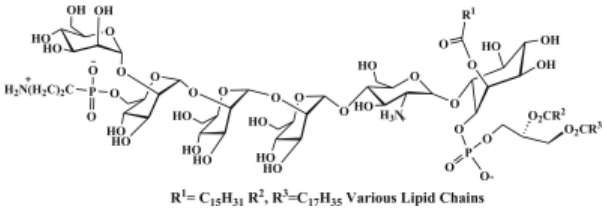

Figure 15. Consensus structure and retrosynthetic analysis of lipidates *P. falciparum* GPIs.

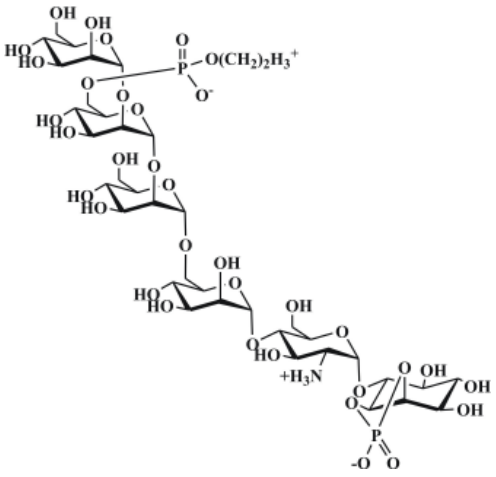

Figure 16. Hexasaccharide GPI malaria toxin-I.

and innovative approaches are still needed. For many infectious diseases it is possible to produce an attenuated (harmless) version of the pathogen or a pathogen subunit that will lead to protective immunity without causing disease. Although in the case of malaria this is technically possible (irradiated malaria sporozoites given by infected mosquito bite can lead to protective immunity), it is impractical to do this on a large scale.

3. Conclusion

All vaccines which have failed in different phases or are in the pipeline toward success have been covered in this review. Many clinical trials and unresolved issues related to stability, immunogenicity and targeting to the site of the parasite life cycle give hope for further development of antimalarial vaccines. The development of a vaccine of therapeutic and protective benefit against the malaria parasite requires a novel approach and to date there are no vaccines available that can effectively target a parasitic infection. Traditional approaches to vaccine development against malaria have met with limited success. The search for an efficacious vaccine against malaria is ongoing and it is now widely believed that to confer protection a vaccine must induce very strong cellular and humoral immunity concurrently, but the vaccine, which has been promised to be 'just round the corner' for many years, remains elusive. Development of an effective and deployable malaria vaccine seems technically feasible in the view of most malaria researchers. New vaccine delivery methods and adjuvants could continue to increase the antibody and cellular immunogenicity of subunit vaccination. The development of a vaccine to protect human subjects against malaria is a feasible goal and the emergence of DNA vaccine technology offers a simple approach to formulating such a multivalent vaccine.

Highly purified subunit vaccines require potent adjuvants in order to elicit optimal immune responses and therefore an efficient adjuvant is also needed. A vaccine that would reduce both mortality and morbidity secondary to *P. falciparum* infection would be a valuable resource in the fight against this disease. A safe, effective and affordable malaria vaccine is expected to provide a long-lasting approach to prevent infection, reduce disease severity, prevent death and interrupt transmission. A vaccine that completely prevented infection, even for a relatively short time, would be very satisfactory for travelers.

References

1. *http://rbm.who.int/globaladvocacy/pr2010-03-18.html* (accessed April 1, 2010).
2. *http://whqlibdoc.who.int/publications/2009/9789241563901_eng.PDF* (accessed April 1, 2010).
3. Araújo MJ, Bom J, Capela R, Casimiro C, Chambel P, Gomes P, Iley J, Lopes F, Morais J, Moreira R, de Oliveira E, do Rosário V, Vale N. Imidazolidin-4-one derivatives of primaquine as novel transmission-blocking antimalarials. J Med Chem. 2005; 48:888-892.
4. White NJ. Antimalarial drug resistance. J Clin Invest. 2004; 113:1084-1092.
5. Gemma S, Campiani G, Butini S, *et al*. Design and synthesis of potent antimalarial agents based on clotrimazole scaffold: Exploring an innovative pharmacophore. J Med Chem. 2007; 50:595-598.
6. Hay SI, Guerra CA, Tatem AJ, Noor AM, Snow RW. The global distribution and population at risk of malaria: Past, present and future. Lancet Infect Dis. 2004; 4:327-336.
7. Bozdech Z, Llinás M, Pulliam BL, Wong ED, Zhu J, DeRisi JL. The transcriptome of the intraerythrocytic developmental cycle of *Plasmodium falciparum*. PLoS Biol. 2003; 1:E5.
8. Patarroyo ME, Patarroyo MA. Emerging rules for subunit-based multiantigenic multistage chemically synthesized vaccines. Acc Chem Res. 2008; 41:377-386.
9. Le Roch KG, Zhou Y, Blair PL, Grainger M, Moch JK, Haynes JD, De La Vega P, Holder AA, Batalov S, Carucci DJ, Winzeler EA. Discovery of gene function by expression profiling of the malaria parasite life cycle. Science. 2003; 301:1503-1508.
10. Garcia JE, Puentes A, Patarroyo ME. Developmental biology of sporozoite-host interactions in *Plasmodium falciparum* malaria: Implications for vaccine design. Clin Microbiol Rev. 2006; 4:686-707.
11. *www.malariavaccine.org/files/Backgrounder2.pdf* (accessed April 1, 2010).
12. Chaudhuri R, Ahmed S, Ansari FA, Singh HV, Ramachandran S. MalVac: Database of malarial vaccine candidates. Malar J. 2008; 7:184.
13. Sauerwein RW. Clinical malaria vaccine development. Immunol Lett. 2009; 122:115-117.
14. Haldar K, Murphy SC, Milner DA, Taylor TE. Malaria: Mechanisms of erythrocytic infection and pathological correlates of severe disease. Annu Rev Pathol. 2007; 2:217-249.
15. Targett GA, Greenwood BM. Malaria vaccines and their potential role in the elimination of malaria. Malar J. 2008; 7 (Suppl 1):S10.
16. Hviid L. Naturally acquired immunity to *Plasmodium falciparum* malaria in Africa. Acta Trop. 2005; 95:270-275.
17. Mackintosh CL, Christodoulou Z, Mwangi TW, Kortok M, Pinches R, Williams TN, Marsh K, Newbold CI. Acquisition of naturally occurring antibody responses to recombinant protein domains of *Plasmodium falciparum* erythrocyte membrane protein 1. Malar J. 2008; 7:155.
18. Ménard R. Medicine: Knockout malaria vaccine? Nature. 2005; 433:113-114.
19. Stevenson MM, Riley EM. Innate immunity to malaria. Nat Rev Immunol. 2004; 4:169-180.
20. Druilhe P, Barnwell JW. Pre-erythrocytic stage malaria vaccines: Time for a change in path. Curr Opin Microbiol. 2007; 10:371-378.
21. Stoute JA, Slaoui M, Heppner DG, Momin P, Kester KE, Desmons P, Wellde BT, Garçon N, Krzych U, Marchand M. A preliminary evaluation of a recombinant circumsporozoite protein vaccine against *Plasmodium falciparum* malaria. RTS,S malaria vaccine evaluation group. N Engl J Med. 1997; 336:86-91.

22. Graves P, Gelband H. Vaccines for preventing malaria (pre-erythrocytic). Cochrane Database Syst Rev. 2006; 18:CD006198.
23. Hill AV. Pre-erythrocytic malaria vaccines: Towards greater efficacy. Nat Rev Immunol. 2006; 6:21-32.
24. Zavala F, Cochrane AH, Nardin EH, Nussenzweig RS, Nussenzweig V. Circumsporozoite proteins of malaria parasites contain a single immunodominant region with two or more identical epitopes. J Exp Med. 1983; 157:1947-1957.
25. Kumar KA, Sano G, Boscardin S, Nussenzweig RS, Nussenzweig MC, Zavala F, Nussenzweig V. The circumsporozoite protein is an immunodominant protective antigen in irradiated sporozoites. Nature. 2006; 444:937-940.
26. Bermúdez A, Vanegas M, Patarroyo ME. Structural and immunological analysis of circumsporozoite protein peptides: A further step in the identification of potential components of a minimal subunit-based chemically synthesised antimalarial vaccine. Vaccine. 2008; 26:6908-6918.
27. Bongfen SE, Ntsama PM, Offner S, Smith T, Felger I, Tanner M, Alonso P, Nebie I, Romero JF, Silvie O, Torgler R, Corradin G. The N-terminal domain of *Plasmodium falciparum* circumsporozoite protein represents a target of protective immunity. Vaccine. 2009; 27:328-335.
28. Zavala F, Tam JP, Hollingdale MR, Cochrane AH, Quakyi I, Nussenzweig RS, Nussenzweig V. Rationale for development of a synthetic vaccine against *Plasmodium falciparum* malaria. Science. 1985; 228:1436-1440.
29. Ballou WR, Hoffman SL, Sherwood JA, *et al*. Safety and efficacy of a recombinant DNA *Plasmodium falciparum* sporozoite vaccine. Lancet. 1987; 1:1277-1281.
30. Herrington DA, Clyde DF, Losonsky G, Cortesia M, Murphy JR, Davis J, Baqar S, Felix AM, Heimer EP, Gillessen D, Nardin E, Nussenzweig RS, Nussenzweig V, Hollingdale MR, Levine MM. Safety and immunogenicity in man of a synthetic peptide malaria vaccine against *Plasmodium falciparum* sporozoites. Nature. 1987; 328:257-259.
31. Sun P, Schwenk R, White K, Stoute JA, Cohen J, Ballou WR, Voss G, Kester KE, Heppner DG, Krzych U. Protective immunity induced with malaria vaccine RTS, S, is linked to *Plasmodium falciparum* circumsporozoite protein-specific CD4+ and CD8+ T cells producing IFN-gamma. J Immunol. 2003; 171:6961-6967.
32. Dunachie SJ, Walther M, Vuola JM, *et al*. A clinical trial of prime-boost immunisation with the candidate malaria vaccines RTS, S/AS02A and MVA-CS. Vaccine. 2006; 24:2850-2859.
33. Bojang KA, Milligan PJ, Pinder M, *et al.* Efficacy of RTS, S/AS02 malaria vaccine against *Plasmodium falciparum* infection in semi-immune adult men in The Gambia: A randomised trial. Lancet. 2001; 358:1927-1934.
34. Alonso PL, Sacarlal J, Aponte JJ, *et al*. Efficacy of the RTS, S/AS02A vaccine against *Plasmodium falciparum* infection and disease in young African children: Randomised controlled trial. Lancet. 2004; 364:1411-1420.
35. Aponte JJ, Aide P, Renom M, *et al*. Safety of the RTS, S/AS02D candidate malaria vaccine in infants living in a highly endemic area of Mozambique: A double blind randomised controlled phase I/IIb trial. Lancet. 2007; 370:1543-1551.
36. Abdulla S, Oberholzer R, Juma O, *et al*. Safety and immunogenicity of RTS, S/AS02D malaria vaccine in infants. N Engl J Med. 2008; 359:2533-2544.
37. Bejon P, Lusingu J, Olotu A, *et al*. Efficacy of RTS, S/AS01E vaccine against malaria in children 5 to 17 months of age. N Engl J Med. 2008; 359:2521-2532.
38. *www.malariavaccine.org/files/05272009_Phase_3_Fact_Sheet_FINAL.pdf* (accessed April 1, 2010).
39. Bejon P, Mwacharo J, Kai OK, Todryk S, Keating S, Lang T, Sarah C, Gilbert SC, Peshu N, Marsh K, Hill AV. Immunogenicity of the candidate malaria vaccines FP9 and modified vaccinia virus Ankara encoding the pre-erythrocytic antigen ME-TRAP in 1-6 year old children in a malaria endemic area. Vaccine. 2006; 24:4709-4715.
40. Bejon P, Mwacharo J, Kai O, *et al*. A phase 2b randomised trial of the candidate malaria vaccines FP9 ME-TRAP and MVA ME-TRAP among children in Kenya. PLoS Clin Trials. 2006; 1:e29.
41. Oliveira GA, Wetzel K, Calvo-Calle JM, Nussenzweig R, Schmidt A, Birkett A, Dubovsky F, Tierney E, Gleiter CH, Boehmer G, Luty AJ, Ramharter M, Thornton GB, Kremsner PG, Nardin EH. Safety and enhanced immunogenicity of a hepatitis B core particle *Plasmodium falciparum* malaria vaccine formulated in adjuvant Montanide ISA 720 in a phase I trial. Infect Immun. 2005; 73:3587-3597.
42. Langermans JA, Schmidt A, Vervenne RA, Birkett AJ, Calvo-Calle JM, Hensmann M, Thornton GB, Dubovsky F, Weiler H, Nardin E, Thomas AW. Effect of adjuvant on reactogenicity and long-term immunogenicity of the malaria Vaccine ICC-1132 in macaques. Vaccine. 2005; 23:4935-4943.
43. Gregson AL, Oliveira G, Othoro C, Calvo-Calle JM, Thorton GB, Nardin E, Edelman R. Phase I trial of an alhydrogel adjuvanted hepatitis B core virus-like particle containing epitopes of *Plasmodium falciparum* circumsporozoite protein. PLoS One. 2008; 3:e1556.
44. Romero P, Maryanski JL, Corradin G, Nussenzweig RS, Nussenzweig V, Zavala F. Cloned cytotoxic T cells recognize an epitope in the circumsporozoite protein and protect against malaria. Nature. 1989; 341:323-326.
45. Aidoo M, Lalvani A, Gilbert SC, Hu JT, Daubersies P, Hurt N, Whittle HC, Druihle P, Hill AV. Cytotoxic T-lymphocyte epitopes for HLA-B53 and other HLA types in the malaria vaccine candidate liver-stage antigen 3. Infect Immun. 2000; 68:227-232.
46. Guerin-Marchand C, Druilhe P, Galey B, Londono A, Patarapotikul J, Beaudoin RL, Dubeaux C, Tartar A, Mercereau-Puijalon O, Langsley G. A liver-stage-specific antigen of *Plasmodium falciparum* characterized by gene cloning. Nature. 1987; 329:164-167.
47. Joshi SK, Bharadwaj A, Chatterjee S, Chauhan VS. Analysis of immune response against T- and B-cell epitopes from *Plasmodium falciparum* liver-stage antigen 1 in rodent malaria models and malaria exposed human subject in India. Infect Immun. 2000; 68:141-150.
48. Taylor Robinson AW, Heal KG. Candidacy of liver stage antigen-1 for *Plasmodium falciparum* vaccine development. J Protozool Res. 2001; 14:1-18.
49. Hillier CJ, Ware LA, Barbosa A, Angov E, Lyon JA, Heppner DG, Lanar DE. Process development and analysis of liver-stage antigen 1, a preerythrocyte-stage protein-based vaccine for *Plasmodium falciparum*. Infect

Immun. 2005; 73:2109-2115.
50. Perlaza BL, Sauzet JP, Balde AT, Brahimi K, Tall A, Corradin G, Druilhe P. Long synthetic peptides encompassing the *Plasmodium falciparum* LSA3 are the target of human B and T cells and are potent inducers of B helper, T helper and cytolytic T cell responses in mice. Eur J Immunol. 2001; 31:2200-2209.
51. Webster D, Hill AV. Progress with new malaria vaccines. Bull World Health Organ. 2003; 81:902-909.
52. Brando C, Ware LA, Freyberger H, Kathcart A, Barbosa A, Cayphas S, Demoitie MA, Mettens P, Heppner DG, Lanar DE. Murine immune responses to liver-stage antigen 1 protein FMP011, a malaria vaccine candidate, delivered with adjuvant AS01B or AS02A. Infect Immun. 2007; 75:838-845.
53. Trager W, Jensen JB. Human malaria parasites in continuous culture. Science. 1976; 193:673-675.
54. Siddiqui WA, Tam LQ, Kramer KJ, Hui GS, Case SE, Yamaga KM, Chang SP, Chan EB, Kan SC. Merozoite surface coat precursor protein completely protects *Aotus* monkeys against *Plasmodium falciparum* malaria. Proc Natl Acad Sci U S A. 1987; 84:3014-3018.
55. Sagara I, Dicko A, Ellis RD, *et al*. A randomized controlled phase 2 trial of the blood stage AMA1-C1/Alhydrogel malaria vaccine in children in Mali. Vaccine. 2009; 27:3090-3098.
56. Holder AA, Guevara Patiño JA, Uthaipibull C, Syed SE, Ling IT, Scott-Finnigan T, Blackman MJ. Merozoite surface protein 1, immune evasion, and vaccines against asexual blood stage malaria. Parassitologia. 1999; 41:409-414.
57. Druilhe P, Spertini F, Soesoe D, Corradin G, Mejia P, Singh S, Audran R, Bouzidi A, Oeuvray C, Roussilhon C. A malaria vaccine that elicits in humans antibodies able to kill *Plasmodium falciparum*. PLoS Med. 2005; 2: e344.
58. McColl DJ, Silva A, Foley M, Kun JF, Favaloro JM, Thompson JK, Marshall VM, Coppel RL, Kemp DJ, Anders RF. Molecular variation in a novel polymorphic antigen associated with *Plasmodium falciparum* merozoites. Mol Biochem Parasitol. 1994; 68:53-67.
59. McColl DJ, Anders RF. Conservation of structural motifs and antigenic diversity in the *Plasmodium falciparum* merozoite surface protein-3 (MSP-3). Mol Biochem Parasitol. 1997; 90:21-31.
60. Haldar K, Ferguson MA, Cross GA. Acylation of a *Plasmodium falciparum* merozoite surface antigen *via sn*-1,2-diacyl glycerol. J Biol Chem. 1985; 260:4969-4974.
61. Oeuvray C, Bouharoun-Tayoun H, Gras-Masse H, Bottius E, Kaidoh T, Aikawa M, Filgueira MC, Tartar A, Druilhe P. Merozoite surface protein-3: A malaria protein inducing antibodies that promote *Plasmodium falciparum* killing by cooperation with blood monocytes. Blood. 1994; 84:1594-1602.
62. Oeuvray C, Bouharoun-Tayoun H, Grass-Masse H, Lepers JP, Ralamboranto L, Tartar A, Druilhe P. A novel merozoite surface antigen of *Plasmodium falciparum* (MSP-3) identified by cellular-antibody cooperative mechanism antigenicity and biological activity of antibodies. Mem Inst Oswaldo Cruz. 1994; 89:77-80.
63. Blackman MJ, Heidrich HG, Donachie S, McBride JS, Holder AA. A single fragment of a malaria merozoite surface protein remains on the parasite during red cell invasion and is the target of invasion-inhibiting antibodies. J Exp Med. 1990; 172:379-382.
64. Morgan WD, Birdsall B, Frenkiel TA, Gradwell MG, Burghaus PA, Syed SE, Uthaipibull C, Holder AA, Feeney J. Solution structure of an EGF module pair from the *Plasmodium falciparum* merozoite surface protein 1. J Mol Biol. 1999; 289:113-122.
65. Uthaipibull C, Aufiero B, Syed SE, Hansen B, Guevara Patiño JA, Angov E, Ling IT, Fegeding K, Morgan WD, Ockenhouse C, Birdsall B, Feeney J, Lyon JA, Holder AA. Inhibitory and blocking monoclonal antibody epitopes on merozoite surface protein 1 of the malaria parasite *Plasmodium falciparum*. J Mol Biol. 2001; 307:1381-1394.
66. O'Donnell RA, de Koning-Ward TF, Burt RA, Bockarie M, Reeder JC, Cowman AF, Crabb BS. Antibodies against merozoite surface protein (MSP)-1(19) are a major component of the invasion-inhibitory response in individuals immune to malaria. J Exp Med. 2001; 193:1403-1412.
67. Darko CA, Angov E, Collins WE, Bergmann-Leitner ES, Girouard AS, Hitt SL, McBride JS, Diggs CL, Holder AA, Long CA, Barnwell JW, Lyon JA. The clinical-grade 42-kilodalton fragment of merozoite surface protein 1 of *Plasmodium falciparum* strain FVO expressed in *Escherichia coli* protects *Aotus nancymai* against challenge with homologous erythrocytic-stage parasites. Infect Immun. 2005; 73:287-297.
68. Carvalho LJ, Daniel-Ribeiro CT, Goto H. Malaria vaccine: Candidate antigens, mechanisms, constraints and prospects. Scand J Immunol. 2002; 56:327-343.
69. Chesne-Seck ML, Pizarro JC, Vulliez-Le Normand B, Collins CR, Blackman MJ, Faber BW, Remarque EJ, Kocken CH, Thomas AW, Bentley GA. Structural comparison of apical membrane antigen 1 orthologues and paralogues in apicomplexan parasites. Mol Biochem Parasitol. 2005; 144:55-67.
70. Bannister LH, Hopkins JM, Dluzewski AR, Margos G, Williams IT, Blackman MJ, Kocken CH, Thomas AW, Mitchell GH. *Plasmodium falciparum* apical membrane antigen 1 (PfAMA-1) is translocated within micronemes along subpellicular microtubules during merozoite development. J Cell Sci. 2003; 116:3825-3834.
71. Nair M, Hinds MG, Coley AM, Hodder AN, Foley M, Anders RF, Norton RS. Structure of domain III of the blood-stage malaria vaccine candidate. *Plasmodium falciparum* apical membrane antigen 1 (AMA1). J Mol Biol. 2002; 322:741-753.
72. Hodder AN, Crewther PE, Matthew ML, Reid GE, Moritz RL, Simpson RJ, Anders RF. The disulfide bond structure of *Plasmodium* apical membrane antigen-1. J Biol Chem. 1996; 271:29446-29452.
73. Dicko A, Diemert DJ, Sagara I, *et al*. Impact of a *Plasmodium falciparum* AMA1 vaccine on antibody responses in adult Malians. PLoS One. 2007; 2:e1045.
74. Anders RF, McColl DJ, Coppel RL. Molecular variation in *Plasmodium falciparum*: Polymorphic antigens of asexual erythrocytic stages. Acta Trop. 1993; 53:239-253.
75. Escalante AA, Lal AA, Ayala FJ. Genetic polymorphism and natural selection in the malaria parasite *Plasmodium falciparum*. Genetics. 1998; 149:189-202.
76. Marshall VM, Zhang L, Anders RF, Coppel RL. Diversity of the vaccine candidate AMA-1 of *Plasmodium falciparum*. Mol Biochem Parasitol. 1996; 77:109-113.

77. Cooper CL, Davis HL, Morris ML, Efler SM, Adhami MA, Krieg AM, Cameron DW, Heathcote J. CPG 7909, an immunostimulatory TLR9 agonist oligodeoxynucleotide, as adjuvant to Engerix-B HBV vaccine in healthy adults: A double-blind phase I/II study. J Clin Immunol. 2004; 24:693-701.
78. Mullen GE, Giersing BK, Ajose-Popoola O, Davis HL, Kothe C, Zhou H, Aebig J, Dobrescu G, Saul A, Long CA. Enhancement of functional antibody responses to AMA1-C1/Alhydrogel, a *Plasmodium falciparum* malaria vaccine, with CpG oligodeoxynucleotide. Vaccine. 2006; 24:2497-2505.
79. Mullen GE, Ellis RD, Miura K, Malkin E, Nolan C, Hay M, Fay MP, Saul A, Zhu D, Rausch K, Moretz S, Zhou H, Long CA, Miller LH, Treanor J. Phase 1 trial of AMA1-C1/Alhydrogel plus CPG 7909: An asexual blood-stage vaccine for *Plasmodium falciparum* malaria. PLoS One. 2008; 3:e2940.
80. Gilberger TW, Thompson JK, Reed MB, Good RT, Cowman AF. The cytoplasmic domain of the *Plasmodium falciparum* ligand EBA-175 is essential for invasion but not protein trafficking. J Cell Biol. 2003; 162:317-327.
81. Tolia NH, Enemark EJ, Sim BK, Joshua-Tor L. Structural basis for the EBA-175 erythrocyte invasion pathway of the malaria parasite *Plasmodium falciparum*. Cell. 2005; 122:183-193.
82. Pattnaik P, Shakri AR, Singh S, Goel S, Mukherjee P, Chitnis CE. Immunogenicity of a recombinant malaria vaccine based on receptor binding domain of *Plasmodium falciparum* EBA-175. Vaccine. 2007; 25:806-813.
83. Camus D, Hadley TJ. A *Plasmodium falciparum* antigen that binds to host erythrocytes and merozoites. Science. 1985; 230:553-556.
84. Sim BK, Chitnis CE, Wasniowska K, Hadley TJ, Miller LH. Receptor and ligand domains for invasion of erythrocytes by *Plasmodium falciparum*. Science. 1994; 264:1941-1944.
85. Adams JH, Sim BK, Dolan SA, Fang X, Kaslow DC, Miller LH. A family of erythrocyte binding proteins of malaria parasites. Proc Natl Acad Sci U S A. 1992; 89:7085-7089.
86. Narum DL, Haynes JD, Fuhrmann S, Moch K, Liang H, Hoffman SL, Sim BK. Antibodies against the *Plasmodium falciparum* receptor binding domain of EBA-175 block invasion pathways that do not involve sialic acids. Infect Immun. 2000; 68:1964-1966.
87. Piper KP, Roberts DJ, Day KP. *Plasmodium falciparum*: Analysis of the antibody specificity to the surface of the trophozoite-infected erythrocyte. Exp Parasitol. 1999; 91:161-169.
88. van Schravendijk MR, Rock EP, Marsh K, Ito Y, Aikawa M, Neequaye J, Ofori-Adjei D, Rodriguez R, Patarroyo ME, Howard RJ. Characterization and localization of *Plasmodium falciparum* surface antigens on infected erythrocytes from West African patients. Blood. 1991; 78:226-236.
89. Kaul DK, Roth EF Jr, Nagel RL, Howard RJ, Handunnetti SM. Rosetting of *Plasmodium falciparum*-infected red blood cells with uninfected red blood cells enhances microvascular obstruction under flow conditions. Blood. 1991; 78:812-819.
90. Mac Pherson GG, Warrell MJ, White NJ, Looareesuwan S, Warrell DA. Human cerebral malaria. A quantitative ultrastructural analysis of parasitized erythrocyte sequestration. Am J Pathol. 1985; 119:385-401.
91. Maier AG, Cooke BM, Cowman AF, Tilley L. Malaria parasite proteins that remodel the host erythrocyte. Nat Rev Microbiol. 2009; 7:341-354.
92. Smith JD, Gamain B, Baruch DI, Kyes S. Decoding the language of *var* genes and *Plasmodium falciparum* sequestration. Trends Parasitol. 2001; 17:538-545.
93. Howell DP, Samudrala R, Smith JD. Disguising itself-insights into *Plasmodium falciparum* binding and immune evasion from the DBL crystal structure. Mol Biochem Parasitol. 2006; 148:1-9.
94. Su XZ, Heatwole VM, Wertheimer SP, Guinet F, Herrfeldt JA, Peterson DS, Ravetch JA, Wellems TE. The large diverse gene family *var* encodes proteins involved in cytoadherence and antigenic variation of *Plasmodium falciparum*-infected erythrocytes. Cell. 1995; 82:89-100.
95. Baruch DI, Pasloske BL, Singh HB, Bi X, Ma XC, Feldman M, Taraschi TF, Howard RJ. Cloning the *P. falciparum* gene endcoding PfEMP1, a malarial variant antigen and adherence receptor on the surface of parasitized human erythrocytes. Cell. 1995; 82:77-87.
96. Kyes S, Horrocks P, Newbold C. Antigenic variation at the infected red cell surface in malaria. Ann Rev Microbiol. 2001; 55:673-707.
97. Vogt AM, Barragan A, Chen Q, Kironde F, Spillmann D, Wahlgren M. Heparan sulfate on endothelial cells mediates the binding of *Plasmodium falciparum*-infected erythrocytes *via* the DBL1alpha domain of PfEMP1. Blood. 2003; 101:2405-2411.
98. Pan W, Huang D, Zhang Q, Qu L, Zhang D, Zhang X, Xue X, Qian F. Fusion of two malaria vaccine candidate antigens enhances product yield, immunogenicity, and antibody-mediated inhibition of parasite growth *in vitro*. J Immunol. 2004; 172:6167-6174.
99. Langermans JA, Hensmann M, van Gijlswiik M, Zhang D, Pan W, Giersing BK, Locke E, Dubovsk F, Wittes J, Thomas AW. Preclinical evaluation of a chimeric malaria vaccine candidate in Montanide ISA 720: Immunogenicity and safety in *rhesus macaques*. Hum Vaccin. 2006; 2:222-226.
100. Malkin E, Hu J, Li Z, *et al*. A phase 1 trial of PfCP2.9: An AMA1/MSP1 chimeric recombinant protein vaccine for *Plasmodium falciparum* malaria. Vaccine. 2008; 26:6864-6873.
101. Hu J, Chen Z, Gu J, Wan M, *et al*. Safety and immunogenicity of a malaria vaccine, *Plasmodium falciparum* AMA-1/MSP-1 chimeric protein formulated in montanide ISA 720 in healthy adults. PLoS One. 2008; 3:e1952.
102. Theisen M, Soe S, Brunstedt K, Follmann F, Bredmose L, Israelsen H, Madsen SM, Druilhe P. A *Plasmodium falciparum* GLURP-MSP3 chimeric protein; expression in *Lactococcus lactis*, immunogenicity and induction of biologically active antibodies. Vaccine. 2004; 22:1188-1198.
103. Carvalho LJ, Alves FA, Bianco C Jr, Oliveira SG, Zanini GM, Soe S, Druilhe P, Theisen M, Muniz JA, Daniel-Ribeiro CT. Immunization of *Saimiri sciureus* monkeys with a recombinant hybrid protein derived from the *Plasmodium falciparum* antigen glutamate-rich protein and merozoite surface protein 3 can induce partial protection with Freund and Montanide ISA720 adjuvants. Clin Diagn Lab Immunol. 2005; 12:242-248.

104. Rener J, Graves PM, Carter R, Williams JL, Burkot TR. Target antigens of transmission-blocking immunity on gametes of *Plasmodium falciparum*. J Exp Med. 1983; 158:976-981.
105. Riley EM, Williamson KC, Greenwood BM, Kaslow DC. Human immune recognition of recombinant proteins representing discrete domains of the *Plasmodium falciparum* gamete surface protein, Pfs230. Parasite Immunol. 1995; 17:11-19.
106. Gwadz RW. Successful immunization against the sexual stages of *Plasmodium gallinaceum*. Science. 1976; 193:1150-1151.
107. Carter R, Chen DH. Malaria transmission blocked by immunisation with gametes of the malaria parasite. Nature. 1976; 263:57-60.
108. Coban C, Ishii KJ, Gursel M, Klinman DM, Kumar N. Effect of plasmid backbone modification by different human CpG motifs on the immunogenicity of DNA vaccine vectors. J Leukoc Biol. 2005; 78:647-655.
109. Haddad D, Maciel J, Kumar N. Infection with *Plasmodium berghei* boosts antibody responses primed by a DNA vaccine encoding gametocyte antigen Pbs48/45. Infect Immun. 2006; 74:2043-2051.
110. Wu Y, Ellis RD, Shaffer D, *et al*. Phase 1 trial of malaria transmission blocking vaccine candidates Pfs25 and Pvs25 formulated with montanide ISA 51. PLoS One. 2008; 3:e2636.
111. Thompson FM, Porter DW, Okitsu SL, *et al*. Evidence of blood stage efficacy with a virosomal malaria vaccine in a phase IIa clinical trial. PLoS One. 2008; 3:e1493.
112. Tine JA, Lanar DE, Smith DM, *et al*. NYVAC-Pf7: A poxvirus-vectored, multiantigen, multistage vaccine candidate for *Plasmodium falciparum* malaria. Infect Immun. 1996; 64:3833-3844.
113. Schofield L, Villaquiran J, Ferreira A, Schellekens H, Nussenzweig R, Nussenzweig V. Gamma-interferon, CD8+ T cells and antibodies required for immunity to malaria sporozoites. Nature. 1987; 330:664-666.
114. Weiss WR, Sedegah M, Beaudoin RL, Miller LH, Good MF. CD8+ T cells (cytotoxic/suppressors) are required for protection in mice immunized with malaria sporozoites. Proc Natl Acad Sci U S A. 1988; 85:573-576.
115. Robinson HL, Amara RR. T cell vaccines for microbial infections. Nat Med. 2005; 11 (Suppl 4):S25-S32.
116. Bolton DL, Roederer M. Flow cytometry and the future of vaccine development. Expert Rev Vaccines. 2009; 8:779-789.
117. Reyes-Sandoval A, Pearson FE, Todryk S, Ewer K. Potency assays for novel T-cell-inducing vaccines against malaria. Curr Opin Mol Ther. 2009; 11:72-80.
118. Berthoud TK, Dunachie SJ, Todryk S, Hill AV, Fletcher HA. MIG (CXCL9) is a more sensitive measure than IFN-gamma of vaccine induced T-cell responses in volunteers receiving investigated malaria vaccines. J Immunol Methods. 2009; 340:33-41.
119. Tyagi RK, Sharma PK, Vyas SP, Mehta A. Various carrier system(s)-mediated genetic vaccination strategies against malaria. Expert Rev Vaccines. 2008; 7:499-520.
120. Müller HM, Reckmann I, Hollingdale MR, Bujard H, Robson KJ, Crisanti A. Thrombospondin related anonymous protein (TRAP) of *Plasmodium falciparum* binds specifically to sulfated glycoconjugates and to HepG2 hepatoma cells suggesting a role for this molecule in sporozoite invasion of hepatocytes. EMBO J. 1993; 12:2881-2889.
121. Sinnis P, Sim BK. Cell invasion by the vertebrate stages of *Plasmodium*. Trends Microbiol. 1997; 5:52-58.
122. Templeton TJ, Kaslow DC. Cloning and cross-species comparison of the thrombospondin-related anonymous protein (TRAP) gene from *Plasmodium knowlesi*, *Plasmodium vivax* and *Plasmodium gallinaceum*. Mol Biochem Parasitol. 1997; 84:13-24.
123. Robson KJ, Hall JR, Jennings MW, Harris TJ, Marsh K, Newbold CI, Tate VE, Weatherall DJ. A highly conserved amino-acid sequence in thrombospondin, properdin and in proteins from sporozoites and blood stages of a human malaria parasite. Nature. 1988; 355:79-82.
124. Lawler J, Hynes RO. The structure of human thrombospondin, an adhesive glycoprotein with multiple calcium-binding sites and homologies with several different proteins. J Cell Biol. 1986; 103:1635-1648.
125. Cowan G, Krishna S, Crisanti A, Robson K. Expression of thrombospondin-related anonymous protein in *Plasmodium falciparum* sporozoites. Lancet. 1992; 339:1412-1413.
126. Rogers WO, Malik A, Mellouk S, Nakamura K, Rogers MD, Szarfman A, Gordon DM, Nussler AK, Aikawa M, Hoffman SL. Characterization of *Plasmodium falciparum* sporozoite surface protein 2. Proc Natl Acad Sci U S A. 1992; 89:9176-9180.
127. Robson KJ, Frevert U, Reckmann I, Cowan G, Beier J, Scragg IG, Takehara K, Bishop DH, Pradel G, Sinden R, Saccheo S, Müller HM, Crisanti A. Thrombospondin-related adhesive protein (TRAP) of *Plasmodium falciparum*: Expression during sporozoite ontogeny and binding to hepatocytes. EMBO J. 1995; 14:3883-3894.
128. Castellanos A, Arevalo-Herrera M, Restrepo N, Gulloso L, Corradin G, Herrera S. *Plasmodium vivax* thrombospondin related adhesion protein: Immunogenicity and protective efficacy in rodents and *Aotus* monkeys. Mem Inst Oswaldo Cruz. 2007; 102:411-416.
129. Dhanawat M, Shrivastava SK. Solid-phase synthesis of oligosaccharide drugs: A review. Mini Rev Med Chem. 2009; 9:169-185.
130. Liu X, Kwon YU, Seeberger PH. Convergent synthesis of a fully lipidated glycosylphosphatidylinositol anchor of *Plasmodium falciparum*. J Am Chem Soc. 2005; 127:5004-5005.
131. Schofield L, Hewitt MC, Evans K, Siomos MA, Seeberger PH. Synthetic GPI as a candidate anti-toxic vaccine in a model of malaria. Nature. 2002; 418:785-789.
132. Hewitt MC, Snyder DA, Seeberger PH. Rapid synthesis of a glycosylphosphatidylinositol-based malaria vaccine using automated solid-phase oligosaccharide synthesis. J Am Chem Soc. 2002; 124:13434-13436.

(Received April 21, 2010; Revised June 9, 2010; Accepted July 8, 2010)

Review

Fruit and vegetable peels: Paving the way towards the development of new generation therapeutics

Hamendra S. Parmar[1,*], Yamini Dixit[2], Anand Kar[2]

[1] *School of Biotechnology, Devi Ahilya University, Takshashila Campus, Indore, India;*
[2] *Thyroid Research Unit, School of Life Sciences, Devi Ahilya University, Takshashila Campus, Indore, India.*

ABSTRACT: Cardiovascular diseases (CVDs), diabetes mellitus (DM), cancer, and thyroid abnormalities are major health problems prevalent around the world and are responsible for a large portion of morbidity and mortality out of health problems overall. Advances in genomics and proteomics in recent years have led to an explosion in the number of possible therapeutic targets and drug candidates through use of molecular approaches, chemical synthesis, traditional medicinal chemistry, and phyto-chemistry and through the exploration of novel herbal preparations. However, virtually none of these candidates are devoid of potential adverse drug reaction(s) or undesirable side effects. Therefore, the clear need is to look to alternative ways to develop novel drug candidates with fewer side effects and less cost. Interestingly, the last few years have seen an increase in the number of available reports on fruits and vegetable peels, and particularly on their biological activity, their content of different bioactive compounds, their chemical characterization, understanding of their structure-activity relationships, isolation and purification of commercially important chemicals without using high throughput techniques, *etc.* Therefore, research in the field of fruit and vegetable peels should present immense possibilities for drug discovery and development of cost-effective therapies that have fewer or practically no side effects. This virtual explosion of interest in fruit and vegetable peels as a source of medicinal and nutritional value has led to the present review.

Keywords: Cardiovascular problems, cancer, diabetes mellitus, thyroid problems, peels

**Address correspondence to:*
Dr. Hamendra Singh Parmar, School of Biotechnology, Devi Ahilya University, Takshashila Campus, Khandwa Road, Indore 452001, M.P., India.
e-mail: hamendrasingh999@yahoo.co.in

1. Introduction

Cardiovascular diseases including coronary heart disease (heart attacks), cerebrovascular disease, raised blood pressure (hypertension), peripheral artery disease, rheumatic heart disease, congenital heart disease and heart failure, diabetes mellitus (both types 1 and 2), thyroid abnormalities (broadly hypo- and hyper-thyroidism), and cancer are among the most prevalent diseases around the world and are responsible for a large portion of morbidity and mortality out of health problems overall (*1-9*).

A vast body of literature is available on the possible therapeutic targets for those diseases, although many substances are either in clinical trials or used in practice (*10-37*). However, they have some major drawbacks including their high cost and adverse effects like cardiovascular events, cancer, aging, cardiac and renal toxicity, and increased oxidative stress (*38-51*). Oxidative stress is itself known to be a root cause for the progression and development of the diseases mentioned (*6*), and modern medicines should be designed in a way to maintain a healthy homeostasis between oxidants and antioxidants. As most herbal preparations are antioxidative in nature, they improve health directly by reducing oxidative stress (*6,52,53*). In fact, many herbal extracts are known to be antiperoxidative, anti-cancer, cardio-protective, anti-diabetic, and thyro-regulatory in nature (*3,4,54-58*). However, the identification of the plant(s) and its availability, precise chemical composition, dose, potential use for ailment(s), precise mechanism of action, unpredictable toxicity, and cost are major concerns that hinder the use of herbal preparations (*59*). That said, fruit and vegetable peels have advantages over other herbal extracts, as they are easily identifiable, commonly used by people, rich in various bioactive compounds, and some of their compounds have been characterized in terms of their chemical structures and biological properties through use of structure-activity relationships (SAR). Additionally, peels are usually considered waste, so they are obviously cost-effective (*60-64*).

Therefore, the present review has attempted to

assess the emerging potential of fruit and vegetable peels for use in developing new generation therapeutics.

2. Anti-peroxidative or radical-scavenging properties

Free radical production in any organism can either be accidental or deliberate. Free radicals have increasingly been accepted as commonplace and important biochemical intermediates, leading to these compounds being implicated in a large number of human diseases including cardiovascular problems, diabetes mellitus, cancer, thyroid disorders, and Alzheimer's disease (*6*).

Various fruit and vegetable peel extracts or compounds are known to be antiperoxidative in nature and their different *in vitro* or *in vivo* mechanism(s) have also been reported (Table 1). The antiperoxidative or radical-scavenging potential of the peel extracts from *C. sinensis*, *P. granatum*, *M. paradisiaca*, *C. vulgaris*, *C. melo*, and *M. indica* is well documented in both *in vivo* and *in vitro* models (*52,53,63-67*). In fact, the current authors have demonstrated that these peel extracts work mainly through the direct radical scavenging of various types of radicals in a dose-specific manner (*64*). Possible mechanism(s) of their antiperoxidative potential might be mediated *via* the presence of a variety of polyphenols and flavonoids in different concentrations. Specifically, *C. sinensis* was found to be an efficient scavenger for DPPH, singlet oxygen, and various peroxyradicals. *P. granatum* and *M. paradisiaca* were also found to be effective against all the aforementioned radicals and nitric oxide (NO) radicals as well, while *M. indica* was found to be effective only against peroxyradicals and *C. vulgaris* and *C. melo* were similarly found to be effective only against singlet oxygen and peroxyradicals. All of the aforementioned peels also have a minor influence on enzymatic and non-enzymatic oxidative defense, which includes catalase (CAT), superoxide dismutase (SOD), and reduced glutathione (GSH), particularly in the event of disease (*53,66*). Other citrus fruit peels including *C. reticulata* and *C. paradisi* are also known to have an antiperoxidative effect (*68,69*). Similarly, extracts of *P. liguralis* peels are reported to have considerable antioxidant activity, as represented by the trolox equivalent antioxidant capacity (TEAC) value, due to the presence of various antioxidative bioactive compounds, certainly indicating the importance of this peel as an alternative source of bioactive compounds (*70*). Peach, pear, and apple peels are also reported to have antioxidative potential according to various *in vitro* methods such as total radical-trapping antioxidative potential (TRAP) values, which also correlate with their polyphenolic content. Peels of those fruits have also been found to be antiperoxidative in hypercholesterolemic diet-fed animals (*71*). Pears and apples were further characterized by beta-carotene bleaching and NO and DPPH radical-scavenging potential (*60*). Peels from Red grape marc have also been found to be a radical quencher according to a beta-carotene bleaching assay (*72*). Solanum melongena is known to contain very strong antioxidants, including nasunin, and its antioxidative potential has been demonstrated using electron spin resonance spectrometric analysis, 5,5-dimethyl-1-pyrroline-*N*-oxide (DMPO), spin trapping, hydroxyl (•OH) or superoxide anion radicals (O^{2-}) generated by a Fenton reaction, and hypoxanthine-xanthine oxidase systems (*73*). Both *S. melongena* L. and *C. annuum* L. peels are also reported to have *in vitro* antiperoxidative potential due to the presence of some other strong antioxidant compounds (*74*). *Solanum tuberosum* peel extract has also been found to have an antioxidative effect on erythrocytes and in rats with streptozotocin-induced diabetes (*75,76*). Jaffa grapefruit peels have been evaluated in DPPH and beta-carotene linoleate model systems and have been found to be radical scavengers *in vitro* (*77*). The peel extract of *L. siceraria* has also recently been reported to have antiperoxidative potential in both *in vitro* and *in vivo* studies; *in vitro* analysis demonstrated that this peel extract not only quenches DPPH radicals but also lowers hepatic lipid peroxidation values induced by CCl_4 and H_2O_2 (*62*). A parallel *in vivo* study on normal healthy and hyperthyroid mice further confirmed its antioxidative efficacy (*62*).

Table 1. Antiperoxidative potential of fruit and vegetable peels

Botanical name	English name	References
1. *Citrus sinensis*	Sweet orange	(*64-66*)
2. *Citrus reticulata*	Mandarin	(*68,149*)
3. *Citrus paradisi*	Jaffa grapefruit	(*68*)
4. *Musa paradisiaca*	Banana	(*52,64,65,94*)
5. *Citrullus vulgaris*	Watermelon	(*63,64,67*)
6. *Cucumis melo*	Melon	(*63,64,67*)
7. *Mangifera indica*	Mango	(*63,64,67,150,151*)
8. *Punica granatum*	Pomegranate	(*52,64,65,99,135*)
9. *Passiflora liguralis*	Sweet granadilla	(*153*)
10. *Legenaria siceraria*	Bottle gourd	(*62*)
11. *Solanum melongena* L.	Brinjal	(*73,74*)
12. *Solanum tuberosam*	Potato	(*75,76*)
13. *Capsicum annuum* L.	Sweet pepper	(*74*)
14. *Cydonia vulgaris*	Quince	(*154*)
15. *Pyrus malus*	Apple	(*60,71,133*)
16. *Pyrus pashia*	Pear	(*60,71*)
17. *Prunus persica*	Peaches	(*71*)

3. Cardiovascular protective effect

Many flavonoids and their glycosides present in herbal extracts are known for their cardiovascular regulatory properties (Table 2) and many are abundantly available in fruit and/or vegetable peels including rutin, isoquercetin, narirutin, narcissin, quercetin, kaempferol, luteolin, and apigenin are known to have a vasodilatory and hypotensive effect (*78-80*). Some of the flavonoids, such as quercetin and quercetin glycosides, are reported to have lipid-lowering and anti-atherosclerotic activity (*79,81-83*). In fact, hesperidin and naringin, both citrus

Table 2. Fruit and vegetable peels known for their cardiovascular effect

Botanical name	English name	References
1. *Citrus sinensis*	Sweet orange	(*52*)
2. *Citrus reticulata*	Mandarin	(*84*)
3. *Musa paradisiaca*	Banana	(*52*)
4. *Citrullus vulgaris*	Watermelon	(*65,118*)
5. *Cucumis melo*	Melon	(*65*)
6. *Mangifera indica*	Mango	(*52,115*)
7. *Punica granatum*	Pomegranate	(*52*)
8. *Citrus paradisi*	Jaffa grapefruit	(*77*)
9. *Pyrus malus*	Apple	(*60,71*)
10. *Pyrus pashia*	Pear	(*60,71*)
11. *Prunus persica*	Peaches	(*60*)

bioflavonoids also present in citrus fruit peels, exhibit biological and pharmacological properties, such as anti-inflammatory, lipid-lowering, and antioxidative behavior; all are related to cardiovascular health (*84,85*).

The mechanism(s) of the aforementioned effects may be explained by the fact that oxidative modification of low-density lipoproteins (LDL) by free radicals is an early event in the pathogenesis of atherosclerosis. The rapid uptake of oxidatively modified LDL *via* a scavenger receptor leads to the formation of foam cells. Oxidized LDL also has a number of other atherogenic properties. A number of mechanisms are likely to contribute to inhibition of LDL oxidation by flavonoids. Flavonoids may directly scavenge some radical species by acting as chain-breaking antioxidants (*86*). In addition, they may recycle other chain-breaking antioxidants such as α-tocopherol by donating a hydrogen atom to the tocopheryl radical (*87*). Transition metals such as iron and copper are important pro-oxidants, and some flavonoids can chelate divalent metal ions, hence preventing free radical formation.

A detailed *in vivo* study of *C. sinensis, P. granatum, M. paradisiaca*, *C. vulgaris*, *C. melo,* and *M. indica* peels in a diet-induced animal model of atherosclerosis revealed the anti-atherogenic potential of extracts. The study also revealed their direct benefit of maintaining cardiovascular health by positively influencing serum lipids (including total cholesterol, triglycerides, LDL-cholesterol, and VLDL-cholesterol), the atherogenic index, glucose, tissue lipid peroxidation, the serum level of creatinine kinase-MB enzyme, and histopathological alterations (*52,67*). The possible reasons for this beneficial role correlated with the presence of a variety of total flavonoids, phenolic compounds, and ascorbic acid content of the peel extracts (*66,67*). The aforementioned fruit peels are specifically known to contain various bioactive compounds that are already known for their cardiovascular or related benefits, including antiperoxidative, anti-inflammatory, and cardioprotective action. In brief, the protective effect of *C. sinensis* peels might be due to the presence of polymethoxylated flavones, *C*-glycosylated flavones, *O*-glycosylated flavones, flavonols, phenolic acids, nobiletin, hesperidin, and naringin (*88-92*). In *M. paradisiaca*, dopamine seems to be responsible as it is known to have strong antiperoxidative properties that are known to be associated with the amelioration of cardiovascular problem(s) (*6,93-97*). In *P. granatum*, some compounds are already known for their antiperoxidative and anti-inflammatory properties, including oleanolic, ursolic, and gallic acids, punicalagin, ellagitannin, ellagic acid, and catechin (*98-107*). Similarly, the anti-atherogenic activity of the peel extract of *M. indica* could be the result of the action of its rich polyphenolic content. Q 3-galactoside, Q 3-glucoside, and Q 3-arabinoside, gallic acid, and mangiferin are reported to have an antioxidative, anti-inflammatory, and cardioprotective role (*108-115*). The protective activity of *C. vulgaris* and *C. melo* peels mainly relates to their high content of citrulline, an essential amino acid that helps in nitric oxide synthesis that, in turn, enhances vasodilatation (*116-118*). Peels from Jaffa grapefruit (*C. paradisi*), pears, peaches, and apples were also evaluated for their possible cardiovascular benefits in hypercholesterolemic diet-fed animals. These peels increased plasma antioxidant capacity and improved plasma levels of different lipids. Further correlation studies revealed that the observed benefits of these peels might be mediated *via* the presence of total flavonoids, phenolics, phenolic acids, and dietary fiber at various levels of correlation (*77*).

Table 3. Anti-diabetic or gluco-regulatory potential of fruit and vegetable peels

Botanical name	English name	References
1. *Citrus sinensis*	Sweet orange	(*65-67,119*)
2. *Punica granatum*	Pomegranate	(*65,67*)
3. *Mangifera indica*	Mango	(*63*)
4. *Citrullus vulgaris*	Watermelon	(*63*)
5. *Solanum tuberosum*	Potato	(*75*)
6. *Legenaria siceraria*	Bottle gourd	(*62*)

4. Antidiabetic or gluco-regulatory potential of fruit and vegetable peels

Dietary antioxidant compounds such as bio-flavonoids may offer some protection against the early stage of diabetes mellitus and the development of complications (Table 3). Available reports describe the known mechanism(s) of bioflavonoids that are present in peels, such as hesperidin and naringin as are present in citrus fruit peels. These peels play an antidiabetic role in C57BL/KsJ-db/db mice *via* regulation of gluco-regulatory enzymes *i.e.*, they decrease the activity of glucose-6-phosphatase and phosphoenol pyruvate with a concomitant increase in the activity of hepatic glucokinase, increased hepatic glycogen content, and increased serum insulin along with a decrease in serum glucose concentrations (*80*).

C. sinensis and *P. granatum* peel extracts have also been found to be thyroid-stimulating in nature

when evaluated in normal healthy animals (*65*). Their antidiabetic potential was further confirmed by the experimentation using alloxan induced diabetes mellitus, hypercholesterolemic diet fed, and hyperthyroid animal models of study, which indentified the mechanism for the observed effects of *C. sinensis* peels and suggested that the antidiabetic potential of this peel extract might be mediated *via* antiperoxidation, α-amylase enzyme activity inhibition that is responsible for the conversion of complex carbohydrates to glucose, increased hepatic glycogen content, insulin-stimulating activity, and repair of secretory defects in β-cells (*53*). Inhibition of α-amylase enzyme activity by *Citrus sinensis* peel extract was also reported by other authors (*119*). *P. granatum* is suggested to have intrinsic antiperoxidative and hypoglycemic properties that may be attributed to some of its bioactive compounds, including oleanolic, ursolic, and gallic acids, punicalagin, ellagitannin, ellagic acid, and catechin (*98-107*). This protective effect was further correlated with the total phenolic and flavonoid compound content in the peels (*53*). However, *M. indica* and *C. vulgaris* have displayed neither any intrinsic hypoglycemic potential nor any antidiabetic potential in diabetic models (data not shown) but have been found to produce hypoglycemia in hyperlipidemia-induced diabetes (*67*). Therefore, these peel extracts may work *via* gluconeogenesis or glycogenolysis or glucose uptake in hypercholesterolemic animals. Therefore, it seems that these peels may be beneficial in obesity induced type 2 diabetic condition or in metabolic syndrome. Antidiabetic role of potato or *S. tuberosum* peels against streptozotocin induced diabetic model was also reported where, reversal in almost all the diabetic changes including serum glucose, body weight, polydipsia, polyuria, elevated activity of serum transaminases (ALT and AST) and hepatic MDA levels, and reduced glutathione (GSH) was observed (*75*). However, the plausible mechanism for this antidiabetic effect has not been completely elucidated but antiperoxidative potential was presumably a major contributing factor to the effect observed. Similarly, the peel extract of *L. siceraria* has been found to cause hypoglycemia in normal healthy and hyperthyroid mice. The hypoglycemic potential observed might be the outcome of thyroid and glucose-6-phosphatase inhibitory activity of the peel extract (*62*).

5. Thyro-regulatory potential

Some plant compounds are already known to influence the thyroid hormone homeostasis at various levels, including that of binding of TSH-receptor, thyroid-iodide transport and conversion of T_4 to T_3 (*120*). However, few reports (Table 4) have demonstrated the thyro-regulatory potential of fruit and vegetable peels (*52*,*53*,*62-67*). Peels from *C. sinensis* and *M. paradisiaca* have been found to inhibit the thyroid. Where, reduction in both the thyroid hormones was observed, in response to either of the peel extract. Therefore, it was suggested that both *C. sinensis* and *M. paradisiaca* might be inhibiting thyroid hormones not only at glandular level, but also at the level of peripheral conversion of T_4 to T_3. The antithyroidal role of *C. sinensis* might be mediated through the inhibition of thyroid peroxidase (TPO); the key enzyme in thyroid hormone biosynthesis, as it contains the phenolic compound naringin which inhibits the activity of TPO (*121-123*). Similarly, the antithyroidal role of *M. paradisiaca* might be mediated by its high dopamine content, which is already known to inhibit the thyroid as previously indicated (*94*,*124*,*125*).

The peel extracts of *M. indica*, *C. vulgaris*, and *C. Melo* were found to be thyro-stimulatory in nature. This thyroid stimulatory nature was further confirmed by a study of rats with chemically-induced hypothyroidism in which the administration of test peel extracts restored the serum levels of two thyroid hormones to normal in hypothyroid animals (*63*). These results clearly demonstrated the role the aforementioned peel extracts had in ameliorating hypothyroidism. An increased level of both thyroid hormones T_3 and T_4 demonstrated the thyroid stimulatory potential of these peel extracts on both the glandular level (the only source for T_4 synthesis) and at the level of peripheral monodeiodination of T_4, the main source of T_3.

Thus far, the mechanism for the effect(s) observed may relate to the presence of various small polyphenolic molecules that might play a major role in thyroid stimulatory activity, as they are already reported to influence thyroid hormone metabolism at genomic level. For instance, they increase the activity of the type 2 iodothyronine deiodinase gene (*126*). Secondly, other mechanisms are also possible, such as TPO stimulation, enhanced glandular functionality, and 5'-deiodinase activity, and could not be ruled out by these studies.

Table 4. Influence of fruit and vegetable peels on thyroid status

Botanical name	English name	Nature	References
1. *Citrus sinensis*	Sweet orange	Thyroid-inhibiting	(*65*,*66*)
2. *Musa paradisiaca*	Banana	Thyroid-inhibiting	(*65*)
3. *Legenaria siceraria*	Bottle gourd	Thyroid-inhibiting	(*62*)
4. *Citrullus vulgaris*	Watermelon	Thyroid-stimulating	(*63*)
5. *Cucumis melo*	Melon	Thyroid-stimulating	(*64*)
6. *Mangifera indica*	Mango	Thyroid-stimulating	(*63*)

6. Anticancer potential

Cancer is one of the most devastating diseases for which various remedies have been reported, but development of suitable therapeutics to treat this disease is still a major challenge for biomedical professionals. In the search for novel therapies and exploration of hitherto unknown compounds with anticancer potential, some reports have described herbal preparations including fruit and vegetable peels (Table 5) (*127-132*). A few important biochemical *in vitro* studies using different cancer cell lines and *in vivo* studies have revealed the potential some fruit peels have to combat variety of cancers, including cancer of the liver, colon, breast, and lung. Peels from different varieties of apples (Rome Beauty, Idared, Cortland, and Golden Delicious) are reported to have an antiproliferative effect (*130*). Golden delicious apple peels have been reported to inhibit the cell proliferation of HepG2 human liver cancer cells and MCF-7 human breast cancer cells (*133*). Some of the active principles present in these peels, such as quercetin and quercetin-3-*O*-beta-D-glucopyranoside, have been found to be responsible for the anticancer activity observed (*130*,*134*). The anticancer effect(s) observed might be mediated *via* inhibition of NF-kappa B activation (*131*). Some of the triterpenoids are also present in apple peels, including 2 alpha-hydroxyursolic acid, 2 alpha-hydroxy-3 beta-{[(2E)-3-phenyl-1-oxo-2-propenyl]oxy}olean-12-en-28-oic acid, 3 beta-trans-*p*-coumaroyloxy-2 alpha-hydroxyolean-12-en-28-oic acid, and 2 alpha-hydroxyursolic acid, and are known to possess anticancer potential *via* the inhibition of NF-kappa B activation (*134*). Similarly, peels of *Punica granatum* are also thought to have an anticancer effect in inflammation-associated cancers (*135*). Different *Citrus* varieties including *C. reticulata*, *C. unshiu*, and *C. natsudaidai* are known to prevent tumorigenesis (*136,137*). *C. reticulata* peels have displayed potent tumor-suppressing activity in SNU-C4 human colon cancer cells; the mechanism for this is believed to be *via* the up-regulation of the pro-apoptotic gene *Bax* and apoptotic gene *caspase-3* along with a concomitant decrease in the expression of the anti-apoptotic gene *bcl-2* (*138*).

The peel extract of *C. natsudaidai* has also been demonstrated to act on tumors in B-16 mouse melanoma and human lung carcinoma cells; it is theorized to contain hydrophobic antitumor compounds (*137*). In fact, 78 species of the genus *Citrus* are known to inhibit the Epstein-Barr virus early antigen (EBV-EA) activation (responsible for some cancers, including Burkitt's lymphoma) induced by 12-*O*-tetradecanoylphorbol 13-acetate (TPA); this serves as a useful screening method for anti-tumor promoters and further underscores the importance of peels in the development of potential anti-tumor therapies (*139*).

Isolated fractions of *D. kaki* (persimmon) peels have potent cytotoxic activity against human oral squamous cell carcinoma cells (HSC-2) and human submandibular gland tumor (HSG) cells (*140*). Interestingly, these fractions also had activity to reverse multiple drug resistance (MDR), further encouraging research on persimmon peels in the prevention and treatment of cancers as MDR is a frequently occurring event in most of the available cancer therapies (*140*). Similarly, cytotoxic and MDR reversal activity were also reported in response to treatment with Feijoa peel extract (*141*).

7. Active principles available in peels and their potential health benefits

Various compounds are present in both vegetable and fruit peels and are known for their different biological activities; these compounds are thought to be the active principles in these peels (Table 6). Different species of *S. melongena* contain various anthocyanins such as delphinidin 3-(*p*-coumaroylrutinoside)-5-glucoside (nasunin), delphinidin 3-rutinoside, delphinidin 3-glucoside, and petunidin 3-(*p*-coumaroylrutinoside)-5-glucoside (petunidin 3RGc5G). These compounds are all reported to have a varying degree of radical-scavenging potential. Delphinidin 3RGcaf5G is reported to have the highest level of radical-scavenging activity in 1,1-diphenyl-2-picrylhydrazyl (DPPH) radical and linoleic acid radical systems, followed by nasunin and petunidin 3RGc5G, in that order (*73,142*). Interestingly, an *ex vivo* angiogenesis assay using a rat aortic ring revealed the antiangiogenic and antioxidative potential of nasunin (*78*). Similarly, delphinidin-3-rutinoside from *S. melongena* and delphinidin-3-*trans*-coumaroylrutinoside-5-glucoside from *C. annuum* L. are also reported to

Table 5. Fruit and vegetable peels known for their anticancer efficacy

Botanical name	English name	References
1. *Pyrus malus*	Apple	(*130,131,133,134*)
2. *Punica granatum*	Pomegranat	(*135*)
3. *Solanum lycopersicum*	Tomato	(*155*)
4. *Citrus reticulata blanco*	Mandarin orange	(*138*)
5. *Citrus unshiu*	Mikan	(*136,137*)
6. *Citri Reticulatae Viride*	Green Tangerine Orange	(*136,137*)
7. *Citrus natsudaidai*	Japanese summer grape fruit	(*137*)
8. *Diospyros kaki*	Persimmon	(*140*)
9. *Feijoa sellowiana*	Feijoa	(*141*)

Table 6. Active principles isolated from fruit and/or vegetable peels and known for their various biological properties

Name	Source	Biological activity	References
1. Different varieties of delphinidin anthocyanins, delphinidin-3-rutinoside, nasunin	*Solanum melongena*	Antioxidant	(*73,74,78,142*)
2. Flavonoids including quercetin-3-*O*-beta-D-glucopyranoside, quercetin-3-*O*-beta-D-galactopyranoside, quercetin, (−)-catechin, (−)-epicatechin, quercetin-3-*O*-alpha-L-arabinofuranoside, 2 alpha-hydroxyursolic acid	*Pyrus malus*	Anticancer	(*61,130,134*)
3. Various triterpenoids including ursolic acid, 3 beta-*trans*-*p*-coumaroyloxy-2 alpha-hydroxyolean-12-en-28-oic acid, (−)-epicatechin, procyanidin B2, chlorogenic acid, and catechins and flavonol glycosides, especially rutin	*Pyrus malus*	Antioxidant	(*61,130,134*)
4. Epicatechin, gallic, and *p*-coumaric acids	*Diospyros kaki* *Pyrus malus*	Antiatherosclerotic	(*143*)
5. Caffeic, *p*-coumaric, and ferulic acids	*Pyrus malus* *Pyrus pashia* *Prunus persica*	Lipid lowering	(*144,148*)
6. Mangiferin, penta-*O*-galloyl-glucoside, gallic acid, methyl gallate, quercetin *O*-glycosides, kaempferol *O*-glycoside, xanthone *C*-glycosides, mangiferin, isomangiferin, gallotannins	*Mangifera indica* L.	Antioxidant	(*150,151*)
7. Resorcinols including 5-(11'Z-Heptadecenyl)-resorcinol, 5-(8'Z, 11'Z-Heptadecadienyl)-resorcinol	*Mangifera indica* L.	Anti-inflammatory	(*152*)
8. Fatty acid esters of hydroxybenzoic acid, fatty acid esters of hydroxybenzaldehyde, glucosides of aromatic acids, chlorogenic acids, flavonols, and benzylamine	*Cydonia vulgaris*	Antioxidant	(*154*)
9. Xyloglucan (carbohydrate)	*Passiflora liguralis*	Antioxidant	
10. Flavanon glycosides hesperidin and naringin aglycones hesperetin and naringenin	Some *Citrus* fruits	Antioxidant	(*144,148*)
5-Hydroxy-3,6,7,8,3',4'-hexamethoxyflavone	*Citrus sinensis*	Anticancer	(*136,145*)
11. Cyclonatsudamine A	*Citrus natsudaidai*	Vasodilatation	(*146*)
12. Naringin, naringenin, hesperidin, hesperetin, rutin, nobiletin, and tangeretin	Some *Citrus* fruit peels	NO radical inhibition	(*149*)
13. Delphinidin-3-*trans*-coumaroylrutinoside-5-glucoside	*Capsicum annuum* L.	Antioxidant	(*74*)
14. Lycopene and carotenoids	*Solanum lycopersicum*	Cancer prevention	(*155*)
15. Hesperidin	*Citrus unshiu*	Decreased plasma triglycerides	(*148*)
16. Auraptene and umbelliferone	*Citrus natsudaidai*	Anticancer	(*136*)

be antiperoxidative according to two different *in vitro* antioxidant capacity assessment assays (*74*). Similarly, apple peels contain a number of major flavonoids, including quercetin-3-*O*-beta-D-glucopyranoside, quercetin-3-*O*-beta-D-galactopyranoside, and trace amounts of quercetin, (−)-catechin, (−)-epicatechin, and quercetin-3-*O*-alpha-L-arabinofuranoside (*130*). Among the compounds isolated, quercetin and quercetin-3-*O*-beta-D-glucopyranoside had potent antioxidative and antiproliferative activity against HepG2 (liver) and MCF-7 (breast) cancer cells, while caffeic acid, quercetin, and quercetin-3-*O*-beta-D-arabinofuranoside, all phenolic compounds, also had antioxidant activity (*134*). Interestingly, most of the flavonoids and phenolic compounds tested were found to be stronger antioxidants when compared to ascorbic acid and might be directly responsible for the antioxidative and antiproliferative activity of apple peels. The presence of triterpenoids, including 2 alpha-hydroxyursolic acid and ursolic acid, in apple peels also makes them a potent cytotoxic or anticancer agent, as evidenced by their inhibitory activity against four tumor cell lines (HL-60, BGC, Bel-7402, and Hela) (*61*). These compounds have anticancer activity *via* inhibition of NF-kappa B activation. Interestingly, structure-activity relationships (SAR) revealed that these triterpenes possess two hydrogen bond-forming

groups (an H-donor and a carbonyl group) at positions 3 and 28 with cytotoxic activity. The configuration at C-3 was found to be important for anticancer activity, as introduction of an amino group was found to greatly increase cytotoxicity. Other evidence has also confirmed the importance of the C-3 and 28 positions, *e.g.* a 3 beta-amino derivative had 20 times the potency of its parent ursolic acid and 28-aminoalkyl dimer compounds had selective cytotoxicity (*61*).

The peels of persimmons and apples have also been recommended as part of an antiatherosclerotic diet due to their rich amounts of total, soluble, and insoluble dietary fiber, total phenols, epicatechin, and gallic and *p*-coumaric acids along with concentrations of Na, K, Mg, Ca, Fe, and Mn (*143*).

The different active components isolated from citrus fruit peels are also known for their various health benefits and disease protection, including antiperoxidative and anticancer activity, vasodilatation, decreased serum triglycerides, and improved cardiovascular health (*144-148*). Caffeic acid, *p*-coumaric acid, ferulic acid, and *p*-hydroxybenzoic acid isolated from *C. unshiu* Marc. peels had antioxidative or radical-scavenging properties as represented by trolox equivalent antioxidant capacity (TEAC) values. Similarly, hesperidin isolated from the same citrus variety was found to decrease the level of serum triglycerides (*144,148*). A polymethoxyflavone compound, 5-hydroxy-3,6,7,8,3',4'-hexamethoxyflavone (5-OH-HxMF), from the sweet orange (*C. sinensis*) is found exclusively in the *Citrus genus* and known for its anticancer and anti-inflammatory potential according to 12-*O*-tetradecanoylphorbol-13-acetate (TPA)-induced expression of inducible nitric oxide synthase (iNOS) and cyclooxygenase-2 (COX-2), which lead to tumor progression, in mouse skin (*145*). Pre-treatment with a topical application of 5-OH-HxMF has been found to inhibit the TPA-induced nuclear translocation of nuclear factor-kappa B (NF-kappa B) subunit and DNA binding by blocking phosphorylation of inhibitor kappa B (IkappaB) alpha and p65 and subsequent degradation of IkappaB alpha (*145*). Another study also suggested the potential of OH-HxMF to inhibit 7,12-dimethylbenz[a] anthracene/TPA-induced skin tumor formation, as evidenced by a reduction in tumor incidence and tumor multiplicity of papillomas at 20 weeks (*136*). Because of its anti-inflammatory and anti-tumor properties, 5-OH-HxMF may prove to be a novel functional agent to prevent inflammation-associated tumorigenesis (*145*). A novel compound, cyclonatsudamine A, was isolated from *C. natsudaidai* and evaluated for its vasodilatory potential in a rat aorta model with norepinephrine-induced contractions. The mechanism of vasodilatation was presumably mediated by increased NO release from endothelial cells (*146*).

In fact, some citrus fruit peel extracts have been reported to have varying degrees of NO radical-scavenging activity, and these levels have been further correlated with the content of some flavonoids, including naringin, naringenin, hesperidin, hesperetin, rutin, nobiletin, and tangeretin (*149*). *M. indica* peels contain compounds such as quercetin *O*-glycosides, kaempferol *O*-glycoside, xanthone *C*-glycosides, mangiferin, and isomangiferin that may serve as natural antioxidants or functional food ingredients (*150*). Other components, including mangiferin, penta-*O*-galloyl-glucoside, gallic acid, and methyl gallate, are already reported to scavenge DPPH radicals, suggesting radical-scavenging activity (*151*). Similarly, two other compounds, 5-(11'Z-heptadecenyl)-resorcinol and 5-(8'Z,11'Z-heptadecadienyl)-resorcinol, are also reported to exhibit potent cyclooxygenase-1 (COX-1) and COX-2 inhibitory activity (*152*). Understanding structure-activity relationships revealed that the degree of unsaturation in the alkyl chain plays a key role in this COX inhibitory activity (*152*). In a TEAC assay system, an unknown polysaccharide xyloglucan from *Passiflora liguralis* or granadilla fruit peels was also reported to have antioxidative potential (*153*). Reports on assessing the capacity to scavenge the 2,2'-diphenyl-1-picrylhydrazyl (DPPH) radical and anion superoxide radical and to induce the reduction of Mo(VI) to Mo(V) indicated that various chlorogenic acids and the flavonols isolated from the peels of *Cydonia vulgaris* have antioxidative and radical-scavenging properties greater than those of alpha-tocopherol and ascorbic acid (*154*). Tomato consumption is associated with a lower incidence of upper aerodigestive tract and prostate cancers due to presence of carotenoids, lycopene, and/or beta-carotene, but interestingly the content of these compounds is higher in peels than in other parts of the fruit (*155*). In fact, an *in vitro* digestion model using human intestinal cells (Caco-2) revealed that tomato paste enriched with 6% peel increased lycopene absorption into intestinal cells 75% and beta-carotene absorption 41%, clearly demonstrating the important role that active principles present in peels might play in cancer prevention (*155*).

8. Future scenario

Reviewing all of the findings on fruit and vegetable peels leads to the conclusion that fruit and vegetable peels have immense potential as novel and promising therapies against the most prevalent diseases, *i.e.*, cardiovascular problems, diabetes mellitus, thyroid abnormalities, and various cancers.

Interestingly, most peels are considered to be waste and are believed to adversely affect the cleanliness of urban areas, so their utilization in pharma or nutraceuticals will certainly offer the potential for cost-effective new generation therapeutics and also enhance the value of fruits and vegetables. As oxidative stress is one of the major factors responsible for various diseases and tissue damage, the presence of strong antioxidants in peels suggests a reduced likelihood of potential drug

toxicity or adverse drug reaction(s). However, well planned pre-clinical studies exploring toxicity and efficacy evaluations that provide an understanding of molecular pathways of the biological effects observed are still needed before any clinical trials can be conducted.

Based on the available literature, evidence, and first-hand experience working in this field, the current authors are quite optimistic that the path from fruit and vegetable peels used in the laboratory to peels available on the market will only take a few more years; soon, they may serve as new generation therapeutics to treat cancer, cardiovascular diseases, diabetes mellitus and thyroid abnormalities.

Acknowledgements

The authors wish to sincerely thank the University Grants Commission (UGC) and Department of Biotechnology (DBT), New Delhi, India for their financial assistance *via* a departmental grant for this research.

References

1. Smletzer SG, Bare BG. Brunner and Suddhath's Text Book of Medical-Surgical Nursing. 7th ed., J.B. Lippincott, Philadelphia, PA, USA, 1992.
2. Chockalingam A, Chalmers J, Lisheng L, Labarthe D, MacMahon S, Martin I, Whitworth J. Prevention of cardiovascular diseases in developing countries: Agenda for action (statement from a WHO-ISH Meeting in Beijing, October 1999). J Hypertens. 2000; 18:1705-1708.
3. Kar A, Panda S. Ayurvedic therapies for thyroid dysfunction. In: Scientific Basis of Ayurvedic Therapies (Mishra L, ed.), Chapter 8. CRC Press, Boca Raton, FL, USA, 2004; pp. 133-148.
4. Kar A, Panda S. Plant extracts in the regulation of hypothyroidism. In: Recent Progress in Medicinal Plants (Sharma SK, Govil JN, Singh VK, eds.), Vol. 10, Phytotherapeutics. Studium Press LLC, Houston, TX, USA, 2005; pp. 419-426.
5. Carter D. British Medical Association Board of Science and Education. BMA Publications Unit, London, UK, 2004.
6. Tiwari AK. Antioxidants: New generation therapeutic base for treatment of polygenic disorders. Curr Sci. 2004; 86:1092-1102.
7. Chun AK. Thyroid disorders. In: Fundamentals of Geriatric Medicine (Chun AK, ed.), Chapter 25. Springer, New York, USA, 2007; pp. 450-469.
8. Lindholm LH, Mendis S. Prevention of cardiovascular disease in developing countries. Lancet. 2007; 370:720-722.
9. Faquin WC. The thyroid gland: Recurring problems in histologic and cytologic evaluation. Arch Pathol Lab Med. 2008; 132:622-632.
10. Nattrass M, Bailey CJ. New agents for Type 2 diabetes. Baillieres Best Pract Res Clin Endocrinol Metab. 1999; 13:309-329.
11. Klotz U, Sailer D. Drug interactions – Their impact on safe drug therapy in the example of the new thiazolidinedione group (glitazone). Arzneimittelforschung. 2001; 51:112-117. (in German)
12. Kajinami K, Takekoshi N, Saito Y. Pitavastatin: Efficacy and safety profiles of a novel synthetic HMG-CoA reductase inhibitor. Cardiovasc Drug Rev. 2003; 21:199-215.
13. Cavero I, Crumb W. ICH S7B draft guideline on the non-clinical strategy for testing delayed cardiac repolarisation risk of drugs: A critical analysis. Expert Opin Drug Saf. 2005; 4:509-530.
14. Chatterjee S, Tringham JR, Davies MJ. Insulin glargine and its place in the treatment of Types 1 and 2 diabetes mellitus. Expert Opin Pharmacother. 2006; 7:1357-1371.
15. Cabebe E, Wakelee H. Role of anti-angiogenesis agents in treating NSCLC: Focus on bevacizumab and VEGFR tyrosine kinase inhibitors. Curr Treat Options Oncol. 2007; 8:15-27.
16. Cravedi JP, Zalko D, Savouret JF, Menuet A, Jégou B. The concept of endocrine disruption and human health. Med Sci (Paris). 2007; 23:198-204.
17. Espinosa AV, Porchia L, Ringel MD. Targeting BRAF in thyroid cancer. Br J Cancer. 2007; 96:16-20.
18. Ivachtchenko AV, Kiselyov AS, Tkachenko SE, Ivanenkov YA, Balakin KV. Novel mitotic targets and their small-molecule inhibitors. Curr Cancer Drug Targets. 2007; 7:766-784.
19. Nelkin BD, de Bustros AC, Mabry M, Baylin SB. The molecular biology of medullary thyroid carcinoma. A model for cancer development and progression. JAMA. 1989; 261:3130-3135.
20. Gertz MA. New targets and treatments in multiple myeloma: Src family kinases as central regulators of disease progression. Leuk Lymphoma. 2008; 49:2240-2245.
21. Tulis DA. Novel therapies for cyclic GMP control of vascular smooth muscle growth. Am J Ther. 2008; 15:551-564.
22. Heng DY, Bukowski RM. Anti-angiogenic targets in the treatment of advanced renal cell carcinoma. Curr Cancer Drug Targets. 2008; 8:676-682.
23. Mohamed Q, Wong TY. Emerging drugs for diabetic retinopathy. Expert Opin Emerg Drugs. 2008; 13:675-694.
24. Rovere RK, Awada A. Treatment of recurrent thyroid cancers – is there a light in the horizon? Curr Opin Oncol. 2008; 20:245-248.
25. Szczepankiewicz BG, Ng PY. Sirtuin modulators: Targets for metabolic diseases and beyond. Curr Top Med Chem. 2008; 8:1533-1544.
26. Collino M, Patel NS, Thiemermann C. PPARs as new therapeutic targets for the treatment of cerebral ischemia/reperfusion injury. Ther Adv Cardiovasc Dis. 2008; 2:179-197.
27. Haverslag R, Pasterkamp G, Hoefer IE. Targeting adhesion molecules in cardiovascular disorders. Cardiovasc Hematol Disord Drug Targets. 2008; 8:252-260.
28. Hermansen K, Mortensen LS, Hermansen ML. Combining insulins with oral antidiabetic agents: Affect on hyperglycemic control, markers of cardiovascular risk and disease. Vasc Health Risk Manag. 2008; 4:561-574.
29. Krentz AJ, Patel MB, Bailey CJ. New drugs for Type 2 diabetes mellitus: What is their place in therapy? Drugs. 2008; 68:2131-2162.
30. Khama-Murad AKh, Pavlinova LI, Mokrushin AA. Hemorrhagic stroke: Molecular mechanisms of pathogenesis and perspective therapeutic targets. Usp Fiziol Nauk. 2008; 39:45-65. (in Russian)
31. Thomas M. Molecular targeted therapy for hepatocellular

carcinoma. J Gastroenterol. 2009; 44:136-141.
32. Steigen SE, Eide TJ. Gastrointestinal stromal tumors (GISTs): A review. APMIS. 2009; 117:73-86.
33. Haberland M, Montgomery RL, Olson EN. The many roles of histone deacetylases in development and physiology: Implications for disease and therapy. Nat Rev Genet. 2009; 10:32-42.
34. Idelevich E, Kirch W, Schindler C. Current pharmacotherapeutic concepts for the treatment of obesity in adults. Ther Adv Cardiovasc Dis. 2009; 3:75-90.
35. Maiese K, Chong ZZ, Shang YC, Hou J. FoxO proteins: Cunning concepts and considerations for the cardiovascular system. Clin Sci (Lond). 2009; 116:191-203.
36. Singh V, Tiwari RL, Dikshit M, Barthwal MK. Models to study atherosclerosis: A mechanistic insight. Curr Vasc Pharmacol. 2009; 7:75-109.
37. Sogno I, Vannini N, Lorusso G, Cammarota R, Noonan DM, Generoso L, Sporn MB, Albini A. Anti-angiogenic activity of a novel class of chemopreventive compounds: Oleanic acid terpenoids. Recent Results Cancer Res. 2009; 181:209-212.
38. Katzung BG. Basic & Clinical Pharmacology. 7th ed., Applenton and Lange, Stamford, CT, USA, 1998.
39. Michaelson J. Thiazolidinedione associated volume overload and pulmonary hypertension. Ther Adv Cardiovasc Dis. 2008; 2:435-438.
40. Gallwitz B. Saxagliptin, a dipeptidyl peptidase IV inhibitor for the treatment of Type 2 diabetes. IDrugs. 2008; 11:906-917.
41. Steinberg M. Ixabepilone: A novel microtubule inhibitor for the treatment of locally advanced or metastatic breast cancer. Clin Ther. 2008; 30:1590-1617.
42. Mazzini MJ, Monahan KM. Pharmacotherapy for atrial arrhythmias: Present and future. Heart Rhythm. 2008; 5 (Suppl):S26-S31.
43. Barry PJ, Gallagher P, Ryan C. Inappropriate prescribing in geriatric patients. Curr Psychiatry Rep. 2008; 10:37-43.
44. Barni S, Cabiddu M, Petrelli F. Toxicity of targeted therapies in elderly patients. Expert Rev Anticancer Ther. 2008; 8:1965-1976.
45. Hoffman AG, Schram SE, Ercan-Fang NG, Warshaw EM. Type I allergy to insulin: Case report and review of localized and systemic reactions to insulin. Dermatitis. 2008; 19:52-58.
46. Hausner E, Fiszman ML, Hanig J, Harlow P, Zornberg G, Sobel S. Long-term consequences of drugs on the paediatric cardiovascular system. Drug Saf. 2008; 31:1083-1096.
47. Jones RL. Utility of dexrazoxane for the reduction of anthracycline-induced cardiotoxicity. Expert Rev Cardiovasc Ther. 2008; 6:1311-1317.
48. Nakae D, Onodera H, Fueki O, Urano T, Komiyama N, Sagami F, Kai S, Nishimura C, Inoue T. Points to consider on the non-clinical safety evaluation of anticancer drugs. J Toxicol Sci. 2008; 33:123-126.
49. Pourpak Z, Fazlollahi MR, Fattahi F. Understanding adverse drug reactions and drug allergies: Principles, diagnosis and treatment aspects. Recent Pat Inflamm Allergy Drug Discov. 2008; 2:24-46.
50. Yap KY, Chui WK, Chan A. Drug interactions between chemotherapeutic regimens and antiepileptics. Clin Ther. 2008; 30:1385-1407.
51. Hellberg V, Wallin I, Eriksson S, Hernlund E, Jerremalm E, Berndtsson M, Eksborg S, Arnér ES, Shoshan M, Ehrsson H, Laurell G. Cisplatin and oxaliplatin toxicity: Importance of cochlear kinetics as a determinant for ototoxicity. J Natl Cancer Inst. 2008; 101:37-47.
52. Parmar HS, Kar A. Protective role of *Citrus sinensis*, *Musa paradisiaca* and *Punica granatum* peels against diet-induced atherosclerosis and thyroid dysfunctions in rats. Nutr Res. 2007; 27:710-718.
53. Parmar HS, Kar A. Antidiabetic potential of *Citrus sinensis* and *Punica granatum* peel extracts in alloxan treated male mice. Biofactors. 2007; 31:17-24.
54. Eddouks M, Maghrani M, Louedec L, Haloui M, Michel JB. Antihypertensive activity of the aqueous extract of *Retama raetam* Forssk. leaves in spontaneously hypertensive rats. J Herb Pharmacother. 2007; 7:65-77.
55. Oliveira HC, dos Santos MP, Grigulo R, Lima LL, Martins DT, Lima JC, Stoppiglia LF, Lopes CF, Kawashita NH. Antidiabetic activity of *Vatairea macrocarpa* extract in rats. J Ethnopharmacol. 2008; 115:515-519.
56. Reddy SS, Karuna R, Baskar R, Saralakumari D. Prevention of insulin resistance by ingesting aqueous extract of *Ocimum sanctum* to fructose-fed rats. Horm Metab Res. 2008; 40:44-49.
57. Venables MC, Hulston CJ, Cox HR, Jeukendrup AE. Green tea extract ingestion, fat oxidation, and glucose tolerance in healthy humans. Am J Clin Nutr. 2008; 87:778-784.
58. Yiming L, Wei H, Aihua L, Fandian Z. Neuroprotective effects of breviscapine against apoptosis induced by transient focal cerebral ischaemia in rats. J Pharm Pharmacol. 2008; 60:349-355.
59. Agarwal A. Current issues in quality control of natural products. Pharma Times. 2005; 37:9-11.
60. Leontowicz M, Gorinstein S, Leontowicz H, Krzeminski R, Lojek A, Katrich E, Cíz M, Martin-Belloso O, Soliva-Fortuny R, Haruenkit R, Trakhtenberg S. Apple and pear peel and pulp and their influnce on plasma lipids an antioxidant potentials in rats fed cholesterol-containing diets. J Agric Food Chem. 2003; 51:5780-5785.
61. Ma CM, Cai SQ, Cui JR, Wang RQ, Tu PF, Hattori M, Daneshtalab M. The cytotoxic activity of ursolic acid derivatives. Eur J Med Chem. 2005; 40:582-589.
62. Dixit Y, Panda S, Kar A. *Lagenaria siceraria* peel extract in the regulation of hyperthyroidism, hyperglycemia and lipid peroxidation in mice. Int J Biomed Pharma Sci. 2008; 2:79-83.
63. Parmar HS, Kar A. Protective role of *Mangifera indica*, *Cucumis melo* and *Citrullus vulgaris* peel extracts in chemically induced hypothyroidism. Chem Biol Interac. 2009; 177:254-258.
64. Parmar HS, Kar A. Comparative analysis of free radical scavenging potential of several fruit peel extracts by *in vitro* methods. Drug Disc Ther. 2009; 3:49-55.
65. Parmar HS, Kar A. Medicinal values of fruit peels from *Citrus sinensis, Punica granatum* and *Musa paradisiaca* with respect to alterations in tissue lipid peroxidation and serum concentration of glucose, insulin and thyroid hormones. J Med Food. 2008; 11:376-381.
66. Parmar HS, Kar A. Antiperoxidative, antithyroidal, antihyperglycemic and cardioprotective role of *Citrus sinensis* peel extracts in male mice. Phytother Res. 2008; 22:791-795.
67. Parmar HS, Kar A. Possible amelioration of atherogenic diet induced dyslipidemia, hypothyroidism and hyperglycemia by the peel extracts of *Mangifera indica*, *Cucumis melo* and *Citrullus vulgaris* fruits in rats.

Biofactors. 2008; 33:13-24.
68. Rincón AM, Vásquez AM, Padilla FC. Chemical composition and bioactive compounds of flour of orange (*Citrus sinensis*), tangerine (*Citrus reticulata*) and grapefruit (*Citrus paradisi*) peels cultivated in Venezuela. Arch Latinoam Nutr. 2005; 55:305-310. (in Spanish)
69. Ho SC, Lin CC. Investigation of heat treating conditions for enhancing the anti-inflammatory activity of citrus fruit (*Citrus reticulata*) peels. J Agric Food Chem. 2008; 56:7976-7982.
70. Tommonaro G, Rodríguez CS, Santillana M, Immirzi B, Prisco RD, Nicolaus B, Poli A. Chemical composition and biotechnological properties of a polysaccharide from the peels and antioxidative content from the pulp of *Passiflora liguralis* fruits. J Agric Food Chem. 2007; 55:7427-7433.
71. Leontowicz H, Gorinstein S, Lojek A, Leontowicz M, Cíz M, Soliva-Fortuny R, Park YS, Jung ST, Trakhtenberg S, Martin-Belloso O. Comparative content of some bioactive compounds in apples, peaches and pears and their influence on lipids and antioxidants capacity in rats. J Nutr Biochem. 2002; 13:603-610.
72. Negro C, Tommasi L, Miceli A. Phenolic compounds and antioxidant from red grape marc extracts. Bioresour Technol. 2003; 87:41-44.
73. Noda Y, Kaneyuki T, Igarashi K, Mori A, Packer L. Antioxidant activity of nasunin, an anthocyanin in eggplant. Res Commun Mol Pathol Pharmacol. 1998; 102:175-187.
74. Sadilova E, Stintzing FC, Carle R. Anthocyanins, colour and antioxidant properties of eggplant (*Solanum melongena* L.) and violet pepper (*Capsicum annuum* L.) peel extracts. Z Naturforsch C. 2006; 61:527-535.
75. Singh N, Kamath V, Rajini PS. Protective effect of potato peel power in ameliorating oxidative stress in streptozotocin diabetic rats. Plant Foods Hum Nutr. 2005; 60:49-54.
76. Singh N, Rajini PS. Antioxidant-mediated protective effect of potato peel extract in erythrocytes against oxidative damage. Chem Biol Interact. 2008; 173:97-104.
77. Gorinstein S, Leontowicz H, Leontowicz M, Drzewiecki J, Jastrzebski Z, Tapia MS, Katrich E, Trakhtenberg S. Red Star Ruby (Sunrise) and blond qualities of Jaffa grapefruits and their influence on plasma lipid levels and plasma antioxidant activity in rats fed with cholesterol-containing and cholesterol-free diets. Life Sci. 2005; 77:2384-2397.
78. Matsubara Y, Kumamoto H, Iizuka Y, Murakami T, Okamoto K, Miyake H, Yokoi K. Structure and hypertensive effect of flavonoids glycosides in *Citrus unshiu* peelings. Agric Biol Chem. 1985; 49:909-914.
79. Narayana RK, Reddy MS, Chaluvadi MR, Krishna DR. Bioflavonids classification, pharmacological, biochemical effects and therapeutic potential. Ind J Pharmacol. 2001; 33:2-16.
80. Jung UJ, Lee MK, Jeong KS, Choi MS. The hypoglycemic effects of hesperidin and naringin are partly mediated by hepatic glucose-regulating enzymes in C57BL/KsJ-db/db mice. J Nutr. 2004; 134:2499-2503.
81. Fuhrman B, Lavy A, Aviram M. Consumption of red wine with meals reduces the susceptibility of human plasma and low-density lipoproteins to lipid peroxidation. Am J Clin Nutr. 1995; 61:549-554.
82. Igarashi K, Ohmuna M. Effect of Isoharnneti, Rhamnetin and Quercetin on the concentrations of cholesterol and lipoperoxide in the serum and liver and on the blood and liver antioxidative enzyme activities in rats. Biosci Biotech Biochem. 1995; 59:595-601.
83. McAnlis GT, McEneny J, Pearce J, Young IS. The effect of various dietary flavonoids on the susceptibility of low density lipoproteins to oxidation *in vitro* using both metallic and non-metallic oxidising agents. Biochem Soc Trans. 1997; 25:142S.
84. Bok SH, Lee SH, Park YB, Bae KH, Son KH, Jeong TS, Choi MS. Plasma and hepatic cholesterol and hepatic activities of 3-hydroxyl-3-methyl-glutaryl-CoA reductase and acyl CoA: Cholesterol transferase are lower in rats fed citrus peel extract or a mixture of citrus bioflavonoids. J Nutr. 1999; 129:1182-1185.
85. Choi MS, Do KM, Park YS, Jeon SM, Jeong TS, Lee YK, Lee MK, Bok SH. Effect of naringin supplementation on cholesterol metabolism and antioxidant status in rats fed high cholesterol with different levels of vitamin E. Ann Nutr Metab. 2001; 45:193-201.
86. de Whalley CV, Rankin SM, Hoult JR, Jessup W, Leake DS. Flavonoids inhibit the oxidative modification of low density lipoproteins by macrophages. Biochem Pharmacol. 1990; 39:1743-1750.
87. Francel EN, Kanner J, German JB, Parks E, Kinsella JE. Inhibition of oxidation of human low-density lipoprotein by phenolis substances in red wine. Lancet. 1993; 341:454-457.
88. Kroyer G. The antioxidant activity of citrus fruit peels. Z Ernahrungswiss. 1986; 25:63-69. (in German)
89. Böhm H, Boeing H, Hempel J, Raab B, Kroke A. Flavonols, flavone and anthocyanins as natural antioxidants of food and their possible role in the prevention of chronic diseases. Z Ernahrungswiss. 1998; 37:147-163. (in German)
90. Murakami A, Nakamura Y, Ohto Y, Yano M, Koshiba T, Koshimizu K, Tokuda H, Nishino H, Ohishi H. Suppressive effects of citrus fruits on free radical generation and nobiletin, an anti-inflammatory polymethoxylated flavonoid. Biofactors. 2000; 12:187-192.
91. Choe SC, Kim HS, Jeong TS, Bok SH, Park YB. Naringin has an antiatherogenic effect with the inhibition of intercellular adhesion molecule-1 in hypercholesterolemic rabbits. J Cardiovasc Pharmacol. 2001; 38:947-955.
92. Anagnostopoulou MA, Kefalas P, Kokkalou E, Assimopoulou AN, Papageorgiou VP. Analysis of antioxidant compounds in sweet orange peel by HPLC-diode array detection-electrospray ionization mass spectrometry. Biomed Chromatogr. 2005; 19:138-148.
93. Lyte M. Induction of gram-negative bacterial growth by neurochemical containing banana (*Musa x paradisiaca*) extracts. FEMS Microbiol Lett. 1997; 154:245-250.
94. Kanazawa K, Sakakibara H. High content of dopamine, a strong antioxidant, in Cavendish banana. J Agric Food Chem. 2000; 48:844-848.
95. Deepa PR, Varalakshmi P. Salubrious effect of low molecular weight heparin on atherogenic diet-induced cardiac, hepatic and renal lipid peroxidation and collapse of antioxidant defences. Mol Cell Biochem. 2003; 254:111-116.
96. Deepa PR, Varlakshmi P. Protective effects of certoparin sodium, a low molecular weight heparin derivative in experimental atherosclerosis. Clin Chim Acta. 2004; 339:105-115.
97. Jatwa R, Kar A. Cardio-protective role of terazosin is possibly mediated through alteration in thyroid function.

Eur J Pharmacol. 2006; 551:87-91.
98. Vedavanam K, Srijayanta S, O'Reilly J, Raman A, Wiseman H. Antioxidant action and potential antidiabetic properties of an isoflavonoid-containing soyabean phytochemical extract (SPE). Phytother Res. 1999; 13:601-608.
99. Murthy KN, Reddy VK, Veigas JM, Murthy UD. Study on wound healing activity of *Punica granatum* peel. J Med Food. 2004; 7:256-259.
100. Seeram NP, Adams LS, Henning SM, Niu Y, Zhang Y, Nair MG, Heber D. *In vitro* antiproliferative, apoptotic and antioxidant activities of punicalagin, ellagic acid and a total pomegranate tannin extract are enhanced in combination with other polyphenols as found in pomegranate juice. J Nutr Biochem. 2005; 16:360-367.
101. Cazarolli LH, Zanatta L, Jorge AP, de Sousa E, Horst H, Woehl VM, Pizzolatti MG, Szpoganicz B, Silva FR. Follow-up studies on glycosylated flavonoids and their complexes with vanadium: Their anti-hyperglycemic potential role in diabetes. Chem Biol Interact. 2006; 163:177-191.
102. Aslan M, Deliorman Orhan D, Orhan N, Sezik E, Yesilada E. *In vivo* antidiabetic and antioxidant potential of *Helichrysum plicatum* ssp. *plicatum* capitulums in streptozotocin-induced-diabetic rats. J Ethnopharmacol. 2007; 109:54-59.
103. Chemler JA, Lock LT, Koffas MA, Tzanakakis ES. Standardized biosynthesis of flavan-3-ols with effects on pancreatic beta-cell insulin secretion. Appl Microbiol Biotechnol. 2007; 77:797-807.
104. Hsu CL, Yen GC. Effect of gallic acid on high fat diet-induced dyslipidaemia, hepatosteatosis and oxidative stress in rats. Br J Nutr. 2007; 98:727-735.
105. Katz SR, Newman RA, Lansky EP. *Punica granatum* L.: Heuristic treatment for diabetes mellitus. J Med Food. 2007; 10:213-217.
106. Jang A, Srinivasan P, Lee NY, Song HP, Lee JW, Lee M, Jo C. Comparison of hypolipidemic activity of synthetic gallic acid-linoleic acid ester with mixture of gallic acid and linoleic acid, gallic acid, and linoleic acid on high-fat diet induced obesity in C57BL/6 Cr Slc mice. Chem Biol Interact. 2008; 174:109-117.
107. Kato A, Nasu N, Takebayashi K, Adachi I, Minami Y, Sanae F, Asano N, Watson AA, Nash RJ. Structure-activity relationships of flavonoids as potential inhibitors of glycogen phosphorylase. J Agric Food Chem. 2008; 56:4469-4473.
108. Mitchell DE, Madore MA. Patterns of assimilate production and translocation in Muskmelon (*Cucumis melo* L.): II. Low temperature effects. Plant Physiol. 1992; 99:966-971.
109. Ganong W. Review of Medical Physiology. 17th ed., Applenton and Lange, Stamford, CT, USA, 2005.
110. Percival SS, Talcott ST, Chin ST, Mallak AC, Lounds-Singleton A, Pettit-Moore J. Neoplastic transformation of BALB/3T3 cells and cell cycle of HL-60 cells are inhibited by mango (*Mangifera indica* L.) juice and mango juice extracts. J Nutr. 2006; 136:1300-1304.
111. Rodríguez J, Di Peirro D, Gioia M, Monaco S, Delgado R, Coletta M, Marini S. Effects of a natural extract from *Mangifera indica* L., and its active compound, mangiferin, on energy state and lipid peroxidation of red blood cells. Biochim Biophys Acta. 2006; 1760:1333-1342.
112. Sa-Nunnes A, Rogerio AP, Medeiros AI, Fabris VE, Andreu GP, Rivera DG, Delgado R, Faccioli LH. Modulation of eosinophil generation and migration by *Mangifera indica* L. extract (Vimang). Int Immunopharmacol. 2006; 6:1515-1523.
113. Hernandez P, Rodriguez PC, Delgado R, Walczak H. Protective effect of *Mangifera indica* L. polyphenols on human T lymphocytes against activation-induced cell death. Pharmacol Res. 2007; 55:167-173.
114. Selles AJ, Rodriguez MD, Balseiro ER, Gonzalez LN, Nicolais V, Rastrelli L. Comparison of major and trace element concentrations in 16 varieties of Cuban mango stem bark (*Mangifera indica* L.). J Agric Food Chem. 2007; 55:2176-2181.
115. Knödler M, Conrad J, Wenzig EM, Bauer R, Lacorn M, Beifuss U, Carle R, Schieber A. Anti-inflammatory 5-(11'Z-heptadecenyl)-and 5-(8'Z,11'Z-heptadecadienyl)-resorcinols from mango (*Mangifera indica* L.) peels. Phytochem. 2008; 69:988-993.
116. Castillo L, Sanchez M, Vogt J, Chapman TE, De Rojas-Walker TC, Tannenbaun SR, Ajami AM, Young VR. Plasma arginine, citrulline, and ornithine kinetics in adults, with observations on nitric oxide synthesis. Am J Physiol. 1995; 268:E360-E367.
117. Edwards AJ, Vinyard BT, Wiley ER, Brown ED, Collins JK, Perkins-Veazie P, Baker RA, Clevidence BA. Consumption of watermelon juice increases plasma concentrations of lycopene and beta-carotene in humans. J Nutr. 2003; 133:1043-1050.
118. Collins JK, Wu G, Perkins-Veazie P, Spears K, Claypool PL, Baker RA, Clevidence BA. Watermelon consumption increases plasma arginine concentration in adults. Nutrition. 2007; 23:261-266.
119. Chau CF, Huang YL, Lee MH. *In vitro* hypoglycemic effects of different insoluble fiber-rich fractions prepared from the peel of *Citrus sinensis* L. cv, Liucheng. J Agric Food Chem. 2003; 51:6623-6626.
120. Auf'mkolk M, Köhrle J, Gumbinger H, Winterhoff H, Hesch RD. Antihormonal effects of plant extracts: Iodothyronine deiodinase of rat liver is inhibited by extracts and secondary metabolites of plants. Horm Metab Res. 1984; 16:188-192.
121. Piattelli M, Impellizzeri G. Fungistatic flavones in the leaves of citrus species resistant and susceptible to *deuterophoma tracheiphila*. Phytochemistry. 1971; 10:2657-2659.
122. Tatum JH, Berry RE. Six new flavonoids from *Citrus*. Phytochemistry. 1972; 11:2283-2288.
123. Divi RL, Doerge DR. Inhibition of thyroid peroxidase by dietary flavonoids. Chem Res Toxicol. 1996; 9:16-23.
124. Wilding J, Williams G. Textbook of Medicine. 3rd ed., Churchill Livingstone, London, UK, 1997.
125. Filippi L, Cecchi A, Tronchin M, Dani C, Pezzati M, Seminara S, Gasperini S, Zammarchi E, Rubaltelli FF. Dopamine infusion and hypothyroxinaemia in very low birth weight preterm infants. Eur J Pediatr. 2004; 163:7-13.
126. da-Silva WS, Harney JW, Kim BW, Li J, Bianco SD, Crescenzi A, Christoffolete MA, Huang SA, Bianco AC. The small polyphenolic molecule kaempferol increases cellular energy expenditure and thyroid hormone activation. Diabetes. 2007; 56:767-776.
127. Wolfe KL, Liu RH. Apple peels as a value-added food ingredient. J Agric Food Chem. 2003; 51:1676-1683.
128. Yance DR Jr, Sagar SM. Targeting angiogenesis with integrative cancer therapies. Integr Cancer Ther. 2006;

5:9-29.
129. Mahadevan S, Park Y. Multifaceted therapeutic benefits of *Ginkgo biloba* L.: Chemistry, efficacy, safety, and uses. J Food Sci. 2008; 73:R14-R19.
130. He X, Liu RH. Phytochemicals of apple peels: Isolation, structure elucidation, and their antiproliferative and antioxidant activities. J Agric Food Chem. 2008; 56:9905-9910.
131. Yoon H, Liu RH. Effect of 2alpha-hydroxyursolic acid on NF-kappaB activation induced by TNF-alpha in human breast cancer MCF-7 cells. J Agric Food Chem. 2008; 56:8412-8417.
132. Li-Weber M. New therapeutic aspects of flavones: The anticancer properties of *Scutellaria* and its main active constituents *wogonin*, *baicalein* and *baicalin*. Cancer Treat Rev. 2009; 35:57-68.
133. Chinnici F, Bendini A, Gaiani A, Riponi C. Radical scavenging activities of peels and pulps from cv. Golden Delicious apples as related to their phenolic composition. J Agric Food Chem. 2004; 52:4684-4689.
134. He X, Liu RH. Triterpenoids isolated from apple peels have potent antiproliferative activity and may be partially responsible for apple's anticancer activity. J Agric Food Chem. 2007; 55:4366-4370.
135. Lansky EP, Newman RA. *Punica granatum* (pomegranate) and its potential for prevention and treatment of inflammation and cancer. J Ethnopharmacol. 2007; 109:177-206.
136. Murakami A, Kuki W, Takahashi Y, Yonei H, Nakamura Y, Ohto Y, Ohigashi H, Koshimizu K. Auraptene, a citrus coumarin, inhibits 12-*O*-tetradecanoylphorbol-13-acetate-induced tumor promotion in ICR mouse skin, possibly through suppression of superoxide generation in leukocytes. Jpn J Cancer Res. 1997; 88:443-452.
137. Kadota Y, Taniguchi C, Masuhara S, Yamamoto S, Furusaki S, Iwahara M, Goto K, Matsumoto Y, Ueoka R. Inhibitory effects of extracts from peels of *Citrus natsudaidai* encapsulated in hybrid liposomes on the growth of tumor cells *in vitro*. Biol Pharm Bull. 2004; 27:1465-1467.
138. Kim MJ, Park HJ, Hong MS, Park HJ, Kim MS, Leem KH, Kim JB, Kim YJ, Kim HK. Citrus reticulate blanco induces apoptosis in human gastric cancer cells SNU-668. Nutr Cancer. 2005; 51:78-82.
139. Iwase Y, Takemura Y, Ju-ichi M, Kawaii S, Yano M, Okuda Y, Mukainaka T, Tsuruta A, Okuda M, Takayasu J, Tokuda H, Nishino H. Inhibitory effect of Epstein-Barr virus activation by *Citrus fruits*, a cancer chemopreventor. Cancer Lett. 1999; 139:227-236.
140. Kawase M, Motohashi N, Satoh K, Sakagami H, Nakashima H, Tani S, Shirataki Y, Kurihara T, Spengler G, Wolfard K, Molnár J. Biological activity of persimmon (*Diospyros kaki*) peel extracts. Phytother Res. 2003; 17:495-500.
141. Motohashi N, Kawase M, Shirataki Y, Tani S, Saito S, Sakagami H, Kurihara T, Nakashima H, Wolfard K, Mucsi I, Varga A, Molnár J. Biological activity of feijoa peel extracts. Anticancer Res. 2000; 20:4323-4329.
142. Azuma K, Ohyama A, Ippoushi K, Ichiyanagi T, Takeuchi A, Saito T, Fukuoka H. Structures and antioxidant activity of anthocyanins in many accessions of eggplant and its related species. J Agric Food Chem. 2008; 56:10154-10159.
143. Gorinstein S, Zachwieja Z, Folta M, Barton H, Piotrowicz J, Zemser M, Weisz M, Trakhtenberg S, Màrtín-Belloso O. Comparative contents of dietary fiber, total phenolics, and minerals in persimmons and apples. J Agric Food Chem. 2001; 49:952-957.
144. Kawaguchi K, Mizuno T, Aida K, Uchino K. Hesperidin as an inhibitor of lipases from porcine pancreas and Pseudomonas. Biosci Biotechnol Biochem. 1997; 61:102-104.
145. Lai CS, Li S, Chai CY, Lo CY, Ho CT, Wang YJ, Pan MH. Inhibitory effect of citrus 5-hydroxy-3,6,7,8,3',4'-hexamethoxyflavone on 12-*O*-tetradecanoylphorbol 13-acetate-induced skin inflammation and tumor promotion in mice. Carcinogenesis. 2007; 28:2581-2588.
146. Morita H, Enomoto M, Hirasawa Y, Iizuka T, Ogawa K, Kawahara N, Goda Y, Matsumoto T, Takeya K. Cyclonatsudamine A, a new vasodilator cyclic peptide from *Citrus natsudaidai*. Bioorg Med Chem Lett. 2007; 17:5410-5413.
147. Ma YQ, Ye XQ, Fang ZX, Chen JC, Xu GH, Liu DH. Phenolic compounds and antioxidant activities of extracts from ultrasonic treatment of Satsuma Mandarin (*Citrus unshiu* Marc.) peels. J Agric Food Chem. 2008; 56:5682-5690.
148. Xu GH, Chen JC, Liu DH, Zhang YH, Jiang P, Ye XQ. Minerals, phenolic compounds, and antioxidant capacity of citrus peel extract by hot water. J Food Sci. 2008; 73: C11-C18.
149. Choi SY, Ko HC, Ko SY, Hwang JH, Park JG, Kang SH, Han SH, Yun SH, Kim SJ. Correlation between flavonoid content and the NO production inhibitory activity of peel extracts from various citrus fruits. Biol Pharm Bull. 2007; 30:772-778.
150. Schieber A, Berardini N, Carle R. Identification of flavonol and xanthone glycosides from mango (*Mangifera indica* L., Cv. "TommyAtkins") peels by high-performanceliquid chromatography-electrospray ionization mass spectrometry. J Agric Food Chem. 2003; 51:5006-5011.
151. Barreto JC, Trevisan MT, Hull WE, Erben G, de Brito ES, Pfundstein B, Würtele G, Spiegelhalder B, Owen RW. Characterization and quantitation of polyphenolic compounds in bark, kernel, leaves, and peel of mango (*Mangifera indica* L.). J Agric Food Chem. 2008; 56:5599-5610.
152. Knödler M, Conrad J, Wenzig EM, Bauer R, Lacorn M, Beifuss U, Carle R, Schieber A. Anti-inflammatory 5-(11'Z-heptadecenyl)- and 5-(8'Z,11'Z-heptadecadienyl)-resorcinols from mango (*Mangifera indica* L.) peels. Phytochemistry. 2008; 69:988-993.
153. Tommonaro G, Rodriguez CS, Santillana M, Immirzi B, Prisco RD, Nicolaus B, Poli A. Chemical composition and biotechnological properties of a polysaccharide from the peels and antioxidative content from the pulp of *Passiflora liquralis* fruits. J Agric Food Chem. 2007; 55:7427-7433.
154. Fiorentino A, D'Abrosca B, Pacifico S, Mastellone C, Piscopo V, Caputo R, Monaco P. Isolation and structure elucidation of antioxidant polyphenols from quince (*Cydonia vulgaris*) peels. J Agric Food Chem. 2008; 56:2660-2667.
155. Reboul E, Borel P, Mikail C, Abou L, Charbonnier M, Caris-Veyrat C, Goupy P, Portugal H, Lairon D, Amiot MJ. Enrichment of tomato paste with 6% tomato peel increases lycopene and beta-carotene bioavailability in men. J Nutr. 2005; 135:790-794.

(Received May 24, 2010; Accepted August 5, 2010)

Review

Potential application of arginine in interaction analysis

Kentaro Shiraki[1], Atsushi Hirano[1], Yoshiko Kita[2], A. Hajime Koyama[3], Tsutomu Arakawa[4,*]

[1] *Institute of Applied Physics, University of Tsukuba, Tsukuba, Ibaraki, Japan;*
[2] *Department of Pharmacology, KEIO University School of Medicine, Shinjuku-ku, Tokyo, Japan;*
[3] *Division of Virology, Department of Cellular and Molecular Medicine, Wakayama Medical University Graduate School of Medicine, Wakayama, Japan;*
[4] *Alliance Protein Laboratories, Thousand Oaks, CA, USA.*

ABSTRACT: Aqueous solution of 0.1-2 M arginine at mildly acidic to neutral pH is widely used in biotechnology and protein research, including protein refolding, purification, and formulation. This is largely because of its ability to suppress non-specific protein-protein and protein-surface interactions. Here we propose potential applications of arginine in interaction analysis for proteins. One of the important goals of such analysis is discovery of small molecule antagonistic or agonistic ligands that bind to target proteins and thereby modulate their function. Such research is often hampered by the low solubility of the small molecules, the instability of target proteins and the non-specific protein-ligand interactions. Aqueous arginine solution increases the solubility of small molecules, which should give an alternative to conventional dissolution method of small molecules by organic solvents. Arginine may also directly impact on the analysis of protein-protein or protein-ligand interactions by suppressing weak non-specific interactions.

Keywords: Small molecule, solubility, arginine, interaction analysis, aggregation suppression

1. Introduction

One of the important goals of protein-ligand interaction studies is discovery of novel small molecule ligands that bind to the target proteins and affect their functions (*1*). Such small molecules should help understand *in vitro* and *in vivo* functional roles of the proteins and may be developed as a therapeutic drug. A major problem in the analysis of ligand-protein interaction is a poor aqueous solubility of small molecules, instability of target proteins and non-specific ligand-protein interactions. There have been a number of studies to increase the solubility of small molecule drug substances, *e.g.*, micronization (*2*), generation of crystalline formulation (*3*), salt form with hydrophilic counterions (*4*), or formulation with delivery vehicles (*5-7*). Solvent additives, such as arginine, have also been used to enhance the solubility of the drug substances that had been formulated with cyclodextrins (*8,9*).

Aqueous solution of 0.1-2 M arginine at mildly acidic to neutral pH is widely used in biotechnology field and protein research, including protein refolding, purification and formulation (*10-16*). While arginine is not a protein stabilizer, it suppresses aggregation of proteins and non-specific interaction of proteins with chromatographic resins (*17-21*). In addition, arginine has been observed to increase the solubility of small molecules (*22-24*). In this review we wish to propose that arginine may prevent non-specific interactions between the small molecules and proteins and aggregation of the target proteins during interaction analysis, and thereby find applications in the drug discovery research.

2. Effects of arginine on small molecules

There is no systematic study of the effects of arginine on the solubility of small molecules and hence we summarize below the data mostly from our laboratories. Coumarin is used as an anti-coagulant and has a poor aqueous solubility (*25,26*). It is a small organic compound with a molecular weight of 146.15 and contains an aromatic ring structure (see Figure 1 for chemical structure). Figure 2 plots the solubility of coumarin as a function of additive concentration in 50 mM citrate-phosphate buffer, pH 7.5. It is evident that arginine and guanidine hydrochloride (GdnHCl) increase the coumarin solubility concentration-dependently to a similar degree. Arginine as well as GdnHCl at 1.0 M increased the coumarin solubility by about 2-fold. Considering the non-denaturing property of arginine and its safety, 1.0 M arginine should be a

**Address correspondence to:*
Dr. Tsutomu Arakawa, Alliance Protein Laboratories, 3957 Corte Cancion, Thousand Oaks, CA 91360, USA.
e-mail: tarakawa2@aol.com

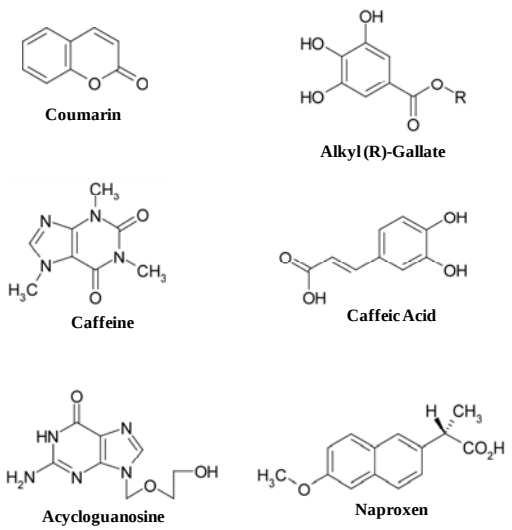

Figure 1. Chemical structure of small molecule drug substances.

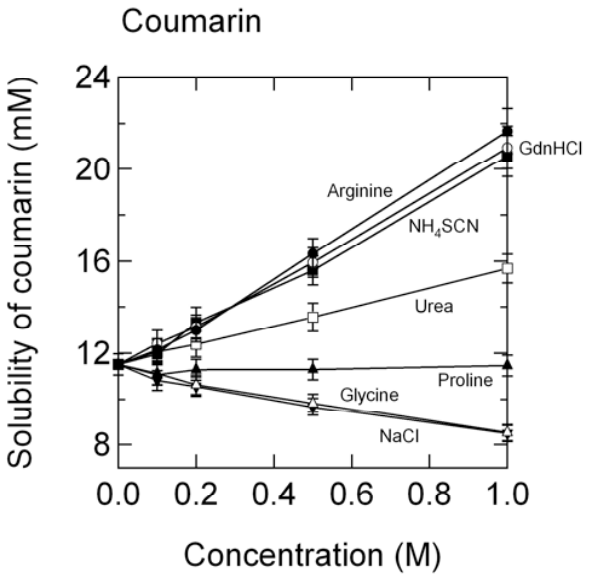

Figure 2. Solubility of coumarin in 50 mM citrate-phosphate buffer at pH 7.5. Closed circles, arginine; Open circles, GdnHCl; Closed squares, NH_4SCN; Open squares, urea; Closed triangles, proline; Open triangles, glycine; Closed inverse triangles, NaCl. The excess amounts of powder of coumarin were added into the stock aqueous additive solutions. Coumarin solutions were boiled at 100°C for 30 min, followed by incubation at 25°C for 2 h. After the incubation, the samples were centrifuged at 15,000 × g for 20 min at 20°C. The supernatants of the sample were diluted 20-fold with distilled water, and then the concentrations of soluble coumarin in the supernatant were measured by absorbance at 278 nm. Reformatted from *ref. 23*.

better additive, as GdnHCl may denature or destabilize the proteins when used in the interaction analysis. As shown in Figure 2, protein folding assisting osmolyte, proline (*27*), has essentially no effect on coumarin solubility at any concentration up to 1 M. Urea, a protein denaturant, is significantly less effective than GdnHCl at the same concentration, consistent with its weaker denaturing potency for proteins (*28*). Figure 2 also shows that another osmolyte, glycine, decreases the coumarin solubility. Other amino acids tested, *i.e.*, alanine, serine, and lysine, also decreased the coumarin solubility (data not shown). These four amino acids are similar, within experimental errors, to each other, decreasing the coumarin solubility by about 0.7-0.8-fold (data not shown). It is interesting to point out that a basic amino acid, lysine, decreased the coumarin solubility, in contrast to the effect of basic arginine. This demonstrates that the basic nature is not the factor responsible for the observed effectiveness of arginine.

Conversely, thiocyantates, salting-in salts, effectively increased the coumarin solubility (see Figure 2 for ammonium thiocyanate), ammonium salt being more effective than sodium salt (data not shown), consistent with their salting-in effects on proteins (*29-31*). Iodide salts were also slightly effective, with the magnitude similar to the effect observed for urea (data not shown). All the salting-out salts tested, *i.e.*, sulfate salts and chloride salts, decreased the coumarin solubility (data not shown), consistent with their known effects on protein solubility (*29-31*). Sulfate salts were most effective, consistent with the Hofmeister series of salts (*32,33*). Within the group of chloride salts, the salting-out effect increased in the order of $NH_4 < K \sim Li < Na$.

Gallic acid (3,4,5-trihydroxybenzoic acid) is obtained from nutgalls or other plants and fruits or by alkaline or acid hydrolysis of the tannins (see Figure 1 for chemical structure of alkyl-gallates) (*34-36*). Some of gallate derivatives have been extensively characterized in terms of physiological activities and cytotoxicities (*34-42*). Gallates are used as antioxidants in fats and oils and also used in cosmetics and, as food additives, in shortening, baked goods, candy and dried milk (*43*). Solubility of four different alkyl-gallates, *i.e.*, methyl-, ethy-, propyl-, and butyl-gallate, was measured in water as a function of arginine concentration and, for comparison, lysine concentration (*Hirano A, Kameda T, Arakawa T, Shiraki K, unpublished results*). Figure 3 plots the solubility ratio of these gallate derivatives as a function of arginine or lysine concentration. Arginine increased the solubility ratio of all 4 alkyl-gallates concentration-dependently (four closed symbols). It appears that the solubility enhancement by arginine is higher for more water-soluble methyl- and ethyl-gallate than the less soluble propyl- and butyl-gallate. As the alkyl-chain length increases in this order (*i.e.*, from methyl to butyl), the above results suggest that the solubility-enhancing effect of arginine is reduced with the increasing proportion of alkyl-chain length in the gallate-derivatives. In other words, arginine appears to interact with the aromatic structure in the gallates, leading to the enhanced solubility more effectively for shorter chain gallates, as has been observed (*44,45*). Conversely, the solubility-enhancing effect of lysine is marginal (four open symbols). Lysine increased the solubility of methyl- and ethyl-gallate only slightly, at

most 1.3-fold at 1 M and was ineffective for propyl- and butyl-gallate.

Arginine is also effective against a longer alkyl-chain gallate, *i.e.*, octyl-gallate, whose aqueous solubility is only ~ 0.072 mg/mL. The solubility increased by about 1.6- and 2.2-fold by the addition of 0.5 and 1 M arginine. On the contrary, NaCl decreased the solubility by ~ 30 and 50% at 0.5 and 1 M.

Hot water extracts of coffee exhibit strong antiviral and virucidal activities (*46*). Caffeine and caffeic acid are the components of coffee, which both also exhibit antiviral activities (*46-49*). Caffeic acid plays a role as an antioxidant (*50,51*) and exhibits various pharmacological activities as well as antiviral activities (*46,52-54*). Different from the compounds described above, caffeic acid is a weak acid (see Figure 1) and hence its solubility is not only solvent-dependent, but also pH-dependent. The deprotonated, charged state of caffeic acid is much more soluble than the protonated, uncharged state. Thus, the effects of 1 and 2 M arginine were examined in the pH range where the caffeic acid is mostly protonated, *i.e.*, between pH 3.5 and 5.0. At a given pH, 1 and 2 M arginine increased the solubility of caffeic acid by about 5- and 10-fold (data not shown) (*Hirano A, Shiraki K, Uozaki M, Koyama AH, Arakawa T, unpublished results*). Conversely, 1 M NaCl showed negligible effect and 2 M NaCl significantly decreased the solubility, indicating that ionic strength of arginine plays no major role in observed increased solubility. On the other hand, the solubility of caffeine was not affected by arginine (*Hirano A, Shiraki K, Uozaki M, Koyama AH, Arakawa T, unpublished results*), which may be due to its high aqueous solubility, namely, water may already be a good solvent for caffeine.

Acycloguanosine contains a partial nucleoside structure (see Figure 1) and is a potent antiherpetic agent, one of the most commonly used antiviral agents (*55-57*). It has a moderate aqueous solubility (1.5 mg/mL in 50 mM phosphate, pH 7.0). As acycloguanosine is a base (Figure 1), 50 mM phosphate was used to maintain the pH constant. The solubility of acycloguanosine in arginine was expressed as the solubility ratio, namely against the solubility in buffer. The solubility ratio is plotted in Figure 4 as a function of arginine concentration (*24*). Arginine up to 0.1 M showed no effect on the solubility of acycloguanosine, but significantly increased its solubility above 0.5 M. The solubility increased by 1.9- and 2.6-fold at 1 and 2 M.

We have described above that arginine by itself increases the solubility of small molecules in aqueous solution. The following example shows that arginine synergizes with other solubility enhancing additives. One of such solubility-enhancing additives uses the compound that binds or entraps the small molecule

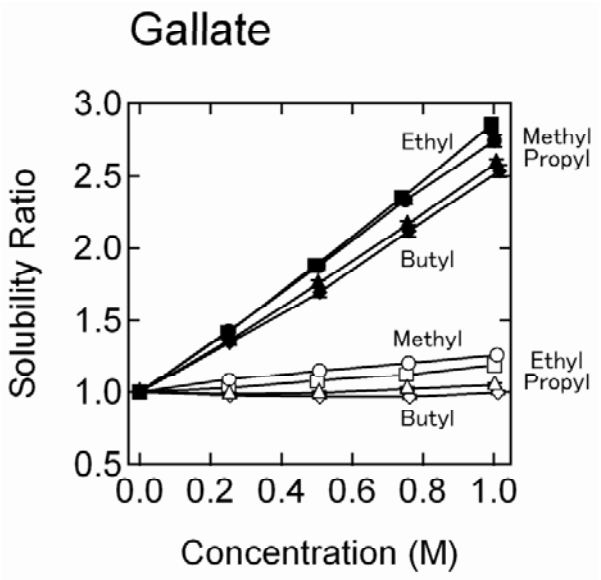

Figure 3. Solubility of alkyl gallates in aqueous lysine and arginine solutions. Ratio of the gallate solubility in the presence of additive to that in water is plotted. Closed symbols, solubility in aqueous arginine solutions; Open symbols, solubility in aqueous lysine solutions; Circle, methyl-gallate; Square, ethyl-gallate; Triangle, propyl-gallate; Diamond, butyl-gallate. Methyl-, ethyl-, propyl-, and butyl-galltes were dried in desiccators. Dried alkyl-galltes were transferred into test tubes, to which 0.5 mL of water or amino acid solutions were added. The suspension was heated at 40°C for 1 h with frequent vortex mixing, resulting in complete resolution of the gallate powders. The solution was then incubated at 25°C for 3 days with frequent vortex mixing, resulting in precipitation. The suspension was centrifuged at 25°C and 16,000 × g to obtain supernatant saturated with alkyl-gallate. After appropriate dilution with water, the absorbance of the supernatant was spectrophotometrically determined at 271 nm. The absorbance value was converted to the concentration based on the standard curve determined for each alkyl-gallate. The solubility thus determined was an average of triplicate experiments and the average and standard deviation were obtained. Reformatted from *Hirano A, Kameda T, Arakawa T, Shiraki K, unpublished results*.

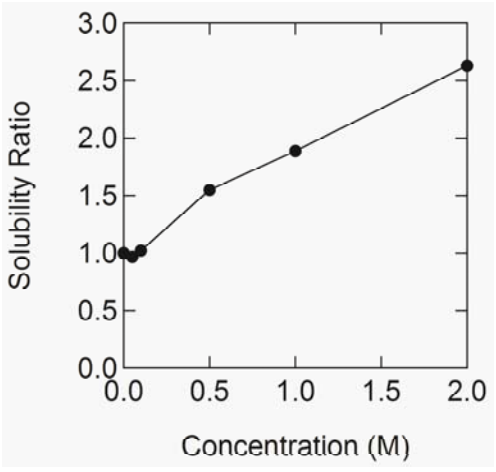

Figure 4. Solubility of acycloguanosine in aqueous arginine solution. About 5-10 mg of acycloguanosine were weighed into eppendolf tubes, into which 1 mL of test solvents in 50 mM phosphate, pH 7.0 was added. Such a strong buffer was required to minimize pH changes upon dissolution of basic acycloguanosine. The suspension was incubated at room temperature for 1 day with frequent vortexing and then centrifuged to separate supernatant. The supernatant was appropriately diluted with water for absorbance measurements. Concentration of acycloguanosine was spectrophotometrically determined at 252 nm. Reformatted from *ref. 24*.

drug. Cyclodextrin is often used as an additive for such purpose, but has limited application in pharmaceutical formulations due to low solubility and high molecular weight (*58*), although hydroxypropyl-β-cyclodextrin (HPC), a more water-soluble and low-cost derivative of cyclodextrin, has been developed. Mura and co-workers (*9,59*) have developed a novel system of multicomponent solution, termed ternary system that increases the solubility of a hydrophobic drug naproxen, a nonsteroidal anti-inflammatory drug (see Figure 1 for chemical structure), using cyclodextrin and amino acid, such as valine, lysine, and arginine, as solution additives. The solubility of naproxen is pH-dependent, due to the fact that naproxen is an acid with a carboxyl group (Figure 1). The solubility of naproxen as a protonated form is very low in acid (below 0.1 mg/mL) and increases with increasing pH by about 100-fold at neutral pH (data not shown), a similar observation for caffeic acid. Nevertheless, the solubility is still low at neutral pH in the absence of the additives (~ 2 mg/mL). When HPC and arginine were combined, both additives acted synergistically to the solubility of naproxen, leading to a 14-fold increase over the solubility of pH 6.9 control.

3. Effects of arginine on proteins

The solubility of small molecules may be increased by arginine. Small molecules solubilized by arginine at high concentrations may be diluted into a solution containing a target protein as well as other macromolecules (*e.g.* in the cell-based analysis). Therefore, it is critical to know how arginine affects the properties of the proteins. Here we summarize our current knowledge on the effects of arginine on proteins.

First, arginine increases the solubility of proteins. In general, salting-in effects are difficult to measure, compared to the salting-out effects, as most globular proteins are highly soluble in aqueous solution. To our knowledge, three poorly water-soluble proteins have been used to assess the ability of arginine to increase the solubility of protein, wheat flour gluten (*22*), S-carboxymethylated lysozyme (*60*) and fibroblast growth factor-20 (*15*). These proteins are barely soluble in aqueous salt solutions. Arginine concentration-dependently increased the gluten solubility up to ~ 3-fold at 1-2 M (data not shown). Interestingly, the magnitude of the increase is similar to that observed for small molecules. S-carboxymethylated lysozyme has a solubility below ~ 0.1 mg/mL in neutral phosphate buffer (*60*). Addition of 0.2 M arginine increased the solubility by about 4-fold, more so than 0.2 M urea or GdnHCl. Other amino acids were either ineffective or less effective (data not shown). Fibroblast growth factor-20 has an extremely low solubility in aqueous solution (*15*). The solubility in 50 mM phosphate buffer is below 0.5 mg/mL at any pH, nearly zero between pH 6.0 and 6.5. The addition of 0.2 M arginine in the same buffer greatly increased the solubility of the fibroblast growth factor-20. The solubility increased to above 1 mg/mL between pH 7.0 and 8.5, reaching 8 mg/mL at pH 5.5 (data not shown). The ability of arginine to increase the solubility of proteins has been utilized to extract insoluble proteins from inclusion bodies (*61-63*). Certain inclusion bodies of recombinant proteins, when expressed in *Escherichia coli*, occur from aggregation of native or native-like structures and can be readily solubilized by 0.2-2 M arginine at neutral pH in the native protein structure.

The solubilizing effect of arginine is consistent with its ability to suppress protein aggregation (*17-19*). Proteins often aggregate during storage and experiment due to various stresses, including such physical stresses as shaking, surface adsorption, pH and temperature fluctuation, concentration, and freezing and such chemical stresses as UV light and metals (*64,65*). Arginine has been used to suppress aggregation of proteins induced by these stresses (*16-19,65*).

Similarly, arginine has been used to suppress protein interactions with surfaces or chromatographic resins (*20,21,66*). Size exclusion chromatography of protein often suffers loss or retention of the proteins due to non-specific binding to the resins. Addition of 0.2-0.5 M arginine in the elution buffer (mobile phase) reduced such non-specific protein binding, leading to normal elution of loaded proteins (*21*). Hydrophobic interaction chromatography uses mildly hydrophobic groups (ligands) conjugated to the resins. Many proteins can only bind to the column in the presence of salting-out salts and elute during descending concentration of the salt. Arginine has been found to facilitate elution of the proteins with both high recovery and earlier elution (*66*). Also, arginine reduced the protein binding when included in the loading sample containing salting-out salts. Thus, arginine reduces hydrophobic interaction.

Such suppression of protein interaction by arginine has been observed for small molecules. Octyl-gallate is highly insoluble in water as described earlier, most likely due to its hydrophobic property. Arginine not only increased the solubility of octyl-gallate, but also inhibited its binding to bovine serum albumin (*24*). In other words, the free concentration of octyl-gallate was reduced by bovine serum albumin and was enhanced when arginine was included. A similar observation was made with a protonated form of caffeic acid. Caffeic acid was shown to bind to the plastic surface and such binding was reduced by arginine (*Hirano A, Shiraki K, Uozaki M, Koyama AH, Arakawa T, unpublished results*).

4. Potential applications

An obvious application of arginine in small molecule-protein interaction analysis is dissolution of small molecules by arginine, instead of organic solvents. As organic solvents are generally stronger in the

solubilization effectiveness, the final concentration in the interaction analysis may be lower than the arginine concentration that would be required and hence may not be high enough to denature the protein of interest. However, the target protein will be exposed to a transient high organic solvent concentration, which may be sufficient to cause protein denaturation. In addition, certain organic solvents are strong protein precipitant, and hence such a transient high concentration may cause irreversible protein aggregation. On the contrary, arginine does not denature proteins nor does it cause aggregation. It even suppresses protein aggregation.

Second potential application is inclusion of arginine to suppress non-specific protein-ligand interactions. Non-specific interactions of small molecules can cause the reduced effective concentration and false positives, as has been observed for benzofuran acyl-sulfonamide: this UDP-*N*-acetylmuramyl-L-alanine ligase inhibitor has been observed to bind to serum proteins (*67*). Arginine has been observed to suppress binding of octyl-gallate to bovine serum albumin (*24*). This raises a possibility that arginine may suppress weak, but specific, protein-ligand interactions, leaving only the strongly bound ligands in the protein-ligand complex.

Third potential application is to use arginine at 0.1-0.5 M level to prevent aggregation of target proteins or other proteins during the interaction analysis. Arginine is an effective suppressor of protein aggregation against various stresses as described above. This implies that care must be exercised for handling weakly associating oligomeric proteins. Arginine at 0.2 M has been found to cause dissociation of hemoglobin tetramer to the dimers (*Arakawa T, unpublished observation*).

Arginine may also prevent aggregation of small molecules. Small molecules have been observed to form a promiscuous cluster that presents non-polar surface, leading to non-specific binding of target proteins to the cluster (*68*). Inclusion of arginine in the interaction analysis may prevent such clustering of small molecules and also reduce non-specific interactions of the proteins with the cluster, if formed. Arginine has been observed to reduce non-specific binding of protein to chromatographic resins. In addition, arginine concentration-dependently prevented binding of caffeic acid to a plastic tube.

Finally, one of the ultimate goals of small molecule-protein interaction analysis may be the structure determination of the interacting complex. X-ray structure determination requires production of high quality crystals. Recently, arginine as well as some amino acids and their derivatives have been shown to assist production of high quality crystal of lysozyme, which otherwise tends to form amorphous precipitates. The effects of arginine to assist crystallization were ascribed to its suppressive effect on protein aggregation (*69,70*). Similarly, arginine assisted crystallization of hemoglobin (*71*).

5. Mechanism

Arginine increases the solubility of both small organic molecules and proteins as described above. The effects of arginine on protein solubility can be explained from its interaction with the proteins as determined by equilibrium dialysis and amino acid solubility measurements. Arginine shows an interaction pattern different from other solvent additives that enhance protein stability and decrease protein solubility (*72-75*). Salting-out salts are the typical additives, whose physical mechanisms can be explained by an increase in the surface tension of water. Namely, the higher the surface tension increment of water by the salts, the greater the decrease in the solubility of proteins is (*76*). Such correlation was also found in the solubility data for coumarin and caffeine as shown in Figure 5A (coumarin) and Figure 5B (caffeine). Although the data are somewhat scattering, there is a similar trend, *i.e.*, the more effectively the surface tension increase by the salts, the more they decrease the solubility of

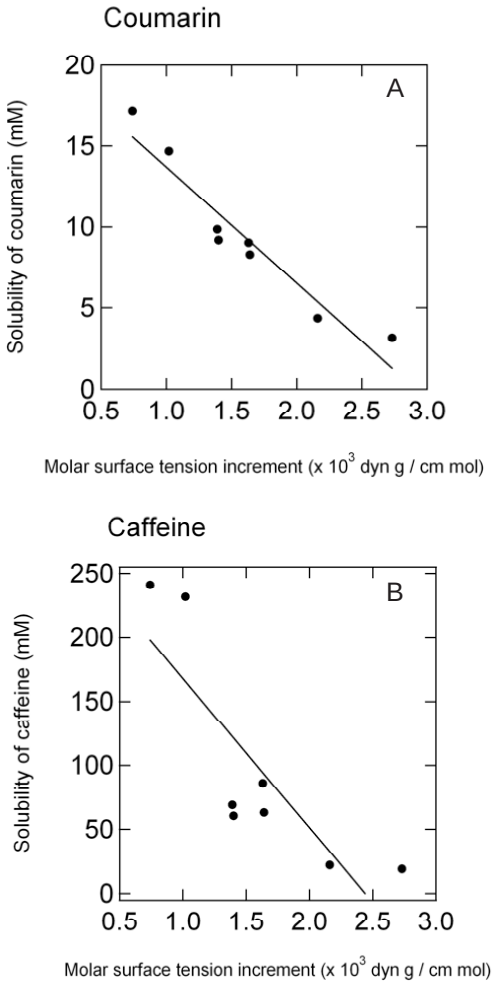

Figure 5. Correlation between the solubility of coumarin (A) or caffeine (B) and the molar surface tension increment. Linear lines indicate the least-square fitting of the line with correlation coefficients of –0.9573 ± 0.0006 (**A**, coumarin) and –0.8345 ± 0.0024 (**B**, caffeine).

coumarin and caffeine. The mechanism of surface tension effect is due to interfacial free energy at the molecule surface. Surface tension of water creates the surface free energy at the interface between water and the compound. The free energy becomes greater with increasing surface tension, as schematically shown in Figure 6. The solubility of the compound is determined by the difference in the free energy between the liquid phase and the solid phase. Here it is assumed that the precipitate has a lower interfacial free energy than the soluble form, as the surface area per compound is smaller in precipitate than in the soluble form. Smaller interface of the precipitate also means that the increment of the interfacial free energy, upon transfer of the precipitate from water to salt solution, is smaller than that of the soluble form, as shown in Figure 6 (*lower panel*). Thus, the free energy difference between the soluble form and precipitate phase is larger in salting-out salt solution than in water, leading to decreased solubility of the compound.

This mechanism, however, does not apply for arginine, as it also increases the surface tension of water (*73*). This is exactly identical to the case of urea that also increases the surface tension of water, yet is a solubilizing agent (*76*). Urea binding has been used to explain its solubilizing and denaturing effects (*76-78*). Can binding also explain the arginine effects? Preferential interaction measurements suggest such possibility for proteins (*72-75*). Formation of arginine clusters and their binding to proteins were also suggested (*79*). A plenty of evidence exists for binding of arginine with π-electron of aromatic ring structures (*44,45,80*). The chemical structures of some of the compounds used here are shown in Figure 1. Such binding mechanism clearly applies to coumarin, alkyl-gallates, caffeic acid and naproxen. Due to this mechanism, solubilization could be most likely observed for small molecules containing one or more aromatic ring structures. It is not clear whether arginine can increase the solubility of non-aromatic compounds. It is possible that arginine may not increase the solubility of non-aromatic compounds, but may suppress their binding to proteins, if the protein contains aromatic groups involved in binding non-aromatic compounds. Although acycloguanosine and caffeine have a similar structure without aromatic ring structures, only acycloguanosine solubility increased in the presence of arginine. This may be due to the different electrostatic properties between the two compounds. It suggests, however, that aromatic ring structure may not be an absolute requirement for arginine to exert solubilizing effects. Thus, more studies are required to fully understand how arginine interacts with the small molecules. We have initiated molecular dynamic simulation to examine molecular detail of the interactions between gallates and arginine (*Hirano A, Kameda T, Arakawa T, Shiraki K, unpublished results*).

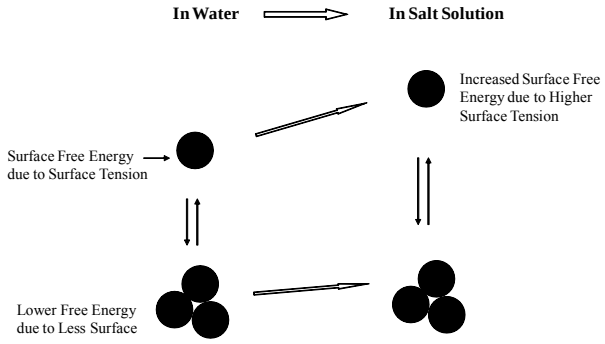

Figure 6. Schematic diagram of free energy of a compound in soluble form (*upper panel*) and in precipitate (*lower panel*) in the absence (*left panel*) and presence (*right panel*) of salting-out salt.

6. Conclusion

We have summarized the effects of arginine on small molecules and proteins. Arginine increases the solubility of proteins and small molecules and suppresses protein-protein and protein-surface interactions. These effects of arginine may find application in the analysis of drug-protein interactions and in solubilization of small molecules, and suppressing aggregation of target proteins and non-specific interactions.

References

1. Fuentes G, Oyarzabai J, Rojas AM. Databases of protein-protein interactions and their use in drug discovery. Curr Opin Drug Discov Devel. 2009; 12:358-366.
2. Chaumeil JC. Micronization: A method of improving the bioavailablilty of poorly soluble drugs. Methods Find Exp Clin Pharmacol. 1998; 20:211-215.
3. Blagden N, de Matas M, Gavan PT, York P. Crystal engineering of active pharmaceutical ingredients to improve solubility and dissolution rates. Adv Drug Deliv Rev. 2007; 59:617-630.
4. Agharkar S, Lindenbaum S, Higuchi T. Enhancement of solubility of drug salts by hydrophilic counter ions: Properties of organic salts of an antimalarial drug. J Pharm Sci. 1976; 65:747-749.
5. Amin K, Dannenfelser RM, Zielinski J, Wang B. Lyophilization of polyethylene glycol mixtures. J Pharm Sci. 2004; 93:2244-2249.
6. Torchillin VP. Micellar nanocarriers: Pharmaceutical perspectives. Pharm Res. 2007; 24:1-16.
7. Humberstone AJ, Charman WN. Lipid-based vehicles for the oral delivery of poorly water soluble drugs. Adv Drug Deliv Rev. 1997; 25:103-128.
8. Rajewski RA, Stella VJ. Pharmaceutical applications of cyclodextrins. 2. *In vivo* drug delivery. J Pharm Sci. 1996; 85:1142-1169.
9. Mura P, Maestrelli F, Cirri M. Ternary systems of naproxen with hydroxypropyl-beta-cyclodextrin and aminoacids. Int J Pharm. 2003; 260:293-302.
10. Buchner J, Rudolph R. Renaturation, purification and characterization of recombinant Fab-fragments produced

in *Escherichia coli*. Biotechnology (N Y). 1991; 9:157-162.
11. Arora D, Khanna N. Method for increasing the yield of properly folded recombinant human gamma interferon from inclusion bodies. J Biotechnol. 1996; 52:127-133.
12. Arakawa T, Philo JS, Tsumoto K, Yumioka R, Ejima D. Elution of antibodies from a Protein-A column by aqueous arginine solutions. Protein Expr Purif. 2004; 36:244-248.
13. Yumioka R, Tsumoto K, Arakawa T, Ejima D. Screening of effective column rinse solvent for Protein-A chromatography. Protein Expr Purif. 2010; 70:218-223.
14. Arakawa T, Kita Y, Sato H, Ejima D. MEP chromatography of antibody and Fc-fusion protein using aqueous arginine solution. Protein Expr Purif. 2009; 63:158-163.
15. Maity H, Karkaria C, Davagnino J. Effects of pH and arginine on the solubility and stability of a therapeutic protein (Fibroblast Growth Factor 20): Relationship between solubility and stability. Curr Pharm Biotechnol. 2009; 10:609-625.
16. Arakawa T, Dix DB, Chang BS. The effects of protein stabilizers on aggregation induced by multiple-stresses. Yakugaku Zasshi. 2003; 123:957-961. (in Japanese)
17. Arakawa T, Tsumoto K. The effects of arginine on refolding of aggregated proteins: Not facilitate refolding, but suppress aggregation. Biochem Biophys Res Commun. 2003; 304:148-152.
18. Tsumoto K, Ejima D, Kita Y, Arakawa T. Review: Why is arginine effective in suppressing aggregation? Protein Pept Lett. 2005; 12:613-619.
19. Arakawa T, Ejima D, Tsumoto K, Obeyama N, Tanaka Y, Kita Y, Timasheff SN. Suppression of protein interactions by arginine: A proposed mechanism of the arginine effects. Biophys Chem. 2007; 127:1-8.
20. Arakawa T, Tsumoto K, Nagase K, Ejima D. The effects of arginine on protein binding and elution in hydrophobic interaction and ion-exchange chromatography. Protein Expr Purif. 2007; 54:110-116.
21. Ejima D, Yumioka R, Arakawa T, Tsumoto K. Arginine as an effective additive in gel permeation chromatography. J Chromatogr A. 2005; 1094:49-55.
22. Arakawa T, Kita Y, Koyama AH. Solubility enhancement of gluten and organic compounds by arginine. Int J Pharm. 2008; 355:220-223.
23. Hirano A, Arakawa T, Shiraki K. Arginine increases the solubility of coumarin: Comparison with salting-in and salting-out additives. J Biochem. 2008; 144:363-369.
24. Arakawa T, Uozaki M, Koyama AH. Modulation of small molecule solubility and protein binding by arginine. Mol Med Report. 2010; 3:833-836.
25. Kamali F, Pirmohamed M. The future prospects of pharmacogenetics in oral anticoagulation therapy. Br J Clin Pharmacol. 2006; 61:746-751.
26. Thacker SM, Grice GR, Milligan PE, Gage BF. Dosing anticoagulant therapy with coumarin drugs: Is genotyping clinically useful? Yes. J Thromb Haemost. 2008; 6:1445-1449.
27. Samuel D, Kumar TK, Jayaraman G, Yang PW, Yu C. Proline is a protein solubilizing solute. Biochem Mol Biol Int. 1997; 41:235-242.
28. Nozaki Y, Tanford C. The solubility of amino acids and related compounds in aqueous urea solutions. J Biol Chem. 1963; 238:4074-4081.
29. Baldwin RL. How Hofmeister ion interactions affect protein stability. Biophys J. 1996; 71:2056-2063.
30. Hofmeister F. Zur Lehre von der Wirkung der Salze. Naunyn Schmiedebergs Arch Exp Pathol Pharmakol. 1888; 24:247-260. (in German)
31. Melander W, Horváth C. Salt effect on hydrophobic interactions in precipitation and chromatography of proteins: An interpretation of the lyotropic series. Arch Biochem Biophys. 1977; 183:200-215.
32. Arakawa T, Timasheff SN. Preferential interactions of proteins with salts in concentrated solution. Biochemistry. 1982; 21:6545-6552.
33. Arakawa T, Timasheff SN. Mechanism of protein salting in and salting out by divalent cation salts: Balance between hydration and salt binding. Biochemistry. 1984; 23:5912-5923.
34. Xu J, Wang J, Deng F, Hu Z, Wang H. Green tea extract and its major component epigallocatechin gallate inhibits hepatitis B virus *in vitro*. Antiviral Res. 2008; 78:242-249.
35. Ahn YJ, Lee HS, Oh HS, Kim HT, Lee YH. Antifungal activity and mode of action of *Galla rhois*-derived phelolics against phytopathogenic fungi. Pestic Biochem Physiol. 2005; 81:105-112.
36. Uozaki M, Yamasaki H, Katsuyama Y, Higuchi M, Higuti T, Koyama AH. Antiviral effect of octyl gallate against DNA and RNA viruses. Antiviral Res. 2007; 73:85-91.
37. Ow YY, Stupans I. Gallic acid and gallic acid derivatives: Effects on drug metabolizing enzymes. Curr Drug Metab. 2003; 4:241-248.
38. van der Heijden CA, Janssen PJ, Strik JJ. Toxicology of gallates: A review and evaluation. Food Chem Toxicol. 1986; 24:1067-1070.
39. Bub A, Watzl B, Blockhaus M, Briviba K, Liegibel U, Müller H, Pool-Zobel BL, Rechkemmer G. Fruit juice consumption modulates antioxidative status, immune status and DNA damage. J Nutr Biochem. 2003; 14:90-98.
40 Chung KT, Wong TY, Wei CI, Huang YW, Lin Y. Tannins and human health: A review. Crit Rev Food Sci Nutr. 1998; 38:421-464.
41. Isaacs CE, Wen GY, Xu W, Jia JH, Rohan L, Corbo C, Di Maggio V, Jenkins EC Jr, Hillier S. Epigallocatechin gallate inactivates clinical isolates of herpes simplex virus. Antimicrob Agents Chemother. 2008; 52:962-970.
42. Cowan MM. Plant products as antimicrobial agents. Clin Microbiol Rev. 1999; 12:564-582.
43. Surh Y. Molecular mechanisms of chemopreventive effects of selected dietary and medicinal phenolic substances. Mutat Res. 1999; 428:305-327.
44. Woods AS. The mighty arginine, the stable quaternary amines, the powerful aromatics, and the aggressive phosphate: Their role in the noncovalent minuet. J Proteome Res. 2004; 3:478-484.
45. Nakakido M, Tanaka Y, Mitsuhori M, Kudou M, Ejima D, Arakawa T, Tsumoto K. Structure-based analysis reveals hydration changes induced by arginine hydrochloride. Biophys Chem. 2008; 137:105-109.
46. Utsunomiya H, Ichinose M, Uozaki M, Tsujimoto K, Yamasaki H, Koyama AH. Antiviral activities of coffee extracts *in vitro*. Food Chem Toxicol. 2008; 46:1919-1924.
47. Yamazaki Z, Tagaya I. Antiviral effects of atropine and caffeine. J Gen Virol. 1980; 50:429-431.
48. Shiraki K, Rapp F. Effects of caffeine on herpes simplex virus. Intervirology. 1988; 29:235-240.

49. Murayama M, Tsujimoto K, Uozaki M, Katsuyama Y, Yamasaki H, Utsunomiya H, Koyama AH. Effect of caffeine on the multiplication of DNA and RNA viruses. Mol Med Report. 2008; 1:251-255.
50. Tapiero H, Tew KD, Ba GN, Methé G. Polyphenols: Do they play a role in the prevention of human pathologies? Biomed Pharmacother. 2002; 56:200-207.
51. Yoshida Y, Hayakawa M, Niki E. Evaluation of the antioxidant effects of coffee and its components using the biomarkers hydroxyoctadecadienoic acid and isoprostane. J Oleo Sci. 2008; 57:691-697.
52. Chiang LC, Chiang W, Chang MY, Ng LT, Lin CC. Antiviral activity of *Plantago* major extracts and related compounds *in vitro*. Antiviral Res. 2002; 55:53-62.
53. Benković V, Orsolić N, Knezević AH, Ramić S, Dikić D, Basić I, Kopjar N. Evaluation of the radioprotective effects of propolis and flavonoids in gamma-irradiated mice: The alkaline comet assay study. Biol Pharm Bull. 2008; 31:167-172.
54. Vlietinck AJ, De Bruyne T, Apers S, Pieters LA. Plant-derived leading compounds for chemotherapy of human immunodeficiency virus (HIV) infection. Planta Med. 1998; 64:97-109.
55. Dawson CR, Beck R, Wilhelmus KR, Cohen EJ. Herpetic eye disease study. You can help. Arch Ophthalmol. 1996; 114:89-90.
56. Shiraki K, Kurokawa M. Antiherpetic chemotherapy. Nippon Rinsho. 2000; 58:939-943. (in Japanese)
57. Shiraki K. Antiherpetic chemotherapeutic drugs. Nippon Rinsho. 2003; 61:792-797. (in Japanese)
58. Loftsson T, Brewster ME. Pharmaceutical applications of cyclodextrins. 1. Drug solubilization and stabilization. J Pharm Sci. 1996; 85:1017-1025.
59. Mura P, Bettinetti GP, Cirri M, Maestrelli F, Sorrenti M, Catenacci L. Solid-state characterization and dissolution properties of naproxen-arginine-hydroxypropyl-beta-cyclodextrin ternary system. Eur J Pharm Biopharm. 2005; 59:99-106.
60. Matsuoka T, Hamada H, Matsumoto K, Shiraki K. Indispensable structure of solution additives to prevent inactivation of lysozyme for heating and refolding. Biotechnol Prog. 2009; 25:1515-1524.
61. Tsumoto K, Umetsu M, Kumagai I, Ejima D, Arakawa T. Solubilization of active green fluorescent protein from insoluble particles by guanidine and arginine. Biochem Biophys Res Commun. 2003; 312:1383-1386.
62. Umetsu M, Tsumoto K, Nitta S, Adschiri T, Ejima D, Arakawa T, Kumagai I. Nondenaturing solubilization of beta2 microglobulin from inclusion bodies by L-arginine. Biochem Biophys Res Commun. 2005; 328:189-197.
63. Tsumoto K, Abe R, Ejima D, Arakawa T. Non-denaturing solubilization of inclusion bodies. Curr Pharm Biotechnol. 2010; 11:309-312.
64. Wang W. Protein aggregation and its inhibition in biopharmaceutics. Int J Pharm. 2005; 289:1-30.
65. Maity H, O'Dell C, Srivastava A, Goldstein J. Effects of arginine on photostability and thermal stability of IgG1 monoclonal antibodies. Curr Pharm Biotechnol. 2009; 10:761-766.
66. Tsumoto K, Ejima D, Nagase K, Arakawa T. Arginine improves protein elution in hydrophobic interaction chromatography. The cases of human interleukin-6 and activin-A. J Chromatogr A. 2007; 1154:81-86.
67. Ehmann DE, Demeritt JE, Hull KG, Fisher SL. Biochemical characterization of an inhibitor of *Escherichia coli* UDP-*N*-acetylmuramyl-L-alanine ligase. Biochim Biophys Acta. 2004; 1698:167-174.
68. Coan KE, Maltby DA, Burlingame AL, Shoichet BK. Promiscuous aggregate-based inhibitors promote enzyme unfolding. J Med Chem. 2009; 52:2067-2075.
69. Ito L, Shiraki K, Yamaguchi H. Comparative analysis of amino acids and amino-acid derivatives in protein crystallization. Acta Crystallogr Sect F Struct Biol Cryst Commun. 2010; 66:744-749.
70. Ito L, Shiraki K, Yamaguchi H. Amino acids and glycine ethyl ester as new crystallization reagents for lysozyme. Acta Crystallogr Sect F Struct Biol Cryst Commun. 2010; 66:750-754.
71. Ito L, Kobayashi T, Shiraki K, Yamaguchi H. Effect of amino acids and amino acid derivatives on crystallization of hemoglobin and ribonuclease A. J Synchrotron Radiat. 2008; 15:316-318.
72. Kita Y, Arakawa T, Lin TY, Timasheff SN. Contribution of the surface free energy perturbation to protein-solvent interactions. Biochemistry. 1994; 33:15178-15189.
73. Lin TY, Timasheff SN. On the role of surface tension in the stabilization of globular proteins. Protein Sci. 1996; 5:372-381.
74. Arakawa T, Kita Y, Ejima D, Tsumoto K, Fukada H. Aggregation suppression of proteins by arginine during thermal unfolding. Protein Pept Lett. 2006; 13:921-927.
75. Schneider CP, Trout BL. Investigation of cosolute-protein preferential interaction coefficient: New insight into the mechanism by which arginine inhibits aggregation. J Phys Chem B. 2009; 113:2050-2058.
76. Breslow R, Guo T. Surface tension measurements show that chaotropic salting-in denaturants are not jusy water-structure breakers. Proc Natl Acad Sci U S A. 1990; 87:167-169.
77. Prakash V, Loucheux C, Scheufele S, Gorbunoff MJ, Timasheff SN. Interactions of proteins with solvent components in 8 M urea. Arch Biochem Biophys. 1981; 210:455-464.
78. Timasheff SN, Xie G. Preferential interactions of urea with lysozyme and their linkage to protein denaturation. Biophys Chem. 2003; 105:421-448.
79. Das U, Hariprasad G, Ethayathulla AS, *et al*. Inhibition of protein aggregation: Supramolecular assemblies of arginine hold the key. PLoS One. 2007; 2:e1176.
80. Crowley PB, Golovin A. Cation-pi interactions in protein-protein interfaces. Proteins. 2005; 59:231-239.

(Received June 27, 2010; Revised August 6, 2010; Accepted August 7, 2010)

Original Article

Anti-hyperlipidemic activity of *Withania coagulans* in streptozotocin-induced diabetes: A potent anti-atherosclerotic agent

Bhagawati Saxena*

Pharmacology Research laboratory, Department of Pharmaceutics, Meerut Institute of Engineering and Technology, Meerut, India.

ABSTRACT: Dyslipidemia is one of the most common complications in diabetes mellitus, which increases risk of premature atherosclerosis. Drugs having antihyperlipidemic activity in addition to their hypoglycemic effect in diabetes may be suitable anti-atherosclerotic agents in diabetic patients. The present study was aimed to investigate the anti-atherosclerotic activity of an aqueous extract of *Withania coagulans* (AWC) in terms of atherogenic index (AI) in normal and streptozotocin (STZ)-induced diabetes. AWC (1,000 mg/kg body weight, BW) was orally administrated in normal and STZ (70 mg/kg)-induced diabetic rats and levels of glucose, total cholesterol (CHL), high density lipoprotein (HDL)-cholesterol and triglyceride (TG) levels in the plasma were analyzed spectrophotometrically. BW was measured and AI was calculated in each group. Results show that after sub-chronic dosing, AWC reduced plasma glucose levels both in normal and diabetic rats, while significantly decreasing plasma levels of CHL, HDL and TG only in STZ-induced diabetic rats. Repeated administration of AWC also significantly decreased AI and prevented weight loss in STZ-induced diabetic animals. Hence, AWC showed anti-hyperlipidemic activity in diabetic rats and was suggested to be a suitable candidate for the treatment of atherosclerosis associated with diabetes.

Keywords: *Withania coagulans*, diabetes, anti-hyperlipidemic, hypoglycemic, atherosclerosis

1. Introduction

Diabetes mellitus, an endocrine disorder, is a major source of morbidity in developed countries. The number of people with diabetes mellitus is rapidly increasing worldwide. There is a report by the International Diabetes and Federation in the year 2005 which shows that more than 150 million people are suffering from diabetic disease. Diabetes patients show several complications including coronary insufficiency, cerebrovascular, peripheral vascular disease, neuropathy, retinopathy, and nephropathy *etc.* (*1,2*). Diabetes and its associated complications are the major cause of disability and hospitalization which ultimately results in a significant financial burden. One of the complications of diabetes is dyslipidemia (alterations in the plasma lipid and lipoprotein profile). Dyslipidemia is one of the most common complications in diabetes mellitus, which is found in about 40% of diabetic patients. Abnormality in lipid profile increases risk of premature atherosclerosis, coronary and myocardial infarction (*3*), which is a major cause of cardiovascular (CV) morbidity and mortality in diabetic patients (*4-6*). Thus, an anti-diabetic drug having a favorable effect on lipid profile would be beneficial in the treatment of lipid abnormalities and the accompanying premature atherosclerosis of CV disease in diabetic patients.

Currently there is no oral antidiabetic drug approved for the treatment of diabetes which has a favorable effect on CV disease (*7*). Some of the available oral anti-diabetic drugs are associated with serious adverse effects (*8,9*). Injection of insulin to treat type 1 diabetes has its own limitations (*10*). Thus, there emerges the need for new, relatively non-toxic, therapeutic agents for the treatment of hyperglycemia, which also would be able to correct dyslipidemia and reduce the risk of CV complications of diabetes. With growing emphasis on therapy of dyslipidemia associated with diabetes and a need to develop drugs which do not have side effects and which avoid recurrences of cardiovascular diseases associated with diabetes on drug withdrawal, researchers during the last decade started to investigate several indigenous plants. There is a need to explore more indigenous plants through application of modern evaluation protocols, so as to evaluate the ability of these plants in the treatment of atherosclerosis associated with the diabetes. In ayurveda many indigenous plants have been mentioned and well established as anti-atherosclerotic agents. Yet there

**Address correspondence to:*
Bhagawati Saxena, P-18, New Medical Enclave, B.H.U., Varanasi-221005 (U.P.), India.
e-mail: bsaxenapharm@gmail.com

is a paucity of information regarding the activity of *Withania coagulans* in atherosclerosis. Thus this study was undertaken to fulfill the lacunae in this regard.

Withania coagulans Dunal (Family: Solanaceae) is commonly known as Indian cheese and is found in drier parts of India. Different parts of this plant have been reported to possess a variety of ethnopharmacological activities (*11*). Traditional healers in Varanasi and its surrounding area, use dry fruits of *Withania coagulans* for the treatment of diabetic patients. The hypoglycemic activity of an aqueous extract of the fruit of *Withania coagulans* (AWC) was previously demonstrated in streptozotocin (STZ)-induced diabetic rats (*12*). There is no report showing an anti-hyperlipidemic and anti-atherosclerotic effect of AWC in STZ-induced diabetes.

For this reason, in our present investigation we evaluated AWC for its hypolipidemic activity such as reduction in plasma total cholesterol (CHL) and triglycerides (TG) levels, body weight as well as atherogenic index after oral administration, in normal as well as STZ-diabetic rats, using the latter animals as a model for human type 1 diabetes (*13*) for elucidating its activity in atherosclerosis associated with diabetes. The sulfonylurea, glibenclamide (GLB), and the semi-essential amino acid taurine (TR) were used as reference compounds.

2. Materials and Methods

2.1. *Chemicals*

STZ, taurine and glibenclamide were procured from Sigma-Aldrich, St. Louis, MO, USA. All other chemicals used were of analytical grade.

2.2. *Plant material*

Dried fruits of *Withania coagulans* were purchased from the market and identified by chief botanist of TAMPCOL Arumbakkam, Chennai. The fruits (with persistent calyx and pedicle) were coarsely powdered and boiled with distilled water repeatedly. The aqueous extract was concentrated and dried in a vacuum dessicator. The dried extract, which was dark brown in color with coca-like smell was dissolved in distilled water and used for experimental work.

2.3. *Animals*

Male Albino rats were purchased from Central Drug Research Institute, Lucknow, Uttar Pradesh, India. The body weights of the animal ranged between 175 and 225 g. The rats were housed in polypropylene cages (one in each cage) at an ambient temperature of 25 ± 2°C and 55-60% relative humidity. The animals were acclimatized to in-house conditions and were fed a commercial pellet diet (Hindustan Lever Ltd., Bangalore, India) and water *ad libitum*. The experimental protocol was undertaken in accordance with "Principles of laboratory animal care" (NIH publication number 85-23, revised 1985) guidelines.

2.4. *Experimental induction of diabetes in rats*

Diabetes was induced in animals by intraperitoneal administration of a freshly prepared solution of STZ dissolved in citrate buffer (0.1 M, pH 4.5) at a dose of 70 mg/kg body weight to overnight fasted animals. Blood glucose levels were determined 72 h after STZ injection. Rats with stable (yield = 90-95%) (up to three days) blood glucose levels above 250 mg% were selected to use in further studies.

2.5. *Experimental treatment protocol*

Normal and STZ-diabetic rats were randomly assigned to groups of six each. The acute study consists of four normal and four diabetic groups while subchronic study includes four normal and four diabetic groups. Among the four groups of acute study, one received a single oral dose of distilled water, a second group received AWC at a dose of 1,000 mg/kg of body weight (BW), while the third and fourth groups received the first reference compound taurine (TR) (10 mg/kg) and the second reference drug glibenclamide (GLB) (10 mg/kg) respectively. Similarly, the four groups of STZ-diabetic rats received water, AWC, TR and GLB, at the same doses described above, respectively. Selection of the dose of AWC was based upon a previous study done by Hemalatha *et al.* (*12*) in which AWC at the stated dose showed considerable hypoglycemic activity in normal and diabetic rats. For the sub-chronic treatment, groups of normal and STZ-induced diabetic rats received oral doses (by gavage) of water or the three test materials (AWC, TR and GLB) daily for 28 days. For the acute study, blood was collected before administered dose (0 h) and then at 6 h after the single dose. For the sub-chronic study, blood samples were collected before treatment *i.e.*, for baseline estimation (D0), after 14 days of treatment (D14) and after 28 days of treatment (D28). Plasma, obtained by centrifugation, was stored at −20°C until analyzed for glucose, plasma high density lipoprotein (HDL)-cholesterol and TG levels.

2.6. *Analytical methods*

Blood glucose (collected at 0 and 6 h post dose in the single dose study and 6 h post dose on D0, D14 and D28 in the sub-chronic study), total cholesterol, HDL-cholesterol and triglyceride levels in serum (6 h post dose on D0, D14 and D28 in the sub-chronic study) were measured spectrophotometrically with the Span Diagnostic kit (Span Diagnostics Ltd., Surat, India). Atherogenic index was calculated by using the

following formula (*14*):

Atherogenic index = (CHL – HDL-cholesterol)/ HDL-cholesterol

2.7. *Statistical analysis*

All grouped data were statistically evaluated with SigmaStat 3.5 software. Hypothesis testing methods included one way analysis of variance (ANOVA) followed by Dunnett test for more than two groups while using student's *t*-test for two groups. $p < 0.05$ was considered to indicate statistical significance. All the results were expressed as mean ± S.E.M. for six animals in each group.

3. Results

3.1. *Effect of a single (acute) and sub-chronic oral doses of test substances (AWC, TR, and GLB) on body weight*

Effect of a single (acute) and sub-chronic oral doses of test substances (AWC, TR, and GLB) on body weight are shown in Table 1. In normal rats, body weight significantly ($p < 0.05$) increased after 28 days treatment with distilled water, AWC, TR as well as GLB compared to the baseline (D0) values. There was no significant difference in weights between the treatment groups. However, in the STZ-diabetic rats, a very significant ($p < 0.05$) weight loss occurred in rats that were given water. The TR group also showed a slight but significant ($p < 0.05$) loss in body weight. On the other hand, there was no change in the weight of rats given daily doses of AWC. GLB administration caused a small but significant ($p < 0.05$) increase in body weight.

3.2. *Effect of a single (acute) and sub-chronic oral doses of test substances (AWC, TR and GLB) on plasma glucose levels*

The effect of single (acute) oral doses of water (10 mL/kg) and the test materials (AWC, TR, and GLB) on blood glucose levels in normal and STZ-diabetic rats is presented in Table 2; the values are compared with the baseline values (before treatment). In normal rats, with a single dose of water, AWC caused little decrease (not significant) in plasma glucose levels but a significant ($p < 0.05$) decrease occurred in glucose levels with TR. GLB had no effect. In the diabetic rats, two standard drugs TR and GLB showed significant ($p < 0.05$) hypoglycemia. TR produced normal glycemia post dose. With GLB glucose levels remained slightly higher than the normal values.

The effect of daily oral dosing for 28 days with the test materials (AWC, TR, and GLB) and water at the doses indicated above on blood glucose levels in normal and STZ-induced diabetic rats is presented in Table 3. The values are compared with the baseline values (D0). In normal rats, daily dosing with the AWC reduced plasma glucose significantly ($p < 0.05$) after 14 days as well as 28 days. The hypoglycemic response to TR was significant ($p < 0.05$) after 28 days. Administration of GLB, like water, had no effect on plasma glucose levels. In the diabetic rats, daily dosing with AWC produced significant hypoglycemia ($p < 0.05$) on D14 as well as on D28. Rats became normoglycemic after 2 weeks of daily treatment with levels going down further at the end of the 28 days of treatment. GLB treatment reduced glucose levels on D14, but the decrease was far less than that produced by AWC. Continuous administration of GLB resulted in a further decrease ($p < 0.05$) in glucose levels. After 28 days of treatment, once again the reduction was not as great as with AWC, and the rats did not achieve normoglycemia even after 4 weeks of continuous treatment. TR significantly ($p < 0.05$) reduced glucose levels after 2 weeks. However, normoglycemia was achieved after 28 days of treatment

Table 1. Effect of repeated daily oral treatment with the aqueous extract of *Withania coagulance* (AWC), taurine (TR) and glibenclamide (GLB) on body weight in normal and STZ-induced diabetic rats

Treatment	Dose (mg/kg)	Body weight (g)	
		D0	D28
Normal			
Water	a	201.2 ± 2.8	251.5 ± 5.4*
AWC	1,000	198.4 ± 3.8	236.7 ± 9.6*
TR	10	228.6 ± 1.5	273.1 ± 4.8*
GLB	10	187.4 ± 2.7	218.3 ± 6.3*
STZ-induced diabetic rats			
Water	a	223.3 ± 1.7	191.9 ± 2.4*
AWC	1,000	249.1 ± 10.2	237.0 ± 13.8
TR	10	210.2 ± 1.6	195.5 ± 1.4*
GLB	10	197.6 ± 9.2	224.7 ± 4.3*

The values are expressed as mean ± S.E.M. ($n = 6$). a: 10 mL/kg. * $p < 0.05$, when compared to baseline values. Data of D0 and D28 were analyzed within the treatment groups by *t*-test.

Table 2. The effect of a single oral dose of aqueous extract of *Withania coagulance* (AWC), taurine (TR), and glibenclamide (GLB) on plasma glucose levels after acute oral administration in normal and STZ-diabetic rats

Treatment	Dose (mg/kg)	Plasma glucose level (mg%)	
		Before treatment	After treatment
Normal			
Water	a	94.6 ± 2.9	93.5 ± 3.1
AWC	1,000	93.5 ± 4.5	81.9 ± 2.1
TR	10	95.5 ± 1.6	77.4 ± 0.8*
GLB	10	96.5 ± 1.3	98.3 ± 2.4
STZ-induced diabetic rats			
Water	a	303.4 ± 6.6	288.0 ± 2.5
AWC	1,000	330.3 ± 5.2	307.8 ± 4.7
TR	10	365.2 ± 5.0	106.6 ± 3.6*
GLB	10	370.8 ± 2.5	191.9 ± 9.5*

The values are expressed as mean ± S.E.M. ($n = 6$). a: 10 mL/kg. * $p < 0.05$, when compared to baseline values. Data of treatment groups before treatment and after treatment were analyzed by *t*-test.

with TR. Water had no significant effect on glucose levels. Since acute administration of AWC was not effective, further study was conducted in the chronic administered group.

3.3. *Effect of repeated oral doses (sub-chronic) of test substances (AWC, TR, and GLB) on plasma lipids (CHL, HDL, and TG)*

The effect of oral sub-chronic treatment with AWC, TR, and GLB on plasma CHL levels in normal and STZ-induced diabetic rats are represented in Table 4. In normal rats, repeated daily administration of AWC induced a significant ($p < 0.05$) fall in plasma total CHL levels on the 28th day of continuous treatment. The effect of daily treatment with TR was similar to that of AWC. GLB and water had no significant effect on total CHL levels. In the STZ-diabetic rats all the materials tested (except water) at the daily doses indicated above, showed a significant ($p < 0.05$) hypocholesterolemic effect. AWC induced a significant fall in plasma CHL levels on D14, with an additional decrease occurring with continued treatment on D28. TR was more effective than AWC in decreasing CHL levels on D14, while less so on D28. GLB was less effective than AWC on D28 ($p < 0.05$). Water had no effect.

The effect of oral sub-chronic treatment with AWC, TR, and GLB on plasma CHL levels and HDL levels in normal and STZ-induced diabetic rats are represented in Table 5. Oral sub-chronic treatment with AWC, TR, and GLB are ineffective in plasma HDL level in normal animals while AWC and TR at doses indicated above show a significant ($p < 0.05$) increase in plasma HDL-cholesterol levels on D14 as well as D28 in normal and

Table 3. The effect of sub-chronic oral administration of the aqueous extract of *Withania coagulance* (AWC), taurine (TR), and glibenclamide (GLB) for up to 28 days on plasma glucose levels in normal and STZ-diabetic rats

Days of chronic treatment	Plasma glucose level (mg%)			
	Water (10 mL/kg)	AWC (1 g/kg)	TR (10 mg/kg)	GLB (10 mg/kg)
Normal				
D0	98.2 ± 2.7	103.7 ± 3.1	106.2 ± 3.5	99.6 ± 3.7
D14	100.4 ± 2.0	87.6 ± 1.0*	95.1 ± 2.6	98.2 ± 2.2
D28	91.7 ± 4.7	73.6 ± 2.7*	89.0 ± 3.1*	96.2 ± 3.7
STZ-induced diabetes				
D0	333.6 ± 14.5	363.4 ± 9.9	391.0 ± 16.5	31.0 ± 19.8
D14	372.8 ± 13.8	107.1 ± 10.2*	178.8 ± 9.4*	177.0 ± 8.8*
D28	376.3 ± 10.1	83.1 ± 6.3*	2.9 ± 9.1*	27.6 ± 10.8*

The values are expressed as mean ± S.E.M. ($n = 6$). * $p < 0.05$, when compared to baseline values. Data within the treatment groups was analyzed by one way ANOVA followed by Dunnett test.

Table 4. The effect of sub-chronic oral administration of the aqueous extract of *Withania coagulance* (AWC), taurine (TR), and glibenclamide (GLB) for up to 28 days on plasma total cholesterol levels (mg/dL) in normal and STZ-diabetic rats

Days of chronic treatment	Plasma total cholesterol level (mg/dL)			
	Water (10 mL/kg)	AWC (1 g/kg)	TR (10 mg/kg)	GLB (10 mg/kg)
Normal				
D0	66.2 ± 1.2	62.3 ± 1.1	66.6 ± 2.5	62.4 ± 3.7
D14	65.1 ± 2.1	58.8 ± 1.6	64.8 ± 1.1	60.1 ± 2.3
D28	64.6 ± 2.0	55.2 ± 0.9*	60.0 ± 1.2*	59.6 ± 2.1
STZ-induced diabetes				
D0	131.3 ± 4.3	122.5 ± 3.4	106.3 ± 2.7	116.3 ± 2.2
D14	123.8 ± 3.9	94.6 ± 1.1*	91.2 ± 2.0*	107.3 ± 3.4
D28	115.0 ± 5.1	60.2 ± 1.4*	70.2 ± 1.0*	105.8 ± 2.0*

The values are expressed as mean ± S.E.M. ($n = 6$). * $p < 0.05$, when compared to baseline values. Data within the treatment groups was analyzed by one way ANOVA followed by Dunnett test.

Table 5. The effect of sub-chronic oral administration of the aqueous extract of *Withania coagulance* (AWC), taurine (TR), and glibenclamide (GLB) for up to 28 days on plasma HDL-cholesterol levels (mg/kg) in normal and STZ-diabetic rats

Days of chronic treatment	Plasma HDL-cholesterol level (mg/dL)			
	Water (10 mL/kg)	AWC (1 g/kg)	TR (10 mg/kg)	GLB (10 mg/kg)
Normal				
D0	29.0 ± 0.4	28.8 ± 0.6	28.7 ± 0.9	26.5 ± 0.9
D14	29.7 ± 0.5	29.0 ± 0.3	27.5 ± 0.9	25.9 ± 0.5
D28	28.2 ± 0.4	27.4 ± 0.6	27.0 ± 0.7	25.2 ± 0.5
STZ-induced diabetes				
D0	23.3 ± 0.7	20.3 ± 0.4	20.0 ± 0.1	21.7 ± 0.4
D14	21.1 ± 0.4	26.6 ± 0.4*	22.5 ± 0.3*	22.9 ± 0.9
D28	23.5 ± 0.6	29.0 ± 0.3*	22.5 ± 0.7*	23.8 ± 0.3*

The values are expressed as mean ± S.E.M. ($n = 6$). * $p < 0.05$, when compared to baseline values. Data within the treatment groups was analyzed by one way ANOVA followed by Dunnett test.

STZ-diabetic rats.

The effect of oral sub-chronic treatment with AWC, TR, and GLB, at doses indicated above, on plasma TG levels in normal and STZ-diabetic rats is shown in Figure 1. In normal rats, daily dosing with either AWC or TR reduced TG levels significantly ($p < 0.05$) only after 28 days of treatment (Figure 1A). GLB showed only an insignificant reduction in TG levels, while water had no effect (Figure 1A). In the STZ-diabetic rats, daily administration of either AWC or TR caused a significant ($p < 0.05$) decrease in plasma TG levels on D14 (Figure 1B). The decrease with GLB was insignificant. With continued administration, serum TG values fell further significantly ($p < 0.05$) with AWC and TR on D28 with respect to baseline (D0), while GLB and water had no significant effect.

3.4. *Effect of repeated oral doses (sub-chronic) of test substances (AWC, TR and GLB) on AI (atherogenic index)*

The effect of oral sub-chronic treatment with AWC, TR, and GLB, at doses indicated above, on AI in normal and STZ-diabetic rats is shown in Figure 2. In normal rats, daily dosing with neither AWC, TR nor GLB reduced AI significantly on D14 as well as D28 of continuous treatment. In the STZ-diabetic rats, daily administration of either AWC ($p < 0.05$) or TR ($p < 0.05$) caused a significant decrease in plasma TG levels on D14 (Figure 2B). The decrease with GLB was insignificant. With continued administration, AI values fell further significantly ($p < 0.05$) with AWC and TR on D28, while GLB and water had no significant effect.

4. Discussion

Until now, no previous study has been performed with *Withania coagulans* on dyslipidemia associated with diabetes, which results in premature atherosclerosis and is one of the important causes of CV disease in diabetic patients. In the present study, we investigated, whether AWC has any effect on levels of lipids (plasma CHL and TG), in addition to its hypoglycemic action, in normal and STZ-diabetic rats as well as on the atherogenic index.

One report showed that AWC has a hypolipidemic effect in high fat diets as well as triton induced hypercholesterolemia (*15*). However, the mechanism underlying diabetes induced dyslipidemia is different from hyperlipidemia, resulting from administration of triton and high fat diets in normal

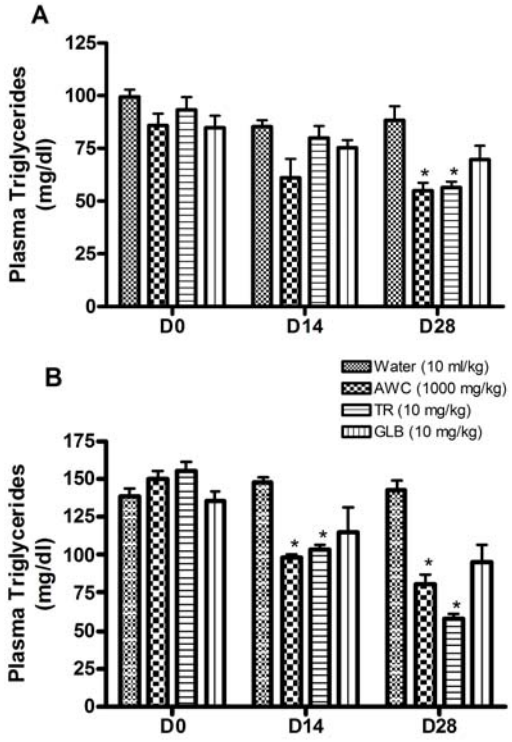

Figure 1. Plasma triglyceride levels (mg/dL) at baseline (D0), on 14th day (D14) and on 28th day (D28) after repeated daily oral administration (sub-chronic dosing) of water (10 mL/kg/day), aqueous extract of *Withania coagulace* (AWC) (1,000 mg/kg/day), taurine (TR) (10 mg/kg/day) and glibenclamide GLB (10 mg/kg/day) in normal (A) and STZ-diabetic (B) rats. Values are expressed as mean ± S.E.M. ($n = 6$). * $p < 0.05$ compared with respective baseline values (D0). Data within the treatment groups was analyzed by one way ANOVA followed by Dunnett test.

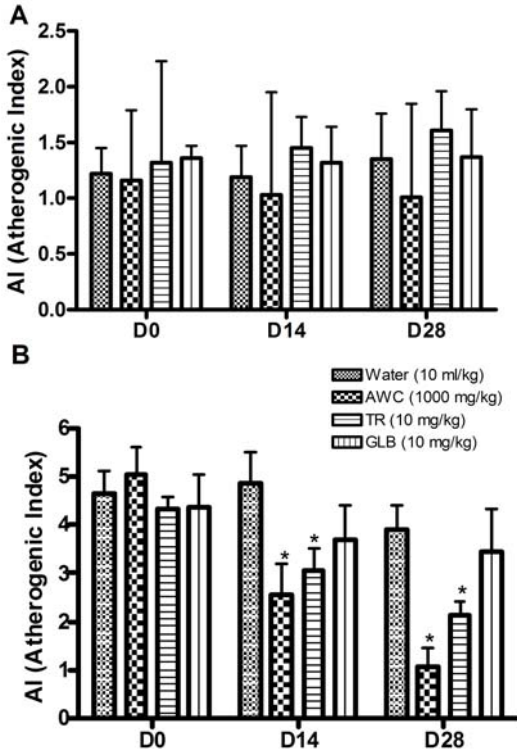

Figure 2. Atherogenic index (AI) at baseline (D0), on 14th day (D14) and on 28th day (D28) after repeated daily oral administration (sub-chronic dosing) of water (10 mL/kg/day), aqueous extract of *Withania coagulace* (AWC) (1,000 mg/kg/day), taurine (TR) (10 mg/kg/day) and glibenclamide (GLB) (10 mg/kg/day) in normal (A) and STZ-diabetic (B) rats. Values are expressed as mean ± S.E.M. ($n = 6$). * $p < 0.05$ compared with respective baseline values (D0). Data within the treatment groups was analyzed by one way ANOVA followed by Dunnett test.

animals. Triton first causes a sharp increase in serum cholesterol levels (phase I) followed by a decrease in hypercholesterolemia nearly to control levels (phase II). The mechanism of triton induced hypercholesterolemia in phase I is thought to be due to increased hepatic synthesis of cholesterol through the ability of triton to interfere with the uptake of plasma lipids by the tissues. Drugs interfering with cholesterol biosynthesis were shown to be active in phase I, while those interfering with cholesterol excretion and metabolism were active in phase II triton induced hyperlipidemia (*16-19*).

In high fat diets, higher levels of glucose and lipid are maintained in blood for a longer duration of time and result in insulin resistance. STZ-induced diabetes mimics type 1 diabetes where insulin secretion decreases greatly. Therefore, drugs active in STZ induced diabetes and high fat diets are effective in decreased insulin secretion as well as in insulin resistance (*20-23*). Thus different models are used for screening different antihyperlipidemic drugs. Moreover, different hypercholesterolemia affecting drugs show different activities using different tests (*17*). Therefore, the study of the effect of drugs on lipid profiles in different models reveals a clearer picture about their mechanism of action.

Induction of diabetes in rats by STZ, also led to the development of dyslipidemia (hypercholesterolemia and hypertriglyceridemia) (Tables 4 and 5) and weight loss as has been reported previously (*24,25*). Administration of daily doses of AWC protected the STZ-diabetic rats from weight loss, which was not the case with rats given water, TR or GLB (Table 1). A single oral dose of AWC and water had no effect on glucose levels in normal as well as in STZ-induced diabetes. TR caused lowering of glucose levels in normal as well as STZ-induced diabetes. GLB had no effect on normal animals and caused a lowering of glucose levels in STZ-induced diabetes (Table 2). Daily dosing with AWC (sub-chronic study) caused a gradual decrease in plasma glucose in normal rats, which became significant on D28 (Table 3). In the diabetic rats, daily dosing with AWC produced a significant euglycemic effect on D14, with glucose levels going down further by D28. GLB was less potent and not able to decrease glucose levels up to normal. TR had a slower onset of action and caused a euglycemic effect on D28 (Table 3). The lower hypoglycemic response in normoglycemic animals compared to diabetic rats may be due to homeostasis mechanisms of glucose/carbohydrate metabolism (*26*). AWC and TR reduced TG levels in normal rats, while TR performed at a slower rate (Figure 1A); GLB and water had no effect. In the diabetic rats, daily dosing with either AWC or TR reduced TG levels significantly, and the effect increased with repeated dosing (Figure 1B). GLB had no significant effect. Thus, our study shows that repeated oral administration of AWC caused significant hypolipidemia, especially in the diabetic rats.

The mechanism(s) of hypolipidemic and hypoglycemic actions of AWC are not known. However, in view of the similar reduction in plasma glucose as well as the hypolipidemic effect of AWC and TR, the mechanism of hypoglycemic action of AWC may be like that of TR, which involves insulin and in turn causes increased glucose utilization *via* insulin sensitization in peripheral tissues (*27,28*). This also normalizes plasma lipids in STZ-diabetic rats (*25*). Plants like *Momordica charantia* fruit (*29*) and *Scoparia dulcis* leaves (*30*) also show similar effects. The mechanism of action of AWC is not like that of the sulfonylurea GLB, since it has only a weak hypolipidemic action. Additionally its hypolipidemic activity in triton induced as well as high fat diet induced hyperlipidemia also reveals its interference in synthesis, metabolism and excretion of lipids. Insulin receptor sensitization would also explain its mechanism of action.

The chronic elevation of glucose levels in diabetes causes oxidative stress (*31*). It leads to protein oxidation, glycation (*32*), and dyslipidemia. Together they play a significant role in the manifestation and development of premature atherosclerosis. Thus drugs effective in lipid profiles in diabetic animals are assumed to be effective in protection from atherosclerosis. It is further supported by the result of the atherogenic index (Figure 2) which shows AWC decreases the AI significantly in STZ-induced diabetes.

A preliminary phytochemical analysis of AWC revealed that it contains several withanolides and lactones (*33-35*). There is report which shows that withanolides are effective in cardiovascular complications (*36*). Thus hypolipidemic and hypoglycemic activities of AWC may be attributed to one or more of the identified or as-yet-unidentified compounds. Studies are still in progress to isolate and identify the active principle(s) of *Withania coagulans*, which may be valuable in the treatment of dyslipidemia and atherosclerosis in diabetic patients.

It can be concluded that AWC exhibited strong hypolipidemic activity in addition to its hypoglycemic action in diabetic animals. This has clinical implications in that the relatively nontoxic AWC, if used as a hypoglycemic agent, may also reverse dyslipidemia associated with diabetes (types 1 and 2), and prevent the CV complications which are very prevalent in diabetic patients. Our results suggest that AWC has the potential to be a suitable candidate for further investigations as an anti-atherogenic agent in humans with diabetes. Further studies are warranted to confirm our results and fractionate AWC to isolate and identify the active principle(s), and to determine the exact mechanism(s) of action.

References

1. Brown WV. Lipoprotein disorders in diabetes mellitus. Med Clin North Am. 1994; 78:143-161.

2. Stamler J, Vaccaro O, Neaton JD, Wentworth D. Diabetes, other risk factors, and 12-yr cardiovascular mortality for men screened in the Multiple Risk Factor Intervention Trial. Diabetes Care. 1993; 16:434-444.
3. Betteridge J. Lipid disorders in diabetes mellitus. In: Text Book of Diabetes (Pickup JC, Williams G, eds.). Blackwell Science, London, UK, 1997; pp. 1-35.
4. Feher MD. Diabetes: Preventing coronary heart disease in a high risk group. Heart. 2004; 90 (Suppl 4):iv18-iv21.
5. Tang WH, Maroo A, Young JB. Ischemic heart disease and congestive heart failure in diabetic patients. Med Clin North Am. 2004; 88:1037-1061, xi-xii.
6. American Diabetes Association. Diagnosis and classification of diabetes mellitus. Diabetes Care. 2004; 27 (Suppl 1):S5-S10.
7. Fisman EZ, Tenenbaum A, Motro M, Adler Y. Oral antidiabetic therapy in patients with heart disease. A cardiologic standpoint. Herz. 2004; 29:290-298.
8. Albertini JP, McMorn SO, Chen H, Mather RA, Valensi P. Effect of rosiglitazone on factors related to endothelial dysfunction in patients with type 2 diabetes mellitus. Atherosclerosis. 2007; 195:e159-e166.
9. Koro C, Barrett S, Qizilbash N. Cancer risks in thiazolidinedione users compared to other anti-diabetic agents. Pharmacoepidemiol Drug Saf. 2007; 16:485-492.
10. Yoo MH, Yoon YH, Chung H, Cho KS, Koh JY. Insulin increases retinal hemorrhage in mild oxygen-induced retinopathy in the rat: Inhibition by riluzole. Invest Ophthalmol Vis Sci. 2007; 48:5671-5676.
11. Kirthikar KR, Basu BD. Indian Medical Plants. In: C.M. Basu: Vol. 2. Allahabad, India, 1933; p. 1777.
12. Hemalatha S, Wahi AK, Singh PN, Chansouria JP. Hypoglycemic activity of *Withania coagulans* Dunal in streptozotocin induced diabetic rats. J Ethnopharmacol. 2004; 93:261-264.
13. Tenner TE Jr, Zhang XJ, Lombardini JB. Hypoglycemic effects of taurine in the alloxan-treated rabbit, a model for type 1 diabetes. Adv Exp Med Biol. 2003; 526:97-104.
14. Nikkilä EA, Kekki M. Plasma triglyceride transport kinetics in diabetes mellitus. Metabolism. 1973; 22:1-22.
15. Hemalatha S, Wahi AK, Singh PN, Chansouria JP. Hypolipidemic activity of aqueous extract of *Withania coagulans* Dunal in albino rats. Phytother Res. 2006; 20:614-617.
16. Frantz ID Jr, Hinkelman BT. Acceleration of hepatic cholesterol synthesis by triton WR-1339. J Exp Med. 1955; 101:225-232.
17. Garattini S, Paoletti R, Bizzi L, Grossi E, Vertua R. A comparative evaluation of hypocholesteremizing drugs on several tests. In: Drugs affecting lipid metabolism (Garattini S, Paoletti R, eds.). Elsevier Publishing Company, Amsterdam, Holland, 1961; pp. 144-157.
18. Holmes WL. Drugs affecting lipid synthesis. In: Lipid Pharmacology (Paoletti R, ed.). Academic Press, New York, NY, USA, 1964; pp. 131-184.
19. Moss JN, Dajani EZ. Antihyperlipidemic agents. In: Screening Methods in Pharmacology: Vol. 2 (Turner RA, Hebborn P, eds.). Academic Press, New York, NY, USA, 1971; pp. 121-143.
20. Poveda E, Trujillo P, Ruiz F, López E. Glucose and insulin levels in Wistar rats submitted to high fat diet and treatment with mimetic leptin peptides. Biomedica. 2008; 28:50-63. (in Spanish)
21. Matsuzawa-Nagata N, Takamura T, Ando H, Nakamura S, Kurita S, Misu H, Ota T, Yokoyama M, Honda M, Miyamoto K, Kaneko S. Increased oxidative stress precedes the onset of high-fat diet-induced insulin resistance and obesity. Metabolism. 2008; 57:1071-1077.
22. Afonso RA, Lautt WW, Ribeiro RT, Legare DJ, Macedo MP. Insulin resistance in two animal models of obesity: A comparison of HISS-dependent and HISS-independent insulin action in high-fat diet-fed and Zucker rats. Proc West Pharmacol Soc. 2007; 50:110-114.
23. Yamanouchi T, Akanuma H, Takaku F, Akanuma Y. Marked depletion of plasma 1,5-anhydroglucitol, a major polyol, in streptozoc-ininduced diabetes in rats and the effect of insulin treatment. Diabetes. 1986; 35:204-209.
24. Peungvicha P, Thirawarapan SS, Watanabe H. Possible mechanism of hypoglycemic effect of 4-hydroxybenzoic acid, a constituent of *Pandanus odorus* root. Jpn J Pharmacol. 1998; 78:395-398.
25. Pepato MT, Mori DM, Baviera AM, Harami JB, Vendramini RC, Brunetti IL. Fruit of the jambolan tree (*Eugenia jambolana* Lam.) and experimental diabetes. J Ethnopharmacol. 2005; 96:43-48.
26. Roman-Ramos R, Flores-Saenz JL, Alarcon-Aguilar FJ. Anti-hyperglycemic effect of some edible plants. J Ethnopharmacol. 1995; 48:25-32.
27. Nandhini AT, Thirunavukkarasu V, Anuradha CV. Stimulation of glucose utilization and inhibition of protein glycation and AGE products by taurine. Acta Physiol Scand. 2004; 181:297-303.
28. Da Ros R, Assaloni R, Ceriello A. The preventive anti-oxidant action of thiazolidinedione: A new therapeutic prospect in diabetes and insulin resistance. Diabet Med. 2004; 21:1249-1252.
29. Miura T, Itoh C, Iwamoto N, Kato M, Kawai M, Park SR, Suzuki I. Hypoglycemic activity of the fruit of the *Momordica charantia* in type 2 diabetic mice. J Nutr Sci Vitaminol (Tokyo). 2001; 47:340-344.
30. Pari L, Venkateswaran S. Hypoglycaemic activity of *Scopariadulcis* L. extract in alloxan induced hyperglycaemic rats. Phytother Res. 2002; 16:662-664.
31. Mohamed AK, Bierhaus A, Schiekofer S, Tritschler H, Ziegler R, Nawroth PP. The role of oxidative stress and NF-kappaB activation in late diabetic complication. Biofactors. 1999; 10:157-167.
32. King GL, Loeken MR. Hyperglycemia-induced oxidative stress in diabetic complications. Histochem Cell Biol. 2004; 122:333-338.
33. ur-Rahman A, Dur-e-Shahwar, Naz A, Choudhary MI. Withanolides from *Withania coagulans*. Phytochemistry. 2003; 63:387-390.
34. ur-Rahman A, Shabbir M, Yousaf M, Qureshi S, Dur-e-Shahwar, Naz A, Choudhary MI. Three withanolides from *Withania coagulans*. Phytochemistry. 1999; 52:1361-1364.
35. Subramanian SS, Sethi PD, Glotter E, Kirson I, Lavie D. 5,20α(R)-dihydroxy-6α,7α-epoxy-1-oxo-(5α) witha-2,24-dienolide, a new steroidal lactone from *withania coagulans*. Phytochemistry. 1971; 10:685-688.
36. Budhiraja RD, Sudhir S, Garg KN. Cardiovascular effects of a withanolide from *Withania coagulans*, dunal fruits. Indian J Physiol Pharmacol. 1983; 27:129-134.

(Received June 15, 2010; Accepted August 7, 2010)

Original Article

Investigation of phenolic leaf extract of *Heimia myrtifolia* (Lythraceae): Pharmacological properties (stimulation of mineralization of SaOS-2 osteosarcoma cells) and identification of polyphenols

Nahla Ayoub[1,*], Abdel Naser Singab[1], Mohamed El-Naggar[1], Ulrike Lindequist[2]

[1] *Department of Pharmacognosy, Faculty of Pharmacy, Ain-Shams University, Cairo, Egypt;*
[2] *Pharmazeutische Biologie, Institut für Pharmazie, Ernst-Moritz-Arndt-Universität, Greifswald, Germany.*

ABSTRACT: Evaluation of the activity of an aqueous alcoholic extract obtained from the leaves of *Heimia myrtifolia* (Lythraceae) by determining its stimulating effect on two human osteoblastic cell lines HOS58 and SaOS-2 indicated its potential for use in the prevention and treatment of osteoporosis. In addition, the extract was found to significantly increase the mineralization of cultivated human bone cell SaOS-2, in which a strong dose-dependent increase was observed. A phytochemical investigation of the extract also confirmed that *H. myrtifolia* is capable of synthesizing and accumulating appreciable amounts of several phenolics, thus leading to the isolation and characterization of sixteen of these constituents. Identified among these isolates were a new natural product, 1,6-di-*O*-dehydrotrigalloyl-β-D-$^4C_1$-glucopyranose, and a rare natural product (this marks its second report), 5,7,4'-trihydroxy-3-methoxyflavanone (dihydrokaempferol-3-*O*-methyl ether). Structures of these isolates were fully elucidated on the basis of conventional methods of analysis and confirmed by ESI/MS and ^{1}H and ^{13}C-NMR analysis.

Keywords: *Heimia myrtifolia*, phenolics, osteoporosis, 1,6-di-*O*-dehydrotrigalloyl-β-D-$^4C_1$-glucopyranose

1. Introduction

Due to interest in biological activity as well as in the diverse phenolic metabolite production of terrestrial plants (*1-3*), the current authors investigated an aqueous alcoholic leaf extract of *Heimia myrtifolia* Cham. for its potential use in the prevention or treatment of osteoporosis by evaluating its stimulant effect on two human osteoblastic cell lines HOS58 and SaOS-2. Phytochemical screening, including color reactions and chromatographic analysis of this extract, has shown that it contains mainly phenolic compounds (*4*).

A comprehensive analysis of the constitutive phenolics of the plant leave extract was therefore undertaken. Sixteen compounds (compounds **1-16**), including a new natural product, 1,6-di-*O*-dehydrotrigalloyl-β-D-$^4C_1$-glucopyranose (compound **7**), and a rare natural product (this is its second report in nature), 5,7,4'-trihydroxy-3-methoxyflavanone (dihydrokaempferol-3-*O*-methyl ether) (compound **9**), were subsequently isolated and identified. Structures were confirmed by electrospray ionization/mass spectrometry (ESI/MS) and nuclear magnetic resonance (NMR) analysis.

H. myrtifolia Cham., known as sun opener or shrubby yellow crest, is one of the Lythraceous species that is native to South America, ranging from Brazil to Uruguay, where it is common along the sides of streams. It is a deciduous shrub growing up to 1 m tall. The yellow flowers are 5 petaled and 1 cm in diameter. The leaves are approximately 2-5 cm long and 1 cm wide and are variably arranged in alternate, opposite, or whorled fashion on the stem. *H. myrtifolia* flowers from August to September. The flowers are hermaphrodite (*5*).

Extracts from *H. myrtifolia* that contain Lythrine and Lythridine alkaloids exhibit diuretic activity (*6*). Strong anti-inflammatory activity of *H. myrtifolia* originates from an alkaloidal fraction containing vertine (Cryogenine) (*7*), while 70% acetone extract of *H. myrtifolia* has a strong cytotoxic effect on human promyelocytic leukemia cells (HL-60) (*8*).

Three biphenylquinolizidine lactone alkaloids were isolated from *H. myrtifolia*, namely Vertine (Cryogenine), Lythrine, and Lythridine (*9,10*). The fatty acid composition of seed lipids consists of linoleic

**Address correspondence to:*
Dr. Nahla Ayoub, Department of Pharmacognosy, Faculty of Pharmacy, Ain-Shams University, Cairo, Egypt.
e-mail: Ayoub.n@link.net

acid (18:2) as the primary or dominant fatty acid of *H. myrtifolia*, while palmitic acid (16:0) is the only secondary component, constituting 10% or more of the total fatty acid composition (*11*). Nothing in literature indicated the phenolic content or bone mineralization activity of *H. myrtifolia* Cham. and Schl., thus leading the present study to investigate the aqueous alcoholic extract in depth for its phenolic content and its activity in preventing or treating osteoporosis.

2. Materials and Methods

2.1. *Instruments and materials for phytochemical investigation*

^{1}H-NMR spectra were measured by a Jeol ECA 500 MHz NMR spectrometer (JEOL, Tokyo, Japan) at 500 MHz. ^{1}H chemical shifts (δ) were measured in ppm, relative to TMS and ^{13}C-NMR chemical shifts to dimethyl sulfoxide (DMSO)-d_6 and converted to the tetramethylsilane (TMS) scale by adding 39.5. Typical conditions: spectral width = 8 kHz for ^{1}H and 30 kHz for ^{13}C, 64 K data points, and a flip angle of 45.

ESI/MS spectra were measured on a Finnigan LTQ-ESI/MS (Thermo Electron, Bremen, Germany) (Department of Chemistry, Humboldt-Universität zu Berlin). UV recording was done on a Shimadzu UV-Visible-1601 spectrophotometer (Shimadzu, Kyoto, Japan).

Paper chromatographic analysis was carried out on Whatman No. 1 paper (Whatman, Kent, UK) using solvent systems: 1) H_2O; 2) 6% AcOH; and 3) BAW (*n*-BuOH/AcOH/H_2O, 4:1:5, v/v, upper layer). Solvents 2 and 3 were also used for preparative paper chromatography (PPC).

2.2. *Plant material*

The leaves of *H. myrtifolia* Cham. were collected from El-Orman Botanical Garden, Cairo, Egypt, in March 2007 and identified by Mrs. Tereize Labib, Agricultural Engineer, El-Orman Botanical Garden, Giza, Egypt. Vouchered specimens of the authenticated plant were deposited at the Department of Pharmacognosy, Faculty of Pharmacy, Ain-Shams University, Cairo, Egypt.

2.3. *Extraction, isolation, and purification of phenolics from H. myrtifolia*

The air dried plant material (2 kg) was extracted with 70% ethanol. The aqueous alcohol extract was filtered and evaporated *in vacuo* at ~ 45ºC until dry to yield 90 g of a sticky dark brown material. The dried residue was applied to a polyamide 6s column (250 g, 125 cm L × 5 cm D) (Riedel-de Haen AG, Seelze-Hannover, Germany) and eluted with H_2O followed by H_2O/MeOH mixtures of decreasing polarities to yield 36 individual fractions (2 L each) that were examined separately under UV light. Similar fractions were pooled to yield eleven main fractions (I-XI) that were separately dried in a vacuum and subjected to two-dimensional paper chromatographic investigation (2D-PC). Compounds **1-7** were individually isolated from 5.6 g of fraction III (eluted with 20% MeOH), where compound **1** (250 mg) was crystallized from the concentrated fraction and then purified by application to a Sephadex LH-20 column (10 g; GE Healthcare Bio-Sciences, Uppsala, Sweden) eluted with MeOH, while other compounds were separated through column fractionation on a Sephadex LH-20 column (30 g) (eluted with distilled water 100% followed by pure MeOH 100%). This led to the desorption of five successive sub-fractions (III-[i-v]). Sub-fraction III-iv (2.8 g) was fractionated over a Sephadex LH-20 column (20 g) using *n*-butanol saturated with water, leading to the desorption of five successive sub-fractions (III-iv-[ib-vb]). PPC using BAW as a solvent of the dried material (700 mg) of sub-fractions (III-iv-iib) led to the separation of pure samples of compounds **2** (90 mg), **3** (82 mg), and **4** (96 mg), while PPC using BAW as an eluent of the dried material (570 mg) of sub-fractions (III-iv-ivb) yielded the pure compounds **5** (137 mg), **6** (112 mg), and **7** (136 mg). Compounds **8** (1.4 g), and **9** (150 mg) were individually separated from 5.5 g of fraction VI (eluted with 60% MeOH) through initial crystallization of a yellow amorphous powder (1.7 g) from the concentrated fraction followed by purification over a Sephadex LH-20 column (20 g) using *n*-butanol saturated with water as a solvent. Compound **10** (180 mg) was separated from Fraction IX (2.2 g, eluted with 80% MeOH) by purification of (500 mg) using column chromatography with a Sephadex LH-20 column and MeOH as an eluent.

PPC of the material of fraction X (2.9 g, eluted with 90% MeOH) with BAW as a solvent led to the separation of four pure samples of compounds **11** (95 mg), **12** (125 mg), **13** (89 mg), and **14** (119 mg). Polyamide 6s (25 g) column fractionation (1 g) of fraction XI (6.5 g, eluted with 100% MeOH) using EtOAc saturated with water for elution afforded individual pure samples of compounds **15** (570 mg) and **16** (280 mg).

2.4. *Spectral data for the new natural product 1,6-di-O-dehydrotrigalloyl-β-D-$^{4}C_1$-glucopyranose (compound 7)*

The new natural product was a white amorphous powder (136 mg), R_f values (×100): 50 (6% AcOH), 28 (BAW). UV λ_{max} (nm) in MeOH: 273 nm. UV λ_{max} (nm) in MeOH after acid hydrolysis: 273 nm. Negative ESI/MS indicated a molecular ion at $[M-H]^-$, m/z 1,155, which corresponded to a molecular mass (M_r) of 1,156. ^{1}H-NMR (DMSO-d_6) δ (ppm): 7.10 and 6.99 (1H, *d*, *J* = 2.5 Hz, H-2 and H-2'), 6.96 (2H, *s*, H-8 and H-8'), 6.42

and 6.40 (1H, *d*, *J* = 2.5 Hz, H-8b and H-8b'), 6.53 and 6.54 (1H, *s*, H-14 and H-14'), 4.70 (1H, *d*, *J* = 8 Hz, H-1''), 4.40 (1H, *d*, *J* = 12 Hz, Ha-6''), 4.22 (1H, *dd*, *J* = 3.5, 12 Hz, Hb-6''), 3.1-3.8 (*m*, sugar protons) (see the structural formula).

^{13}C-NMR (DMSO-d_6) δ (ppm): 119.95 (C-1 and C-1'), 168.16 (C-1b and C-1b'), 102.79 and 102.93 (C-2 and C-2'), 148.59 (C-3 and C-3'), 138.95 (C-4 and C-4'), 151.07 (C-4a and C-4a'), 138.90 (C-4b and C-4b'), 140.02 (C-5 and C-5'), 140.00 (C-6 and C-6'), 146.05 (C-7 and C-7'), 108.20 (C-8 and C-8'), 115.68 and 115.80 (C-8a and C-8a'), 110.70 and 110.80 (C-8b and C-8b'), 166.27 (C-8c, C-8c', C-9b and C-9b'), 114.74 (C-9 and C-9'), 136.89 (C-10 and C-10'), 141.90 (C-11 and C-11'), 141.92 (C-12 and C-12'), 148.31 (C-13 and C-13'), 109.16 (C-14 and C-14'), 94.53 (C-1''), 74.29 (C-2''), 76.82 (C-3''), 70.33 (C-4''), 73.76 (C-5''), 66.24 (C-6'').

2.5. *Spectral data for the rarely reported natural product 5,7,4'-trihydroxy-3-methoxyflavanone (dihydrokaempferol-3-O-methyl ether) (compound **9**)*

The rarely reported natural product was a yellow amorphous powder (150 mg), R_f values (×100): 6 (6% AcOH), 48 (BAW). UV λ_{max} (nm) in MeOH: 290, 324 sh; ^{1}H-NMR (DMSO-d_6) δ (ppm): 4.99 (1H, *d*, *J* = 11 Hz, H-2), 4.6 (1H, *d*, *J* = 11 Hz, H-3), 5.96 (1H, *d*, *J* = 2.5 Hz, H-6), 6.10 (1H, *d*, *J* = 2.5 Hz, H-8), 7.47 (2H, *d*, *J* = 8.5 Hz, H-2' and H-6'), 7.05 (2H, *d*, *J* = 8.5 Hz, H-3' and H-5'), 4.04 (3H, *s*, OMe). UV spectral data and ^{1}H-NMR data for compound **9** were identical to those reported in the literature (*12*).

2.6. *Chemicals and biochemicals for biochemical assays*

Cell culture plastics, fetal bovine serum (FBS), phosphate buffered saline (PBS), L-glutamine, trypsin, and antibiotics were purchased from Biochrom KG (Berlin, Germany). Bovine serum albumin (BSA; fraction V) and Iscove's modification of Dulbecco's medium (IMDM), with or without phenol red, were purchased from Invitrogen (Karlsruhe, Germany). All other reagents were obtained from Sigma (Deisenhofen, Germany). HOS58 cells were obtained from H. Siggelkow (Heidelberg, Germany). SaOS-2 cells were purchased from DSZM (Braunschweig, Germany). Other chemicals used were of analytical grade. All cell culture plastics were provided by Biochrom KG (Berlin, Germany).

2.7. *Cell culture*

Human osteosarcoma cells HOS58 and SaOS-2 were grown as a monolayer in IMDM with 10% FBS, 2 mM L-glutamine, and 1% penicillin-streptomycin solution (penicillin 10,000 IE/mL, streptomycin 10,000 µg/mL). Both cell lines were grown at 37ºC in 95% air humidity and 5% CO_2 and were routinely sub-cultured.

For assays, HOS58 and SaOS-2 cells were grown to 90% confluence in 96-well plates for 48 h. After cells were washed twice with PBS, the medium was changed to IMDM without phenol red supplemented with 0.05% BSA, 2 mM L-glutamine, and 1% antibiotics (assay medium).

Different concentrations of *Heimia* extract in assay medium were prepared using a stock solution (10 mg/mL DMSO) and serial dilution with medium. The final DMSO concentration did not exceed 0.05%. The procedure was further carried out as indicated below.

2.8. *Cell viability and cell proliferation assays (Neutral Red assay)*

The Neutral Red assay was used to measure the cell proliferation rate and cell viability. HOS58 cells (see "Cell culture") were incubated with different concentrations of *H. myrtifolia* (3.9-250 µg/mL) for 43 h. A 0.4% aqueous stock solution of Neutral Red (NR; Sigma) was prepared and an aliquot added to bring the IMDM medium to a final concentration of 50 µg/mL.

Pre-incubating NR-containing medium overnight at 37°C proved advantageous in terms of removing fine precipitate and dye crystals that formed when NR was mixed with medium. Deposition of such precipitated crystals onto the cell cultures during incubation would interfere with the assay. The NR-medium was centrifuged for 10 min at 1,500 × g before use to facilitate removal of crystals. After washing, 0.2 mL of the NR-medium was added to the wells and the plates were incubated at 37ºC in 95% air humidity and 5% CO_2 for a further 3 h, resulting in the uptake of the vital dye into viable cells.

The dye-medium was removed and the cells were washed rapidly with 1% formaldehyde-1% $CaCl_2$ to remove extraneously adhering, unincorporated dye and simultaneously promote adhesion of the cells to the substratum. The formaldehyde had to be left only briefly in contact with the cells since longer exposure would result in extraction of the dye. Removal of the formaldehyde and addition of 0.2 mL of a mixture of 1% acetic acid/50% ethanol to each well then resulted in the extraction of the NR into the solution. After 20 min the trays were placed on a microtiter plate shaker for a few seconds and the absorbance of the extracted dye was measured with a Dynatech microplate reader equipped with a 540-nm filter. Cell viability was calculated as the percent of vehicle control (*13-15*).

2.9. *Cell maturation assay*

A cell maturation assay was used to determine the osteoblastic activity of osteoblastic cells. HOS58 cells (see "Cell culture") were incubated with different concentrations of *H. myrtifolia* for 5 days and the

medium was exchanged on day 3. Cells were then lysed and the enzyme activity of alkaline phosphatase (ALP) was determined in the supernatant.

2.9.1. *Cell lysis*

Upon the conclusion of incubation, cells treated with *H. myrtifolia* extract or vehicle were washed twice with PBS and disrupted (lysed) by adding 100 µL of 0.1% Triton X-100 in 0.1 M Tris-HCl, pH 9.8 (lysis buffer) followed by freeze/thawing and vigorous mixing. The obtained suspension was centrifuged and the supernatant (cell lysate) assayed for protein content (Roti-Nanoquant, Roth GmbH, Karlsruhe, Germany) and ALP activity (cleavage of 4-nitrophenylphosphate under basic conditions).

2.9.2. *Protein quantification*

The total cellular protein was determined using Roti-Nanoquant reagent (Roth GmbH, Karlsruhe, Germany) and a modified Bradford method in accordance with the manufacturer's instructions (*16*). Briefly, 10 µL cell lysates was diluted with PBS (1:4) in a microtiter plate. Roti-Nanoquant (200 µL) reagent was added and mixed and the OD was read out at 405 and 620 nm using a spectrophotomer (Anthos Labtec, Salzburg, Austria). The total protein content was calculated from a standard curve using BSA.

2.9.3. *ALP activity*

Cellular ALP activity was determined by the release of 4-nitrophenol (4-NP) from 4-nitrophenylphosphate (4-NPP). An aliquot of cell lysates was mixed with 0.2 M aminopropanol buffer, pH 9.8 (AMP) and 24 mM 4-NPP in AMP. After incubation at 37ºC, the reaction was stopped by 0.5 M NaOH (50 µL), and the OD was read out at 405 nm. The concentration of 4-NP was calculated utilizing a calibration curve.

Here, for ALP determination assay two independent experiments were carried out with six replicates each and results were expressed as mean ± S.D. Statistical differences were analyzed using single side ANOVA; p values < 0.05 were considered significant.

2.10. *Mineralization assay*

SaOS-2 cells were seeded into 24 well-plates (10^4 cells/well) using growth medium (see "Cell culture") and grown to 90% confluence. The medium was discarded and cells were maintained in assay medium (see "Cell culture") with or without *H. myrtifolia* crude extract (1, 5, and 25 µg/mL) for 21 days. The medium was changed every 3 days. Mineralization was triggered by continuously adding 2 mM β-glycerophosphate (bGP) to the medium, while Zn was added to other cells as a positive control. Upon the conclusion of incubation, cells were stained for mineral deposition by the arsenazo III method for measuring calcium (*17*). After cells were washed with warm PBS, they were fixed with 5% buffered glutardialdehyde (Grade II, Sigma) in cold PBS for 30 min. Cell layers were washed twice with deionized water and Arsen-Azo III dye was added. Cells were then incubated at room temperature for 2 min. After cells were mixed thoroughly, the absorbance at 650 nm was measured for the bluish-purple color formed after complex formation between Ca^{2+} and Arsen-Azo III dye, which is directly proportional to calcium deposition. In the mineralization assay, each bar represents mean ± S.D. of 1 experiment with 4 parallels.

2.11. *Statistical analysis*

For ALP determination assay, two independent experiments were carried out with six replicates each and results were expressed as mean ± S.D. Statistical differences were analyzed using one-way ANOVA; p values < 0.05 were considered significant. In the mineralization assay, each bar represents the mean ± S.D. of 1 experiment with 4 parallels.

3. Results and Discussion

Little phytochemical investigation has been conduced into the phenolic metabolites and biological activities of *H. myrtifolia*. Thus, this study describes the isolation and characterization of different phenolic compounds and the influence of the aqueous alcoholic extract of *H. myrtifolia* on the growth and maturation of human osteoblastic osteosarcoma cell lines, HOS58 and SaOS-2.

3.1. *Isolation and structure elucidation of phenolics*

Phytochemical investigation indicated the presence of complicated phenolic mixtures in the aqueous alcoholic extract of *H. myrtifolia*. Following column chromatographic fractionation of the *H. myrtifolia* leaf extract, sixteen compounds (compounds **1-16**) were isolated. Conventional and spectral analysis mainly by UV, ^{1}H-NMR, and ^{13}C-NMR spectroscopy and by ESI/MS spectrometry indicated that one of these compounds, 1,6-di-*O*-dehydrotrigalloyl-β-D-$^4C_1$-glucopyranose (**7**), was a new natural product (Figure 1) and that another, 5,7,4'-trihydroxy-3-methoxyflavanone (dihydrokaempferol-3-*O*-methyl ether) (**9**), was a rare natural product (noted for the second time in the present study) that was isolated as a new natural product in 1992 (*12*) from *Prunus domestica* (family Rosaceae). Compounds **9** and **10** are the first such compounds reported from the family Lytheraceae while the compounds **1-6, 8,** and **11-16** are the first such compounds reported from the genus *Heimia*.

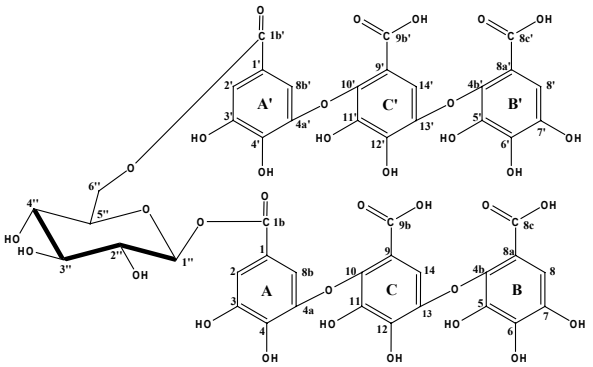

Figure 1. Compound 7: 1,6-di-*O*-dehydrotrigalloyl-β-D-$^4C_1$-glucopyranose. Numbering of the carbons is for convenience.

3.1.1. *Known compounds*

The present study has described the isolation and structural elucidation of sixteen phenolic compounds where chromatographic behavior, UV spectral, ESI/MS (negative mode), and ^{1}H and ^{13}C NMR data were consistent with those previously reported for apigenin-7-*O*-rutinoside (**1**) (*18-20*); protocatechuic acid (**2**) (*21*); vanillic acid (**3**) (*22*); apigenin-4'-*O*-methyl ether 7-*O*-glucoside (acacetin-7-*O*-β-glucoside) (**4**) (*23,24*); methyl gallate (**5**) (*25,26*); gallic acid (**6**) (*27-30*); apigenin-7-*O*-β-D-$^4C_1$-glucoside (**8**) (*24,31*); 5,7,4'-trihydroxy-3-methoxyflavanone (dihydrokaempferol-3-*O*-metyhl ether) (**9**) (*12*); dehydrotrigallic acid (**10**) (*32*); 3,4,3'-trimethoxyellagic acid (**11**) (*33*); 3,3'-dimethoxyellagic acid (**12**) (*27,34*); 3-methoxyellagic acid (**13**) (*27,34*); ellagic acid (**14**) (*32*); apigenin (**15**) (*24,35*); and kaempferol (**16**) (*36,37*).

3.1.2. *The new natural product 1,6-di-O-dehydrotrigalloyl-β-D-$^4C_1$-glucopyranose (compound **7**)*

The new natural product, compound **7** (Figure 1), was obtained as a white amorphous powder that possesses gallic acid-like characteristics (intense blue color with $FeCl_3$, rosy red color with KIO_3 and UV spectral maximum in MeOH at 273 nm). Negative ESI mass spectral analysis established that compound **7** was a di-dehydrotrigalloyl glucose ($[M-H]^-$, m/z 1,155) with a M_r of 1,156, which on complete acid hydrolysis yielded dehydrotrigallic acid (Comparative paper chromatography (CoPC), UV, and ^{1}H and ^{13}C-NMR spectral analyses) (*32*) together with glucose (CoPC). Partial acid hydrolysis of compound **7** yielded, besides glucose and dehydrotrigallic acid (CoPC), an intermediate (**7a**) that was purified by preparative PC. This was found to have a M_r of 668 (negative ESI mass spectrum: $[M-H]^-$, m/z 667) and UV spectral maximum in MeOH at 273 nm, thus suggesting its structure to be a monodehydrotrigalloyl glucose (*38*).

To determine the site of attachment of the dehydrotrigalloyl moieties in the molecule of the parent compound (**7**), ^{1}H-NMR spectral analysis was then carried out. The spectrum, recorded in DMSO-d_6, revealed a characteristic doublet at δ ppm 4.70 (*d*, *J* = 8 Hz) attributable to the β-anomeric glucose protons in compound **7**. The spectrum also showed two downfield glucose proton resonances at 4.40 (*d*, *J* = 12 Hz) and 4.22 (*dd*, *J* = 3.5 Hz and 12 Hz) attributable to the two methylenic glucose protons at C-6.

In addition, two different patterns of proton signals each belonging to a dehydrotrigalloyl moiety were also noted in this spectrum at δ ppm 7.10 (*d*, *J* = 2.5 Hz); 6.99 (*d*, *J* = 2.5 Hz); 6.96 (*s*) (2H); 6.40 (*d*, *J* = 2.5 Hz); 6.42 (*d*, *J* = 2.5 Hz); 6.53 (*s*); and 6.54 (*s*). This assignment was based on comparison with the ^{1}H-NMR spectrum of free dehydrotrigallic acid, which had signals at δ ppm: 7.02 (*d*, *J* = 2.5 Hz); 6.95 (*s*); 6.48 (*d*, *J* = 2.5 Hz); and 6.42 (*s*) (*32*).

Dehydrotrigalloylation at the anomeric and the 6-positions of glucose in compound **7** was evidenced by an upfield shift of the anomeric carbon at δ ppm 94.53 in the ^{13}C NMR spectrum and the low field of methylenic proton signals in the ^{1}H NMR spectrum in comparison to the corresponding chemical shifts in free β-glucose (*39*).

The weight of evidence described above indicated that compound **7** is 1,6-di-*O*-dehydrotrigalloyl-β-D-$^4C_1$-glucopyranose. Final proof of its structure was then obtained through ^{13}C-NMR spectral analysis, which resulted in a spectrum containing essentially double signals for most of the dehydrotrigalloyl carbons. In this spectrum, resonances were assigned by comparing them to the ^{13}C-NMR data reported for free dehydrotrigallic acid (*32*) as well as for 1,6-di-*O*-galloyl glucose (*40,41*), β-anomeric carbon signals were readily identified from the characteristic chemical shift values at δ ppm 94.53, attributable to glucose C-1β, and at 66.24, attributable to C-6 glucose carbon. Other resonances in this spectrum exhibited chemical shift values [74.29 (C-2"), 76.82 (C-3"), 70.33 (C-4"), 73.76 (C-5")] that were in accordance with the proposed structure of compound **7**. Furthermore, the measured chemical shift values of the glucose carbon resonances proved that this moiety existed in a pyranose form (*39*), thus confirming the final structure of compound **7** to be 1,6-di-*O*-dehydrotrigalloyl-β-D-$^4C_1$-glucopyranose, which represents, to the extent known, a new natural product.

3.2. *Influence on human osteoblastic cell cultures*

Osteoblastic-mediated bone formation can be divided into three phases: proliferation, matrix maturation, and mineralization (*42*). Cell vitality was estimated in the Neutral Red assay (*13,14*) as a parameter for the proliferation phase, and protein content and ALP activity were determined as indicators for matrix maturation and finally mineralization of the

extracellular matrix (ECM). In order to increase the validity of the results and to eliminate false positives, two different cell lines, namely HOS58 and SaOS-2 cell lines, were used.

3.2.1. *Cell viability and cell proliferation assay (NR assay)*

Neutral red (3-amino-*m*-dimetyhlamino-2-methyl-phenazine hydrochloride)-based colorimetric assay is one of the best methods to detect mammalian cell survival and proliferation and is frequently used (*13,14*). The NR assay is based on the incorporation of the supravital dye, neutral dye, into lysosomes of viable uninjured cells after incubation of the cell culture with the extract. This weakly cationic dye penetrates cell membranes by nonionic diffusion and binds intracellularly to anionic carboxylic and/or phosphate groups of the lysosomal matrix. Xenobiotics that injure the plasma or lysosomal membrane decrease the uptake and subsequent retention of the dye. Dead cells cannot retain the dye after washing/fixation (*14,15*). After extraction from the lysosomes, the neutral dye is quantified spectrophotometrically and this amount is compared to the amount of dye extracted from control cell cultures (*13-15*). Cytotoxicity testing of *H. myrtifolia* did not indicate any reduction in cell viability (Figure 2). Even at the highest concentration tested (125 µg/mL), HOS58 cells retained their metabolic activity.

3.2.2. *Cellular protein content and ALP activity of HOS58 cells*

The extract was slightly toxic to HOS58 cells up to 125 µg/mL (Figure 2), suggesting that it was tolerated by the cell line prior to this concentration.

Total protein content assay – There was a transient increase in total cellular protein at doses between 15.6 and 62.5 µg/mL. Given a lack of cytotoxicity at this concentration, this can be considered the stimulation of cell maturation (Figure 3). At higher concentrations (> 100 µg/mL), protein production decreased.

ALP activity assay – ALP activity is commonly used as an indicator of osteoblastic cell maturation. The enzyme is considered to mark the middle stage of bone formation and generally appears during the matrix maturation phase (*43,44*). It plays an unclear, but crucial role in matrix mineralization (*44*). The level of cellular ALP activity of HOS58 human osteoblastic osteosarcoma cells was significantly reduced in a dose-dependent manner within the *H. myrtifolia* non-toxic concentration range tested (15.6 and 62.5 µg/mL) to values between 90% and 75% of vehicle treated control (4,100 and 3,200 nmol/min/mg) (Figure 4). A higher concentration (125 µg/mL) of *H. myrtifolia* resulted in an even more pronounced reduction of ALP.

This finding supports the proposed triggering of cell maturation by *H. myrtifolia* in terms of increased formation of ECM. This matrix provides support for subsequent mineralization. The enzyme ALP plays an important but yet undefined role in the mineralization

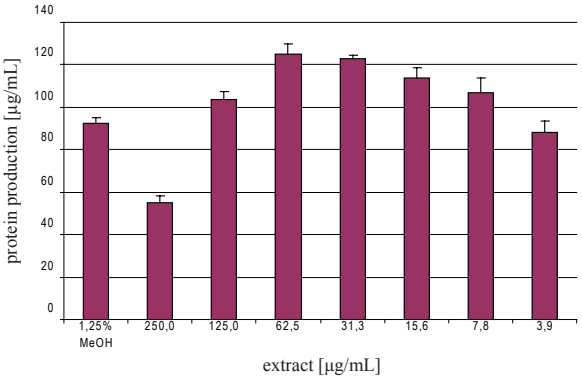

Figure 3. Total cellular protein produced by HOS58 human osteosarcoma cells under the influence of *H. myrtifolia* leaf extract. A dose-dependent increase was observed for medium doses (15.6 to 62.5 µg/mL). Two independent experiments with 6 parallels each were performed.

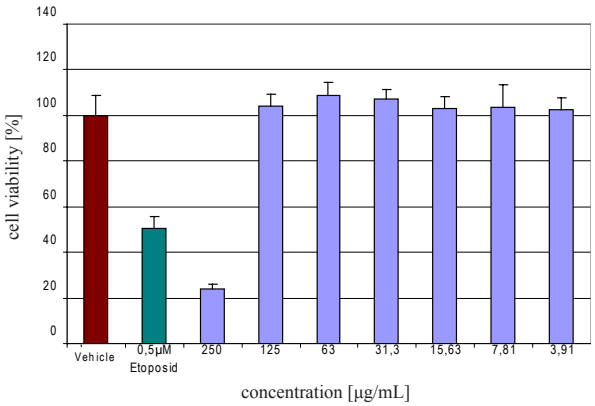

Figure 2. Cytotoxicity on HOS58 human osteosarcoma cells. No significant toxicity was observed up to 125 µg/mL, suggesting that the cells continued to be viable in the experimental setup. Two independent experiments with 6 parallels each were performed.

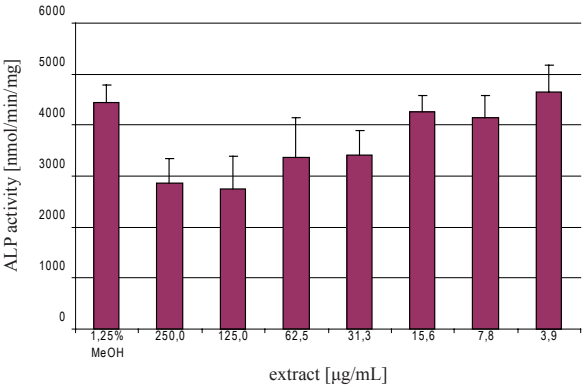

Figure 4. ALP activity of HOS58 human osteosarcoma cells under the influence of *H. myrtifolia* leaf extract. A dose-dependent decrease of enzyme activity was observed. Two independent experiments with 6 parallels each were performed**.**

process and its abundance varies considerably with cell activation. It is usually down-regulated when ECM is produced (as it is not necessary for this process). The model substance bGP (2 mM) was used as a positive control and led to a significant increase in ALP activity within the usual range, thus indicating quite normal cell behavior.

3.2.3. *Mineralization assay of SaOS-2 cells and enhanced activity of the crude extract*

To accomplish the testing of *H. myrtifolia* crude extract, the effect of *H. myrtifolia* on *in vitro* mineralization was studied using SaOS-2 cells. This delicate process is not fully understood but it requires a highly sophisticated ECM, an active ALP (at least in the beginning), and a certain concentration of inorganic phosphorus. Mineralization as the last step of bone formation unambiguously shows the bone character of cells (*43*). It is therefore used as an endpoint for *in vitro* studies of cells with an osteoblastic lineage. After 21 days of cultivation, unstimulated cells (containing no bGP) did lack calcium deposition (data not shown). The addition of bGP (2 mM) was found to be essential for the activation of the mineralization process and led to detectable calcium deposits of SaOS-2 of about 30 µg/mL (data not shown). This finding has been noted by others, and bGP is frequently used to trigger mineralization (*45*). Zn is added as a positive control as it helps in calcium deposition or aids in calcium deposition inside the matrix (*46*). The aqueous alcoholic leaf extract of *H. myrtifolia* has a stimulating effect on the mineralization of SaOS-2 cells. There was a highly significant increase (280 µg/mL) in calcium deposition or mineralization when using 25 µg/mL of *H. myrtifolia* leaf extract (Figure 5). Using 1 and 5 µg/mL of leaf extract did significantly alter positive cell mineralization to 175 and 205 µg/mL, respectively, indicating strong dose-dependent activity (Figure 5).

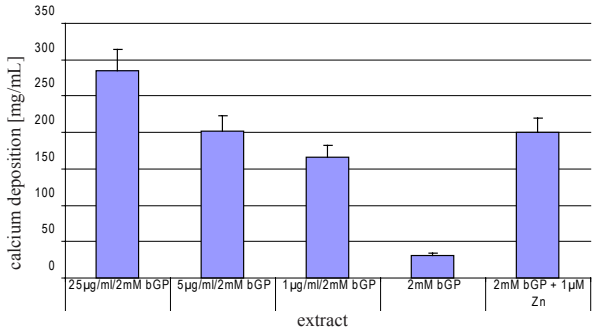

Figure 5. Mineralization (calcium deposition) of SaOS-2 human osteosarcoma cells *in vitro* under the influence of *H. myrtifolia* leaf extract. A strong dose-dependent increase was observed for *Heimia* extract. Calcium deposition was triggered by 2 mM bGP (glycerophosphate). One experiment with 4 parallels each was performed.

4. Conclusion

Sixteen compounds were isolated from the genus *Heimia* for the first time. These compounds included 5,7,4'-trihydroxy-3-methoxyflavanone (dihydrokaempferol-3-*O*-methyl ether) (compound **9**), which was recorded for the second time, and a new natural product, 1,6-di-*O*-dehydrotrigalloyl-β-D-$^4C_1$-glucopyranose (compound **7**).

Further, an aqueous alcohol extract of *H. myrtifolia* was found to stimulate mineralization and protein production of SaOS-2 human osteosarcoma osteoblastic cell cultures for the first time. Utilizing pharmacologically relevant concentrations (< 30 µg/mL), the current data thus show that the *H. myrtifolia* aqueous alcoholic extract enhances the osteogenicity of cultured bone cells. This positive effect on bone cells with comparatively low doses of *H. myrtifolia* extract is, at least partly, attributed to its high phenolic content.

In conclusion, *H. myrtifolia* extract has been found to have a bone-enhancing effect *in vitro*. Its high content of phenolic compounds, which help in calcium deposition in the bone cells matrix, may lead to the extract playing a role in the prevention of osteoporosis.

References

1. Ayoub NA. Unique phenolic carboxylic acids from *Sanguisorba minor*. Phytochemistry. 2003; 63:433-436.
2. Ayoub NA, Hussein SA, Hashim AN, Hegazi NM, Linscheid M, Harms M, Wende K, Lindequist U, Nawwar MA. Bone mineralization enhancing activity of a methoxyellagic acid glucoside from a *Feijoa sellowiana* leaf extract. Pharmazie. 2009; 64:137-141.
3. Ayoub NA. A trimethoxyellagic acid glucuronide from *Conocarpus erectus* leaves: Isolation, characterization and assay of antioxidant capacity. Pharm Biol. 2010; 48:328-332.
4. Harborne JB. Phytochemical Methods. Chapman & Hall, London, UK, 1973.
5. Malone MH, Rother A. *Heimia salicifolia*: A phytochemical and phytopharmacologic review. J Ethnopharmacol. 1994; 42:135-159.
6. Weisbach JA. Heimia Alkaloids (Patent No. 3184446). Smith Kline & French Laboratories, Philadelphia, PA, USA, 1965. (*http://www.freepatentsonline.com/3184446.html*)
7. Otsuka H, Tsukui M, Toyosato T, Fujioka S, Matsuoka T, Fujimura H. Anti-inflammatory agents, anti-inflammatory activity of crude drugs and plants. Takeda Kenkyusho Ho. 1972; 31:238-246.
8. Yang LL, Lee CY, Yen KY. Induction of apoptosis by hydrolysable tannins from *Eugenia jambos* L. on human leukemia cells. Cancer Lett. 2000; 157:65-75.
9. Douglas B, Kirkpatrick JL, Raffauf RF, Ribeiro O, Weisbach JA. Problems in chemotaxonomy. II. The major alkaloids of the genus *Heimia*. Lloydia. 1964; 27:25-31.
10. Ferris JP, Douglas B, Boyce CB, Briner RC, Kirkpatrick JL, Weisbach JA. Lythraceae alkaloids: Structure and stereochemistry of the major alkaloids of *Decodon* and

Heimia. Tetrahedron Lett. 1966; 30:3641-3649.
11. Graham SA, Kleiman R. Seed lipids of lythraceae. Biochem Syst Ecol. 1987; 15:433-439.
12. Parmar VS, Vardhan A, Nagarajan GR, Jain R. Dihydroflavonols from *Prunus Domestica*. Phytochemistry. 1992; 31:2185-2186.
13. Borenfreund E, Puerner JA. Toxicity determined *in vitro* by morphological alterations and neutral red absorption. Toxicol Lett. 1985; 24:119-124.
14. Babich H, Borenfreund E. Structure-activity relationship (SAR) models established *in vitro* with the neutral red cytotoxicity assay. Toxicol In Vitro. 1987; 1:3-9.
15. Borenfreund E, Puerner JA. A simple quantitative procedure using monolayer cultures for cytotoxicity assays (HTD/NR-90). Methods Cell Sci. 1984; 9:7-9.
16. Zor T, Selinger Z. Linearization of the Bradford protein assay increases its sensitivity: Theoretical and experimental studies. Anal Biochem. 1996; 236:302-308.
17. Morgan BR, Artiss JD, Zak B. Calcium determination in serum with stable alkaline Arsenazo III and triglyceride clearing. Clin Chem. 1993; 39:1608-1612.
18. Wang M, Simon JE, Aviles IF, He K, Zheng QY, Tadmor Y. Analysis of antioxidative phenolic compounds in artichoke (*Cynaras colymus* L.). J Agric Food Chem. 2003; 51:601-608.
19. Fan CQ, Yue JM. Biologically active phenols from *Saussurea medusa*. Bioorg Med Chem. 2003; 11:703-708.
20. Siciliano T, De Tommasi N, Morelli I, Braca A. Study of flavonoids of *Sechium edule* (Jacq) Swartz (Cucurbitaceae) different edible organs by liquid chromatography photodiode array mass spectrometry. J Agric Food Chem. 2004; 52:6510-6515.
21. Lee EJ, Kim JS, Kim HP, Lee JH, Kang SS. Phenolic constituents from the flower buds of *Lonicera japonica* and their 5-lipoxygenase inhibitory activities. Food Chem. 2010; 120:134-139.
22. Prachayasittikul S, Suphapong S, Worachartcheewan A, Lawung R, Ruchirawat S, Prachayasittikul V. Bioactive metabolites from *Spilanthes acmella* Murr. Molecules. 2009; 14:850-867.
23. Li YL, Li J, Wang NL, Yao XS. Flavonoids and a new polyacetylene from *Bidens parviflora* Willd. Molecules. 2008; 13:1931-1941.
24. Chaudhary G, Goyal S, Poonia P. *Lawsonia inermis* Linnaeus: A phytopharmacological review. International Journal of Pharmaceutical Sciences and Drug Research. 2010; 2:91-98.
25. Barakat HH, Hussein SAM, Marzouk MS, Merfort I, Linscheid M, Nawwar MAM. Polyphenolic metabolites of *Epilobium hirsutum*. Phytochemistry. 1997; 46:935-941.
26. Méndez J, Mato MC. Methyl gallate and related polyphenols as auxin protectors. Phytochemistry. 1997; 44:41-43.
27. Nawwar MAM, Buddrus J, Bauer H. Dimeric phenolic constituents from the roots of *Tamarix nilotica*. Phytochemistry. 1982; 21:1755-1758.
28. Barakat HH, Nawwar MAM, Buddrus J, Linsheid M. Niloticol, a phenolic glyceride and two phenolic aldehydes from the roots of *Tamarix nilotica*. Phytochemistry. 1987; 26:1837-1838.
29. Sakar MK, Petereit F, Nahrstedt A. Two phloroglucinol glucosides, flavan gallates and flavonol glycosides from *Sedum sediforme* flowers. Phytochemistry. 1993; 33:171-174.
30. Nawwar MAM, Hussein SAM, Merfort I. NMR spectral analysis of polyphenols from *Punica granatum*. Phytochemistry. 1994; 36:793-798.
31. Nawwar MAM, EI-Mousallamy AMD, Barakat HH, Buddrus J, Linscheid M. Flavonoid lactates from the leaves of *Marrubium vulgare*. Phytochemistry. 1989; 28:3201-3206.
32. Nawwar MAM, Hussein SAM, Buddrus J, Linscheid M. Tamarix ellagic acid, an ellagitannin from the galls of *Tamarix aphylla*. Phytochemistry. 1994; 35:1349-1354.
33. Khac DD, Tran-Van S, Campos AM, Lallemand JY, Fetizon M. Ellagic compounds from *Diplopanax stachyanthus*. Phytochemistry. 1990; 29:251-256.
34. Sata T. Spectral differentiation of 3,3'-di-*O*-methylellagic acid from 4,4'-di-*O*-methylellagic acid. Phytochemistry. 1987; 26:2124-2125.
35. Mabry TJ, Markham RK, Thomas MB. The Systematic Identification of Flavonoids. Springer, New York, USA, 1970; p. 280.
36. Mabry TJ, Markham RK, Thomas MB. The Systematic Identification of Flavonoids. Springer, New York, USA, 1970; p. 292.
37. Nawwar MAM, Souleman AMA, Buddrus J, Bauer H, Linscheid M. Polyphenolic constituents of the flowers of *Tamarix nilotica*: The structure of nilocitin, a new digalloylglucose. Tetrahedron Lett. 1984; 25:49-52.
38. Bikbulatova TN, Erzhanova MS, Terent'ev PB, Beisekova KD, Seifullina A. A hydrolyzable tannin substance from the fruit of *Rosa platyacantha*. Chemistry of Natural Compounds. 1985; 21:789-791.
39. Kalinowski HO, Berger S, Braun S. ^{13}C-NMR Spektroskopie. Georg Thieme, Stuttgart, Germany, 1984.
40. Kashiwada Y, Nonaka GI, Nishioka I. Tannins and related compounds. XXIII. Rhubarb (4): Isolation and structures of new classes of gallotannins. Chem Pharm Bull. 1984; 32:3461-3470.
41. Kashiwada Y, Nonaka GI, Nishioka I, Yamagishi T. Galloyl and hydroxycinnamoylglucoses from rhubarb. Phytochemistry. 1988; 27:1473-1477.
42. Stein GS, Lian JB, Owen TA. Relationship of cell growth to the regulation of tissue-specific gene expression during osteoblast differentiation. FASEB J. 1990; 4:3111-3123.
43. Saif A, Lindequist U, Wende K. Stimulating effects of *Grifola frondosa* (Maitake) on human osteoblastic cell cultures. J Nat Med. 2007; 61:231-238.
44. Perizzolo D, Lacefield WR, Brunette DM. Interaction between topography and coating in the formation of bone nodules in culture for hydroxyapatite- and titanium-coated micromachined surfaces. J Biomed Mater Res. 2001; 56:494-503.
45. zur Nieden NI, Kempka G, Ahr HJ. *In vitro* differentiation of embryonic stem cells into mineralized osteoblasts. Differentiation. 2003; 71:18-27.
46. Hsu HH, Anderson HC. Effects of zinc and divalent cation chelators on ATP hydrolysis and Ca deposition by rachitic rat matrix vesicles. Bone. 1995; 17:473-477.

(*Received July 3, 2010; Revised August 11, 2010; Re-revised August 18, 2010; Accepted August 21, 2010****)***

Original Article

Evaluation of therapeutic effects and pharmacokinetics of antibacterial chromogenic agents in a silkworm model of *Staphylococcus aureus* infection

Tomoko Fujiyuki, Katsutoshi Imamura, Hiroshi Hamamoto, Kazuhisa Sekimizu*

Graduate School of Pharmaceutical Sciences, The University of Tokyo, Tokyo, Japan.

ABSTRACT: The therapeutic effect of dye compounds with antibacterial activity was evaluated in a silkworm model of *Staphylococcus aureus* infection. Among 13 chromogenic agents that show antibacterial activity against *S. aureus* (MIC = 0.02 to 19 μg/mL), rifampicin had a therapeutic effect. The ED_{50} value in the silkworm model was consistent with that in a murine model. Other 12 dyes did not increase survival of the infected silkworms. We examined the reason for the lack of therapeutic efficacy. Amidol, pyronin G, and safranin were toxic to silkworms, which explained the lack of therapeutic effects. Fuchsin basic and methyl green disappeared quickly from the hemolymph after injection, suggesting that they are not stable in the hemolymph. Although coomassie brilliant blue R250/G250, cresyl blue, and nigrosin showed no toxic effects or instability in the hemolymph, they also did not have a therapeutic effect. The *in vitro* antibacterial actions of these dyes were inhibited by silkworm plasma or bovine serum albumin and filtration experiments demonstrated that cresyl blue bound to plasma proteins in the silkworm, suggesting that plasma protein binding inhibited the therapeutic efficacy of these four dyes. These findings indicate that drug screening using the silkworm infection model is useful for evaluating toxicity and pharmacokinetics of potential antibiotics.

Keywords: Silkworm, plasma protein binding, antibacterial, dye

1. Introduction

In the course of developing drugs to treat infectious diseases, chemical compounds with antibacterial activity *in vitro* are tested for their therapeutic efficacy *in vivo* in animal infection models. A serious problem is that most of compounds that exhibit antibacterial activity *in vitro* do not have therapeutic effects in animal infection models due to toxicity and pharmacokinetic issues. Thus, for efficient drug discovery, protocols must be established to exclude agents without therapeutic effects at earlier stages of drug development. Evaluation of the therapeutic effects of potential antibiotics has been performed using mammalian models, but conventional methods using a large number of mammals are problematic due to high costs and ethical concerns. Therefore, the development of a non-vertebrate infection model to test drug efficacy in the early stages of development is highly desirable.

We have established insect models of human pathogenic bacterial and viral infection using the silkworm, *Bombyx mori* (*1-3*), and proposed the utilization of the silkworm model for drug discovery (*4*). Our previous studies indicated that lethal doses of chemicals in silkworm were consistent with those in mammals, when normalized by body weights (*5*). Silkworms and mammals share conserved mechanisms for the pharmacokinetics of chemicals: absorption, distribution, metabolism, and excretion (ADME) (*5-7*). Therefore, the silkworm infection model is potentially useful for the evaluation of toxicity and ADME of candidate compounds in therapeutic drug screening for infectious diseases.

In mammals, the binding of drugs to plasma proteins like albumin is an important factor in the distribution of drugs in the animal body. In invertebrates, however, information regarding interactions of drugs with plasma proteins is scarce. Therefore, it is not known whether the silkworm model can be used to evaluate the inhibition of therapeutic effects induced by plasma protein binding of drug candidate agents.

To evaluate factors that affect pharmacokinetics, including plasma protein binding, on the therapeutic effects of antibacterial agents in the silkworm infection model, we considered dyestuffs as suitable model agents. Some of dyes have antibacterial activity (*8,9*).

**Address correspondence to:*
Dr. Kazuhisa Sekimizu, Graduate School of Pharmaceutical Sciences, The University of Tokyo, 7-3-1 Hongo, Bunkyo-ku, Tokyo 113-0033, Japan.
e-mail: sekimizu@mol.f.u-tokyo.ac.jp

In addition, dye concentration in samples can be easily quantified by measuring absorbance. Here we describe the therapeutic effects and pharmacologic properties of dyes in the silkworm model of *S. aureus* infection.

2. Materials and Methods

2.1. *Animals*

Bombyx mori eggs (Fu•Yo × Tsukuba•Ne) were purchased from Ehima Sansyu (Ehime, Japan), and raised to the fifth instar larval stage by feeding with artificial food Silkmate 2S (Nosan Corporation, Yokohama, Japan). All of the animals used in this study were fifth instar larvae.

2.2. *Chromogenic compounds*

Rifampicin, methyl green, amidol (Wako Pure Chemical Industries, Osaka, Japan), Coomassie brilliant blue (CBB) R250, CBB G250, nigrosin (Nakalai Tesque, Kyoto, Japan), malachite green (Tokushu Chemicals, Tokyo, Japan), crystal violet (Sigma, St. Louis, MO, USA), cresyl blue, pyronin G (Tokyo Chemical Industry, Tokyo, Japan), toluidine blue O (Chroma-gesellschaft Schmid, Stuttgart, Germany), fuchsin basic, and safranin (Kanto Chemical, Tokyo, Japan) were dissolved in phosphate buffered saline (PBS, 10 mM sodium phosphate, 137 mM sodium chloride, 3 mM potassium chloride, pH 7.4) or dimethyl sulfoxide. Commercially available CBB R250 is a mixture of chromogenic compounds in different forms (*10-12*). Therefore, we purified CBB R250 from the purchased reagent using thin layer chromatography (TLC). The sample (30 mg) in methanol was applied to a preparative TLC plate (silica gel 60 F254, Merck KGaA, Darmstadt, Germany) and developed in 1-butanol/acetic acid/water (15:3:7). The main band with blue color was scraped off, eluted with methanol, and filtered through a 0.45-μm filter. The methanol was removed by evaporation and the sample was analyzed using liquid chromatography-mass spectrometry. The molecular mass of the principal compound in the fraction was estimated to be 804, which is previously reported molecular mass of CBB R250 (*11*).

2.3. *Assay of antibacterial activity of dyes*

A clinical strain of *S. aureus*, MSSA1 (*13*), was cultured in Luria-Bertani 10 (LB 10) medium (10 g bactotryptone, 5 g yeast extract, 10 g NaCl per liter) at 37°C for 24 h. The full growth culture was diluted to 1/1,000 in Mueller-Hinton (MH) medium and then a 100-μL aliquot was added to each well of 96-well plate. The dye solution was serially diluted 2-fold and 100 μL of each dilution was added to the bacterial solution, and cultured at 37°C for 18 to 24 h. Bacterial growth was visually determined. The MIC (minimum inhibitory concentration) was defined as the lowest concentration of the dye that inhibited the bacterial growth. To evaluate the effect of silkworm plasma or bovine serum albumin (BSA) on the antibacterial activity of the dyes, the silkworm plasma (final concentration, 25%) or BSA (fraction V, Nakalai Tesque; final concentration, 25 mg/mL) was added to MH medium, and the MICs of the dyes were determined. The silkworm plasma was prepared as follows: the legs of fifth instar larvae were cut and the hemolymph was collected. 2-Mercaptoethanol (2-ME; final concentration, 0.1%) was added to the samples to inhibit melanization and the hemocytes were removed by centrifugation for 5 min at 8,000 rpm (R10A2, Hitachi Koki, Tokyo, Japan).

2.4. *Calculation of the theoretically minimal effective dose of antibacterial dye required for the treatment of infected silkworms*

The fifth instar larva (2 g) used for therapeutic assay has a hemolymph with volume of approximately 500 μL (*5*). Therefore, injection of 50 μL dye solution into the silkworm hemolymph results in a 1:10 dilution. The putative minimal effective dose of dye minimally required to achieve therapeutic effect on the infected silkworm, tEDmini (μg/g•larva), was theoretically defined based on the following formula using the MIC of the dye.

$$\text{tEDmini (μg/g•larva)} = \frac{\text{MIC (μg/mL)} \times 0.5\text{ (mL)} \times 10}{2\text{ (g•larva)}}$$

2.5. *Determination of the dye LD_{50} in silkworms*

The larvae were reared for 1 day at 27°C with feeding. The larvae (n = 3-5) were injected with 2-fold serial dilutions of the dye solution (50 μL) into the hemolymph and reared at 27°C. The number of surviving larvae was counted 2 days later. The LD_{50} was determined by the survival curve as the dose that killed half of the larvae (LD_{50}).

2.6. *Evaluation of therapeutic effects of dyes*

Full growth *S. aureus* culture was diluted 10-fold with 0.9% NaCl. A 50 μL aliquot was injected into the hemolymph of the silkworm. Dye solution (50 μL) diluted with PBS was further injected into the hemolymph (*6*). The silkworms were reared at 27°C and the number of surviving silkworms was counted 2 days later. Vancomycin (200 μg/mL) was administered as a positive control. To determine the number of viable bacteria in the hemolymph, the hemolymph was collected 1 day after the injection of CBB R250 and diluted in 0.9% NaCl before spreading on mannitol-

salt agar plates. The plates were incubated at 37°C overnight and the colonies were counted.

2.7. *Determination of the concentration of chromogenic compound in the hemolymph of the injected silkworm*

Rifampicin solution (3.5 mg/mL in 30% dimethyl sulfoxide, 0.9% NaCl, 50 μL) was injected into the hemolymph of the silkworm. The animals were reared at 27°C and the hemolymph was collected after 20 sec, 1, 5, 10, 15, 30, 60 min, 1.5, 2, 4, 8 h. 2-ME (1 μL) was added to approximately 100 μL of hemolymph and an equal volume of acetone was added to the hemolymph, followed by vigorous shaking. The sample was then centrifuged at 20,000 × g for 5 min and the OD_{475} of the supernatant was measured. Hemolymph of a silkworm injected with the buffer (30% dimethyl sulfoxide, 0.9% NaCl) was used as the background.

A solution (50 μL, in PBS) of fuchsin basic (5 mg/mL), methyl green (15 mg/mL), CBB R250 (3.7 mg/mL), CBB G250 (5 mg/mL), cresyl blue (8 mg/mL), or nigrosin (9 mg/mL) was injected into the hemolymph of the silkworm. The animals were reared at 27°C and the hemolymph was collected after 2 days and the sample was prepared as described above. The OD value, at absorption maximum of each dye, of the supernatant was measured. Hemolymph of a silkworm injected with PBS was used as the background.

2.8. *Assay for cresyl blue binding to the silkworm plasma proteins*

A solution of cresyl blue (2 μL, 8 mg/mL) was mixed with the silkworm plasma (200 μL) diluted with phosphate buffer (10 mM sodium phosphate, 150 mM sodium chloride, 5 mM potassium chloride, 1 mM calcium chloride, pH 7.2). The sample was applied to YM-3 filter for ultra filtration (3 kDa cut-off, Millipore, Billerica, MA, USA) and centrifuged at 12,000 × g for 30 min at 4°C. The OD_{635} of the filtered solution was measured and the amount of the dye that passed through the membrane was calculated. Protein concentration in the filtered solution was determined by Lowry's method after trichloroacetic acids precipitation. The findings revealed that most of the proteins did not pass through the filter.

3. Results

First, we measured the antibacterial activity *in vitro* of 44 randomly selected chromogenic compounds *in vitro* and chose the 13 dyes for which the MIC was less than 20 μg/mL (Table 1). We then tested whether the dyes were therapeutically effective in silkworms infected with *S. aureus*. Rifampicin had a therapeutic effect and the ED_{50} value was 0.08 μg/g•larva. This is consistent with the value in a murine model (0.062 μg/g) (*14*). None of others had a therapeutic effect, even at various doses. In addition to evaluating the therapeutic effect by counting the number of surviving silkworms, we examined whether CBB R250 suppresses the growth of *S. aureus* in the silkworm hemolymph. Our findings indicated that CBB R250 administration did not decrease the number of viable bacteria in the hemolymph (Figure 1), whereas vancomycin suppressed bacterial growth in the hemolymph. To understand the reason for the lack of therapeutic effects of these dyes in the silkworm infection model, we studied their toxicity, stability in the hemolymph, and plasma protein binding properties as follows.

For antibacterial agents to show therapeutic effects, their concentrations in the hemolymph after injection should be higher than their MIC values and, at the same time, they should not be toxic to the host animals. As the MIC value enables us to calculate the minimal required dose for the therapeutic effect in infected silkworms (see "Material and Methods"), we defined the value as the theoretical minimal effective dose required

Table 1. Antibacterial activity, toxicity, and therapeutic effect of dyes in the silkworm model of *S. aureus* infection

Dye	MIC (μg/mL)	tEDmini (μg/g•larva)	LD_{50} (μg/g•larva)	ED_{50} (μg/g•larva)	ED_{50}/MIC
Rifampicin	0.02	0.05	ND	0.08	4
Amidol	19	48	54	> 9	> 0.5
Pyronin G	2	5	11	> 13	> 7
Safranin	10	25	34	> 23	> 2
Fuchsin basic	6	15	100-500	> 230	> 38
Methyl Green	13	33	530	> 160	> 12
CBB R250	4	10	> 660	> 83	> 17
CBB G250	7	18	> 800	> 72	> 10
Cresyl Blue	4	10	530	> 150	> 39
Nigrosin	5	13	490	> 170	> 33
Crystal Violet	0.2	0.5	15	> 9	> 45
Malachite Green	0.3	0.8	15	> 10	> 33
Toluidine Blue O	14	35	1,000	> 700	> 50
Vancomycin	1	2	ND	0.3*	0.3*

*; the values are cited from Hamamoto *et al.*, 2004. tEDmini; theoretical minimal effective dose required for therapeutic effect in the infected silkworm. ND; not determined.

for the therapeutic effect (tEDmini), and compared it with the LD_{50} value of the dye. The tEDmini values of amidol, pyronin G, and safranin were 48, 5, and 25 μg/g•larva, respectively, which were all greater than 1/3 of the LD_{50} values (Table 1). These results suggest that these three dyes were not therapeutically effective in the silkworm infection model because they were toxic to the silkworms.

The other nine dyes with antibacterial activity showed smaller tEDmini values lower than 1/10 of the LD_{50} (Table 1). These dyes still did not have therapeutic effects in the infected silkworms. We previously proposed that an antibacterial agent whose ED_{50}/MIC values were lower than 10 had proper pharmacokinetics characteristics (*6*). While the ED_{50}/MIC value of rifampicin was 4, the values of the nine dyes were over 10 (Table 1), suggesting that these dyes have pharmacokinetic problem in the silkworm and thus are not therapeutically effective. To test this notion, we examined the stability of these compounds in the silkworm hemolymph. The concentration of the chromogenic compound in the hemolymph can be easily measured by absorbance at the maximum absorption wavelength. This method revealed that the half-life of rifampicin at α phase was 3 min, indicating rapidly distributed (Figure 2). The half-life at β phase was 3 h, suggesting that rifampicin is present in the hemolymph over the MIC during 2 days after injection. The period of the half-life at β phase was consistent with that of human (*15*). As for other dyes, the concentration of fuchsin basic and methyl green in the hemolymph was below the MIC at 2 days after injection (Table 2), suggesting that these dyes are rapidly eliminated from the hemolymph. We concluded that these chromogenic compounds do not have therapeutic effects due to their rapid distribution into the tissues, rapid metabolism, and/or rapid excretion.

The concentrations of CBB R250, CBB G250, cresyl blue, and nigrosin in the hemolymph were higher than the MIC values even 2 days after injection, but they still did not show the therapeutic effects (Tables 1 and 2), suggesting that a factor other than distribution, metabolism, and excretion of the dyes inhibited the therapeutic effects.

Therapeutic effects of drugs are sometimes prevented by plasma protein binding, which is included in the issues of distribution of ADME. It is well known that CBB R250, CBB G250, and nigrosin bind to proteins (*16-18*). We examined whether the antibacterial activity of CBB R250, CBB G250, cresyl blue, and nigrosin were inhibited in the presence of the silkworm plasma. Adding the silkworm plasma fraction increased the MICs of these four dyes (Table 3). The protein concentration in the hemolymph of fifth instar larva ranges from approximately 10 to 100 mg/mL (*19,20*). Adding 25 mg/mL BSA also increased the MICs of the dyes, whereas adding the silkworm

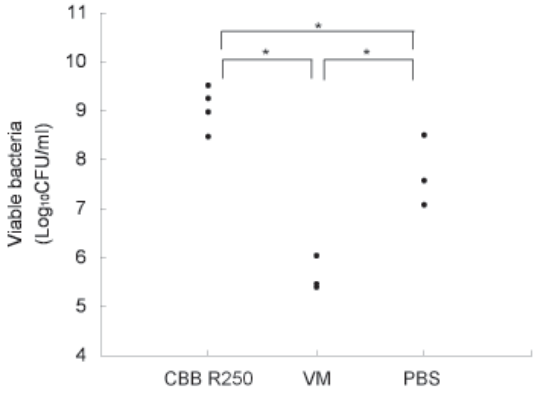

Figure 1. Evaluation of the therapeutic effect of CBB R250 based on the number of viable bacteria in the hemolymph after injection into the silkworm. A 10-fold diluted solution (50 μL) of full growth *S. aureus* culture was injected into the hemolymph of fifth instar larva, and then an equal volume of CBB R250, PBS, or vancomycin was injected into the hemolymph. The hemolymph was collected 1 day later and the number of colonies of viable bacteria was counted. Each dot indicates the number of viable bacteria in the hemolymph from one individual larva. * Student's *t*-test, $p < 0.05$.

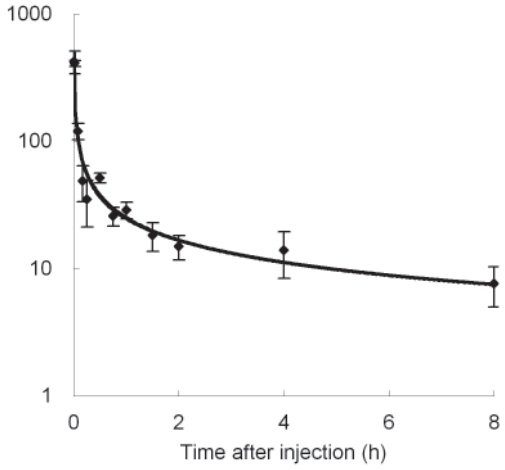

Figure 2. Pharmacokinetics of rifampicin in the silkworm. Rifampicin solution (50 μL, 3.5 mg/mL) was injected into the silkworm hemolymph and then the hemolymph was collected at different time after injection. The rifampicin concentration in the hemolymph was calculated by OD_{475} value. Data are presented as mean ± S.E.M. ($n = 3$).

Table 2. Dye concentration in the silkworm hemolymph after injection

Dye	MIC (μg/mL)	Concentration in hemolymph after 2 days (μg/mL)
Fuchsin basic	6	0 ± 0 ($n = 5$)
Methyl green	13	1 ± 1 ($n = 5$)
CBB R250	4	14 ± 5 ($n = 7$)
CBB G250	7	7 ± 3 ($n = 5$)
Cresyl blue	4	12 ± 4 ($n = 4$)
Nigrosin	5	9 ± 1 ($n = 4$)

Data shown are the MICs and the concentrations in the hemolymph of dyes (μg/mL). The concentration was measured 2 days after dye injection (250 μg/larva for fuchsin basic, 750 μg/larva for methyl green, 185 μg/larva for CBB R250, 250 μg/larva for CBB G250, 400 μg/larva for cresyl blue, 450 μg/larva for nigrosin) into the hemolymph. Values are presented as mean ± S.E.M. N; number of the tested silkworms.

plasma or BSA did not affect the MIC of vancomycin. Cresyl blue is a basic dye that binds to various biologic substances such as nucleic acids, although information regarding its protein binding properties is limited to only a few species of proteins (*21*,*22*). To examine whether cresyl blue binds to silkworm plasma proteins, we performed a filtration assay (see "Materials and Methods"). Adding the silkworm plasma decreased the amount of the filtrated dye (Figure 3). When mixed with the maximum amount (99%) of plasma, only 4% of cresyl blue penetrated through the filter, indicating that 96% of the dye wad bound to the plasma proteins. These results suggest that the antibacterial activities of CBB R250, CBB G250, cresyl blue, and nigrosin are inhibited in the hemolymph by plasma protein binding.

4. Discussion

In the present study, we examined the therapeutic effects of 13 different chromogenic compounds with *in vitro* antibacterial activity against *S. aureus*, and demonstrated that rifampicin had a therapeutic effect and the ED_{50} value and the elimination half-life were consistent with those in mammals. The other 12 dyes were not therapeutically effective in the silkworm infection model due to toxicity or ADME problems. Some of the dyes (CBB R250, CBB G250, cresyl blue, and nigrosin) had no therapeutic effects, while apparent concentrations in the hemolymph were maintained higher than their MICs. These dyes lost their antibacterial activity in the presence of silkworm plasma or BSA, which suggested that these dyes bind to silkworm plasma proteins and the concentrations of the free compounds are too small in the hemolymph to produce therapeutic effects in the silkworm infection model. We previously reported that the pharmacokinetics of various compounds are similar between silkworms and mammals (*5*-*7*). Here we reported that the influence of plasma protein binding on drug distribution, which is a known phenomenon in mammals, is also observed in silkworms. To our knowledge, this is the first report that the therapeutic effectiveness of drugs can be inhibited by plasma protein binding in invertebrates as well as in vertebrates.

Table 3. Effect of the presence of the silkworm plasma (25%) and BSA (25 mg/ml) on the antibacterial activity of dyes

Dye	None	Plasma	BSA
CBB R250	7 ± 2 (n = 3)	> 263 (n = 3)	> 1,050 (n = 3)
CBB G250	7 ± 0 (n = 3)	600 ± 184 (n = 3)	> 900 (n = 3)
Cresyl Blue	5 ± 1 (n = 4)	> 16 (n = 4)	> 131 (n = 4)
Nigrosin	3 ± 0 (n = 3)	> 163 (n = 4)	> 325 (n = 3)
Vancomycin	1 ± 0 (n = 2)	1 ± 0 (n = 2)	1 ± 0 (n = 2)

The MICs of the dyes are shown (μg/mL). A CBB R250 reagent was obtained from the supplier and used without purification in this experiment. Values are presented as mean ± S.E.M.

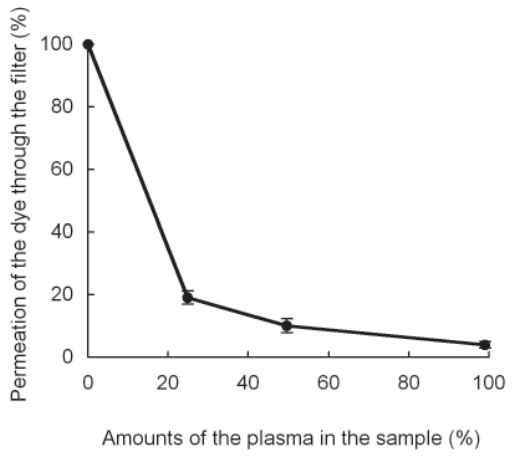

Figure 3. Binding of cresyl blue to the silkworm plasma proteins. Silkworm plasma was mixed with buffer in various ratios and then cresyl blue was added. The sample was applied to ultra-filtration. The OD_{635} of the filtrated solution was determined and the permeation of the dye was calculated. Data are presented as mean ± S.E.M. (n = 3).

Further, we showed that the silkworm model can be used to evaluate the toxicity of candidate agents of drugs for infectious diseases. We previously reported that the LD_{50} values of cytotoxic agents in silkworm are consistent with those in mammals (*5*). Therefore, therapeutically effective agents in the silkworm infection model are expected to show therapeutic effectiveness without toxicity in mammals. The silkworm infection model is advantageous for simultaneous evaluation of the toxicity and therapeutic effects of drug candidates.

Drug candidates whose concentrations in free form in the blood are reduced by plasma protein binding often do not show therapeutic effects. Efficient exclusion of such candidates in the early phase of drug development is necessary for productive drug discovery. To advance drug development, candidate compounds must have the low toxicity and good property of ADME properties. We propose the use of a silkworm model for these aims. Silkworm models of diseases do not cost compared with mammalian models and are associated with fewer ethical issues and biohazard risks. Furthermore, silkworm larvae are large enough to handle for the injection of reagent solutions and for the collection of hemolymph for analysis. Silkworm models of infectious diseases have been established using bacteria, virus, and fungi (*1*,*3*,*6*). Although other invertebrate infection models have also been proposed (*23*,*24*), the silkworm is highly advantageous for studies of pharmacokinetics and this model can likely be extended to various human diseases. Actually a silkworm model of human sepiapterin reductase deficiency was recently reported (*25*). Utilization of

the silkworm model of various diseases will be helpful to exclude candidate therapeutic agents that are not effective at an early stage of drug development.

Acknowledgements

We thank Kiyomi Kyougoku, Yumiko Matsuzawa, and Aya Yoshino for their technical assistance. This study was supported by the Program for the Promotion of Fundamental Studies in Health Sciences of NIBIO and grants from Genome Pharmaceuticals Co. Ltd. T. Fujiyuki is the recipient of a Grant-in-Aid from Japan Society for the Promotion of Science for young scientists (21-40175).

References

1. Kaito C, Akimitsu N, Watanabe H, Sekimizu K. Silkworm larvae as an animal model of bacterial infection pathogenic to humans. Microb Pathog. 2002; 32:183-190.
2. Kaito C, Sekimizu K. A silkworm model of pathogenic bacterial infection. Drug Discov Ther. 2007; 1:89-93.
3. Orihara Y, Hamamoto H, Kasuga H, Shimada T, Kawaguchi Y, Sekimizu K. A silkworm baculovirus model for assessing the therapeutic effects of antiviral compounds: Characterization and application to the isolation of antivirals from traditional medicines. J Gen Virol. 2008; 89:188-194.
4. Kurokawa K, Hamamoto H, Matsuo M, Nishida S, Yamane N, Lee BL, Murakami K, Maki H, Sekimizu K. Evaluation of target specificity of antibacterial agents using *Staphylococcus aureus ddlA* mutants and D-cycloserine in a silkworm infection model. Antimicrob Agents Chemother. 2009; 53:4025-4027.
5. Hamamoto H, Tonoike A, Narushima K, Horie R, Sekimizu K. Silkworm as a model animal to evaluate drug candidate toxicity and metabolism. Comp Biochem Physiol C Toxicol Pharmacol. 2009; 149:334-339.
6. Hamamoto H, Kurokawa K, Kaito C, Kamura K, Manitra Razanajatovo I, Kusuhara H, Santa T, Sekimizu K. Quantitative evaluation of the therapeutic effects of antibiotics using silkworms infected with human pathogenic microorganisms. Antimicrob Agents Chemother. 2004; 48:774-779.
7. Hamamoto H, Kamura K, Razanajatovo IM, Murakami K, Santa T, Sekimizu K. Effects of molecular mass and hydrophobicity on transport rates through non-specific pathways of the silkworm larva midgut. Int J Antimicrob Agents. 2005; 26:38-42.
8. Bentley R. Different roads to discovery; Prontosil (hence sulfa drugs) and penicillin (hence beta-lactams). J Ind Microbiol Biotechnol. 2009; 36:775-786.
9. Sörgel F. The return of Ehrlich's 'Therapia magna sterilisans' and other Ehrlich concepts? Series of papers honoring Paul Ehrlich on the occasion of his 150th birthday. Chemotherapy. 2004; 50:6-10.
10. Wilson CM. Studies and critique of amido black 10B, coomassie blue R, and fast green FCF as stains for proteins after polyacrylamide gel electrophoresis. Anal Biochem. 1979; 96:263-278.
11. Kundu SK, Robey WG, Nabors P, Lopez MR, Buko A. Purification of commercial coomassie brilliant blue R-250 and characterization of the chromogenic fractions. Anal Biochem. 1996; 235:134-140.
12. Rosenthal HL, Berger RA, Tyler AN, Moore BW. Isolation of a component from commercial coomassie brilliant blue R-250 that stains rubrophilin and other proteins red on polyacrylamide gels. Biochim Biophys Acta. 1988; 965:106-113.
13. Akimitsu N, Hamamoto H, Inoue R, Shoji M, Akamine A, Takemori K, Hamasaki N, Sekimizu K. Increase in resistance of methicillin-resistant *Staphylococcus aureus* to beta-lactams caused by mutations conferring resistance to benzalkonium chloride, a disinfectant widely used in hospitals. Antimicrob Agents Chemother. 1999; 43:3042-3043.
14. Rothstein DM, Farquhar RS, Sirokman K, Sondergaard KL, Hazlett C, Doye AA, Gwathmey JK, Mullin S, van Duzer J, Murphy CK. Efficacy of novel rifamycin derivatives against rifamycin-sensitive and -resistant *Staphylococcus aureus* isolates in murine models of infection. Antimicrob Agents Chemother. 2006; 50:3658-3664.
15. Nitti V, Virgilio R, Partricolo MR, Iuliano A. Pharmacokinetic study of intravenous rifampicin. Chemotherapy. 1977; 23:1-6.
16. Congdon RW, Muth GW, Splittgerber AG. The binding interaction of coomassie blue with proteins. Anal Biochem. 1993; 213:407-413.
17. Fazekas de St Groth S, Webster RG, Datyner A. Two new staining procedures for quantitative estimation of proteins on electrophoretic strips. Biochim Biophys Acta. 1963; 71:377-391.
18. Ortega M. Use of nigrosine for staining proteins after electrophoresis on filter paper. Nature. 1957; 179:1086-1087.
19. Fujiwara Y, Yamashita O. Developmental changes and hormonal regulation of mRNA of *Bombyx mori* larval serum protein (BmLSP). J Seric Sci Jpn. 1998; 67:393-401.
20. Etebari K, Matindoost L, Mirhoseini SZ, Turnbull MW. The effect of BmNPV infection on protein metabolism in silkworm (*Bombyx mori*) larva. Invertebrate Survival Journal. 2007; 4:13-17.
21. Kelley EG, Miller EG Jr. Reactions of dyes with cell substances; II. The differential staining of nucleoprotein and mucin by thionine and similar dyes. J Biol Chem. 1935; 110:119-140.
22. Lillie RD, Pizzolato P. Acid alcoholic brilliant cresyl blue stain for gastric and other mucins. Histochimie. 1969; 17:138-144.
23. Mylonakis E, Casadevall A, Ausubel FM. Exploiting amoeboid and non-vertebrate animal model systems to study the virulence of human pathogenic fungi. PLoS Pathog. 2007; 3:e101.
24. Scully LR, Bidochka MJ. Developing insect models for the study of current and emerging human pathogens. FEMS Microbiol Lett. 2006; 263:1-9.
25. Meng Y, Katsuma S, Daimon T, Banno Y, Uchino K, Sezutsu H, Tamura T, Mita K, Shimada T. The silkworm mutant *lemon* (*lemon lethal*) is a potential insect model for human sepiapterin reductase deficiency. J Biol Chem. 2009; 284:11698-11705.

(Received June 8, 2010; Accepted August 8, 2010)

Original Article

Effect of heparin-superoxide dismutase on γ-radiation induced DNA damage *in vitro* and *in vivo*

Jinfeng Liu[1,2,*], Xuan Wang[1,*], Haining Tan[3], Hong Liu[4], Yonggang Wang[4], Renqin Chen[1], Jichao Cao[1], Fengshan Wang[1,3,]**

[1] *Institute of Biochemical and Biotechnological Drugs, School of Pharmaceutical Sciences, Shandong University, Ji'nan, Shandong, China;*
[2] *College of Life Sciences, Qufu Normal University, Qufu, Shandong, China;*
[3] *National Glycoengineering Research Center, Ji'nan, Shandong, China;*
[4] *Qilu Hospital, Shandong University, Ji'nan, Shandong, China.*

ABSTRACT: The effects of heparin-superoxide dismutase (SOD) conjugate (heparin-SOD) on γ-radiation induced DNA damage *in vivo* and *in vitro* were evaluated. Plasmid pcDNA3.0 solution was mixed with heparin-SOD, SOD, and a mixture of heparin and SOD (heparin + SOD), respectively, and irradiated with ^{60}Co at a dosage of 120 Gy. DNA injury was analyzed using agarose gel electrophoresis. The results showed that the degree of injury of pcDNA3.0 mixed with heparin-SOD, SOD, or heparin + SOD was less than that of untreated pcDNA3.0, and among them the degree of injury of pcDNA3.0 mixed with heparin-SOD was the least. It also showed that the protective effect increased with an increase of heparin-SOD concentration. The effects of SOD and heparin-SOD on the DNA damage and tumor inhibition rate of ^{60}Co γ-radiation exposure on tumor-bearing mice were also studied. Agarose gel electrophoresis showed that, when different SOD samples were administered before irradiation, the thymus DNA injuries of heparin-SOD, SOD, or heparin + SOD groups were more serious than that of the control group, and the DNA injuries of heparin-SOD or heparin + SOD groups were the most serious, which contradicted the above *in vitro* experiments. However, when heparin-SOD was administered post irradiation, it showed a repairing effect on the injured DNA.

Keywords: Cu,Zn-superoxide dismutase, low molecular weight heparin (LMWH), LMWH-SOD, DNA fragmentation

1. Introduction

Eighty percent of cancer patients need radiotherapy at some time, either for a curative or palliative purpose. Since human tissues contain 80% water, the major radiation damage is due to aqueous free radicals generated by the action of radiation on water. These free radicals react with cellular macromolecules, such as DNA, RNA, proteins, *etc.*, and cause cell dysfunction and mortality. Oxidative damage to the cellular genetic material, *i.e.*, DNA, plays a major role in mutagenesis and carcinogenesis. Highly reactive oxygen radicals produced by ionizing radiation cause lesions in DNA, which lead to cell death and DNA mutation. In order to obtain better tumor control with a higher radiation dose, normal tissues should be protected from radiation injury. Thus, the role of radioprotective compounds is very important in clinical radiotherapy. However, many of them have severe side effects, such as nausea, vomiting, and hypotension (*1,2*).

Enzymes such as superoxide dismutase, glutathione peroxidase and catalase protect mammalian cells from oxidative radiation damage (*3*). Because of the shortcomings of proteins used as medicines, such as short half-life, antigenicity, and instability, the utilization of these enzymes has been limited and increasing attention has been given to chemical modification of proteins to overcome the shortcomings (*4,5*). In our laboratory, Cu,Zn-superoxide dismutase (Cu,Zn-SOD) has been chemically modified with low molecular weight heparin (LMWH), and it was proved that after modification, the immunogenicity was lowered, the anti-inflammatory activity was increased and the stability of SOD towards acid, alkali, heat and trypsin were enhanced (*4*). Our earlier studies showed that heparin-SOD could prevent the effect of carbon tetrachloride-induced acute liver failure and hepatic fibrosis in mice (*6*). Our earlier studies also showed that heparin-SOD could attenuate bleomycin-induced pulmonary fibrosis *in vivo*, and inhibit the inflammatory cytokine expression

*These two authors made an equal contribution to this work.
***Address correspondence to:*
Dr. Fengshan Wang, Institute of Biochemical and Biotechnological Drugs, School of Pharmaceutical Sciences, Shandong University, Ji'nan 250012, China.
e-mail: fswang@sdu.edu.cn

induced by radiation, demonstrating that heparin-SOD might be useful in the treatment of pulmonary fibrosis (*7*). In the present study, the radioprotective effects and possible mechanisms of heparin-SOD *in vivo* and *in vitro* were investigated.

2. Materials and Methods

2.1. *Materials*

Heparin-SOD was prepared according to the method reported previously (*4,5*). Agarose and ethidium bromide were purchased from Sigma-Aldrich, St. Louis, MO, USA. Plasmid pcDNA3.0 was purified from *Escherichia coli* using a Qiagen Plasmid kit-Pack 500 (Qiagen, Hilden, Germany). S180 tumor cells were supplied by Shandong Academy of Medical Science, China. ^{60}Co γ-radiation exposure was performed in the Academy of Agricultural Sciences of Shandong Province, China. Other chemicals and reagents were of analytical grade.

2.2. *Animals*

Pathogen-free male Kunming mice, weighing 23-27 g, obtained from the Experimental Animal Center of Shandong University (Ji'nan, Shandong, China) were used in the experiments. The mice were housed in animal facilities accredited by the Shandong Council on Animal Care and treated in accordance with approved protocols. Animals were maintained in a specific pathogen-free environment that was temperature-controlled (23 ± 2°C) and humidity-controlled (60 ± 10%), under a 12 h light-dark cycle. The animals used in this study were handled and treated in accordance with the strict guiding principles of the National Institutes of Health for Experimental Care and Use of Animals. The experimental design and procedures were approved by the Institutional Ethical Committee for Animal Care and Use of Shandong University, People's Republic of China.

2.3. *In vitro assessment of the radio-protective effect of heparin-SOD on pcDNA3.0*

One microgram of pcDNA3.0 was put into 4 Eppendorf centrifuge tubes, respectively, and 50 μL of SOD, heparin-SOD, a mixture of heparin and SOD (heparin + SOD), and isotonic sodium chloride (as control) were added respectively before irradiation. The added dosages concerning SOD for the above SOD sample were according to Cu,Zn-SOD enzymatic activity (3,000 units/mL), and the heparin dosage in heparin + SOD was the same heparin proportion as in heparin-SOD. After mixing, the four tubes were exposed to γ-radiation at a dose rate of 1 Gy/min on an ice bath with a total dose of 120 Gy as reported elsewhere (*8-10*). The supercoiled (SC) and open circular (OC) forms of DNA were separated using 1.5% agarose gel electrophoresis and DNA bands were quantified by scanning the resulting optical density with a densitometer (LKB Co. Ltd., Stockholm, Sweden) after staining with ethidium bromide (*11*). Radiation induced damage was assessed as an increase in the OC form of DNA (*12*).

In another experiment, the radio-protective effect of heparin-SOD at different enzyme activity levels on ^{60}Co γ-radiation induced pcDNA3.0 damage was assessed. One microgram of pcDNA3.0 was put into 5 Eppendorf centrifuge tubes respectively, and isochoric heparin-SOD solutions containing enzymatic activities of 7.5×10^2, 1.5×10^3, 3.0×10^3, 6×10^3, and 1.2×10^4 units, respectively, were added before irradiation. After mixing, the five tubes were exposed to γ-radiation at a dose rate of 1 Gy/min and a total dose of 120 Gy on an ice bath as above. An equal quantity of DNA (based on optical density measurements at 260 nm) in different tubes was loaded in each lane, and agarose gel electrophoresis was carried out as above.

2.4. *In vivo experiment of the effect of SOD, heparin-SOD, and heparin + SOD on DNA damage and tumor growth inhibition of sarcoma bearing mice caused by ^{60}Co γ-radiation exposure*

To study the effect of heparin, SOD, and heparin-SOD on DNA damage and tumor growth inhibition caused by ^{60}Co γ-radiation exposure *in vivo*, S180 sarcoma bearing mice were prepared by subcutaneous injection of sarcoma cells. The tumor-bearing mice were randomly divided into the following 5 groups (10 mice in each group) on the seventh day after tumor cell transplantation: group I, control (0.5 mL of isotonic sodium chloride); group II, SOD (35,000 units/kg); group III, heparin + SOD (SOD 35,000 units/kg and the same proportion of heparin as in heparin-SOD); group IV, heparin-SOD (35,000 units/kg); group V, no irradiation exposure. Group I ~ IV received an intraperitoneal injection of the corresponding SODs 40 min before radiation exposure. ^{60}Co γ-radiation exposure was at a dose rate of 0.30 Gy/min and the total dose was 6 Gy. Mice were sacrificed by cervical dislocation on the fifth day after radiation exposure. Tumors were removed carefully and weighed. At the same time the thymus was removed for DNA extraction. Agarose gel electrophoresis was carried out to analyze for DNA fragmentation (*11-13*).

2.5. *In vivo experiment of the effect of heparin-SOD injected at different times and different parts of sarcoma bearing mice on the DNA damage caused by ^{60}Co γ-radiation exposure*

S180 sarcoma bearing mice were prepared by subcutaneous injection of the sarcoma cells as above. The tumor-bearing mice were randomly divided into the following 5 groups (10 mice in each group):

group I, control (no radiation administered); group II, received intraperitoneal injection of 0.5 mL of isotonic sodium chloride; group III, intraperitoneal injection of heparin-SOD (35,000 units/kg) 3 min after exposure to γ-radiation; group IV, intraperitoneal injection of heparin-SOD 40 min before exposure to γ-radiation (35,000 units/kg); group V, received intratumoral injection of heparin-SOD 40 min before exposure to γ-radiation. Mice were sacrificed after ^{60}Co γ-radiation exposure as above. The thymus was removed for DNA extraction and agarose gel electrophoresis was carried out to analyze for DNA fragmentation.

2.6. *Statistical analysis*

The differences between the control and experimental groups were analyzed by Student's *t*-test.

3. Results

3.1. *Radio-protective effect of heparin-SOD on pcDNA3.0*

Effects of heparin-SOD, SOD, and heparin + SOD on plasmid pcDNA3.0 damage induced by γ-radiation are shown in Figures 1 and 2. Exposure of plasmid pcDNA3.0 DNA to γ-radiation resulted in broken DNA strands, shown as SC form of plasmid DNA converted to the OC form or linear form. The disappearance of the SC form of DNA could be taken as an index of DNA damage induced by the radiation exposure. The presence of heparin-SOD or heparin + SOD along with pcDNA3.0 during irradiation protected the DNA from radiation-induced lesions as seen in Figures 1 and 2. Employing integral calculus analysis, we found that the DNA damage of the heparin-SOD group was the least. Figures 2A and 2B showed that with the increase of enzyme activity, the SC proportion increased and the OC proportion decreased, which meant that the heparin-SOD protection of DNA damage induced by radiation *in vitro* was concentration-dependent.

3.2. *Effect of SOD, heparin-SOD, and heparin + SOD on thymus DNA fragmentation induced by radiation in vivo*

As shown in Figures 3 and 4, groups treated with intraperitoneal injection of SOD, heparin + SOD, or heparin-SOD 40 min before irradiation showed more serious thymus DNA injury than the control group (Figure 3, lanes 2-4; Figure 4, lane 4). DNA injuries in groups treated with the intraperitoneal injection of heparin-SOD or heparin + SOD were the most serious, which was a contradiction of the above *in vitro* experiment. However, when heparin-SOD was intraperitoneally injected 3 min shortly after irradiation or intratumorally injected 40 min before irradiation, intact thymus DNA was observed (Figure 4, lanes 3 and 6).

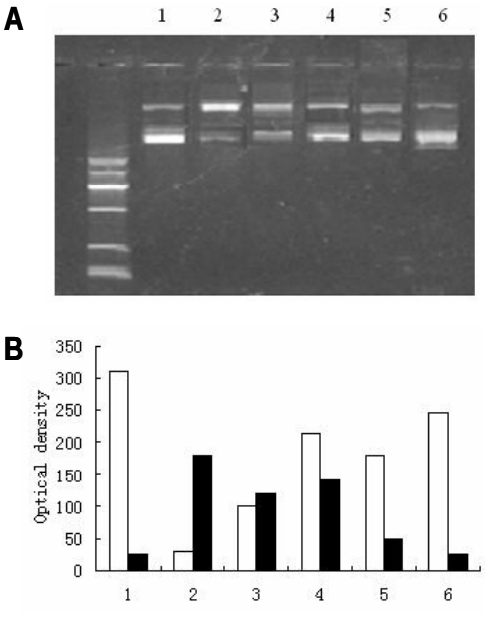

Figure 1. Effect of SOD, heparin-SOD, and heparin + SOD on irradiation induced DNA fragmentation. (A) Agarose gel electrophoresis of pcDNA3.0 after ^{60}Co γ-radiation exposure. The upper and lower bands are the open circular (OC) and the supercoiled (SC) forms respectively. Lane 1, control (no radiation group); Lane 2, isotonic Na chloride group; Lane 3, SOD group; Lane 4, heparin + SOD group; Lanes 5 and 6, heparin-SOD groups. **(B)** Analysis of the pcDNA3.0 agarose gel electrophoresis density integral calculus. Open columns, SC; Closed columns, OC.

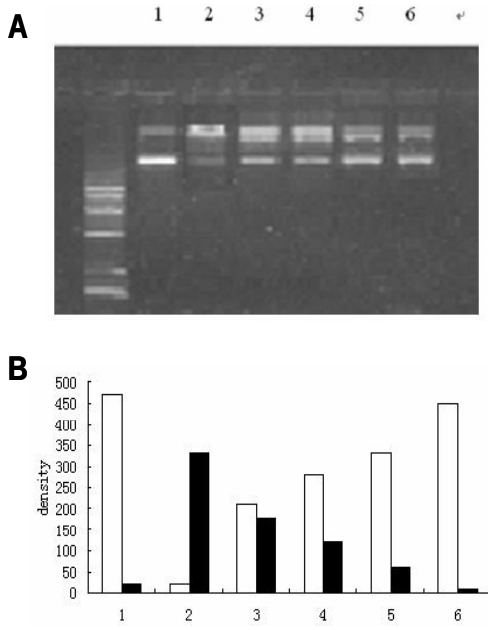

Figure 2. Effect of heparin-SOD with different activities on irradiation induced DNA fragmentation. (A) Agarose gel electrophoresis of pcDNA3.0 exposed to γ-radiation at a dose rate of 1 Gy/min on an ice bath in the presence of heparin-SOD at various enzyme activities. Lanes 1-6 were pcDNA3.0 treated with heparin-SOD with enzyme activity of 0, 7.5×10^2, 1.5×10^3, 3.0×10^3, 6×10^3, 1.2×10^4 units, respectively. **(B)** Analysis of pcDNA3 agarose gel electrophoresis density integral calculus. Open columns, SC, supercoiled DNA; Closed columns, OC, open circular DNA.

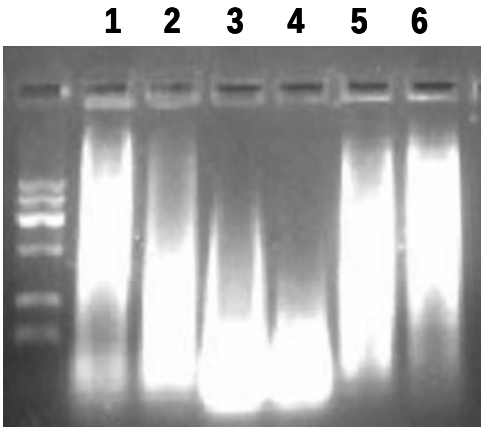

Figure 3. Agarose gel electrophoresis of thymus DNA fragmentation from mice intraperitoneal injection of SOD 40 min before exposure to γ-radiation at a dose rate of 0.30 Gy/min. Lane 1, control (received intraperitoneal injection of 0.5 mL of isotonic sodium chloride 40 min before exposure to γ-radiation); Lane 2, intraperitoneal injection of SOD 40 min before exposure to γ-radiation; Lane 3, intraperitoneal injection of SOD + heparin 40 min before exposure to γ-radiation; Lane 4, intraperitoneal injection heparin-SOD 40 min before exposure to γ-radiation; Lanes 5 and 6, no irradiation exposure.

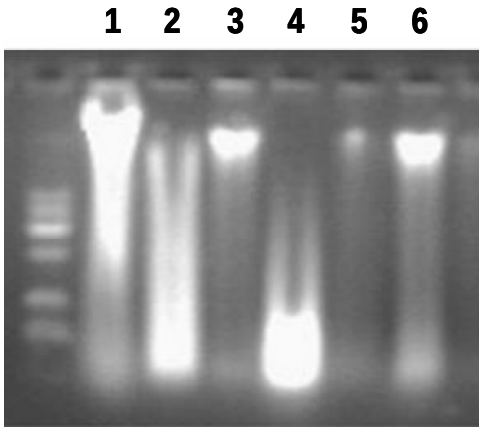

Figure 4. Agarose gel electrophoresis of thymus DNA fragmentation of mice injected with heparin-SOD 3 min after exposure to γ-radiation at a dose rate of 0.30 Gy/min. Lane 1, control (no radiation administered); Lane 2, isotonic Na chloride group; Lane 3, intraperitoneal injection of heparin-SOD 3 min after exposure to γ-radiation; Lane 4, intraperitoneal injection of heparin-SOD 40 min before exposure to γ-radiation; Lanes 5 and 6, tumor injection of heparin-SOD 40 min before exposure to γ-radiation.

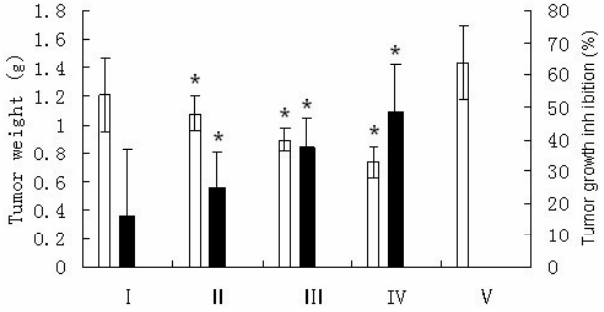

Figure 5. Tumor growth inhibition rates of irradiated S180 sarcoma bearing mice treated with different SODs. Inhibition rate of tumor growth = (tumor weight of untreated group – tumor weight of treated group)/tumor weight of treated group × 100%. I, control (isotonic sodium chloride); II, SOD; III, heparin + SOD; IV, heparin-SOD; V, no irradiation exposure. (I ~ IV: received intraperitoneal injection 40 min before exposure to γ-radiation). * Compared with control group, the difference was considered significant, $p < 0.05$. Open columns, tumor weight; Closed columns, tumor growth inhibition rates.

3.3. *Influence of heparin-SOD on the irradiation effect on tumor growth*

As shown in Figure 5, the tumor inhibition rate of heparin-SOD or heparin + SOD group was significantly higher than that of the control group, and the inhibition rate of the heparin-SOD group was the highest.

4. Discussion

The use of ionizing radiation has become an integral part of modern medicine. In some cases, radiation may be the single best treatment for cancer. Cancer radiation therapy depends on achieving a therapeutic differentiation between cancer cell toxicity and normal tissue toxicity. Therapeutic differentiation may be achieved with chemical radiation sensitizers or protectors (*14,15*). The development of radiation protectors is important not only to enhance the effectiveness of cancer treatment, but also for studying the underlying mechanisms of radiation cytotoxicity (*16*). A wide variety of compounds have been tested. These compounds, though highly effective in *in vitro* studies, may find little use in clinical applications. SODs are one class of essential enzymes in the cellular defense system against the superoxide anion radical ($O_2^{\bullet -}$). Although the importance of SODs as antioxidant enzymes has been demonstrated in various types of cells, whether SODs contribute to the cell's protection against ionizing radiation is still under debate. There are conflicting reports concerning the correlation between the effects of SOD and cellular damage when exposed to ionizing radiation (*17-20*). In the present study, we found that SOD and heparin-SOD rendered protection against γ-radiation induced DNA damage *in vitro* (Figures 1 and 2), but increased sensitivity to ionizing radiation with *in vivo* administered pre-irradiation (Figures 3 and 4).

It is well known that reactive oxygen species (ROS) cause DNA damage and induce cytotoxicity. They induce a variety of lesions in DNA, including oxidized bases, abasic sites, DNA strand-breaks, and cross-links between DNA and proteins (*11,12*). Increase in DNA damage after γ-irradiation has been observed in different studies (*11-13*). DNA constitutes the primary vital target for cellular inactivation of living systems by ionizing radiation. Ionizing radiation-induced damages to cellular DNA are mainly strand breaks of the double- and single-strand types, base damage, elimination of bases, and sugar damage (*21*). The majority of the free radicals may react with DNA by adding to the double bonds

of the bases, forming base radicals, leading to strand breaks (*21*). In this study, the effect of heparin-SOD on the protection of γ-radiation inducted strand breaks in pcDNA3.0 *in vitro* was monitored using agarose gel electrophoresis and observing the disappearance of the SC form of DNA. The reduction in the quantity of the SC form of plasmid DNA was directly related to the radiation-induced damage of DNA. It was found that when pcDNA3.0 was exposed to γ-radiation, the SC form of the molecule was converted to OC form. The presence of heparin-SOD or SOD along with DNA during irradiation prevented this decrease of the SC form, as evidence of attenuating strand breaks. Among all the groups above, the degree of pcDNA3.0 injury when mixed with heparin-SOD was the lowest. It also showed that the protective effect increased with an increase in heparin-SOD concentration (Figures 2A and 2B). Our results revealed that heparin-SOD could effectively protect plasmid DNA against ionizing radiation in an *in vitro* system independent of DNA repair and other cellular defense mechanisms.

Interestingly, the *in vivo* study showed contradictory results for thymus DNA fragmentation when SOD, heparin-SOD, or heparin + SOD was administered pre- and post-irradiation (Figures 3 and 4). When heparin-SOD, SOD, or heparin + SOD was administered pre-irradiation, agarose gel eletrophoresis (Figures 3 and 4) showed that thymus DNA injury was more serious than that of the control group, and when heparin-SOD was administered 3 min shortly after whole body irradiation almost no thymus DNA damage was found (Figure 4, lane 3). The former result was coincident with the early report that overexpression of SOD in *E. coli* had been found to increase sensitivity to ionizing radiation (*22,23*), but contradicted our above *in vitro* experiments (Figures 1 and 2).

The DNA damaging effect of SODs administered pre-irradiation may be explained by the increased level of H_2O_2 in the tissue. It is well known that high levels of H_2O_2 lead to DNA damage. It was reported that human and mouse cell clones overexpressing human Cu,Zn-SOD appeared to have higher levels of H_2O_2 (*24-26*). Other research showed that in some conditions increased amounts of SOD indeed caused increased steady-state levels of H_2O_2 (*27*). In JB6 cells and Chinese hamster fibroblasts, overexpression of Cu,Zn-SOD resulted in increased DNA breakage upon exposure to oxidants (*25,28*). Zhong *et al.* (*29*) reported that overexpression of SOD in rat glioma cells not only inhibited cell growth but also resulted in sensitization to oxidative damage. Researches by Han *et al.* and Wang *et al.* clearly demonstrated that Cu,Zn-SOD could mediate significant DNA cleavage in the presence of either H_2O_2 or mercaptoethanol (*30,31*) implying that any form of the copper-containing SOD enzymes (including Cu,Zn-SOD and its mutants) might have DNA cleavage activity (*32*). In theory, irradiation causes high levels of $O_2^{\bullet -}$, and high levels of $O_2^{\bullet -}$ will produce high levels of H_2O_2 at high levels of SOD. In this study, DNA injury of the intraperitoneal injection group of heparin-SOD before irradiation was the most serious (Figure 4), suggesting that heparin-SOD could serve as a sensitizer in tumor radiotherapy. The contradictory effects of SODs in *in vitro* and *in vivo* experiments imply that irradiation protection or damage is a complex issue and many factors may be involved in the process.

The DNA protecting or repairing effect of heparin-SOD administered post-irradiation is hard to explain. We speculated that when heparin-SOD was absorbed after intraperitoneal injection, the level of $O_2^{\bullet -}$ has become normal or lower, and at this time heparin-SOD does not help to produce a high level of H_2O_2, but helps to recover the activity of DNA repair enzymes. Recently, research indicated that low-molecular-weight heparin could exert beneficial effects on biological macromolecules, such as DNA (*33*). Therefore, we speculated that under some conditions heparin-SOD has DNA repair enzyme activity. In considering the less DNA fragmentation in the thymus in the group which received intratumoral injection of heparin-SOD 40 min before exposure to γ-radiation (lane 6 in Figure 4), we speculate that the intratumoral injection of heparin-SOD was hard to be absorbed into the blood stream due to the solidness of the tumor. The delayed absorption of heparin-SOD acts just like administration of SOD post-irradiation. All these speculations need to be confirmed by experiments. Regardless of the reason, the result suggests that heparin-SOD can be used to treat radiation damage.

Many other studies have clearly demonstrated that SOD suppressed cell growth (*34-44*). SOD had been found to be low in many cancer cells (*34-40*), fetal cells (*41-43*), as well as stem cells (*44*). Forced overexpression of Mn-SOD slowed the growth of cancer cells both *in vitro* and *in vivo* (*41,44*). This growth suppression could be in part a result of increasing the flux of H_2O_2 and thereby pushing the redox status of the cell to a more oxidized state (*43*). The results of our research (Figure 5) showed that the tumor weights of heparin-SOD, SOD, or heparin + SOD groups were lower than that of the control group, and the inhibition rate of the heparin-SOD group was the highest group, suggesting that the use of heparin-SOD could increase the tumor radiotherapy effect.

In summary, the results of our work probably have a meaning to direct selecting a drug administration time when SOD or its modified analogues can be used to prevent or treat radiation injury during tumor radiotherapy, at the same time, a new subject is raised that SOD and its modified analogues may be used to increase tumor sensitivity to radiotherapy.

Acknowledgements

This work was supported by a grant from the National Natural Science Foundation of China (No. 30670637).

References

1. Maisin JR. Bacq and Alexander Award lecture – chemical radioprotection: Past, present, and future prospects. Int J Radiat Biol. 1998; 73:443-450.
2. Maisin JR, Albert C, Henry A. Reduction of short-term radiation lethality by biological response modifiers given alone or in association with other chemical protectors. Radiat Res. 1993; 135:332-337.
3. Fridovich I. The biology of oxygen radicals. Science. 1978; 201:875-880.
4. Zhang HW, Wang FS, Shao W, Zheng XL, Qi JZ, Cao JC, Zhang TM. Characterization and stability investigation of Cu,Zn-superoxide dismutase covalently modified by low molecular weight heparin. Biochemistry (Mosc). 2006; 71 (Suppl 1):S96-S100, 5.
5. Qi JZ, Wang FS, Zhang HW, Cao JC, Zhang TM. Chemical modification of superoxide dismutase by low molecular weight heparin and their physical and chemical properties. Chinese Pharmaceutical Journal. 2006; 41:150-153. (in Chinese)
6. Liu J, Tan H, Sun Y, Zhou S, Cao J, Wang F. The preventive effects of heparin-superoxide dismutase on carbon tetrachloride-induced acute liver failure and hepatic fibrosis in mice. Mol Cell Biochem. 2009; 327:219-228.
7. Liu J, Wang X, Wang F, Teng L, Cao J. Attenuation effects of heparin-superoxide dismutase conjugate on bleomycin-induced lung fibrosis *in vivo* and radiation-induced inflammatory cytokine expression *in vitro*. Biomed Pharmacother. 2009; 63:484-491.
8. Rajgopalan R, Wani K, Huilgol NG, Kagiya TV, Nair CK. Inhibition of γ-radiation induced DNA damage in plasmid pBR322 by TMG, a water-soluble derivative of vitamin E. J Radiat Res (Tokyo). 2002; 43:153-159.
9. Gandhi NM, Nair CK. Protection of DNA and membrane from gamma radiation induced damage by gallic acid. Mol Cell Biochem. 2005; 278:111-117.
10. Maurya DK, Adhikari S, Nair CK, Devasagayam TP. DNA protective properties of vanillin against gamma-radiation under different conditions: Possible mechanisms. Mutat Res. 2007; 634:69-80.
11. Maurya DK, Salvi VP, Nair CK. Radiation protection of DNA by ferulic acid under *in vitro* and *in vivo* conditions. Mol Cell Biochem. 2005; 280:209-217.
12. Yokozawa T, Dong E. Role of ginsenoside-Rd in cisplatin-induced renal injury: Special reference to DNA fragmentation. Nephron. 2001; 89:433-438.
13. Mansour HH, Hafez HF, Fahmy NM, Hanafi N. Protective effect of *N*-acetylcysteine against radiation induced DNA damage and hepatic toxicity in rats. Biochem Pharmacol. 2008; 75:773-780.
14. Coleman CN, Turrisi AT. Radiation and chemotherapy sensitizers and protectors. Crit Rev Oncol Hematol. 1990; 10:225-252.
15. McAleer MF, Davidson C, Davidson WR, Yentzer B, Farber SA, Rodeck U, Dicker AP. Novel use of zebrafish as a vertebrate model to screen radiation protectors and sensitizers. Int J Radiat Oncol Biol Phys. 2005; 61:10-13.
16. Hahn SM, Krishna CM, Samuni A, DeGraff W, Cuscela DO, Johnstone P, Mitchell JB. Potential use of nitroxides in radiation oncology. Cancer Res. 1994; 54 (Suppl 7):2006s-2010s.
17. Marklund SL, Westman NG, Roos G, Carlsson J. Radiation resistance and the Cu,Zn-superoxide dismutase, Mn superoxide dismutase, catalase, and glutathione peroxidase activities of seven human cell lines. Radiat Res. 1984; 100:115-123.
18. Scott MD, Meshnick SR, Eaton JW. Superoxide dismutase amplifies organismal sensitivity to ionizing radiation. J Biol Chem. 1989; 264:2489-2501.
19. Yamaguchi S, Sakurada S, Nagumo M. Role of intracellular SOD in protecting human leukemic and cancer cells against superoxide and radiation. Free Radic Biol Med. 1994; 17:389-395.
20. Lee JH, Choi IY, Kil IS, Kim SY, Yang ES, Park JW. Protective role of superoxide dismutases against ionizing radiation in yeast. Biochim Biophys Acta. 2001; 1526:191-198.
21. Bagchi M, Balmoori J, Ye X, Bagchi D, Ray SD, Stohs SJ. Protective effect of melatonin on naphthalene-induced oxidative stress and DNA damage in cultured macrophage J774A.1 cells. Mol Cell Biochem. 2001; 221:49-55.
22. Scott MD, Meshnick SR, Eaton JW. Superoxide dismutase-rich bacteria. Paradoxical increase in oxidant toxicity. J Biol Chem. 1987; 262:3640-3645.
23. Scott MD, Meshnick SR, Eaton JW. Superoxide dismutase amplifies organismal sensitivity to ionizing radiation. J Biol Chem. 1989; 264:2498-2501.
24. Elroy-Stein O, Bernstein Y, Groner Y. Overproduction of human Cu/Zn-superoxide dismutase in transfected cells: Extenuation of paraquat-mediated cytotoxicity and enhancement of lipid peroxidation. EMBO J. 1986; 5:615-622.
25. Amstad P, Peskin A, Shah G, Mirault ME, Moret R, Zbinden I, Cerutti P. The balance between Cu,Zn-superoxide dismutase and catalase affects the sensitivity of mouse epidermal cells to oxidative stress. Biochemistry. 1991; 30:9305-9313.
26. Buettner GR, Ng CF, Wang M, Rodgers VG, Schafer FQ. A new paradigm: Manganese superoxide dismutase influences the production of H_2O_2 in cells and thereby their biological state. Free Radic Biol Med. 2006; 41:1338-1350.
27. Kowald A, Lehrach H, Klipp E. Alternative pathways as mechanism for the negative effects associated with overexpression of superoxide dismutase. J Theor Biol. 2006; 238:828-840.
28. Teixeira HD, Meneghini R. Chinese hamster fibroblasts overexpressing Cu,Zn-superoxide dismutase undergo a global reduction in antioxidants and an increasing sensitivity of DNA to oxidative damage. Biochem J. 1996; 315:821-825.
29. Zhong W, Oberley LW, Oberley TD, Yan T, Domann FE, St Clair DK. Inhibition of cell growth and sensitization to oxidative damage by overexpression of manganese superoxide dismutase in rat glioma cells. Cell Growth Differ. 1996; 7:1175-1186.
30. Han Y, Shen T, Jiang W, Xia Q, Liu C. DNA cleavage mediated by copper superoxide dismutase *via* two pathways. J Inorg Biochem. 2007; 101:214-224.
31. Wang BZ, Wei XB, Liu WY. Cleavage of supercoiled circular double-stranded DNA induced by a eukaryotic cambialistic superoxide dismutase from *Cinnamomum camphora*. Acta Biochim Biophys Sin (Shanghai). 2004; 36:609-617.
32. Jiang W, Shen T, Han Y, Pan Q, Liu C. Divalent-metal-dependent nucleolytic activity of Cu,Zn-superoxide dismutase. J Biol Inorg Chem. 2006; 11:835-848.
33. Deepa PR, Varalakshmi P. Influence of a low-molecular-

weight heparin derivative on the nitric oxide levels and apoptotic DNA damage in adriamycin-induced cardiac and renal toxicity. Toxicology. 2006; 217:176-183.
34. Rabbani ZN, Anscher MS, Folz RJ, Archer E, Huang H, Chen L, Golson ML, Samulski TS, Dewhirst MW, Vujaskovic Z. Overexpression of extracellular superoxide dismutase reduces acute radiation induced lung toxicity. BMC Cancer. 2005; 5:59.
35. Venkataraman S, Jiang X, Weydert C, Zhang Y, Zhang HJ, Goswami PC, Ritchie JM, Oberley LW, Buettner GR. Manganese superoxide dismutase overexpression inhibits the growth of androgen-independent prostate cancer cells. Oncogene. 2005; 24:77-89.
36. Oberley LW, Buettner GR. Role of superoxide dismutase in cancer: A review. Cancer Res. 1979; 39:1141-1149.
37. Yang J, Lam EW, Hammad HM, Oberley TD, Oberley LW. Antioxidant enzyme levels in oral squamous cell carcinoma and normal human oral epithelium. J Oral Pathol Med. 2002; 31:71-77.
38. Allen RG, Balin AK. Effects of oxygen on the antioxidant responses of normal and transformed cells. Exp Cell Res. 2003; 289:307-316.
39. Weydert C, Roling B, Liu J, Hinkhouse MM, Ritchie JM, Oberley LW, Cullen JJ. Suppression of the malignant phenotype in human pancreatic cancer cells by the overexpression of manganese superoxide dismutase. Mol Cancer Ther. 2003; 2:361-369.
40. Darby Weydert CJ, Smith BB, Xu L, Kregel KC, Ritchie JM, Davis CS, Oberley LW. Inhibition of oral cancer cell growth by adenovirusMnSOD plus BCNU treatment. Free Radic Biol Med. 2003; 34:316-329.
41. Allen RG, Keogh BP, Gerhard GS, Pignolo R, Horton J, Cristofalo VJ. Expression and regulation of superoxide dismutase activity in human skin fibroblasts from donors of different ages. J Cell Physiol. 1995; 165:576-587.
42. Allen RG, Balin AK. Developmental changes in the superoxide dismutase activity of human skin fibroblasts are maintained *in vitro* and are not caused by oxygen. J Clin Invest. 1988; 82:731-734.
43. Balin AK, Pratt L, Allen RG. Effects of ambient oxygen concentration on the growth and antioxidant defenses of human cell cultures established from fetal and postnatal skin. Free Radic Biol Med. 2002; 32:257-267.
44. Oberley TD, Sempf JM, Oberley LW. Immunohistochemical localization of antioxidant enzymes during hamster kidney development. Histochem J. 1995; 27:575-586.

(Received May 19, 2010; Revised July 14, 2010; Accepted August 2, 2010)

Original Article

In vivo evaluation of black and green tea dermal products against UV radiation

Murat Türkoğlu[1,*], Timuçin Uğurlu[1], Gülşah Gedik[1], Ayşe M. Yılmaz[2], A. Süha Yalçin[2]

[1] *Pharmaceutical Technology Department, Faculty of Pharmacy, Marmara University, Istanbul, Turkey;*
[2] *Biochemistry Department, Faculty of Medicine, Marmara University, Istanbul, Turkey.*

ABSTRACT: Aqueous extracts of black and green tea (*Camellia sinensis*) were obtained by freeze-drying for this study. The extracts were evaluated based on tea quality control tests, UV, IR scans, and *in vitro* antioxidant capacity tests. Dermal products from the tea extracts were designed and manufactured. Black and green tea gels were tested *in vivo* in the forearms of six subjects using an artifical UV (200-400 nm) source. The tested formulations were green tea gel, black tea gel, 0.3% caffeine gel, carbomer gel base, and a control. Depending on tea quality, the samples resulted in water soluble fractions of 24.5-39.5%. UV and IR scans specifically showed peaks for alkaloids like caffeine, catechins such as epigallocatechin gallate, and polyphenols with dimeric and polymeric structures such as theaflavins (TFs) and thearubigins (TRs). Antioxidant and free radical scavenging activities of black and green tea samples were found to be high and comparable; activity levels for black tea, green tea, high quality black tea, and L-ascorbic acid were 0.48, 0.50, 0.82, and 1.32 mM TR/mg, respectively. No UV-induced erythema was observed at the black and green tea gel sites in any of the subjects. UV-induced erythema was consistently present in various grades at caffeine gel, carbomer gel, and control sites. Results led to the conclusion that freeze-dried black and green tea extracts had strong UV absorbance. Formulating those extracts into dermal gels protected the skin against UV-induced erythema. Therefore, tea extracts were found to be promising candidates for their ability to protect against the harmful effects of UV radiation, such as erythema and premature aging of the skin.

Keywords: Black tea, green tea, UV, human subjects, CUPRAC, DPPH, erythema, antioxidants, freeze-drying

**Address correspondence to:*
Dr. Murat Türkoğlu, Pharmaceutical Technology Department, Faculty of Pharmacy, Marmara University, 34668 Haydarpasa, Istanbul, Turkey.
e-mail: turkoglu@marmara.edu.tr

1. Introduction

Tea, a valuable plant, has three distinct species: *Camellia sinensis* var. *sinensis*, which has small leaves and is a northern plant grown at higher elevations; *Camellia sinensis* var. *assamica*, which has larger leaves and is a southern plant; and *Camellia assamica* subsp. *lasiocalyx* (*1*). Tea can be studied as tea leaves directly from the plant or as fully fermented black tea. During the fermentation of black tea, polyphenol oxidase leads to the formation of orange-red colored dimeric theaflavins (TFs) and dark-brown polymeric pigment thearubigins (TRs) from smaller catechins (*2*,*3*). Partially fermented oolong tea or unfermented green tea contains epicatechin (EC), epigallocatechin (EGC), epicatechin gallate (ECG), and epigallocatechin gallate (EGCG) as the basic polyphenols of tea leaves. Tea leaves also contain caffeine, theanine, myricetin, quarcetin, and kaempferol as examples of alkaloids, amino acids, and flavonols (*3-6*). This diverse chemical composition of tea with high antioxidant potential makes it a unique drink with great health benefits. The antioxidant activity of black tea was reported to be higher than that of most dietary agents, and among the twenty-one botanical infusions tested black tea had the highest antioxidant activity (*4*,*7*). Yoshino *et al*. (*8*) reported that TFs and TRs of black tea, like green tea catechins, inhibited lipid peroxidation and that black tea was as potent as green tea in terms of antioxidative activity. Green tea extracts are reported to result in the inhibition of UV-induced erythema on the skin and to reduce the DNA damage inside the skin; EGCG and ECG are reported to be the most efficient among the catechins (*9*). Turkoglu *et al*. (*10*) reported that a tea gel formulation produced from the aqueous extract of black tea prevented UV-induced erythema on the forearms of six human subjects. Black tea extract was found to be effective against UVB-induced erythema in human subjects and was found to inhibit UVB-induced tyrosine phosphorilation of epidermal growth factor receptor in mouse skin; TRs are also reported to inhibit mouse skin TPA-induced cell proliferation (*11*,*12*). Furthermore, oral administration of 600 mg geen tea extract per day

for a year was used in the chemoprevention of human prostate cancer (*13,14*) and tea polyphenols and TFs are reported to be present in the prostate tissue of humans and mice after green and black tea consumption. Finally, Mulder *et al*. (*15*) showed that both green and black tea have the same metabolic fate in humans and that they are all converted into hippuric acid. Therefore, a limited human study was carried out here along with *in vitro* antioxidant and free radical scavenging activity tests to compare the skin protection provided by freeze-dried green and black tea extracts.

2. Materials and Methods

2.1. *Materials*

The teas used were cut black and green teas from the Black Sea region of Turkey (Çaykur, Green Tea, 53-18/09 02630, Exp. date: 2012; Çaykur, Black Tea 53-6/04, 29/08966 Exp. Date: 2012), Carbomer Carbopol Ultrez 21 (Lot. EC521ZR291, Noveon, Inc., Cleveland, OH, USA) was obtained as a free sample. Sodium hydroxide and benzyl alcohol were of reagent grade. The artificial UV source used was a Philips HPA 400, which is a high-pressure iron-cobalt metal halide lamp with a 400-W power source (Philips, Turnhout, Belgium). A UVX Radiometer (UVP, Inc., Upland, CA, USA, Serial Number: E27858) was used to monitor UVA (λ_{max} = 365 nm), UVB (λ_{max} = 310 nm), and UVC (λ_{max} = 254 nm) radiation from the UV source with three probes. A UVmini 1240, UV/VIS spectrophotometer, and FTIR 8400S (Shimadzu, Kyoto, Japan) were used for photometrical analyses.

2.2. *Tea infusions and freeze-drying*

Water soluble fractions and the moisture content of tea samples were determined gravimetrically according to ISO 9768 and 1573. Ten-percent (w/w) infusions of tea leaves were prepared from green or black tea as previously described (*10*). The infusions were frozen at –18°C before further processing. Using a laboratory size freeze-dryer (Alpha 1-2 LD Plus, Martin Christ, Osterode, Germany), frozen tea samples were lyophilized at –52°C and 0.1 mBar. Freeze-dried samples were stored at –18°C for further quality control tests and used as tea actives.

2.3. *Preparation of tea gels*

Gels were obtained using a carbomer resin. One hundred mL of 1% (w/w) carbomer solution were prepared and 3 g freeze-dried black or green tea extract was added to the carbomer dispersion. A 20% sodium hydroxide solution was added drop by drop until a viscous gel was obtained by monitoring the pH with a pH meter to determine the end point. One percent benzyl alcohol was added as a preservative. The gels were stored in glass jars at room temperature. A caffeine gel containing 0.3% caffeine and a gel-base that did not contain anything but carbomer were also prepared as described above.

2.4. *Assay of antioxidant activity*

Freeze-dried samples (100 mg) were powdered and suspended in 1 mL ultra-pure water. After vortex mixing, samples were kept at 37°C for 2 h and centrifuged at 9,000 × g for 2 min. The supernatants were diluted 100 times and used for antioxidant activity measurements. The cupric ion-reducing antioxidant capacity (CUPRAC) of samples was determined using an assay described by Apak *et al*. (*7*). Briefly, 0.2 mL of 10 mM $CuCl_2$, 0.2 mL of 7.5 mM neocuproine, and 0.2 mL of 1 M ammonium acetate (pH 7) were added to a test tube. After vortex mixing, a suitable amount of sample (20 or 50 µL) and ultra-pure water was added and the absorbance at 450 nm was read after 30 min. Trolox equivalent antioxidant capacity was calculated using a calibration curve obtained by the serial dilution of 1 mM trolox.

2.5. *Assay of free radical scavenging activity*

The free radical scavenging activity of samples was measured with 1,1-diphenyl-2-picrylhydrazil (DPPH) using an assay described by Peksel *et al*. (*16*). Briefly, DPPH was dissolved in ethanol (4 mg/100 mL) and 100 µL of this solution were added to an equal volume of a sample. The mixture was shaken vigorously and the decrease in absorbance was measured at 515 nm after 30 min. Water was used as a control. The percent inhibition activity was calculated using the following equation: Inhibition activity (%) = $[(A_0 - A_1)/A_0 \times 100]$, where A_0 and A_1 are the absorbance of the control and sample, respectively.

2.6. *In vivo study*

Six subjects, two males and four females (skin types I and II), aged 23-55 were selected after signing an informed consent form. A template made of dermal tape was applied to the forearms of the subjects (See Figure 4A for the template and the position of the formulations). First, three square-shaped openings 4 cm^2 in size were subjected to "black tea gel", "green tea gel", and "caffeine gel". The last opening was divided into two portions; the top was subjected to a "gel-base", which contained 1% carbomer, and the bottom served as the "control" and was left untreated. The forearms were exposed to the artificial UV source through a slit for 2.5 min.

2.7. *Evaluation of erythema after UV exposure*

UV-induced erythema was graded visually as

previously reported (*17*), with 0 indicating no erythema; ± indicating slight patchy erythema; 1 indicating slight but confluent erythema; 2 indicating moderate erythema; and 3 indicating severe erythema with or without edema

3. Results

3.1. *In vitro study*

Table 1 summarizes the water soluble fractions and moisture content of the tea samples studied. The water soluble fraction of the samples ranged between 24.5-39.5% and the moisture content varied between 2.50-3.80% depending on the tea quality and type. Freeze-dried black and green tea samples were freely water soluble and hygroscopic. The free radical scavenging and antioxidant activities of freeze-dried tea samples were compared to those of L-ascorbic acid. As shown in Table 2, the values varied between 0.48-0.82 mM TR/mg based on the water soluble fractions of the tea samples. Green and black tea samples were found to be similar (0.48 *vs.* 0.50). One of the tea samples (black tea A) resulted in a value of 0.82 and L-ascorbic acid resulted in one of 1.32 mM TR/mg. Results based on the DPPH test, which indicates the free radical scavenging activity of the samples, showed that tested black tea samples were similar to each other unlike in the CUPRAC antioxidant activity test (26.3% *vs.* 26.5% inhibition for black teas A and B, respectively, and 18.4% and 41.8% for green tea and L-ascorbic acid, respectively) (Table 2). IR spectra of freeze-dried green and black teas are shown in Figures 1A and 1B, respectively. In those spectra, hydroxyl groups due to stretching were observed between 3,350-3,600 cm^{-1}. Green tea resulted in six bands in that region while black tea resulted in three. For both tea types, caffeine and theobromine bands were observed in the 1,558-1,695 cm^{-1} region. Catechins resulted in peaks in the 800-1,600 cm^{-1} region. With EGCG, a band was observed at 1,238, 1,141, and 1,034 cm^{-1}; with GC, one was observed at 1,373-1,280 cm^{-1}; with ECG, one was observed at 1,238 cm^{-1}; with EC, one was observed at 820 cm^{-1}.

Table 1. Tea samples studied and their water soluble fractions

Tea type	Water soluble fraction (%, w/v)	Moisture (%)
Black tea A	39.51	3.49
Black tea B	38.20	3.80
Black tea C	35.24	2.76
Black tea D	24.50	2.50
Green tea	34.95	2.57

Table 2. Free radical scavenging and antioxidant activity of freeze-dried tea samples in comparison to L-ascorbic acid

Samples	CUPRAC (mM TR/mg)	DPPH (% inhibition)
Freeze-dried black tea A	0.480 ± 0.167	26.3
Freeze-dried green tea	0.506 ± 0.161	18.4
Freeze-dried black tea B	0.818 ± 0.232	26.5
L-Ascorbic acid	1.317 ± 0.503	41.8

3.2. *In vivo study*

For the human study, an artificial UV source was used. UV irradiation were measured and monitored at 0.5 m from the source with a UV radiometer. The values were UVA = 4,550 $\mu W/cm^2$; UVB = 2,800 $\mu W/cm^2$; and UVC = 500 $\mu W/cm^2$. At thsese energy levels, subjects with skin types I and II can be expected to develop moderate UV-induced erythema after 2.5 min. Figure 2 compares the UV irradiation from the Philips HPA 400, used as UV source in the present study, and that from the sun. Table 3 summarizes the formulations used in the human study. Green and black tea gels (formulations **1** and **2**) contained 3 g of freeze-dried extract, which corresponded to a 10% tea infusion. Such an infusion contains 0.3% caffeine, so formulation **3** contained only 0.3% caffeine in a carbomer gel. Formulation **4** was the base, which contained only carbomer. All of the formulations contained 1% benzyl alcohol as a preservative against fungi.

Table 4 summarizes the erythema grades for the aforementioned sites in each subject and Figure 3 graphs erythema depending on the time. In this study, the six human subjects showed no signs of erythema at green tea gel and black tea gel sites on the forearm after being exposed to UV radiation for 2.5 min. In contast, UV-induced erythema was consistently present to a varying degree at the carbomer-base site, 0.3% caffeine site, and control site. As is typical of UV-induced erythema, erythema reached a peak around 24 h and diminished afterwards (Figure 3). Figure 4 shows the application of the templete and grading of UV-induced erythema at 24 h on one subject's forearm.

4. Discussion

Black and green teas contain tea actives such as EGCG, EGC, TF, TR, and caffeine in an aqueous infusion. These components are responsible for the UV protection provided by tea gel formulations. Therefore, determination of the "water soluble fraction" of teas is one of the most important parameters of tea quality control tests and this fraction must be at least 35% (w/v) or more for a high quality tea. Based on the CUPRAC method, the present study found that tea samples were strong antioxidants. Using the CUPRAC test, Apak *et al.* reported that among tea types Ceylon blended black tea resulted in 4.41 mMT/g and ordinary black tea resulted in 0.38 mMT/g (*7*). Yoshino *et al.* (*8*) reported that there was no marked difference between

black and green tea. The current findings agree with both of those reports. A free radical scavenging assay (DPPH) indicated almost the same % inhibition levels for black tea samples (26.3 *vs.* 26.5) as for a green tea sample (18.4%) (Table 2), and results led to the conclusion that the black tea samples were superior in terms of their free radical scavenging effect. The water soluble fractions of those two black tea samples (samples A and B) were also very similar. However, the CUPRAC assay did not confirm these findings. Black tea samples A and B led to a difference of 50% in terms of antioxidant activity while the green tea sample had

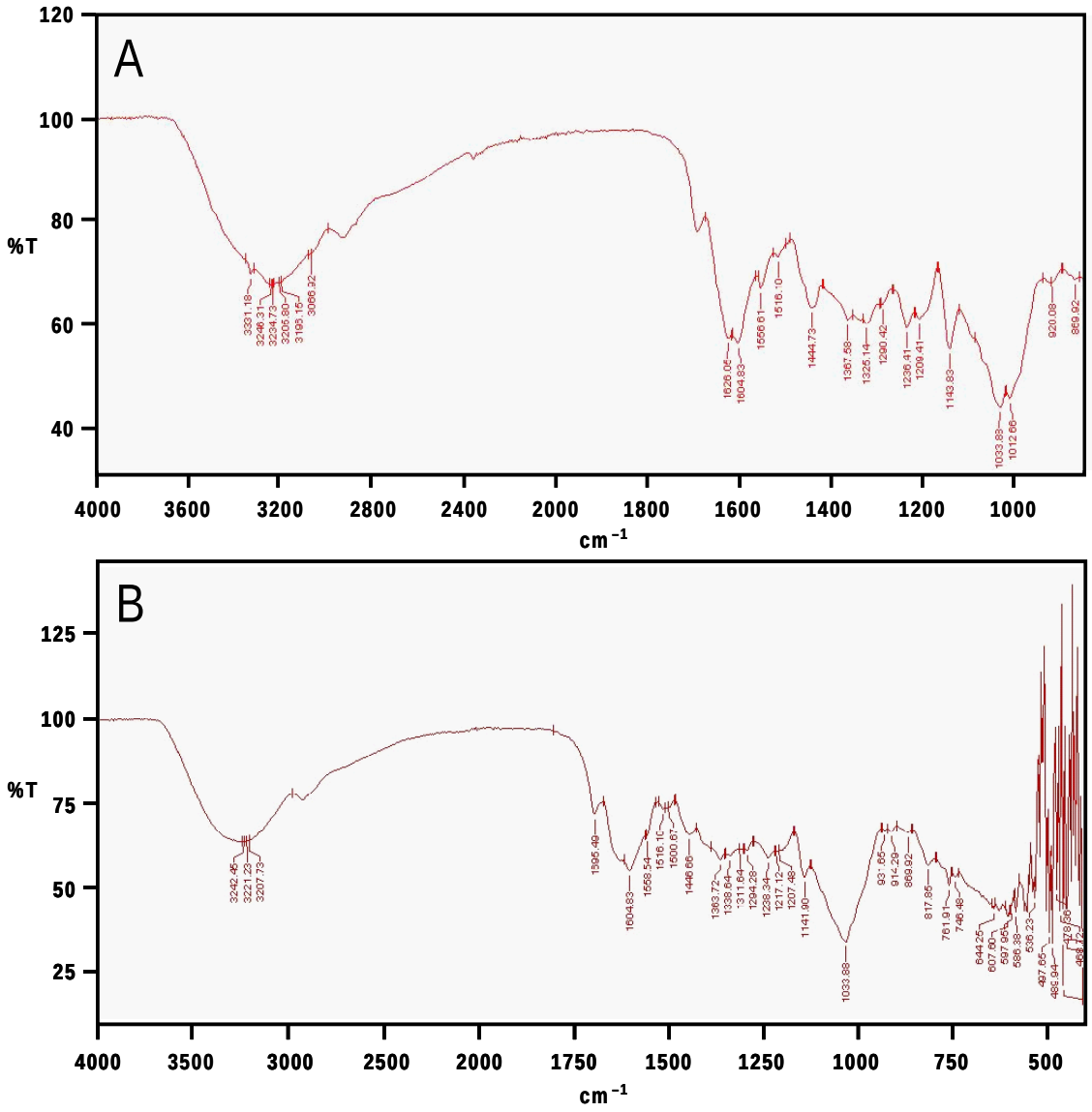

Figure 1. IR scan profiles of freeze-dried green tea (A) and black tea (B).

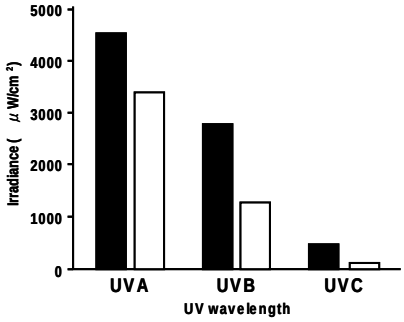

Figure 2. Comparison of UV irradiation from a Philips HPA 400 and the sun. Closed column, HPA 400; Open column, the sun.

Table 3. List of formulations tested on the forearms of subjects

Contents	Formulations (g/100g)			
	#1*	#2*	#3	#4
Freeze-dried black tea extract	3	–	–	–
Freeze-dried green tea extract	–	3	–	–
Caffeine	0.3	0.3	0.3	–
Carbomer, Carbopol Ultrez 21	1	1	1	1
Sodium hydroxide (20% solution)	1.47	1.47	1.47	1.47
Benzyl alcohol	1	1	1	1
Water	q.s.**	q.s.	q.s.	q.s.

* Formulations **1** and **2** naturally contain 0.3% caffeine as part of tea extracts. ** q.s.: quantum sufficit.

Table 4. Forearm erythema grades

Subjects	Erythema score at 6 h					Erythema score at 24 h					Erythema score at 48 h				
	BTG	GTG	CG	GB	C	BTG	GTG	CG	GB	C	BTG	GTG	CG	GB	C
1	0	0	1	1	±	0	0	1	1	±	0	0	±	±	±
2	0	0	0.5	0.5	1	0	0	±	±	±	0	0	0	±	±
3	0	0	1	1	±	0	0	2	2	2	0	0	1	1	1
4	0	0	1	1	±	0	0	1	1	±	0	0	0	±	0
5	0	0	±	1	±	0	0	±	1	±	0	0	±	±	0
6	0	0	±	±	±	0	0	1	±	1	0	0	±	±	±

UV was irradiated by a Philips HPA 400 UV for 2.5 min from a distance of 50 cm. BTG, black tea gel; GTG, green tea gel; CG, caffeine gel; GB, gel base; C, control.

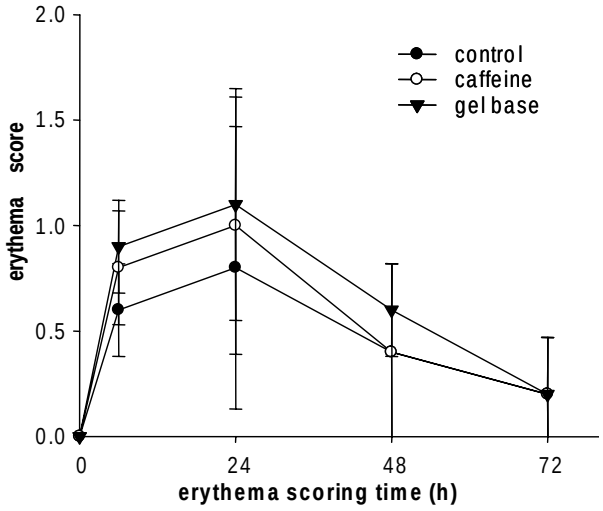

Figure 3. Grades of UV-induced erythema from a human study (*n* = 6) with a caffeine gel, carbomer base, and control site.

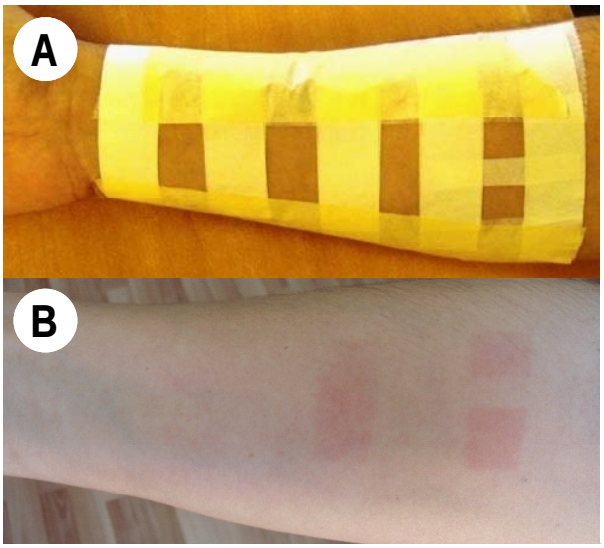

Figure 4. Application of the template and grading of UV-induced erythema on the subject's forearm at 24 h. (A) Application of a template to the forearm before UV irradiation. Starting from the left, the first three regions are "black tea gel", "green tea gel", and "caffeine gel". In the divided region on the right, the upper region is "carbomer gel" and the lower is the "control". **(B)** Typical UV-induced erythema after 24 h at "caffeine gel", "gel-base", and "control" sites. There was no erythema at "green tea gel" or "black tea gel" sites.

activity close to that of black tea sample A. Therefore, different methods must be used to gauge the antioxidant activity of tea samples in order to differentiate between the effects of different chemical groups, *e.g.* EGCG *vs.* TRs or TFs.

Figure 5 shows typical UV absorption for a tea infusion. In the current study, black or green aqueous tea infusions resulted in very similar UV spectra between 200-400 nm with a peak around 272 nm. When this spectrum was overlapped with the UV spectra for human erythema and skin DNA damage, the maximum absorbance region corresponded to that for tea infusions (Figure 5). Therefore, tea extracts are good candidates to provide UV protection against erythema or DNA damage. Aqueous tea samples absorb UV radiation with a maxiumum level where that radiation causes maxiumum damage to the skin.

In the present study, formulation **3** at the selected concentration (0.3% caffeine) did not protect the skin against UV-induced erythema. Caffeine greatly absorbs UV with a peak around 272 nm. However, the concentration in a 10% tea infusion may be insufficient for effective protection. Higher concentrations of caffeine in a dermal formula such as 2% would afford skin protection against UV-induced erythema. Caffeine is also capable of penetrating the skin and could affect the epidermis. Oral administration of green tea or a caffeine solution is reported to inhibit UVB-induced complete carcinogenesis in SKH mice (*18*).

Green tea contains smaller molecules such as EGCG, EC, and EGC, while black tea contains larger molecules (MW 700-1,400) such as TFs and TRs. TFs and TRs cannot penetrate human skin while EGCG, EGC, and caffeine can. However, a previous study by the current authors (*10*) and the current study both found that green tea and black tea gels successfully prevented UV-induced erythema. Based on these results, black tea cannot be considered superior to green tea or *vice versa*. Black tea TFs and TRs have been found to prevent human epidermal carcinoma and human malignant melanoma cell proliferation through apoptosis (*19*). Recent studies have further speculated on the molecular pathways by which tea constituents protect the skin (*20,21*). In conclusion, dermal gels of green or black tea have been found to prevent acute UV-

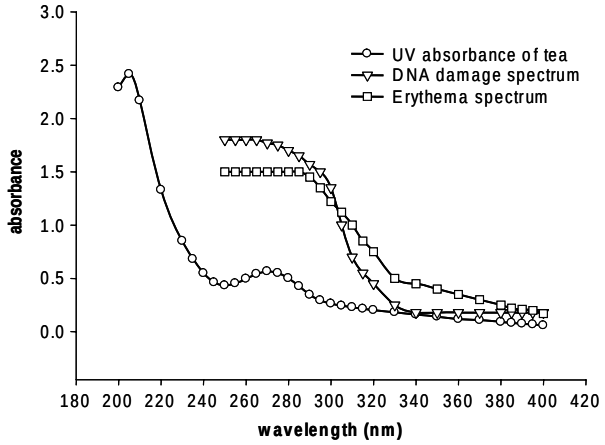

Figure 5. Overlapping spectra of DNA damage and human erythema and typical UV absorption of tea infusions.

induced erythema on human skin. Skin protection and the absence of any gradable erythema were observed in every subject.

Acknowledgements

The authors wish to thank the Pharmaceutical Chemistry Department, Faculty of Pharmacy, Marmara University for use of their IR equipment and Prof. Dr. Oya Gurbuz, Department of Dermatology, Faculty of Medicine, Marmara University for obtaining institutional approval and monitoring this human study.

References

1. Wight W. Tea classification revised. Curr Sci. 1962; 31:298-299.
2. Menet MC, Sang S, Yang CS, Ho CT, Rosen RT. Analysis of theaflavins and thearubigins from black tea extract by MALDI-TOF mass spectrometry. J Agric Food Chem. 2004; 52:2455-2461.
3. Wang H, Provan GJ, Helliwell K. Tea flavonoids: Their functions, utilization and analysis. Trends Food Sci Technol. 2000; 11:152-160.
4. Rechner AR, Wagner E, Van Buren L, Van De Put F, Wiseman S, Rice-Evans CA. Black tea represents a major source of dietary phenolics among regular tea drinkers. Free Radic Res. 2002; 36:1127-1135.
5. Wang H, Helliwell K. Determination of flavonols in green and black tea leaves and green tea infusions by high-performance liquid chromatography. Food Res Int. 2001; 34:223-227.
6. International Agency for Research on Cancer (IARC). Tea chemical composition. In: IARC Monographs, Vol. 51. Lyon, France, 1991; pp. 217-233.
7. Apak R, Güçlü K, Ozyürek M, Esin Karademir S, Erçağ E. The cupric ion reducing antioxidant capacity and polyphenolic content of some herbal teas. Int J Food Sci Nutr. 2006; 57:292-304.
8. Yoshino K, Hara Y, Sano M, Tomita I. Antioxidative effects of black tea theaflavins on lipid peroxidation of rat liver homogenates induced by *tert*-butyl hydroperoxide. Biol Pharm Bull. 1994; 17:146-149.
9. Elmets CA, Singh D, Tubesing K, Matsui M, Katiyar S, Mukhtar H. Cutaneous photoprotection from ultraviolet injury by green tea polyphenols. J Am Acad Dermatol. 2001; 44:425-432.
10. Turkoglu M, Cigirgil N. Evaluation of black tea gel and its protection potential against UV. Int J Cosmet Sci. 2007; 29:437-442.
11. Zhao J, Jin X, Yaping E, Zheng ZS, Zhang YJ, Athar M, DeLeo VA, Mukhtar H, Bickers DR, Wang ZY. Photoprotective effect of black tea extracts against UVB-induced phototoxicity in skin. Photochem Photobiol. 1999; 70:637-644.
12. Patel R, Krishnan R, Ramchandani A, Maru G. Polymeric black tea polyphenols inhibit mouse skin chemical carcinogenesis by decreasing cell proliferation. Cell Prolif. 2008; 41:532-553.
13. Bettuzi S, Brausi M, Rizzi F, Castagnetti G, Peracchia G, Corti A. Chemoprevention of human prostate cancer by oral administration of green tea catechins in volunteers with high-grade prostate intraepithelial neoplasia: A preliminary report from a one-year proof-of-principle study. Cancer Res. 2006; 66:1234-1240.
14. Henning SM, Aronson W, Niu Y, *et al*. Tea polyphenols and theaflavins are present in prostate tissue of humans and mice after green and black tea consumption. J Nutr. 2006; 136:1839-1843.
15. Mulder TP, Rietveld AG, van Amelsvoort JM. Consumption of both black tea and green tea results in an increase in the excretion of hippuric acid into urine. Am J Clin Nutr. 2005; 81 (Suppl 1):256S-260S.
16. Peksel A, Arısan AI, Yanardag R. Antioxidant activities of aqueous extracts of purslane. Ital J Food Sci. 2006; 3:297-311.
17. Turkoglu M, Adel Sakr A, Lichtin JL, Buehler EV, Kruezmann JJ. An *in vivo* assessment of the sun-protection index. Cosmetics & Toiletries. 1989; 104:33-38.
18. Conney AH, Zhou S, Lee MJ, Xie JG, Yang CS, Lou YR, Lu YP. Stimulatory effect of oral administration of tea, coffee, or caffeine on UVB-induced apoptosis in the epidermis of SKH-1 mice. Toxicol Appl Pharmacol. 2007; 224:209-213.
19. Halder B, Bhattacharya U, Mukhopadhyay S, Giri AK. Molecular mechanism of black tea polyphenols induced apoptosis in human skin cancer cells: Involment of Bax translocation and mitochondria mediated death cascade. Carcinogenesis. 2008; 29:129-138.
20. Yang CS, Lambert JD, Ju J, Lu G, Sang S. Tea and cancer prevention: Molecular mechanism and human relevance. Toxicol Appl Pharmacol. 2007; 224:265-273.
21. Casmeron AR, Anton S, Melville L, Houston NP, Dayal S, McDougall GJ, Stewart D, Rena G. Black tea polyphenols mimic insulin/insulin-like growth factor-1 signalling to the longevity factor FOXO1a. Aging Cell. 2008; 7:69-77.

(Received May 7, 2010; Revised June 30, 2010; Accepted July 18, 2010)

Original Article

Reduced expression of *Sytl 1* and *Ccdc21* and impaired induction of *Mt I* by oxidative stress in *SII-K1* knockout mice

Keiko Tano[1], Hiroshi Hamamoto[2], Takahiro Ito[2], Eriko Sumiya[2], Randeep Rakwal[3], Junko Shibato[3], Yoshinori Masuo[3], Kenichi Ijiri[1], Kazuhisa Sekimizu[2], Nobuyoshi Akimitsu[1,*]

[1] *Radioisotope Center, The University of Tokyo, Tokyo, Japan;*
[2] *Department of Developmental Biochemistry, Graduate School of Pharmaceutical Sciences, The University of Tokyo, Tokyo, Japan;*
[3] *Health Technology Research Center, National Institute of Advanced Industrial Science and Technology (AIST) West, Ibaraki, Japan.*

ABSTRACT: SII-K1 is a member of the transcription elongation factor S-II family. In the mouse, SII-K1 is expressed exclusively in the liver, kidney, heart, and skeletal muscle. Here, we report that deletion of the *SII-K1* gene in mice resulted in the downregulation of the synaptotagmin-like 1 (*Sytl 1*) gene in liver and of the coiled-coil domain-containing 21 (*Ccdc21*) gene in liver and kidney. Moreover, the induction of the metallothionein I (*Mt I*) gene in *SII-K1*-deficient mice liver was impaired in diethyl maleate-induced oxidative stress conditions. Our results suggest that SII-K1 regulates these genes *in vivo*.

Keywords: Transcription, elongation, knockout mice, oxidative stress

1. Introduction

The transcription elongation process is highly regulated by RNA polymerase II (RNAPII) and various elongation factors. During elongation of primary transcripts, RNAPII can encounter the DNA sequence, which interferes with the transcription and results in transcriptional arrest (*1*). Cleavage of the nascent RNA *via* the endonucleolytic activity of RNAPII is required to relieve the arrested state. S-II, also designated as TFIIS, is a transcription elongation factor that facilitates the elongation process by promoting RNAPII-mediated cleavage of the nascent RNA, which leads to the resumption of elongation *in vitro* (*2*). Recent studies have revealed that S-II regulates the expression of multiple genes *in vivo* (*3*). For example, mouse S-II, also referred to as general S-II, was involved in the transcription elongation of the *Bcl-*x_L gene in fetal liver *via* its activity of transcription-arrest relief (*4,5*). Yeast S-II is involved in the transcription of the *SSM1* and *IMD2* genes (*6,7*). The requirement of S-II function in mouse development (*4*) and oxidative stress resistance in yeast (*8*) clearly indicate the physiological relevance of S-II *in vivo*.

Mammalian tissues express several S-II-related genes. Among these, general S-II is ubiquitously expressed, whereas the others are expressed in a tissue-specific manner. SII-K1 is one of the tissue-specific S-IIs expressed exclusively in mouse liver, kidney, heart, and skeletal muscle (*9*). There are significant similarities in the N-terminal and C-terminal conserved amino acid regions between general S-II and SII-K1. Purified recombinant SII-K1 stimulates RNAPII *in vitro*, as does general S-II, which suggests that SII-K1 acts as a transcription elongation factor (*9*). The expression of general S-II is detected in throughout mouse development, whereas SII-K1 mRNA is barely detectable before 15- and 17-day-old embryos (*9*). It was demonstrated that *Xenopus* SII-K1 participates in the induction of the mesoderm marker genes and in the development of mesoderm-derived tissues (*10*). These findings raise the possibility that SII-K1 plays roles in the regulation of developmental process and gene expression that are distinct from those of general S-II. To understand the role of SII-K1 in the regulation of mouse development and gene expression, we generated *SII-K1*-deficient mice and assessed the extent of development and gene expression defects.

2. Materials and Methods

2.1. *Generation of SII-K1-deficient mice*

Genomic DNA fragments were cloned from a 129/Sv genomic DNA library (STRATAGENE, La Jolla, CA, USA) using the *SII-K1* cDNA as a probe. The 4.7 kb *XbaI-XhoI* genomic DNA fragment (5' arm) located in the 5' upstream region of exon 1 of the *SII-K1* gene and the 5.2 kb *SacI* genomic DNA fragment

**Address correspondence to:*
Dr. Nobuyoshi Akimitsu, Radioisotope Center, The University of Tokyo, 2-11-16 Yayoi, Bunkyo-ku, Tokyo 113-0032, Japan.
e-mail: akimitsu@ric.u-tokyo.ac.jp

(3' arm) containing exons 2 and 3 of the gene were used to construct the targeting vector (Figure 1A). Electroporation of the targeting vector into E14 embryonic stem (ES) cells, selection of neomycin-resistant clones, and injection of the correctly targeted ES cells into blastocysts were performed as described previously (*11*,*12*). The resulting female chimeric mouse was bred with C57BL/6J male mice (CLEA Japan Inc., Tokyo, Japan) to obtain F_1 mice that were heterozygous for the mutation. Heterozygotes were then backcrossed to C57BL/6J mice.

For genotyping, genomic DNA isolated from mouse tail was analyzed by PCR assay using the following primer pairs (forward primer/reverse primer): wild-type allele, 5'-GGTGCACGAAAGGAGAACTG-3'/5'-CCTGGAATGTCCTGGCAATG-3'; targeted-allele, 5'-GTTATTAGTGGAGAGGCCCCA-3'/5'-AACTGTCAGAGCATGTGCGTCATGC-3'. This four-primer multiplex PCR resulted in a 320-bp product for the wild-type allele and a 430-bp product for the targeted allele. All animal experiments were approved by the institutional committee on animal experimentation and were performed in compliance with the corresponding animal welfare laws.

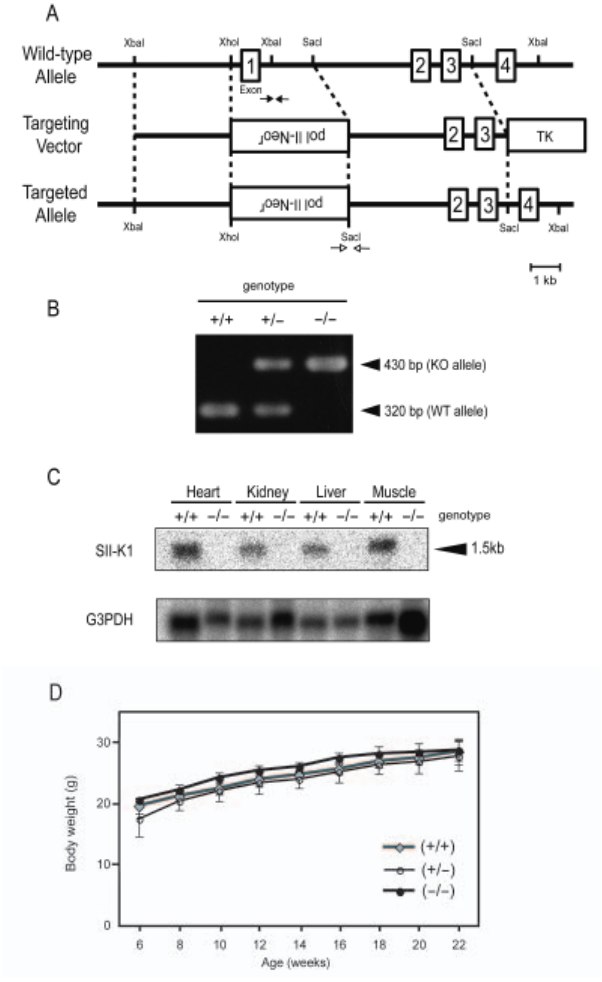

Figure 1. Generation of *SII-K1*-deficient mice. (**A**) Targeted disruption of the *SII-K1* gene. Diagrams of the wild-type allele of the mouse *SII-K1* gene, the targeting vector, and the targeted allele are shown. Numbered boxes indicate exons. Broken lines indicate the regions of homology used for homologous recombination. *Pol-II Neo*^{r} and *TK* represent the neomycin resistant gene and the herpes simplex virus thymidine kinase gene, respectively. (**B**) Genotyping of progeny from the heterozygous intercross using PCR with the indicated primer pairs in Figure 1. (**A**) (arrows). +/+, wild-type; +/–, heterozygous mutant; –/–, homozygous mutant. (**C**) Northern blot analysis of *SII-K1* mRNA from mouse heart, kidney, liver, and skeletal muscle. (**D**) Body weight was measured once every two weeks, from 6 to 22 weeks of age. Results are expressed as the mean ± S.D. (n = 4 in each group).

2.2. *Northern blot analysis of SII-K1*

Northern blot hybridization of SII-K1 mRNA was carried out using a probe that consisted of a PCR product corresponding to nucleotides +34 to +350 of the *SII-K1* cDNA. We used GAPDH mRNA as a control, which was detected with a GAPDH cDNA probe that was amplified using the following primers: 5'-ACCACAGTCCATGCCATCAC-3'/5'-TCCACCACCCTGTTGCTGTA-3'.

2.3. *Total RNA extraction and DNA microarray analysis*

Total RNA was extracted from five livers and four kidneys from *SII-K1*$^{-/-}$ and wild-type mice using the QIAGEN RNeasy Mini Kit (QIAGEN KK, Tokyo, Japan) in accordance with the manufacturer's instructions. To verify the quality of this RNA, the yield and purity were determined spectrophotometrically and visually confirmed using formaldehyde-agarose gel electrophoresis. A pool of RNA samples from each genotype was used for microarray analysis.

Microarray analysis was performed as previously reported (*13*) using a whole mouse genome 4x 44K oligo microarray kit (G4122F, Agilent Technologies, Palo Alto, CA, USA). Total RNA (800 ng) was labeled with either Cy3 or Cy5 dye using an Agilent Low RNA Input Fluorescent Linear Amplification Kit (Agilent). Fluorescently labeled targets of wild-type, as well as *SII-K1*$^{-/-}$ samples were hybridized to the same microarray slide with 60-mer probes. A flip labeling (dye-swap or reverse labeling with Cy3 and Cy5 dyes) procedure was followed to nullify the dye bias associated with unequal incorporation of the two Cy dyes into cDNA. The use of a dye-swap approach provides a more stringent selection condition for changed gene expression profiling than use of a simple single/two-color approach. Hybridization and wash processes were performed according to the manufacturer's instructions, and hybridized microarrays were scanned using an Agilent Microarray scanner G2565BA. For the detection of significantly differentially expressed genes between *SII-K1*$^{-/-}$ and wild-type samples each slide image was processed by Agilent Feature Extraction software (version

9.5.3.1). This program measures Cy3 and Cy5 signal intensities of whole probes. Dye-bias tends to be signal intensity dependent, therefore the software selected probes using a set by rank consistency filter for dye-normalization. Said normalization was performed by LOWESS (locally weighted linear regression) which calculates the log ratio of dye-normalized Cy3- and Cy5-signals, as well as the final error of log ratio. The significance (*p*) value based on the propagate error and universal error models. In this analysis, the threshold of significant differentially expressed genes was < 0.01 (for the confidence that the feature was not differentially expressed). In addition, erroneous data generated due to artifacts were eliminated before data analysis using the software. The differentially expressed gene lists (up- and down-regulated genes) were generated (data not shown) and annotated using the GeneSpring version GX 7.3.1 (Agilent).

2.4. *Reverse transcription and real-time quantitative PCR analysis*

Total RNA (1 μg) was reverse transcribed using TaqMan Reverse Transcription Reagents (Applied Biosystems, Foster City, CA, USA). A real-time PCR assay was performed on the Thermal Cycler Dice Real-Time System TP850 (TaKaRa Bio, Shiga, Japan) using SYBR Premix Ex Taq II (TaKaRa) and the following primer sets: *Sytl 1*, 5'-CCAGGGTCTCCATAGAGGTG-3'/5'-TGAGGGTACATATGGTGAGAACA-3'; *Ccdc21*, 5'-AGATGGAACAGCTGCACTCC-3'/5'-CCCTCTTCTTGTGCCAGTTC-3'; *Mt I*, 5'-CACCAGATCTCGGAATGGAC-3'/5'-AGGAGCAGCAGCTCTTCTTG-3'; *Mt II*, 5'-CATGGACCCCAACTGCTC-3'/5'-GCAGCAGCTTTTCTTGCAG-3'; NAD(P)H quinone oxidoreductase 1 (*Nqo 1*), 5'-AGCGTTCGGTATTACGATCC-3'/5-AGTACAATCAGGGCTCTTCTCG-3'; β-actin, 5'-CTAAGGCCAACCGTGAAAAG-3'/5'-ACCAGAGGCATACAGGGACA-3'. Real-time PCR was performed in duplicate for each sample and was normalized to β-actin expression levels.

2.5. *Diethyl maleate treatment*

Ten- to fourteen-week-old male wild-type and *SII-K1*$^{-/-}$ mice were used (n = 4 in each group). Groups of mice were injected subcutaneously with 10 mmol/kg of diethyl maleate (DEM) (Wako, Osaka, Japan) or with corn oil vehicle at a volume of 10 mL/kg.

3. Results

3.1. *Generation of SII-K1-deficient mice*

To disrupt the *SII-K1* gene, we constructed a targeting vector to replace exon 1, which contains the initiation codon and part of the 5' sequence of exon 2 of the *SII-K1* gene, with a neomycin resistance cassette (Figure 1A). We then introduced this targeting vector into ES cells and established ES cell lines in which the *SII-K1* gene was targeted. Disruption of the *SII-K1* gene by homologous recombination was confirmed by Southern blot hybridization analysis (data not shown). We obtained a chimeric mouse by injecting the heterozygous mutant (*SII-K1*$^{+/-}$) ES cells into C57BL/6J blastocysts. This mouse was crossed with C57BL/6J mice to establish the *SII-K1*$^{+/-}$ mouse line. To determine whether homozygous mutant (*SII-K1*$^{-/-}$) mice were viable, *SII-K1*$^{+/-}$ mice were intercrossed and the genotypes of the progeny were determined (Figure 1B). The distribution of genotypes in the progeny was consistent with a Mendelian distribution, which signifies that *SII-K1*$^{-/-}$ mice are viable (Table 1). Northern blot analysis confirmed the complete loss of SII-K1 mRNA expression in the organs of adult *SII-K1*$^{-/-}$ mice (Figure 1C). We observed little difference in body weight between wild-type and SII-K1 mutant mice up to four months (from six weeks of age after birth) (Figure 1D). *SII-K1*$^{-/-}$ mice were fertile and had no abnormalities in terms of overt appearance and health up to over one year of age (data not shown). These results indicate that SII-K1 is not essential for mouse development.

3.2. *Reduced expression levels of Sytl 1 in the liver and Ccdc21 in the liver and kidney of SII-K1*$^{-/-}$ *mice*

To investigate genes that are regulated by SII-K1, we screened for genes with decreased expression in *SII-K1*$^{-/-}$ mice. From a whole mouse genome 4× 44K oligo microarray analysis, candidate genes were filtered for transcripts that were decreased above 2-fold in *SII-K1*$^{-/-}$ mice compared with wild-type mice and there were 14 transcripts in the liver and 12 transcripts in the kidney that were passed this filtering criteria. To confirm the downregulation of these transcripts observed in microarray analysis above, expression levels of each gene were determined using real-time quantitative PCR analysis. This revealed a significant downregulation of the mRNA levels of the two genes, *Sytl 1* (approximately 20% of wild-type) and *Ccdc21* (approximately 30% of wild-type), in the liver of *SII-K1*$^{-/-}$ mice (Figures 2A and 2B). The Sytl1 protein is a Rab27 effector that is involved in secretion (*16*), whereas the function of Ccdc21 is uncertain. The

Table 1. Genotype of the offspring from the intercross of *SII-K1*$^{+/-}$ mice

Genotype			Total
+/+	+/–	–/–	
60	118	61	239

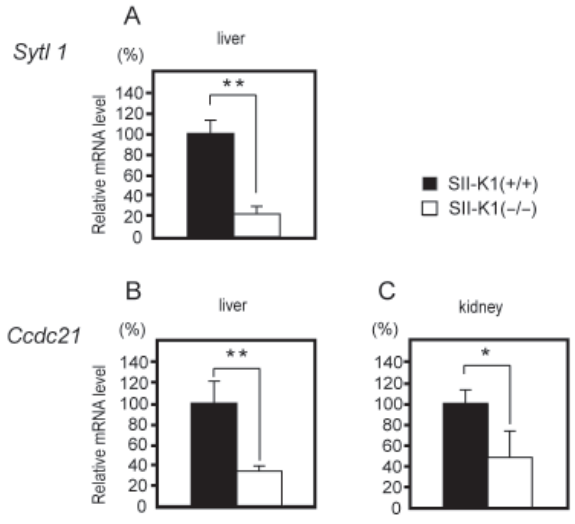

Figure 2. Gene expression analysis in *SII-K1*$^{-/-}$ mice. The expression levels of each gene were analyzed in liver (**A** and **B**) and kidney (**C**) using real-time PCR. The relative mRNA levels in *SII-K1*$^{-/-}$ mice are presented by defining the mean value for wild-type mice as 100% (n = 5 in each group). Error bars show the standard deviation. Asterisks indicate significant differences (Student's t-test, * $p < 0.05$, ** $p < 0.01$).

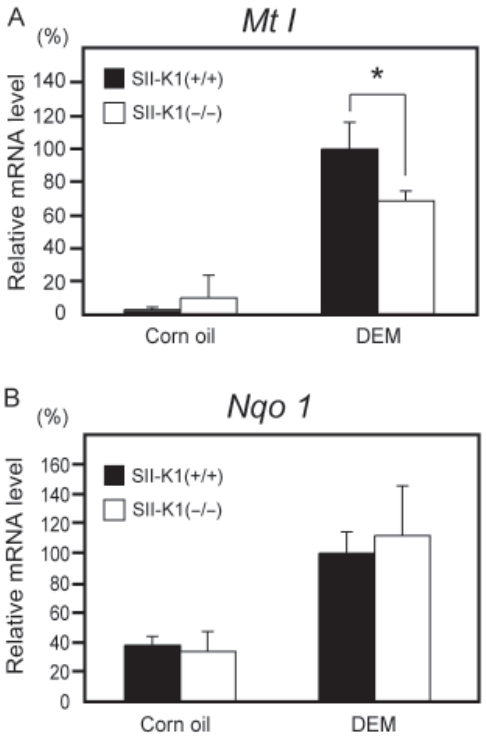

Figure 3. Gene expression analysis in the liver of *SII-K1*$^{-/-}$ mice under DEM-induced oxidative stress conditions. The expression levels of each gene were analyzed by real-time PCR. Relative mRNA levels in *SII-K1*$^{-/-}$ mice are presented by defining the mean value for wild-type mice exposed to DEM as 100% (n = 4 in each group). Error bars show the standard deviation. The asterisk indicates a significant difference (Student's t-test, * $p < 0.05$).

mRNA levels of the *Ccdc21* gene were also reduced in the kidney of *SII-K1*$^{-/-}$ mice (Figure 2C). These results suggest that SII-K1 is involved in the control of the expression levels of a specific subset of genes, *Sytl 1* and *Ccdc21*, *in vivo*.

3.3. *Impaired induction of the Mt I gene in the liver of SII-K1*$^{-/-}$ *mice under DEM-induced oxidative stress conditions*

S-II participates in the induction of certain genes as a response to environmental stimuli (*6,7*). Moreover, it was demonstrated that S-II (*DST1*) confers resistance against oxidative stress in yeast (*8*). It is also well known that certain oxidative stress-inducible genes are activated in response to oxidative stress in the mammalian liver, where SII-K1 is expressed. These findings led us to hypothesize that SII-K1 contributes to the induction of oxidative stress-inducible genes in the liver under oxidative stress conditions. To test this hypothesis, we examined the effect of diethyl maleate (DEM), which is an oxidative stress agent, on *SII-K1*$^{-/-}$ mice. Because *Mt* gene is activated by various oxidative stress agents to protect organs against oxidative stress, especially in the liver (*14*), we analyzed *Mt* gene induction. Real-time PCR assays revealed that the expression levels of the *Mt I* gene were reduced by about 30% in the liver of *SII-K1*$^{-/-}$ mice 7.5 h after DEM treatment when compared with wild-type mice (Figure 3A). In contrast, there was no significant difference in *Mt II* gene expression levels in the liver between *SII-K1*$^{-/-}$ and wild-type mice treated with DEM (data not shown). The level of induction of *Nqo1*, which is also induced by DEM (*15*), in the liver was not significantly different between *SII-K1*$^{-/-}$ and wild-type mice (Figure 3B). These results suggest that SII-K1 is specifically involved in the induction of the *Mt I* gene in the liver under DEM-induced oxidative stress conditions.

4. Discussion

In the present study, we found that the tissue-specific transcription elongation factor SII-K1 is involved in the expression of a specific subset of genes in tissues where SII-K1 is expressed. We also found that SII-K1 is not essential for mouse development.

Previously, we reported that the *Bcl-x*$_L$ gene, which is downregulated in the fetal liver of *S-II* knockout mice, has a transcription arrest site and that the arrest at this site is relieved by general S-II (*4,5*). As SII-K1 is a transcription elongation factor, *Sytl 1* and *Ccdc21*, which were downregulated in *SII-K1* knockout mice, may also have transcription arrest sites that can be relieved by SII-K1. Sytl1, also known as Slp 1, is a Rab27 effector protein and has been reported to be part of secretory machineries, *e.g.* amylase secretion by the exocrine pancreas (*16*). SII-K1 may affect the secretion of certain proteins *via* the transcriptional regulation of the *Sytl 1* gene in the liver.

We provided evidence that SII-K1 participates in

the induction of the *Mt I* gene in the liver under DEM-induced oxidative stress conditions. It was reported that hepatocytes from MT I and II double knockout (MT null) mice exhibited enhanced sensitivity to the oxidative stress and cytotoxicity induced by cadmium or *tert*-butylhydroperoxide (*17*), which suggests that MT is important for the protection of hepatic cells against oxidative stress. Our finding that deficiency of SII-K1 reduced the induction of the *Mt I* gene under DEM-induced oxidative stress conditions suggests that SII-K1 confers oxidative stress resistance through the induction of the *Mt I* gene in the liver. In addition, SII-K1 may be involved in the suppression of carcinogenesis in liver, because MT null mice showed high susceptibility to cisplatin-induced hepatocarcinogenicity (*18*).

Taken together, our results imply that mammals may have acquired SII-K1, in addition to general S-II, to achieve proper expression of certain genes, which include *Sytl 1* and *Ccdc21*. Moreover, the reduced induction of the *Mt I* gene in *SII-K1*$^{-/-}$ mouse liver suggests that SII-K1 participates in the protection of tissues that express SII-K1 against environmental stresses.

Acknowledgements

We would like to thank Dr. Makiko Nagata (Eisai Co., Ltd., Japan) and Dr. Hiroshi Koyama (National Institute of Genetics (NIG), Japan) for providing helpful discussion and pertinent advice.

References

1. Cramer P. RNA polymerase II structure: From core to functional complexes. Curr Opin Genet Dev. 2004; 14:218-226.
2. Fish RN, Kane CM. Promoting elongation with transcript cleavage stimulatory factors. Biochim Biophys Acta. 2002; 1577:287-307.
3. Tano K, Nagata M, Akimitsu N. S-II mediated gene regulation. Drug Discov Ther. 2008; 2:136-139.
4. Ito T, Arimitsu N, Takeuchi M, Kawamura N, Nagata M, Saso K, Akimitsu N, Hamamoto H, Natori S, Miyajima A, Sekimizu K. Transcription elongation factor S-II is required for definitive hematopoiesis. Mol Cell Biol. 2006; 26:3194-3203.
5. Nagata M, Ito T, Arimitsu N, Koyama H, Sekimizu K. Transcription arrest relief by S-II/TFIIS during gene expression in erythroblast differentiation. Genes Cells. 2009; 14:371-380.
6. Shimoaraiso M, Nakanishi T, Kubo T, Natori S. Transcription elongation factor S-II confers yeast resistance to 6-azauracil by enhancing expression of the *SSM1* gene. J Biol Chem. 2000; 275:29623-29627.
7. Shaw RJ, Reines D. *Saccharomyces cerevisiae* transcription elongation mutants are defective in *PUR5* induction in response to nucleotide depletion. Mol Cell Biol. 2000; 20:7427-7437.
8. Koyama H, Ito T, Nakanishi T, Kawamura N, Sekimizu K. Transcription elongation factor S-II maintains transcriptional fidelity and confers oxidative stress resistance. Genes Cells. 2003; 8:779-788.
9. Taira Y, Kubo T, Natori S. Molecular cloning of cDNA and tissue-specific expression of the gene for SII-K1, a novel transcription elongation factor SII. Genes Cells. 1998; 3:289-296.
10. Taira Y, Kubo T, Natori S. Participation of transcription elongation factor X SII-K1 in mesoderm-derived tissue development in *Xenopus laevis*. J Biol Chem. 2000; 275:32011-32015.
11. Arimitsu N, Akimitsu N, Kotani N, Takasaki S, Kina T, Hamamoto H, Kamura K, Sekimizu K. Glycophorin A requirement for expression of O-linked antigens on the erythrocyte membrane. Genes Cells. 2003; 8:769-777.
12. Fukuma N, Akimitsu N, Hamamoto H, Kusuhara H, Sugiyama Y, Sekimizu K. A role of the Duffy antigen for the maintenance of plasma chemokine concentrations. Biochem Biophys Res Commun. 2003; 303:137-139.
13. Hirano M, Shibato J, Rakwal R, Kouyama N, Katayama Y, Hayashi M, Masuo Y. Transcriptomic analysis of rat brain tissue following gamma knife surgery: Early and distinct bilateral effects in the un-irradiated striatum. Mol Cells. 2009; 27:263-268.
14. Bauman JW, Liu J, Liu YP, Klaassen CD. Increase in metallothionein produced by chemicals that induce oxidative stress. Toxicol Appl Pharmacol. 1991; 110:347-354.
15. Lee JM, Moehlenkamp JD, Hanson JM, Johnson JA. Nrf2-dependent activation of the antioxidant responsive element by *tert*-butylhydroquinone is independent of oxidative stress in IMR-32 human neuroblastoma cells. Biochem Biophys Res Commun. 2001; 280:286-292.
16. Saegusa C, Kanno E, Itohara S, Fukuda M. Expression of Rab27B-binding protein Slp1 in pancreatic acinar cells and its involvement in amylase secretion. Arch Biochem Biophys. 2008; 475:87-92.
17. Zheng H, Liu J, Liu Y, Klaassen CD. Hepatocytes from metallothionein-I and II knock-out mice are sensitive to cadmium- and *tert*-butylhydroperoxide-induced cytotoxicity. Toxicol Lett. 1996; 87:139-145.
18. Waalkes MP, Liu J, Kasprzak KS, Diwan BA. Hypersusceptibility to cisplatin carcinogenicity in metallothionein-I/II double knockout mice: Production of hepatocellular carcinoma at clinically relevant doses. Int J Cancer. 2006; 119:28-32.

(Received May 18, 2010; Revised June 14, 2010; Accepted June 24, 2010)

Original Article

Preparation and *in vitro* evaluation of self-nanoemulsifying drug delivery systems (SNEDDS) containing clotrimazole

Alaa A. Kassem, Maha A. Marzouk, Amal A. Ammar*, Ghada H. Elosaily

Department of Pharmaceutics, Faculty of Pharmacy, Al-Azhar University, Nasr City, Cairo, Egypt.

ABSTRACT: This study sought to formulate and evaluate a self-nanoemulsified drug delivery system (SNEDDS) for clotrimazole (CT), a poorly water-soluble antimycotic drug, used in vaginal delivery. SNEDDS was developed to increase the CT dissolution rate, solubility, and ultimately bioavailability. The solubility of CT in various oils, surfactants, and co-surfactants was determined. Based on solubility studies, oil phase (oleic acid without or with coconut oil), surfactant (Tween 20), and co-surfactants (PEG 200 and *n*-butanol) were selected and grouped in two combinations for phase studies. Pseudo-ternary phase diagrams were used to evaluate the area of self-nanoemulsification. Essential properties of the prepared systems with regard to emulsion droplet size and turbidity value were determined. In order to investigate the potential for interaction between any of the SNEDDS ingredients used, FTIR spectroscopy was performed. *In vitro* release studies were performed with SNEDDS formulations in capsules, and the plain drug served as a control. The droplet size of the nanoemulsion was greatly affected by the ratio of the surfactant and co-surfactant. Based on the results with regard to droplet size, turbidity values, and complete drug release after 3 h, three optimized formulations were selected; each contained oleic acid/coconut oil/Tween 20/PEG 200/*n*-butanol in ratios of 10:0:60:15:15 (%, w/w), 7.5:2.5:53.5:13.3:13.3 (%, w/w), and 6.7:3.3:60:10:10 (%, w/w), respectively. Results suggested that the prepared SNEDDS formulations produced acceptable properties in terms of immediate drug release and could increase the bioavailability of CT.

Keywords: Clotrimazole, self-nanoemulsion (SNEDD)

**Address correspondence to:*
Dr. Amal A. Ammar, Department of Pharmaceutics, Faculty of Pharmacy, Al-Azhar University, Nasr city, Cairo, Egypt.
e-mail: amal_mansy@yahoo.com

1. Introduction

Clotrimazole (CT), a lipophilic imidazole derivative with antimycotic action, is widely and effectively employed locally for the treatment of vulvovaginal candidiasis. It is formulated in creams, foams, tablets, gels, irrigations, and pessaries. Unfortunately, oral use of CT is unacceptable due to its severe side effects, so topical administration of CT is recommended. However, its use is limited because of its very low water solubility, resulting in the need for it to be incorporated into a suitable vehicle (*1*). Microemulsion-based formulations offer rapid dispersion and an enhanced drug absorption profile. Microemulsions are thermodynamically stable, isotropically clear dispersions of water, oil, and surfactants with the potential to serve as drug-delivery vehicles (*2*,*3*). Microemulsions appear to have the ability to deliver larger amounts of topically applied agents into the mucosa than do traditional lotions and creams because they provide a better reservoir for a poorly soluble drug through their capacity for enhanced solubilization (*4*). Nanoemulsions or mini-emulsions are transparent or translucent oil-in-water (o/w) or water-in-oil (w/o) droplets with a mean droplet diameter in the range of 100-600 nm. They are also known as submicron emulsions and, unlike thermodynamically stable microemulsions, nanoemulsions are kinetically stable with great stability in suspension due to their small droplet size (*5*). Furthermore, self-nanoemulsion drug delivery systems (SNEDDS) have been reported to result in more reproducible plasma concentration profiles and oral bioavailability of pharmaceuticals (*6*). The aim of the present study was to prepare a CT SNEDDS to enhance the solubility of CT and consequently its absorption profile.

2. Materials and Methods

2.1. *Materials*

CT was generously provided by Alexandria Pharmaceuticals and Chemical Industries Co. (Alexandria, Egypt). Miglyol 812 (medium chain triglyceride oil from coconut oil), α-tocopherol acetate

(vitamin E acetate), Tween® 60 (polyoxyethylene 20 sorbitan monostearate), Arlacel 83 (sorbitan sesquioleate), and Labrafil M 1944 (a polyoxyethylated kernel oil) were generously provided by GlaxoSmithKline (Cairo, Egypt). Oleic acid, citric acid, sodium hydroxide, conc. hydrochloric acid, polyethylene glycol 4000 (PEG 4000), methanol, 1-octanol, and *n*-butanol were from ADWIC (Cairo, Egypt). Castor oil, sesame oil, palm oil, coconut oil, olive oil, corn oil, and linseed oil were from Lab Chemicals Trading (Cairo, Egypt). Sweet almond oil was from Escoda & Nicolau, S.A. (Spain). Sorbitol and Tween® 80 (polyoxyethylene 20 sorbitan monooleate) were from ADCO (Alexandria, Egypt). PEG 200 (polyethylene glycol 200), Span® 80 (sorbitan monooleate), and Tween® 20 (polyoxyethylene 20 sorbitan monolaurate) were from Sigma-Aldrich (St. Louis, MO, USA). PEG 400 (polyethylene glycol 400) and PEG 600 (polyethylene glycol 600) were from Winlab (Middlesex, UK). Isopropyl myristate, propylene glycol (PG), Span® 20 (sorbitan monolaurate), and Tween® 40 (polyoxyethylene 20 sorbitan monopalmitate) were from Fluka (Buchs, Switzerland).

2.2. *Solubility studies*

Solubility of CT in various oils, surfactants, and co-surfactants was determined (*7-9*). Two grams of each of the selected vehicles were added to each cap vial containing an excess of CT. After the vial was sealed, the mixture was heated at 40°C in a water bath to facilitate solubilization using a sonicator (Ultrasonic model SS101H, Sonix IV, Huntington Beach, CA, USA). Mixtures were shaken with a shaker (shaking water bath, Weiss-Gallenkamp, Loughborough, UK) at 25°C for 48 h. Each vial was centrifuged using a centrifuge (Nuve, NF 815, Ankara, Turkey) at 3,000 rpm for 5 min and excess insoluble CT was discarded by filtration using hydrophilic polyvinylidene fluoride (PVDF) Acrodisc LC membrane filter discs (0.2 μm). The clear filtrate was diluted with methanol and was measured spectrophotometrically using a spectrophotometer (Model 6105 UV/V, Jenway Ltd., Essex, UK) at 261 nm.

2.3. *Apparent partition coefficient studies*

The previous saturation of equal volumes of the citrate buffer (pH 4.5) and 1-octanol was accomplished by shaking both in a shaker for 3 h, and the two phases were left to separate overnight. A known concentration of CT was added to the separated 1-octanol phase with gentle shaking until the CT dissolved. The 1-octanol phase containing the dissolved drug was mixed with the citrate buffer (pH 4.5) phase. The mixture was then agitated for 6 h at room temperature, and the two phases were then separated again after centrifugation. The drug concentration in the citrate buffer (pH 4.5) phase was determined spectrophotometrically at 263 nm after suitable dilution.

2.4. *Construction of phase diagrams*

Based on previous solubility studies (*10,11*), an oil phase (oleic acid without or with coconut oil), surfactant (Tween® 20), and co-surfactants (PEG 200 and *n*-butanol) were selected and grouped in two combinations for phase studies (Table 1). Surfactant and co-surfactants were mixed (Smix) in different weight ratios (2:1:1, 4:1:1, and 6:1:1, respectively). These Smix ratios were chosen to reflect increasing concentrations of surfactant with respect to co-surfactants. For each phase diagram, the oil phase (consisting of oleic acid alone or in combination with coconut oil in ratios of 2:1, 3:1, and 4:1) and the specific Smix ratio were mixed thoroughly in different weight ratios from 1:9 to 9:1 in different glass vials. Sixteen different combinations of oil and Smix (1:9, 1:8, 1:7, 1:6, 1:5, 1:4, 1:3.5, 1:3, 1:2.33, 1:2, 1:1.5, 1:1, 1:0.66, 1:0.43, 1:0.25, and 1:0.11) were produced to study phase diagrams. Pseudo-ternary phase diagrams were developed using aqueous titration with a magnetic stirrer (Thermolyne, Dubuque, IA, USA). Slow titration with the aqueous phase was performed for each combination of oil and Smix separately. The amount of the aqueous phase added was varied to produce a water concentration in a range of 5% to 95% of total weight in increments of around 5%.

2.5. *Preparation of SNEDDS*

Based on the pseudo-ternary phase diagrams observed, homogenous mixtures of Tween 20 (surfactant), PEG 200, and *n*-butanol (co-surfactants) in varying ratios were blended with oleic acid with or without coconut oil (groups I and II) in different weight ratios using a magnetic stirrer.

2.6. *Emulsion droplet size analysis*

The morphology and size of the emulsion were studied (*6,12-17*) using a transmission electron microscope (TEM, JEM 1010, JEOL, Tokyo, Japan) capable of point-to-point resolution. The combination of bright field imaging at increasing magnification and diffraction modes was used to reveal the form and size of the emulsion. A drop of CT emulsion was placed on a carbon-coated copper grid, stained with 2% uranyl acetate aqueous solution, and examined using the TEM.

2.7. *Turbidity measurement*

Each formulation (1.6 g) was diluted with citrate buffer (pH 4.5) to 400 mL and gently mixed. The resultant emulsions were evaluated for their turbidity. The turbidity

Table 1. Composition of SNEDDS formulations

Formula	O:Smix	Omix ratio	Smix ratio	Ingredients (%, w/w)				
				Oleic acid	Coconut oil	Tween 20	PEG 200	*n*-butanol
F1	1:9	–	2:1:1	10	–	45	22.5	22.5
F2	1:8	–	2:1:1	10	–	40	20	20
F3	1:7	–	2:1:1	10	–	35	17.5	17.5
F4	1:6	–	2:1:1	10	–	30	15	15
F5	1:9	–	4:1:1	10	–	60	15	15
F6	1:8	–	4:1:1	10	–	53.3	13.3	13.3
F7	1:7	–	4:1:1	10	–	46.7	11.7	11.7
F8	1:6	–	4:1:1	10	–	40	10	10
F9	1:5	–	4:1:1	10	–	33.3	8.3	8.3
F10	1:3.5	–	4:1:1	10	–	23.3	5.8	5.8
F11	1:8	4:1	4:1:1	8	2	53.3	13.3	13.3
F12	1:7	4:1	4:1:1	8	2	46.7	11.7	11.7
F13	1:6	4:1	4:1:1	8	2	40	10	10
F14	1:8	3:1	4:1:1	7.5	2.5	53.3	13.3	13.3
F15	1:9	–	6:1:1	10	–	67.5	11.25	11.25
F16	1:8	–	6:1:1	10	–	60	10	10
F17	1:7	–	6:1:1	10	–	52.5	8.75	8.75
F18	1:6	–	6:1:1	10	–	45	7.5	7.5
F19	1:5	–	6:1:1	10	–	37.5	6.25	6.25
F20	2:8	–	6:1:1	10	–	30	5	5
F21	1:3.5	–	6:1:1	10	–	26.25	4.375	4.375
F22	1:9	4:1	6:1:1	8	2	67.5	11.25	11.25
F23	1:8	4:1	6:1:1	8	2	60	10	10
F24	1:7	4:1	6:1:1	8	2	52.5	8.75	8.75
F25	1:6	4:1	6:1:1	8	2	45	7.5	7.5
F26	1:5	4:1	6:1:1	8	2	37.5	6.25	6.25
F27	1:8	3:1	6:1:1	7.5	2.5	60	10	10
F28	1:7	3:1	6:1:1	7.5	2.5	52.5	8.75	8.75
F29	1:6	3:1	6:1:1	7.5	2.5	45	7.5	7.5
F30	1:5	3:1	6:1:1	7.5	2.5	37.5	6.25	6.25
F31	1:8	2:1	6:1:1	6.7	3.3	60	10	10
F32	1:7	2:1	6:1:1	6.7	3.3	52.5	8.75	8.75

of the resulting emulsions given in nephelometric turbidity units (NTU) was measured using a turbidity meter (TRB 550, WTW, Weilheim, Germany). Turbidity measurements were performed on 15 mL of the emulsion stored in amber screw-capped vials.

2.8. *Fourier transform infrared (FTIR) spectroscopy*

In order to investigate the potential interaction between any of the SNEDDS ingredients used, FTIR spectroscopy was performed using a FTIR spectroscope (FT/IR-5300, JASCO, Tokyo, Japan) fitted with a single cuvette or a single bounce diamond at 45° that internally reflected incident light, providing a sampling area 1 mm in diameter with a sampling depth of several microns. Samples analyzed were CT powder, oleic acid, coconut oil, Tween 20, PEG 200, *n*-butanol, a physical mixture of CT powder, oleic acid, Tween 20, PEG 200, and *n*-butanol at a ratio 1:1:1:1:1, and a physical mixture of CT, oleic acid, coconut oil, Tween 20, PEG 200, and *n*-butanol at a ratio 1:1:1:1:1:1. A small amount of the sample was directly scanned for absorbance over a range from 4,000 to 400 wave numbers (cm^{-1}).

2.9. *In vitro release test*

Release studies were performed with SNEDDS formulations in capsules, and the plain drug served as a control. The *in vitro* release test was performed in a dissolution apparatus I (Dissolution Test Apparatus, USP standard, DA-6D, Bombay, India). Each CT-SNEDDS formulation equivalent to 100 mg of CT was placed in two hard gelatin capsules (*2,18-20*) (size 00) while ensuring that the capsule was completely intact. The same SNEDDS formulation of the same weight but free of CT was placed in two hard gelatin capsules and subjected to dissolution to serve as a blank. These capsules were placed in a basket and rotated at 100 rpm using 400 mL citrate buffer, simulating vaginal

pH (pH 4.5) (*21*) with a temperature maintained at 37 ± 0.5°C. The samples (4 mL each) were removed at specified time intervals, namely, 15, 30, 45, 60, 90, 120, 180, and 240 min (*22*). The withdrawn samples were filtered using PVDF Acrodisc LC membrane filter discs (0.2 μm) and the drug content was determined spectrophotometrically at the predetermined λ_{max} against a blank of the same SNEDDS formulation but free of CT. An equal volume of citrate buffer (pH 4.5) was added to the release medium to maintain constant dissolution volume. The experiments were done in triplicate. The release data were kinetically analyzed using different kinetic models (Zero-order, First-order, and Higuchi diffusion models) to determine the mechanism of CT release from the different SNEDDS.

3. Results and Discussion

3.1. *Screening of oils and surfactants*

Development of microemulsion systems for poorly water-soluble drugs is crucial. The volume of the formulation should be kept to a minimum to deliver the therapeutic dose in an encapsulated form. Components selected for the formulation should have the ability to solubilize the drug at a high level in order to obtain a concentrated form of microemulsion (*23*).

The solubility of CT in various vehicles is shown in Figure 1. The best results in terms of the highest drug solubility were obtained using oleic acid followed by coconut oil (139 and 43.7 mg/mL, respectively). In contrast, Tween 20, PEG 200, and *n*-butanol had a maximum solubility of CT of 47.2, 73.8, and 183 mg/mL. Based on these results, oleic acid (*20,24,25*) and coconut oil (*26*) were chosen as the oil phase, Tween 20 as the surfactant, PEG 200 and *n*-butanol (*27*) as co-surfactants.

An important criterion for the selection of surfactants is that the hydrophilic lipophilic balance (HLB) value required to form an o/w nanoemulsion be greater than

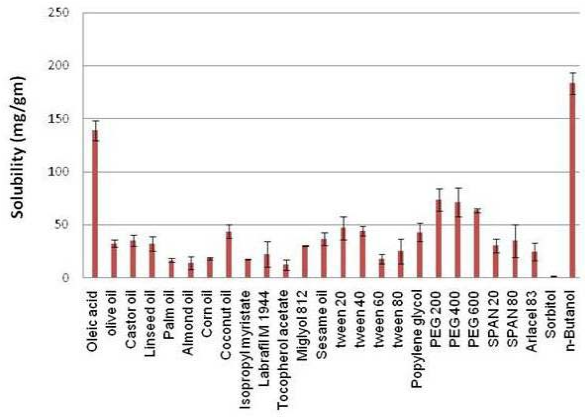

Figure 1. Solubility of CT in different oils, surfactants, and co-surfactants.

10 (*3*). In the present study, Tween 20, a nonionic surfactant, was selected because it has a HLB of 16.7.

Transient negative interfacial tension and a fluid interfacial film are rarely achieved with the use of a single surfactant, usually necessitating the addition of a co-surfactant. The presence of co-surfactants decreases the bending stress of the interface and allows an interfacial film with sufficient flexibility to assume different curvatures required to form a nanoemulsion over a wide range of compositions (*6*) and it also adjusts the HLB value of the formulation by making the polar solvent less hydrophilic. Due to the low water solubility of CT and rigidity of the oily surface, a quantity of alcohol (*n*-butanol) was added to dissolve the drug and increase the curvature of the oil layer. Alcohol incorporated into the nanoemulsion system not only reduces the interfacial tension between the oil phase and the aqueous phase but also makes the lipophilic drug soluble in the system (*28*). Thus, the co-surfactants selected for the study were PEG 200 and *n*-butanol.

3.2. *Apparent partition coefficient*

With a calculated octanol-citrate buffer, pH 4.5 [the pH in the vagina (*21*)], the partition coefficient (log P) value for CT was 2.33. This high value suggested good solubility of CT in lipophilic solvents.

3.3. *Pseudo-ternary phase diagram*

Pseudo-ternary phase diagrams were constructed in the absence of CT (*29*) to identify self nano-emulsifying regions and to select suitable concentrations of oil, surfactant, and co-surfactants for the SNEDDS formulation.

SNEDDS form fine o/w emulsions with only gentle agitation upon introduction into aqueous media. Since the free energy required to form an emulsion is very low, the formation is thermodynamically spontaneous. Surfactants form a layer around the emulsion droplets and reduce the interfacial energy as well as providing a mechanical barrier to coalescence. A visual test is used to measure the apparent spontaneity of emulsion formation (*8*).

Oleic acid and coconut oil (oil), Tween 20 (surfactant), and PEG 200 and *n*-butanol (co-surfactants) were put in two groups to study the phase diagrams in details. Pseudo-ternary phase diagrams were created separately for each group, as shown in Figure 2, so that o/w nanoemulsion regions could be identified. In both groups, increasing the ratio of surfactant/co-surfactants (Tween 20/PEG 200/*n*-butanol) from 2:1:1 to 6:1:1 in SNEDDS formulations was found to increase the spontaneity of the self-emulsification region. Therefore, a much higher concentration of surfactant led to a much higher self-emulsifying region in phase diagrams.

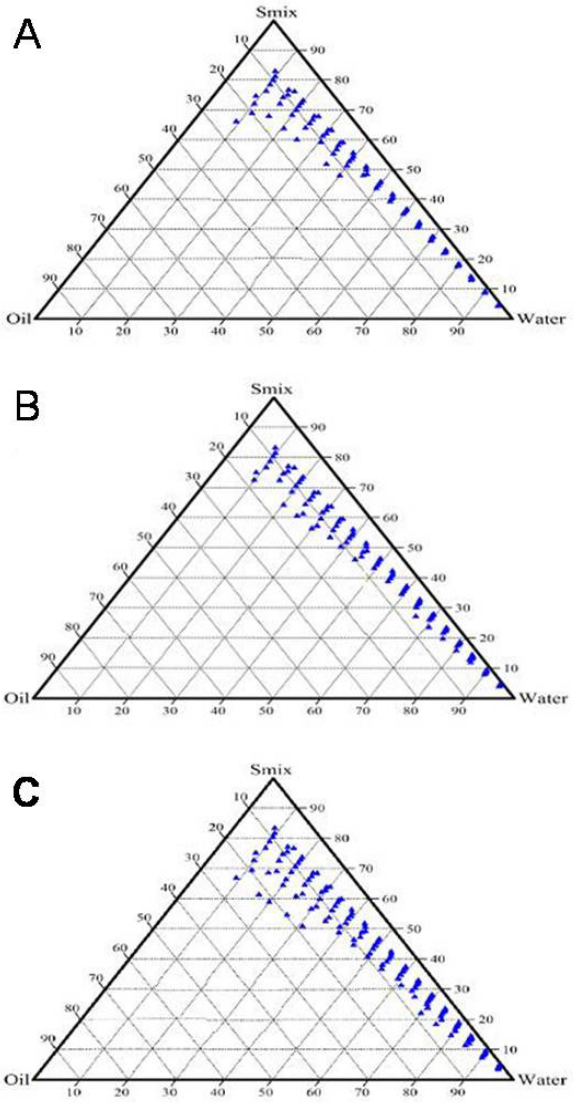

Figure 2. Pseudo-ternary phase diagrams of the o/w nanoemulsion region of certain CT systems at different Smix ratios. Smix ratios (Tween 20/PEG 200/*n*-butanol) were 2:1:1 **(A)**, 4:1:1 **(B)**, and 6:1:1 **(C)**. Closed triangles indicate points with o/w nanoemulsion.

These results agree with those of Derle *et al*. (*28*) who designed topical microemulsions of nimesulide, a poorly water-soluble nonsteroidal anti-inflammatory drug, using olive oil as the oil phase and Tween 80/iso-octanol as surfactant/co-surfactant.

3.4. *Droplet size and turbidity analysis*

TEM analysis revealed that the emulsion droplet was almost spherical in shape (Figure 3). The droplet size of the diluted SNEDDS formulations was evaluated by TEM as described elsewhere (*10,12,14*). Nanoemulsions are characterized in the nanometer size range. Therefore, droplet size analysis was performed to see whether the resultant emulsions were indeed nanoemulsions. All of the formulations prepared were found to be in the nanometer size range except F7, F10,

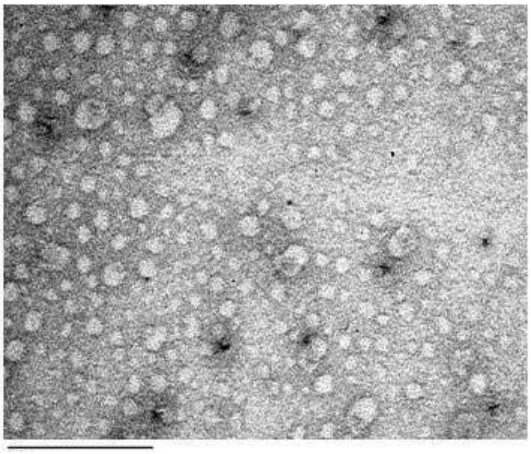

Figure 3. Typical TEM photographs of clotrimazole-containing microemulsion droplets of formulation F14. Bar, 500 nm. Original magnification, ×50,000.

F18, F19, and F26, which were in the micrometer size range (1,500-2,000 nm). The formulations F5-F9, F12, F14, F15, F20, and F31 had a size of < 200 nm, while the formulations F4, F13, F16, F21-25, F27-30, and F32 had a size of 200-500 nm and the formulations F1-3, F11, and F17 had a size of 500-700 nm. The measured turbidity of the formulations is summarized in Table 2. As is apparent, the formulations with a high turbidity (> 1,000) had a droplet size diameter of more than 1.5 µm, indicating a significant correlation between the droplet size and turbidity (in an ANOVA test, the correlation coefficient $r = 0.737$ and the two-tailed p value < 0.001, so the correlation is considered extremely significant).

3.5. *FTIR spectroscopy*

FTIR spectra are mainly used to determine if there is any interaction between the drug and any of the excipients used. The existence of an interaction is detected by the disappearance of an important functional group of the drug. CT compatibility with the ingredients of SNEDDS formulations was tested using FTIR, as shown in Figure 4. The FTIR spectrum of CT was characterized by bands at 1,585.63, 1,487.25, and 1,305.93 cm^{-1} (benzene ring stretching); 904.7, 823.68, and 744.59 cm^{-1} (C-H stretching); 3,169.33 and 3,042.02 cm^{-1} (aromatic C-H stretching); 1,084.09 cm^{-1} (chlorobenzene), and 1,203.69 cm^{-1} (C-N stretching).

After careful inspection of the spectra of the physical mixture of CT with the ingredients of SNEDDS formulations, the –C-N group, benzene ring, and –C-H stretching were found to be affected by the presence of these ingredients, as evidenced by the slightly higher absorption although the activity of the whole compound as well as the activity of characteristic groups of CT were unaffected. This finding confirms that CT did not interact with any of the ingredients of SNEDDS formulations.

Table 2. Mean droplet sizes, turbidity values, and cumulative release of clotrimazole from different SNEDDS formulations

Formulation	Mean droplet size (nm)	Turbidity value (NTU)	Cumulative% release after 240 min
F1	646	893	38.5
F2	723	518	32.6
F3	572	699	43.1
F4	434	344	55.2
F5	81	313	100
F6	144	296	51.8
F7	1,965	> 1,000	13.9
F8	183	816	93.9
F9	191	695	92.7
F10	1,532	> 1,000	32.5
F11	513	263	43.6
F12	179	515	94.4
F13	486	635	46.6
F14	98	88	100
F15	113	551	74.8
F16	492	157	48.7
F17	680	828	38.0
F18	1,714	> 1,000	30.8
F19	1,901	> 1,000	16.7
F20	118	88	29.7
F21	473	458	48.9
F22	303	353	77.7
F23	324	226	73.1
F24	402	276	65.0
F25	454	288	49.3
F26	1,850	> 1,000	20.2
F27	275	671	82.0
F28	404	301	63.2
F29	433	371	51.6
F30	333	438	75.8
F31	168	327	100
F32	345	83	71.0

3.6. *In vitro release study*

Release studies were performed with SNEDDS formulations in capsules as well as with the plain drug. When the release of CT from these formulations was evaluated in citrate buffer (pH 4.5), the percentage release of CT after 240 min from SNEDDS formulations was significantly greater than that of plain CT (13.5%) (Table 2). Complete drug release (100%) was obtained with F5 and F14 after 180 min and with F31 after 240 min (Figure 5). According to correlation coefficient (*r*), the *in vitro* release data suggested diffusion release kinetics except for F5, which displayed first-order release kinetics. The values of n for all of these formulations were ≤ 0.5, indicating Fickian (case I) transport (*20*), except for F31, which had an n that fell between 0.5 and 1, *i.e.*, non-Fickian (anomalous) transport (*30*,*31*).

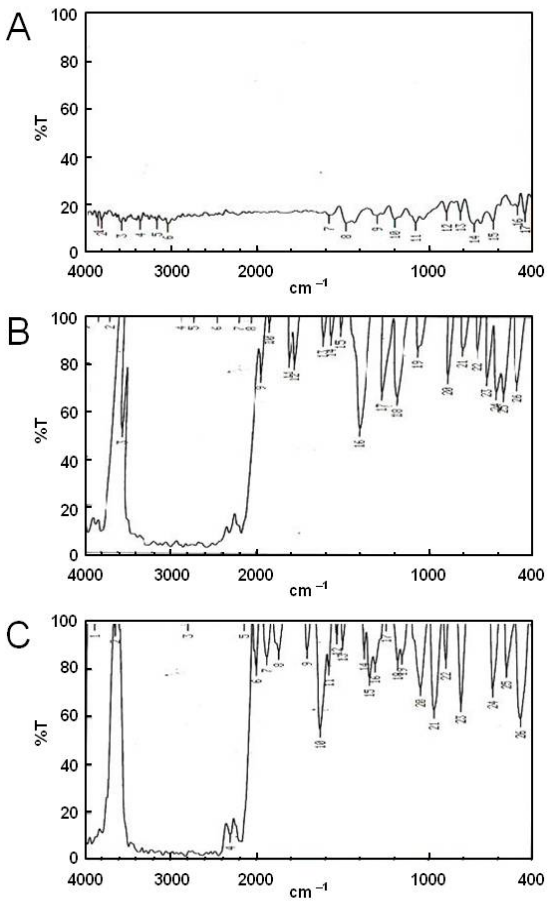

Figure 4. FTIR spectra. (A) clotrimazole; **(B)** physical mixtures of clotrimazole, oleic acid, Tween® 20, PEG 200, and *n*-butanol in a 1:1:1:1:1 ratio; **(C)** physical mixtures of clotrimazole, oleic acid, coconut oil, Tween® 20, PEG 200, and *n*-butanol in a 1:1:1:1:1:1 ratio.

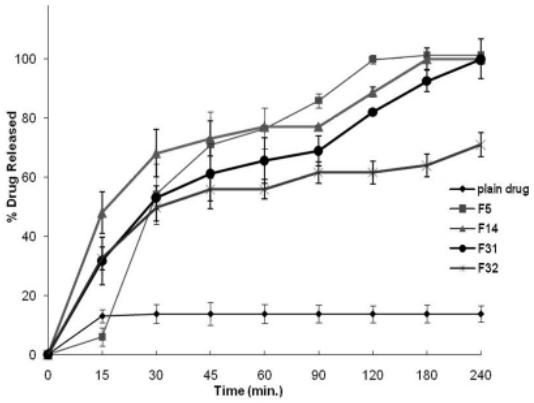

Figure 5. *In vitro* release of clotrimazole from SNEDDS formulations F5, F14, F31, and F32 and plain drug.

4. Conclusion

Results suggested that the prepared self-nanoemulsified formulations of CT produced acceptable properties in terms of droplet size, turbidity values, and immediate drug release that could increase the bioavailability profile of CT.

References

1. Ning MY, Guo YZ, Pan HZ, Yu HM, Gu ZW. Preparation and evaluation of proliposomes containing clotrimazole. Chem Pharm Bull (Tokyo). 2005; 53:620-624.
2. Date AA, Nagarsenker MS. Design and evaluation of self-nanoemulsified drug delivery systems (SNEDDS) for cefpodoxime proxetil. Int J Pharm. 2007; 329:166-172.
3. Constantinides PP. Lipid microemulsions for improving drug dissolution and oral absorption: Physical and biopharmaceutical aspects. Pharm Res. 1995; 12:1561-1572.
4. D'Cruz OJ, Yiv SH, Uckun FM. GM-144, a novel lipophilic vaginal contraceptive gel-microemulsion. AAPS PharmSciTech. 2001; 2:E5.
5. Constantinides PP, Chaubal MV, Shorr R. Advances in lipid nanodispersions for parentral drug delivery and targeting. Adv Drug Deliv Rev. 2008; 60:757-767.
6. Shafiq S, Shakeel F, Talegaonkar S, Ahmad FJ, Khar RK, Ali M. Development and bioavailability assessment of ramipril nanoemulsion formulation. Eur J Pharm Biopharm. 2007; 66:227-243.
7. Limayem Blouza I, Charcosset C, Sfar S, Fessi H. Preparation and characterization of spironolactone-loaded nanocapsules for pediatric use. Int J Pharm. 2006; 325:124-131.
8. Kang BK, Lee JS, Chon SK, Jeong SY, Yuk SH, Khang G, Lee HB, Cho SH. Development of self-microemulsifying drug delivery systems (SMEDDS) for oral bioavailability enhancement of simvastatin in beagle dogs. Int J Pharm. 2004; 274:65-73.
9. D'Cruz OJ, Uckun FM. Influence of long-term stability conditions on microbicidal nucleoside prodrug (WHI-07)-loaded gel-microemulsion. AAPS PharmSciTech. 2006; 7:73.
10. Shafiq-un-Nabi S, Shakeel F, Talegaonkar S, Ali J, Baboota S, Ahuja A, Khar RK, Ali M. Formulation development and optimization using technique: A technical note. AAPS PharmSciTech. 2007; 8:Article 28.
11. Sinko PJ (ed.). Martin's Physical Pharmacy and Pharmaceutical Sciences. 5th ed., Lippincott Williams & Wilkins, Philadelphia, PA, USA, 2006; pp. 54-55.
12. Xi J, Chang Q, Chan CK, Meng ZY, Wang GN, Sun JB, Wang YT, Tong HH, Zheng Y. Formulation development and bioavailability evaluation of a self-nanoemulsified drug delivery system of oleanolic acid. AAPS PharmSciTech. 2009; 10:172-182.
13. Kelmann RG, Kuminek G, Teixeira HF, Koester LS. Carbamazepine parentral nanoemulsions prepared by spontaneous emulsification process. Int J Pharm. 2007; 342:231-239.
14. Kuo F, Subramanian B, Kotyla T, Wilson TA, Yoganathan S, Nicolosi RJ. Nanoemulsions of an anti-oxidant synergy formulation containing gamma tocopherol have enhanced bioavailability and anti-inflammatory properties. Int J Pharm. 2008; 363:206-213.
15. Singh KK, Vingkar SK. Formulation, antimalarial activity and biodistribution of oral lipid nanoemulsion of primaquine. Int J Pharm. 2008; 347:136-143.
16. Vyas TK, Shahiwala A, Amiji MM. Improved oral bioavailability and brain transport of Saquinavir upon administration in novel nanoemulsion formulations. Int J Pharm. 2008; 347:93-101.
17. Wan T, Hu ZW, Ma XL, Yao J, Lu K. Synthesis of silane monomer-modified styrene-acrylate microemulsion coatings by photopolymerization. Prog Org Coat. 2008; 62:219-225.
18. Patil P, Paradkar A. Porous polystyrene beads as carriers for self-emulsifying system containing loratadine. AAPS PharmSciTech. 2006; 7:E28.
19. Zidan AS, Sammour OA, Hammad MA, Megrab NA, Habib MJ, Khan MA. Quality by design: Understanding the formulation variables of a cyclosporin A self-nanoemulsified drug delivery systems by Box-Behnken design and desirability function. Int J Pharm. 2007; 332:55-63.
20. Mehta SK, Kaur G, Bhasin KK. Analysis of tween based microemulsion in the presence of TB drug rifampicin. Colloids Surf B Biointerfaces. 2007; 60:95-104.
21. Pavelić Ž, Škalko-Basnet N, Filipović-Grčić J, Martinac A, Jalšenjak I. Development and *in vitro* evaluation of a liposomal vaginal delivery system for acyclovir. J Control Release. 2005; 106:34-43.
22. Dash AK, Cudworth GC. Evaluation of an acetic acid ester of monoglyceride as a suppository base with unique properties. AAPS PharmSciTech. 2001; 2:E13.
23. Subramanian N, Ray S, Ghosal SK, Bhadra R, Moulik SP. Formulation design of self-microemulsifying drug delivery systems for improved oral bioavailability of celecoxib. Biol Pharm Bull. 2004; 27:1993-1999.
24. Borgia SL, Regehly M, Sivaramakrishnan R, Mehnert W, Korting HC, Danker K, Röder B, Kramer KD, Schäfer-Korting M. Lipid nanoparticales for skin penetration enhancement-correlation to drug localization within the particle matrix as determined by fluorescence and parelectric spectroscopy. J Control Release. 2005; 110:151-163.
25. El-Laithy HM. Preparation and physicochemical characterization of dioctyl sodium sulfosuccinate (aerosol OT) microemulsion for oral drug delivery. AAPS PharmSciTech. 2003; 4:E11.
26. Fang JY, Hung CF, Hua SC, Hwang TL. Acoustically active perfluorocarbon nanoemulsions as drug delivery carriers for camptothecin: Drug release and cytotoxicity against cancer cells. 2009; 49:39-46.
27. Vandamme TF. Microemulsion as ocular drug delivery systems: Recent developments and future challenges. Prog Retin Eye Res. Ultrasonics. 2002; 21:15-34.
28. Derle DV, Sagar BSH, Pimpale S. Microemulsion as a vehicle for transdermal permeation of nimesulide. Indian J Pharm Sci. 2006; 68:622-625.
29. Parikh DK, Ghosh TK. Feasibility of transdermal delivery of fluoxetine. AAPS PharmSciTech. 2005; 6: E144-E149.
30. Attama AA, Nzekwe IT, Nnamani PO, Adikwu MU, Onugu CO. The use of solid self-emulsifying systems in the delivery of diclofenac. Int J Pharm. 2003; 262:23-28.
31. Swarnalatha S, Selvi PK, Ganesh Kumar A, Sekaran G. Nanoemulsion drug delivery by ketene based polyester synthesized using electron rich carbon/silica composite surface. Colloids Surf B Biointerfaces. 2008; 65:292-299.

(Received May 9, 2010; Revised June 4, 2010; Re-revised July 28, 2010; Accepted August 1, 2010)

Original Article

Comparative evaluation of ketoconazole-β-cyclodextrin systems prepared by coprecipitation and kneading

Maha A. Marzouk*, Alaa A. Kassem, Ahmed M. Samy, Reham I. Amer

Department of Pharmaceutics and Industrial Pharmacy, Faculty of Pharmacy, Al-Azhar University, Cairo, Egypt.

ABSTRACT: Ketoconazole (KZ), an imidazole antifungal, was formulated into inclusion complexes *via* coprecipitation and kneading with β-cyclodextrin (β-CD) as a carrier in 1:1 and 1:2 drug to carrier ratios. The KZ-β-CD solid complexes were characterized by X-ray diffraction and differential scanning calorimetry (DSC). The diffraction pattern of the pure drug revealed the drug to be highly crystalline in nature, as indicated by numerous distinctive peaks. The lack of numerous distinctive peaks of the drug in KZ-β-CD complexes prepared by the two methods revealed that a large number of the drug molecules were dissolved in a solid-state carrier matrix with an amorphous structure. The thermograms of the KZ-β-CD complexes showed a strong reduction in the intensity and broadening of drug peaks somewhat in both kneading and coprecipitation systems, suggesting that the drug is monomolecularly dispersed in the β-CD cavity. The prepared tablets of KZ-β-CD solid complexes prepared by the two methods were evaluated for their quality control testing, and an *in vitro* release study and the results of quality control complied with pharmacopeial requirements and the release profiles indicated complete drug release after 30 min. The kinetic parameters obtained from release data were analyzed in order to explain the mechanism of drug release and revealed non-Fickian transport. Accelerated stability testing at 35°C, 45°C, and 55° C and at 75% relative humidity was carried out for six months and revealed somewhat stable systems as indicated by a t_{90} of about 2 years for both KZ-β-CD systems. A microbiological *in vitro* assay of KZ from the prepared tablets was performed using *Candida albicans* as a model fungus, and KZ had improved microbiological activity when administered as an inclusion complex with β-CD. The results confirmed the benefit of using CDs as a useful tool to enhance the dissolution and hence bioavailability of poorly water-soluble drugs by forming solubilizing systems when exposed to gastrointestinal fluid.

Keywords: Ketoconazole, β-cyclodextrin inclusion complex, spectroscopic study, tablets, quality control, *in vitro* release, stability, microbiological study

1. Introduction

A prerequisite for drug absorption and clinical success for all drugs given orally in a solid dosage form is drug dissolution within the gastrointestinal tract, which in many cases can be the rate-limiting step in the overall absorption process *in vivo* (*1*). Ketoconazole (KZ) is a dibasic imidazole antifungal synthetic agent developed for the treatment of human mycotic infections and plays an essential role in antifungal chemotherapy (*2*). It is slightly soluble in water, with a molecular weight of 531.44; it must be administered either topically or by mouth (*3*). Since it is a weak base with limited water solubility, an acid medium is required to transform the drug into the soluble hydrochloride salt (*4-6*).

Cyclodextrins (CDs) are oligosaccharides that have received increasing attention in the pharmaceutical field because of their ability to form inclusion complexes with many lipophilic drugs, thus changing the physicochemical and biopharmaceutical properties of those drugs (*7,8*). Complexation between imidazole derivatives and cyclodextrins has already been studied (*5*) and the antimycotic activity of these complexes has been found to be superior to the activity of drug alone.

The objective of this study was to improve the aqueous solubility and dissolution rate of KZ by preparing inclusion complexes with β-cyclodextrin using coprecipitation and kneading. Furthermore, X-ray diffractometry and differential scanning calorimetry (DSC) were used to study interactions between KZ and β-CD in a solid state. The prepared tablets of KZ-β-CD systems were evaluated for their uniformity of weight, thickness, hardness, friability, disintegration time, and drug content uniformity. The *in vitro* release of KZ

**Address correspondence to:*
Dr. Maha Abd El-hamid Marzouk, Department of Pharmaceutics and Industrial Pharmacy, Faculty of Pharmacy, Al-Azhar University, Cairo, Egypt.
e-mail: ma.marzouk@yahoo.com

tablets was determined and the kinetic parameters were analyzed in order to explain the mechanism of drug release. Accelerated stability testing of KZ at 35°C, 45°C, and 55°C and at 75% relative humidity was carried out for six months, and $t_{1/2}$ and t_{90} were estimated for each formula. A microbiological *in vitro* assay of KZ from the prepared tablets was performed using *Candida albicans* as a model fungus. The inhibition zone diameter in each case was measured, and the obtained value served as a measure of the antifungal activity of KZ.

2. Materials and Methods

2.1. *Materials*

KZ was kindly supplied by Memphis Company for Pharmaceuticals (Cairo, Egypt). β-CD was obtained from Alexandria Chemical Co. (Alexandria, Egypt). Absolute methyl alcohol, hydrochloric acid, sodium chloride, talc, 70% perchloric acid, and glacial acetic acid were from El-Nasr Pharmaceutical Chemicals Co. (Cairo, Egypt). Avicel PH 101 was from Fluka AG (Buchs, Switzerland). Magnesium stearate was from VWR (West Chester, PA, USA). Sodium starch glycolate (Explotab) was kindly supplied by Egyptian International Pharmaceutical Industries Company (EIPICO; Cairo, Egypt). Acetic anhydride was purchased from Eastern Fine Chemicals Co., Ltd. (Milano, Italy). Commercial KZ tablets (Rameda, 200 mg) were from the Tenth of Ramadan for Pharmaceutical Industries and Diagnostic Reagents (6th of October City, Egypt). Sabouraud's agar consisting of 2% glucose, 1% neopeptone, and 2% agar was from Oxoid Ltd. (Cambridge, UK). A strain of *Candida albicans* was from the American Typing Culture Collection (ATCC).

2.2. *Preparation of KZ-β-CD systems*

Inclusion complexes of KZ and β-CD were prepared by coprecipitation and kneading using drug to carrier molar ratios of 1:1 and 1:2 (*5,9*). The coprecipitation system was prepared using methanol as a solvent; the calculated amount of KZ was dissolved homogeneously in the least amount of methanol and mixed with a solution of carrier in distilled water. The solvents were evaporated at room temperature overnight and then dried at 45°C (controlled hot air ovens; VELP Scientifica, Usmate, Italy). The kneading system was prepared by mixing KZ and β-CD powder with a small amount of water and ethanol mixture (1:1) in a mortar so as to obtain a homogeneous paste. The slurries were kneaded for 30 min and then dried at 45°C. The coprecipitation and kneading systems were pulverized and sieved. The fraction of powder passed through a 250-µm sieve and retained on a 125-µm sieve (ASTM; SIEBTECHNIK GmbH, Mulheim/Ruhr, Germany) was collected and used for further investigation.

2.3. *Characterization of KZ-β-CD systems*

2.3.1. *Solubility study of KZ-β-CD systems in 0.1 N HCl*

The solubility of coprecipitated and kneaded KZ-β-CD systems at 1:1 and 1:2 molar ratios was determined by weighing the known excess of both systems in vials containing 0.1 N HCl. The vials containing samples were shaken for 48 h in a thermostatically controlled shaker (Oscillating thermostatically controlled water bath shaker, Weiss-Gallenkamp, Loughborough, UK) at 37°C. The samples were then filtered through a 0.45-µm membrane filter (Millipore, Billerica, MA, USA), suitably diluted, and then analyzed spectrophotometrically (Spectrophotometer Model 6105 UV/Vis Felsted; Jenway Ltd., UK) for KZ content at the determined λ_{max} while referring to the corresponding calibration curve. Each experiment was done in triplicate and the equilibrium solubility served as the average value.

2.3.2. *Drug content and incorporation efficiency*

The drug content of KZ in the prepared inclusion complexes was estimated according to The United States Pharmacopoeia (USP) XXV (*3*). A weight of 200 mg from each system was dissolved in 40 mL glacial acetic acid, shaken for 10 min, and then filtered. The filtrate was treated with a 0.1 N perchloric acid mixture consisting of 8.5 mL of 70% perchloric acid, 900 mL glacial acetic acid, and 30 mL acetic anhydride; this was then left for 24 h in a cold place and was finally adjusted to 1 liter with glacial acetic acid and the end point was determined potentiometrically (*3,10*). A blank sample was prepared, and the necessary corrections were made (each mL of 0.1 N perchloric acid was equivalent to 26.57 mg of KZ). The mean value of triplicate estimates was used to calculate the amount of KZ in each system. The production yield and the incorporation efficiency were calculated according to the following equations:

Production Yield = [Weight of KZ physical mixtures before preparation]/[Weight of KZ inclusion complex after preparation] × 100

--- Eq. 1

Incorporation efficiency = [Drug incorporated]/[Theoretical drug content] × 100

--- Eq. 2

2.3.3. *Spectroscopic study*

X-Ray diffraction (XRD) – Pure KZ, β-CD and the prepared inclusion complexes were evaluated with an XD-610 X-ray diffractometer (Shimadzu, Kyoto, Japan). The samples were exposed to Cu Ka radiation

(40 kV × 30 mA) at a scan rate of 8 deg./min.

Differential scanning calorimetry (DSC) – Pure KZ, β-CD, and the prepared inclusion complexes were subjected to differential scanning calorimetry (Shimadzu DSC TA-50 ESI, Tokyo, Japan). Samples of about 2 mg were accurately weighed and scanned at a rate of 10°C/min over a 20-300°C temperature range in an inert atmosphere of nitrogen.

2.4. *Formulation of KZ tablets*

Tablets of coprecipitated and kneaded KZ-β-CD solid complexes at a molar ratio of 1:2 (*9*) and containing 200 mg of KZ were prepared by direct compression using a tablet compression machine with concave single punches (Erweka, Frankfurt, Germany). The additives used are shown in Table 1 and were talc, magnesium stearate, sodium starch glycolate (Explotab), and Avicel PH 101 as a diluent to yield a tablet of 1,000 mg final weight about 12 mm in diameter. Plain tablets with no inclusion complex and containing 200 mg KZ were also prepared.

2.5. *Evaluation of KZ tablets*

Coprecipitated and kneaded KZ-β-CD tablets at a molar ratio of 1:2 and containing 200 mg of KZ were evaluated for the following parameters. Weight uniformity was determined by a USP XXV procedure (*3*). For drug content determination, random samples of 10 tablets from each system were powdered and treated similarly, as mentioned previously (*10*). Tablet thickness, hardness, disintegration, and friability were determined according to USP XXV (*3*). The experiments were done 6 times in each case and the mean values and standard deviations were calculated.

2.6. In vitro release of KZ tablets

The *in vitro* release of KZ-β-CD systems was investigated by a USP rotating basket method using a USP-Standard Apparatus I Model DA-6D (Veego, Bombay, India). The dissolution media consisted of 900 mL of simulated gastric fluid (pH 1.2) maintained at 37 ± 0.5°C (*11*). Each tablet from the coprecipitated and kneaded KZ-β-CD systems at a molar ratio of 1:2 and containing 200 mg of KZ was held in the basket, which was positioned 2.5 cm from the bottom of the vessel and rotated at 100 rpm. At specified time intervals, 5 mL of sample was withdrawn from each of the six dissolution media and filtered off. This volume was replenished with a similar volume of fresh dissolution medium maintained at the same temperature. The content of KZ was assayed spectrophotometrically at 269 nm against a blank. The same procedure was conducted for the pure KZ tablets containing (200 mg KZ). The experiment was run in triplicate, maintaining sink conditions. The mean percentage of KZ released was calculated.

The dissolution data were fitted to an equation determined by Ritger and Peppas (*12*) as follows:

$$M_t/M_\infty = Kt^n \qquad \text{--- Eq. 3}$$

where M_t/M_∞ is the fraction of drug released at time t, K is the kinetic constant of the system, and n is the exponent characteristic of the release.

2.7. *Stability study*

Accelerated stability studies at 35°C, 45°C, and 55°C ± 1.0°C with thermostatically controlled hot air incubators were carried out for six months on the coprecipitated and kneaded KZ-β-CD tablets at a molar ratio of 1:2 and containing 200 mg of KZ. Relative humidity (RH) was maintained at 75% using saturated solutions of sodium chloride. Adequate samples from each system at each elevated temperature were taken at time intervals of 0, 14, 30, 45, 60, 90, 120, and 180 days. These samples were evaluated according to the method of assay previously mentioned in drug content. The method was carried out in triplicate for each system and the mean value was estimated. Zero-, first-, and second-order kinetics were used to choose the suitable order for the stability study and the relevant kinetic parameters were determined.

2.8. *Microbiological study of KZ tablets*

Coprecipitated and kneaded KZ-β-CD tablets at a molar ratio of 1:2 and commercial KZ tablets were used in this study.

2.8.1. *Preparation of a KZ reference and sample solutions*

An accurately weighed 15 mg KZ reference standard was transferred to a 50-mL volumetric flask and dissolved in methanol (300 µg/mL). An aliquot of this solution (3

Table 1. Formulae of KZ tablets tested

Formula	Inclusion complex wt. (mg)	Magnesium stearate (mg)	Talc (mg)	Explotab (mg)	Avicel (mg)	Total wt. (mg)
Plain KZ*	–	10	10	20	760	1,000
KZ:β-CD 1:2 (Coprecipitated)	950	10	10	20	10	1,000
KZ:β-CD 1:2 (Kneaded)	770	10	10	20	190	1,000

* Plain KZ was 200 mg in weight.

mL) was transferred to a 25-mL volumetric flask and was diluted with 0.1 N HCl solution (pH 1.2) to obtain a solution of concentration (36 µg/mL). Aliquots of 50, 100, and 150 µL from this solution, corresponding to respective drug concentrations of 1.8, 3.6, and 5.4 µg/µL, were used in the assay. Adequate tablets from each formula were weighed, finely powdered, and an amount of powder equivalent to 15 mg of KZ was treated as mentioned previously. Resulting mixtures were then used in the assay as sample solutions.

2.8.2. *Microbiological assay of KZ tablets (Cylinder-plate method)*

Microorganism and inoculum-cultures of *Candida albicans* ATCC were cultivated on 2% Sabouraud's agar (*13*) and maintained in test tubes in a refrigerator at 4 ± 2°C until use. The microorganism was suspended in 0.9% NaCl; the concentration in the obtained suspension was fit to 25 ± 2% of transmittance at 580 nm using a spectrophotometer analyzer and a 10 mm diameter test tube as an absorption cell against 0.9% NaCl as a blank (*14*). For the biological assay of KZ, 1 mL of this suspension was added to 60 mL of 2% Sabouraud's agar using sterile plates; the media was allowed to harden and was used as an inoculated layer. In each plate, three cups were made using a Wasserman tube; each cup was carefully filled with a known quantity of the sample under sterile conditions. The plates were incubated at 37°C for 24 h. The resulting zone diameters of inhibition of growth were then measured in mm. Each determination was done in triplicate and the average zone diameter was calculated (*15*).

3. Results and Discussion

3.1. *Characterization of KZ-β-CD systems*

Solubility of KZ-β-CD is summarized in Table 2. The solubility of pure KZ was found to be greatly enhanced by its incorporation in inclusion complex with β-CD systems prepared by either coprecipitation or kneading. An inclusion complex with a 1:2 drug to β-CD molar ratio had better solubility than one with a 1:1 drug to β-CD molar ratio, and this result agreed with the results of Choi *et al*. (*9*).

Table 2. Solubility of KZ-β-CD systems in 0.1 N HCl

Method of preparation	Drug to β-CD molar ratios	Solubility (mg/mL)
Pure drug	–	0.096
Coprecipitation	1:1	17.9
	1:2	18.3
Kneading	1:1	18.1
	1:2	19.8

The KZ inclusion complex prepared by coprecipitation and kneading using a molar ratio of 1:2 resulted in good production yield of about 99% in relation to the theoretical maximum and also higher incorporation efficiency (Table 3), which was in accordance with the findings of Bergamasco *et al*. (*16*).

3.2. *Spectroscopic study*

Figure 1 shows the X-ray diffraction pattern of a KZ-inclusion complex system (1:1 molar ratio) in comparison to that of pure KZ. The diffraction pattern of KZ showed that the drug has a high degree of crystallinity because of the presence of numerous distinct peaks. The most characteristic peaks at a 2θ-diffraction angle were located at 17.5, 18.52, 19.9, 20.95, 23.5, and 28.6 degrees. The change in the X-ray diffraction pattern of the solid complex, represented by the reduction in intensity of peaks of drug, in the kneaded and coprecipitated products suggested an interaction between drug and the CD used and it also revealed that a portion of KZ was in an amorphous state (*5,17,18*).

Figure 2 shows the DSC thermogram of a KZ-inclusion complex system (1:1 molar ratio) in comparison to that of pure KZ, which is characterized by one sharp endothermic peak at about 152.16°C, indicating that the drug had a melting point like that shown in Figure 2A. Figure 2B shows the DSC thermogram of pure β-CD, which had a shallow and broad endothermic peak at about 105.52°C with the potential to be extended because of the release of water from the molecule (*17*). The DSC thermogram of the inclusion complex of the drug with β-CD is represented in Figure 2C. The characteristic thermal peak of the drug appeared at a lower temperature than 147.73°C and decreased substantially in intensity and broadened somewhat with the kneaded and coprecipitated products (*17*). These results suggest that the drug is monomolecularly dispersed in the β-CD cavity (*19*).

3.3. *Evaluation of KZ tablets*

Solubility in 0.1 N HCl, production yield, and

Table 3. KZ content and incorporation efficiency of KZ-β-CD systems

Method of preparation	Drug to β-CD molar ratio	Production yield (%)	Theoretical drug content (mg)	Actual drug content (mg)	Incorporation efficiency (%)
Coprecipitation	1:1	97.0	200	208.6	104.3
	1:2	99.9	200	211.8	105.9
Kneading	1:1	95.6	200	197.8	98.9
	1:2	98.9	200	213.4	106.7

incorporation efficiency were higher in KZ-β-CD systems prepared by coprecipitation and kneading using a 1:2 molar ratio than in those using a 1:1 molar ratio (*9,16*). Therefore, the 1:2 KZ-β-CD systems were chosen for tablet formulation and further studies.

Table 4 shows the quality control results for KZ tablets. The uniformity of weight of KZ tablets manufactured by direct compression revealed that the weight of the tested tablets complied with the pharmacopeial requirements (*3*). The uniformity of drug content of KZ tablets revealed that the average drug content of KZ tablets ranged from 98.1% to 99.0%, with a standard deviation ranging from 1.00 to 1.80 (Table 4), which complies with the pharmacopeial requirements (*3*).

The uniformity of thickness, although unofficial, can be considered as an additional control to the tablet dimension and increased reproducibility. The average thickness value of KZ tablets ranged from 8.25 mm to 8.54 mm, with standard deviations ranging from 0.07 to 0.14 (Table 4). These results indicate that all of the prepared KZ tablets prepared by different techniques had acceptable limits of thickness uniformity.

The mechanical properties of the investigated tablets were evaluated by testing their hardness and friability. The average hardness values ranged from 8.82 kg to 9.66 kg, with standard deviation values between 0.76 and 0.85 (Table 4). The results of the friability study of different KZ tablets indicated average percent loss of weight ranging from 0.30% to 0.87%, with a standard deviation ranging from 0.01 to 0.08. A maximum weight loss of not more than 1% of the weight of the tablets being tested was considered acceptable for most products.

According to USP XXV (*3*), complete disintegration is defined as that state in which any residue of the unit, except fragments of insoluble coating or capsule shell, remaining on the screen of the test apparatus is a soft mass having no palpably film core. The mean value of the disintegration time for KZ tablets ranged from 2.33 to 5.33 min, with a standard deviation of 0.57 min (Table 4). The aforementioned tests led to the conclusion that all of the prepared KZ tablets complied with the pharmacopeial requirements and demonstrated good inter-batch uniformity.

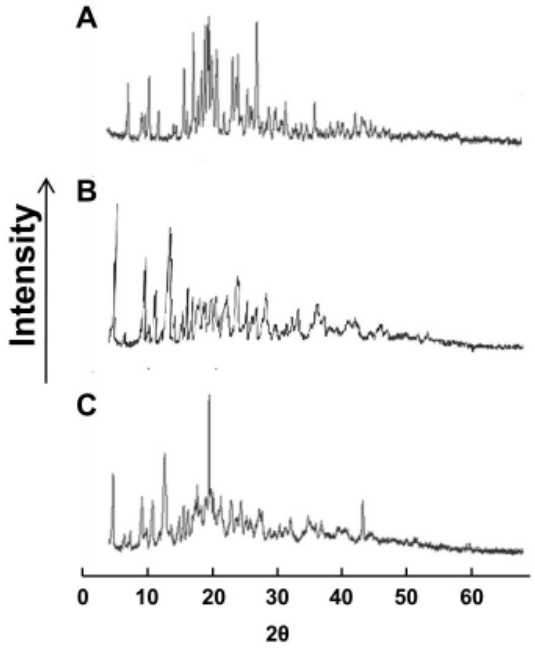

Figure 1. X-Ray Diffraction of (A) Pure KZ, (B) β-cyclodextrin, and (C) KZ-β-CD systems.

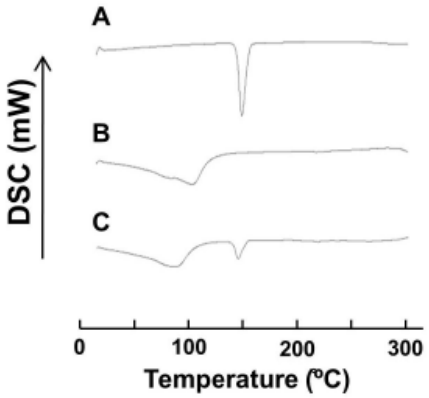

Figure 2. DSC thermograms of pure KZ (A), β-cyclodextrin (B), and KZ-β-CD systems (C).

3.4. *In vitro release of KZ tablets*

The *in vitro* release of KZ tablets containing a β-CD 1:2 molar ratio prepared by coprecipitation and kneading in 0.1 N HCl are shown in Figure 3. Apparent was the fact that the both the coprecipitated and kneaded KZ tablets had maximum drug release (100%) after 30 min, while the plain KZ had release of only 69.6% after the same amount of time. The enhanced dissolution rate might be attributed to the decreased particle size, indicating the high level of energy of drug inclusion complexes.

Table 4. Quality control tests for KZ tablets

Formula	Weight (g)	Drug content (%)	Thickness (mm)	Hardness (kg)	Weight loss (%)	Disintegration time (min)
Coprecipitated KZ-β-CD	0.994 ± 0.006	98.1 ± 1.80	8.25 ± 0.07	9.66 ± 0.76	0.30 ± 0.01	2.33 ± 0.57
Kneaded KZ-β-CD	1.008 ± 0.018	99.0 ± 1.00	8.54 ± 0.14	8.82 ± 0.85	0.87 ± 0.09	5.33 ± 0.57

Data are shown as mean ± S.D.

The medium of 0.1 N HCl has been reported to be one of the most commonly used in such studies to imitate physiological gastric fluid (*11*).

To analyze the release mechanism of the drug from these tablets with hydrophilic matrices, the release data obtained were fit to a simple power equation (*12*) as follows:

$$M_t/M_\infty = Kt^n$$

where M_t/M_∞ is the fraction of drug released at time t, K denotes the constant incorporating structural and geometrical characteristics of the drug/carrier system, n is the diffusion exponent related to the mechanism of the drug release, and M_∞ is the amount of drug incorporated in the tablet, *i.e.*, 200 mg. The values of K and n were estimated by linear regression of log (M_t/M_∞) on log t where log K is the intercept and n is the slope of the straight line.

$$\text{Log } M_t/M_\infty = \log K + n \log t$$

Kinetic analysis of the *in vitro* release data for KZ from all of the tablets revealed that the n value fell between 0.5 and 1, indicating non-Fickian (anomalous) transport (where release is controlled by a combination of diffusion and polymer relaxation), and this finding was in accordance with the findings of Karasulu *et al*. (*13*).

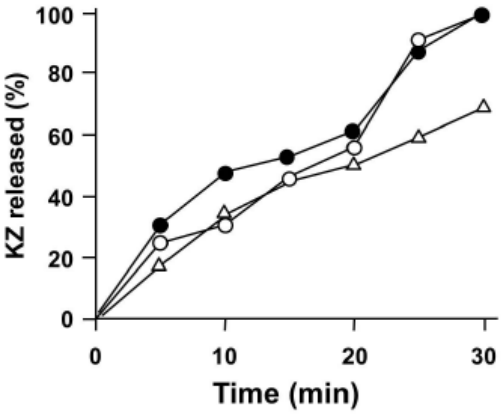

Figure 3. *In vitro* release of coprecipitated and kneaded KZ-β-CD tablets and plain KZ tablets in 0.1 N HCl. Open circles, coprecipitated KZ-β-CD; Closed circles, kneaded KZ-β-CD; Open triangles, plain KZ.

3.5. *Stability study*

Accelerated stability testing could be of value in rating the stability of the tested KZ tablets for scale up studies. The effect of storage of the formulated KZ tablets at three elevated temperatures (35°C, 45°C, and 55°C) on drug chemical stability was studied. Correlation coefficient (*r*) values were determined according to zero-, first-, and second-order equations using the % of drug remaining after specified time intervals over a period of 6 months. The degradation of KZ was found to be a zero-order reaction based on the mean values of the correlation coefficient (*r*). The decomposition rate constants K_{35}, K_{45}, and K_{55} were determined at each temperature using Arrhenius' equation. The energy of activation (E_a) and the decomposition reaction rate constant at room temperature (K_{20}) were determined. $t_{1/2}$ and t_{90} were also estimated for each formula. Figures 4A-4C show the accelerated stability testing of KZ tablets at the three elevated temperatures of 35°C, 45°C, and 55°C, respectively.

Stability results led to the conclusion that the tablets of KZ-β-CD systems at a 1:2 molar ratio prepared by coprecipitation and kneading yielded good stability results as their t_{90} was about 2 years (Table 5).

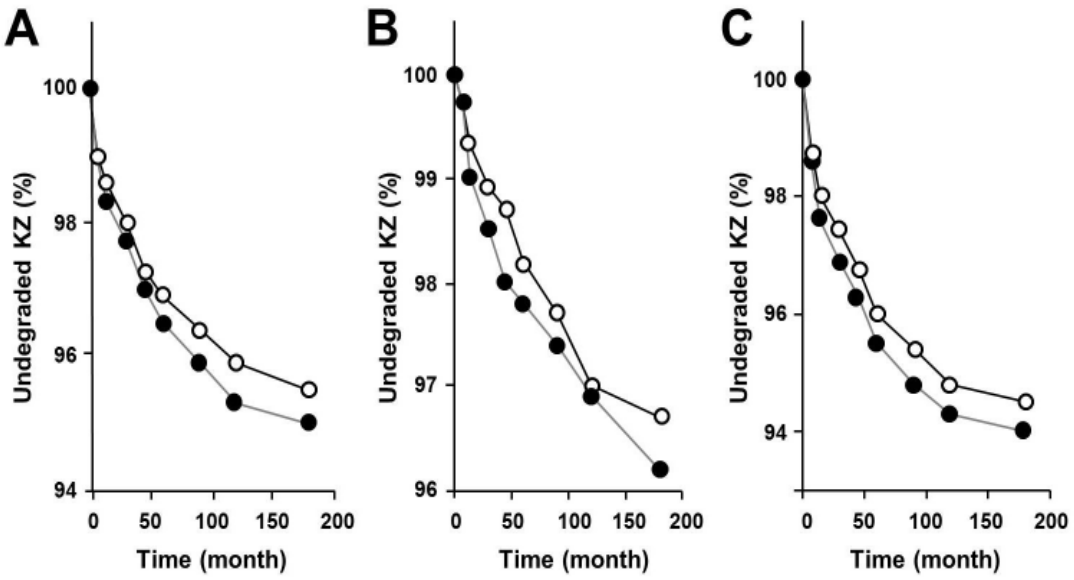

Figure 4. Time course of percent undegraded KZ tablets at various temperatures. (A) 35°C; **(B)** 45°C; **(C)** 55°C. Open circles, coprecipitated KZ-β-CD; Closed circles, kneaded KZ-β-CD.

Table 5. Kinetic parameters for accelerated stability testing of KZ tablets

Method of preparation	K_{35} (days) $^{-1}$	K_{45} (days) $^{-1}$	K_{55} (days) $^{-1}$	E_a (Cal/mol)	K_{20} (days) $^{-1}$	t_{90} (year)	$t_{1/2}$ (year)
Coprecipitated KZ-β-CD	0.017	0.020	0.024	3,072.126	0.01329	2.06	10.30
Kneaded KZ-β-CD	0.018	0.022	0.025	3,857.295	0.01326	2.07	10.32

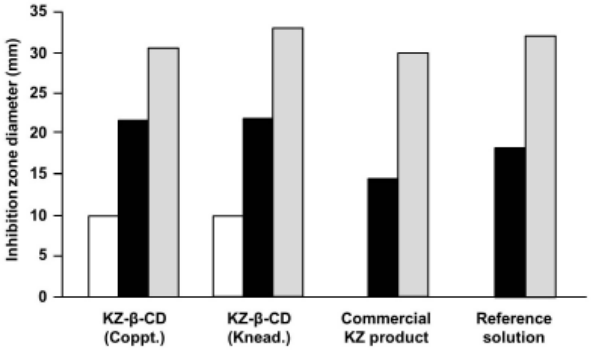

Figure 5. Histogram of the mean values of the inhibition zones diameters of KZ tablets, a commercial product, and a reference solution at different concentrations. Open column, 1.8 µg/µL of KZ; Closed column, 3.6 µg/µL of KZ; Gray column, 5.4 µg/µL of KZ. Coppt. and Knead. represent coprecipitated and kneaded, respectively.

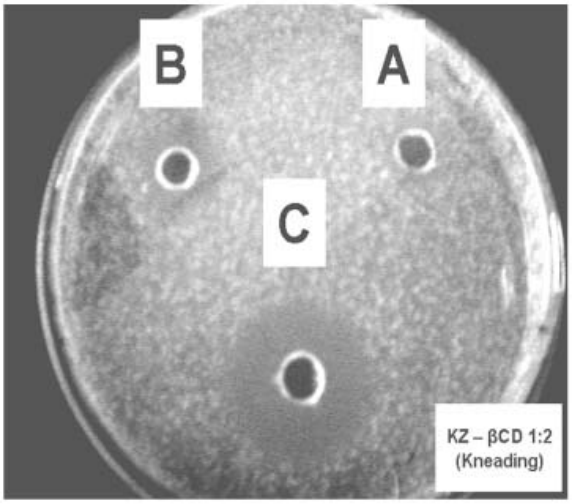

Figure 6. Inhibition zones of kneaded KZ-β-CD 1:2. (A) 1.8 µg/µL; **(B)** 3.6 µg/µL; and **(C)** 5.4 µg/µL.

3.6. *Microbiological study of KZ tablets*

The antifungal activity of KZ-β-CD tablets and a commercial product was studied using *Candida albicans* as a standard fungus. The cylinder plate method (*14*) was used for this study. Figure 5 shows the microbiological data from coprecipitated and kneaded KZ tablets, a KZ commercial product, and a reference KZ sample. The antifungal activity of all of the investigated formulations was determined by measuring the inhibition zone diameter in mm produced by the addition of three volumes (50, 100, and 150 µL) of KZ that were equivalent to three concentrations (1.8, 3.6, and 5.4 µg/µL), respectively. Apparent was the fact that the commercial KZ product and the reference sample had no inhibition zone at the lower concentration (1.8 µg/µL) while the kneaded and coprecipitated KZ tablets prepared at a β-CD 1:2 ratio displayed an increase in the inhibition zone diameter with increasing concentrations ranging from 1.8 to 5.4 µg/µL.

The data obtained, represented by inhibition zone diameters in mm, were statistically analyzed using one-way analysis of variance (ANOVA) followed by Tukey-Kramer post-tests for multiple comparison at $p < 0.05$. The results showed that both KZ-β-CD inclusion complex tablets prepared by coprecipitation and kneading did not differ significantly at 3.6 µg/µL while the reference and commercial formulations differed significantly from both KZ-β-CD systems, especially at low concentrations. The antifungal activity of KZ-β-CD formulations, represented by the inhibition zone diameter of 5.4 µg/µL, were, in descending order, as follows: kneaded KZ-β-CD > coprecipitated KZ-β-CD. Therefore, KZ prepared by kneading as an inclusion complex with a β-CD 1:2 drug/carrier molar ratio yielded the best microbiological results with *Candida albicans* as a fungal model, as shown in Figure 6. The aforementioned results indicate that the KZ-β-CD system tablets have more potent antifungal activity, even at lower concentrations, which may be due to increased drug solubility.

4. Conclusion

The present results confirmed the benefit of using CDs as a useful tool to enhance the dissolution and hence the bioavailability of poorly water-soluble drugs by forming solubilizing systems when exposed to gastrointestinal fluid. The KZ-β-CD system tablets allowed better quality control and had better *in vitro* release and stability values in addition to more potent antifungal activity at low concentrations.

References

1. Remon JP, Belparie F, Van Severen R, Braeckman P. Interaction of antacids with antiarrhythmics. V. Effect of aluminium hydroxide and magnesium oxide on the bioavailability of quinidine, procainamide and propranolol in dogs. Arzneim Forsch. 1983; 33:117-120.
2. Wang L, Tang X. A novel ketoconazole bioadhesive effervescent tablet for vaginal delivery: Design, *in-vitro* and '*in-vivo*' evaluation. Int J pharm. 2008; 350:181-187.
3. USP XXV. The United States Pharmacopoeia, NF 20, US. Pharmacopieal Convention, Inc., Rockville, MD, USA, 2002; p. 1148.

4. Carlson JA, Mann HJ, Canafax DM. Effect of pH on disintegration and dissolution of ketoconazole tablets. Am J Hosp Pharm. 1983; 40:1334-1336.
5. Esclusa-Diaz MT, Guimaraens-Méndez M, Pérez-Marcos MB, Vila-Jato JL, Torres-Labandeira JJ. Characterization and *in vitro* dissolution behaviour of ketoconazole/β- and 2-hydroxypropyl-β-cyclodextrin inclusion compounds. Int J Pharm. 1996; 143:203-210.
6. Heo MY, Piao ZZ, Kim TW, Cao QR, Kim A, Lee BJ. Effect of solubilizing and microemulsifying excipients in polyethylene glycol 6000 solid dispersion on enhanced dissolution and bioavailability of ketoconazole. Arch Pharm Res. 2005; 28:604-611.
7. Jambhekar S, Casella R, Maher T. The physicochemical characterization and bioavailability of indomethacin from β-cyclodextrin, hydroxylethyl-β-cyclodextrin, and hydroxypropyl-β-cyclodextrin complexes. Int J Pharm. 2004; 270:149-166.
8. Nagarsenker MS, Joshi MS. Celecoxib-cyclodextrin systems: Characterization and evaluation of *in vitro* and *in vivo* advantage. Drug Dev Ind Pharm. 2005; 31:169-178.
9. Choi HG, Lee BJ, Han JH, Lee MK, Park KM, Yong CS, Rhee JD, Kim YB, Kim CK. Terfenadine-β-cyclodextrin inclusion complex with antihistaminic activity enhancement. Drug Dev Ind Pharm. 2001; 27:857-862.
10. Svehla G. In: Vogel's Qualitative Inorganic Analysis. 7th ed., Thomson Press India Ltd., Mumbai, India, 1996; p. 207.
11. Lindahl A, Ungell AL, Kunston L, Lennernäs H. Characterization of fluids from stomach and proximal jejunum in men and women. Pharm Res. 1997; 14:497-502.
12. Karasulu HY, Hilmioğlu S, Metin DY, Güneri T. Efficacy of a new ketoconazole bioadhesive vaginal tablet on *Candida albicans*. Farmaco. 2004; 59:163-167.
13. Ritger PL, Peppas NA. A simple equation for description of solute release. II. Fickian and anomalous release from swellable device. J Control Release. 1987; 5:37-42.
14. Vaucher LC, Breier AR, Schapoval EE. Microbiological assay for the determination of telithromycin in tablets. J AOAC Int. 2006; 89:1398-1402.
15. Vanitha J, Saravana Kumar A, Ganesh M, Saravanan VS. Comparative analysis of climbazole in pharmaceutical formulation. Asian J Research Chem. 2008; 1:43-45.
16. Bergamasco Rde C, Zanin GM, de Moraes FF. Sulfluramid volatility reduction by beta-cyclodextrin. J Agric Food Chem. 2005; 53:1139-1143.
17. Tayade PT, Vavia PR. Inclusion complexes of ketoprofen with β-cyclodextrins: Oral pharmacokinetics of ketoprofen in human. Indian J Pharm Sci. 2006; 68:164-170.
18. Abdelkader H, Abdallah OY, Salem HS. Comparison of the effect of tromethamine and polyvinylpyrrolidone on dissolution properties and analgesic effect of nimesulide. AAPS PharmSciTech. 2007; 8:E65.
19. Choi HG, Kim DD, Jun HW, Yoo BK, Yong CS. Improvement of dissolution and bioavailability of nitrendipine by inclusion in hydroxypropyl-β-cyclodextrin. Drug Dev Ind Pharm. 2003; 29:1085-1094.

(*Received July 26, 2010; Revised August 7, 2010; Accepted August 7, 2010****)***

Drug Discoveries & Therapeutics

Guide for Authors

1. Scope of Articles

Drug Discoveries & Therapeutics mainly publishes articles related to basic and clinical pharmaceutical research such as pharmaceutical and therapeutical chemistry, pharmacology, pharmacy, pharmacokinetics, industrial pharmacy, pharmaceutical manufacturing, pharmaceutical technology, drug delivery, toxicology, and traditional herb medicine. Studies on drug-related fields such as biology, biochemistry, physiology, microbiology, and immunology are also within the scope of this journal.

2. Submission Types

Original Articles should be reports new, significant, innovative, and original findings. An Article should contain the following sections: Title page, Abstract, Introduction, Materials and Methods, Results, Discussion, Acknowledgments, References, Figure legends, and Tables. There are no specific length restrictions for the overall manuscript or individual sections. However, we expect authors to present and discuss their findings concisely.

Brief Reports should be short and clear reports on new original findings and not exceed 4,000 words with no more than two display items. *Drug Discoveries & Therapeutics* encourages younger researchers and doctors to report their research findings. Case reports are included in this category. A Brief Report contains the same sections as an Original Article, but Results and Discussion sections must be combined.

Reviews should include educational overviews for general researchers and doctors, and review articles for more specialized readers.

Policy Forum presents issues in science policy, including public health, the medical care system, and social science. Policy Forum essays should not exceed 2,000 words.

News articles should not exceed 500 words including one display item. These articles should function as an international news source with regard to topics in the life and social sciences and medicine. Submissions are not restricted to journal staff - anyone can submit news articles on subjects that would be of interest to Drug Discoveries & Therapeutics' readers.

Letters discuss material published in *Drug Discoveries & Therapeutics* in the last 6 months or issues of general interest. Letters should not exceed 800 words and 6 references.

3. Manuscript Preparation

Preparation of text. Manuscripts should be written in correct American English and submitted as a Microsoft Word (.doc) file in a single-column format. Manuscripts must be paginated and double-spaced throughout. Use Symbol font for all Greek characters. Do not import the figures into the text file but indicate their approximate locations directly on the manuscript. The manuscript file should be smaller than 5 MB in size.

Title page. The title page must include 1) the title of the paper, 2) name(s) and affiliation(s) of the author(s), 3) a statement indicating to whom correspondence and proofs should be sent along with a complete mailing address, telephone/fax numbers, and e-mail address, and 4) up to five key words or phrases.

Abstract. A one-paragraph abstract consisting of no more than 250 words must be included. It should state the purpose of the study, basic procedures used, main findings, and conclusions.

Abbreviations. All nonstandard abbreviations must be listed in alphabetical order, giving each abbreviation followed by its spelled-out version. Spell out the term upon first mention and follow it with the abbreviated form in parentheses. Thereafter, use the abbreviated form.

Introduction. The introduction should be a concise statement of the basis for the study and its scientific context.

Materials and Methods. Subsections under this heading should include sufficient instruction to replicate experiments, but well-established protocols may be simply referenced. *Drug Discoveries & Therapeutics* endorses the principles of the Declaration of Helsinki and expects that all research involving humans will have been conducted in accordance with these principles. All laboratory animal studies must be approved by the authors' Institutional Review Board(s).

Results. The results section should provide details of all of the experiments that are required to support the conclusions of the paper. If necessary, subheadings may be used for an orderly presentation. All figures, tables, and photographs must be referred in the text.

Discussion. The discussion should include conclusions derived from the study and supported by the data. Consideration should be given to the impact that these conclusions have on the body of knowledge in which context the experiments were conducted. In Brief Reports, Results and Discussion sections must be combined.

Acknowledgments. All funding sources should be credited in the Acknowledgments section. In addition, people who contributed to the work but who do not fit the criteria for authors should be listed along with their contributions.

References. References should be numbered in the order in which they appear in the text. Cite references in text using a number in parentheses. Citing of unpublished results and personal communications in the reference list is not recommended but these sources may be mentioned in the text. For all references, list all authors, but if there are more than fifteen authors, list the first three authors and add "*et al.*" Abbreviate journal names as they appear in PubMed. Web references can be included in the reference list.

Example 1:
Hamamoto H, Akimitsu N, Arimitsu N, Sekimizu K. Roles of the Duffy antigen and glycophorin A in malaria infectionand erythrocyte. Drug Discov Ther. 2008; 2:58-63.

Example 2:
Zhao X, Jing ZP, Xiong J, Jiang SJ. Suppression of experimental abdominal aortic aneurysm by tetracycline: a preliminary study. Chin J Gen Surg. 2002; 17:663-665. (in Chinese)

Example 3:
Mizuochi T. Microscale sequencing of *N*-linked oligosacchaides of glycoproteins using hydrazinolysis, Bio-Gel P-4, and sequential exoglycosidase digestion. In: Methods in Molecular Biology: Vol. 14 Glycoprotein analysis in biomedicine (Hounsell T, ed.). Humana Press, Totowa, NJ, USA, 1993; pp. 55-68.

Example 4:
Drug Discoveries & Therapeutics. Hot topics & news: China-Japan Medical Workshop on Drug Discoveries and Therapeutics 2007. http://www.ddtjournal.com/hotnews.php (accessed July 1, 2007).

Figure legends. Include a short title and a short explanation. Methods described in detail in the Materials and methods section should not be repeated in the legend. Symbols used in the figure must be explained. The number of data points represented in a graph must be indicated.

Tables. All tables should have a concise title and be typed double-spaced on pages separate from the text. Do not use vertical rules. Tables should be numbered with Arabic numerals consecutively in accordance with their appearance in the text. Place footnotes to tables below the table body and indicate them with lowercase superscript letters.

Language editing. Manuscripts submitted by authors whose primary language is not English should have their work proofread by a native English speaker before submission. The Editing Support Organization can provide English proofreading, Japanese-English translation, and Chinese-English translation services to authors who want to publish in *Drug Discoveries & Therapeutics* and need assistance before submitting an article. Authors can contact this organization directly at http://www.iacmhr.com/iac-eso .

IAC-ESO was established in order to facilitate manuscript preparation by researchers whose native language is not English and to help edit work intended for international academic journals. Quality revision, translation, and editing services are offered by our staff, who are native speakers of particular languages and who are familiar with academic writing and journal editing in English.

4. Figure Preparation

All figures should be clear and cited in numerical order in the text. Figures must fit a one- or two-column format on the journal page: 8.3 cm (3.3 in.) wide for a single column; 17.3 cm (6.8 in.) wide for a double column; maximum height: 24.0 cm (9.5 in.). Only use the following fonts in the figure: Arial and Helvetica. Provide all figures as separate files. Acceptable file formats are JPEG and TIFF. Please note that files saved in JPEG or TIFF format in PowerPoint lack sufficient resolution for publication. Each Figure file should be smaller than 10 MB in size. Do not compress files. A fee is charged for a color illustration or photograph.

5. Online Submission

Manuscripts should be submitted to *Drug Discoveries & Therapeutics* online at http://www.ddtjournal.com. The manuscript file should be smaller than 10 MB in size. If for any reason you are unable to submit a file online, please contact the Editorial Office by e-mail: office@ddtjournal.com

Editorial and Head Office
Wei TANG, MD PhD
Executive Editor
Drug Discoveries & Therapeutics
Pearl City Koishikawa 603,
2-4-5 Kasuga, Bunkyo-ku,
Tokyo 112-0003, Japan
Tel: 03-5840-9697
Fax: 03-5840-9698
E-mail: office@ddtjournal.com

Cover letter. A cover letter from the corresponding author including the following information must accompany the submission: name, address, phone and fax numbers, and e-mail address of the corresponding author. This should include a statement affirming that all authors concur with the submission and that the material submitted for publication has not been previously published and is not under consideration for publication elsewhere and a statement regarding conflicting financial interests.

Authors may recommend up to three qualified reviewers other than members of Editorial board. Authors may also request that certain (but not more than three) reviewers not be chosen.

The cover letter should be submitted as a Microsoft Word (.doc) file (smaller than 1 MB) at the same time the work is submitted online.

6. Accepted Manuscripts

Proofs. Rough galley proofs in PDF format are supplied to the corresponding author *via* e-mail. Corrections must be returned within 4 working days of receipt of the proofs. Subsequent corrections will not be possible, so please ensure all desired corrections are indicated. Note that we may proceed with publication of the article if no response is received.

Transfer of copyrights. Upon acceptance of an article, authors will be asked to agree to a transfer of copyright. This transfer will ensure the widest possible dissemination of information. A letter will be sent to the corresponding author confirming receipt of the manuscript. A form facilitating transfer of copyright will be provided. If excerpts from other copyrighted works are included, the author(s) must obtain written permission from the copyright owners and credit the source(s) in the article.

Cover submissions. Authors whose manuscripts are accepted for publication in *Drug Discoveries & Therapeutics* may submit cover images. Color submission is welcome. A brief cover legend should be submitted with the image.

Revised June 20, 2009

IACMHR CO., LTD.

Drug Discoveries & Therapeutics

Editorial Office

Pearl City Koishikawa 603,
2-4-5 Kasuga, Bunkyo-ku,
Tokyo 112-0003, Japan

Tel: 03-5840-9697
Fax: 03-5840-9698
E-mail: office@ddtjournal.com
URL: www.ddtjournal.com

IACMHR CO., LTD.

JOURNAL PUBLISHING AGREEMENT

Ms No:

Article entitled:

Corresponding author:

To be published in Drug Discoveries & Therapeutics

Assignment of publishing rights:

I hereby assign to International Advancement Center for Medicine & Health Research Co., Ltd. (IACMHR Co., Ltd.) publishing Drug Discoveries & Therapeutics the copyright in the manuscript identified above and any supplemental tables and illustrations (the articles) in all forms and media, throughout the world, in all languages, for the full term of copyright, effective when and if the article is accepted for publication. This transfer includes the rights to provide the article in electronic and online forms and systems.

I understand that I retain or am hereby granted (without the need to obtain further permission) rights to use certain versions of the article for certain scholarly purpose and that no rights in patent, trademarks or other intellectual property rights are transferred to the journal. Rights to use the articles for personal use, internal institutional use and scholarly posting are retained.

Author warranties:

I affirm the author warranties noted below.

1) The article I have submitted to the journal is original and has not been published elsewhere.
2) The article is not currently being considered for publication by any other journal. If accepted, it will not be submitted elsewhere.
3) The article contains no libelous or other unlawful statements and does not contain any materials that invade individual privacy or proprietary rights or any statutory copyright.
4) I have obtained written permission from copyright owners for any excerpts from copyrighted works that are included and have credited the sources in my article.
5) I confirm that all commercial affiliations, stock or equity interests, or patent-licensing arrangements that could be considered to pose a financial conflict of interest regarding the article have been disclosed.
6) If the article was prepared jointly with other authors, I have informed the co-authors(s) of the terms of this publishing agreement and that I am signing on their behalf as their agents.

Your Status:

☐ I am the sole author of the manuscript.

☐ I am one author signing on behalf of all co-authors of the manuscript.

Please tick one of the above boxes (as appropriate) and then sign and date the document in black ink.

Signature: **Date:**

Name printed:

Please return the completed and signed original of this form by express mail or fax, or by e-mailing a scanned copy of the signed original to:

Drug Discoveries & Therapeutics office
Pearl City Koishikawa 603, 2-4-5 Kasuga, Bunkyo-ku, Tokyo 112-0003, Japan
e-mail: proof-editing@ddtjournal.com
Fax: +81-3-5840-9698